Brain-selective kinase (BRSK) interactions with tau as a cause of neurodegeneration

by

Charles Stuart Cameron

A thesis submitted for the degree of Doctor of Philosophy

School of Life Sciences
University of Warwick

September 2013

For Anna

Table of contents

List of figures

List of tables

Acknowledgements

I would like to thank my supervisors, Dr Kevin Moffat and Prof. Bruno Frenguelli for their guidance and support throughout my PhD, and for giving me the opportunity to participate in some very exciting research.

I am hugely grateful to Dr Alessia Galasso for her help in teaching me most of my lab technique, and for much enriching discussion and critique.

Dr Ceri Lyn-Adams was the source of much of the inspiration behind this project, and was of much help in its early stages.

I would like to thank my mother, father and brother for their love and support, and helping me to come this far.

Others deserving of thanks include:

Dr Guy Tear, Dr Giulia Povellato and Dr Kyung-An Han for their generous provision of fly stocks.

All members of the Moffat and Frenguelli labs, and occupants of rooms C112 and C117, for their friendship, encouragement and advice over the past four years.

My friends in the same boat, Dave, Matt, Matt, Elle and Perry for providing the best possible ways of not thinking about flies for a while.

I must also thank the BBSRC for their financial contribution to this project.

Declaration

Unless otherwise indicated, the entirety of the work contained herein was conducted by me under the supervision of Dr Kevin Moffat, Prof. Bruno Frenguelli and Dr Alessia Galasso with the following exception:

The addition of the S262D mutation to the T212D plasmid was performed by Mr Max Levin under my supervision.

None of the work contained in this thesis has been submitted for any previous degree and all sources of information have been acknowledged by means of references.

Charles Stuart Cameron

September 2013

Abstract

Tauopathies are a group of neurodegenerative diseases associated with the build-up of intracellular aggregates of the microtubule-associated protein (MAP) tau, called neurofibrillary tangles (NFT). The tau found in NFTs is known to be highly phosphorylated, and as such a number of tau kinases have been examined for their ability to affect tau toxicity in animal models, including members of the AMPK-related kinase family. Two members of this family, the brain-selective kinases (BRSKs), have been shown to phosphorylate tau *in vitro* and *in vivo* in an LKB1 and CaMKKα-dependent manner. BRSKs are prevalent in the central nervous system, in which they modulate neuronal polarisation via tau. They have also been shown to dramatically increase 0N4R tau toxicity in a *Drosophila* model.

In order to determine the importance of phosphorylation to tau toxicity in this model, I have generated a group of 2N4R tau phosphorylation mutants. Based upon *in vitro* data linking phosphorylation at T212 to tau aggregation, and S262 to microtubule dissociation, these two residues underwent both non-phosphorylatable and phospho-mimetic mutation and were inserted into *Drosophila*. Each of these mutations was found to alter tau toxicity upon expression in the fly eye, as measured by disruption of ommatidia, with the T212D and S262A mutations producing a milder phenotype.

Each of these sites on tau has previously been shown to be a target of phosphorylation by BRSK2 *in vitro*. Through generation of a T212D S262D double mutant, I was able to investigate whether phenotypic changes caused by BRSK2 were due to phosphorylation. BRSK2 was found to have a different effect on toxicity caused by 2N4R tau, causing a reduction in toxicity. This was found to be comparable to the phenotype of the double mutant. However, examination of the ability of BRSK2 to modulate the toxicity of the single tau mutants demonstrated a more complex phosphorylation profile, also dependent on other residues.

Further experiments examined the consequences of tau and BRSK2 expression in the CNS. This demonstrated the toxicity of BRSK2 overexpression, in the absence of tau, in these tissues. Given that BRSK2 overexpression alone in the eye led to no observable phenotype, this tissue-dependent toxicity of the kinase demonstrates the importance of the choice of model in such studies. In addition, a deficiency screen for modulators of 0N4R tau/BRSK2 toxicity in the eye has generated multiple leads, including the fly homologue of the actin-binding protein profilin.

This project has demonstrated the inequivalence of several phosphorylation sites *in vivo*, as well as an isoform-dependent aspect of tau toxicity. These data suggest that the influence of tau phosphorylation on toxicity is complex; expansion of the work presented here could help decipher the code of tau phosphorylation.

Abbreviations and acronyms

AA: Amino acid
Aβ: β amyloid
Ach: Acetylcholine
AD: Alzheimer's disease
AIF: Apoptosis-inducing factor
AMP: Adenosine monophosphate
Arpc2: Actin-related protein 2/3 complex, subunit 2
ATP: Adenosine triphosphate
AMPK: Adenosine monophosphate-activated protein kinase
ANOVA: Analysis of variance
ApoE: Apolipoprotein E
APP: Amyloid precursor protein
B2WT5: BRSK2 wild-type line 5
BDSC: Bloomington *Drosophila* stock centre
BRSK: Brain-selective kinase
BSA: Bovine serum albumen
CaMKK: Ca^{2+}/calmodulin-dependent protein kinase kinase
CBD: Corticobasal degeneration
Cdc: Cell division cycle
CDK: Cyclin-dependent kinase
cDNA: Complementary DNA
Chk2: Checkpoint kinase 2
CNS: Central nervous system
CSN4: COP9 complex homolog subunit 4
CTE: Chronic traumatic encephalopathy
CyO: Curly of Oster
DAM: *Drosophila* activity monitor
DC: Distortion coefficient
Debcl: Death executioner Bcl-2 homologue
DLG: Discs large
DNA: Deoxyribonucleic acid
EDTA: Ethylene diamine tetra-acetic acid
ECL: Enhanced chemoluminescence
EGTA: Ethylene glycol tetra-acetic acid
ELAV: Embryonic lethal, abnormal vision
ER: Endoplasmic reticulum
ERK: Extracellular signal-related kinase
F-actin: Filamentous actin
FAD: Familial Alzheimer's disease
FLP: Flipase
FRT: Flipase recombination target
FTDP-17: Frontotemporal dementia and Parkinsonism linked to chromosome 17
GlyP: Glycogen phosphorylase
GMR: Glass multimer reporter
GTO: Granular tau oligomers
GSK-3: Glycogen synthase kinase 3
GTP: Guanosine triphosphate

HDAC6: Histone deacetylase 6
Hey: Hairy/E(spl)-related with YRPW motif
HRP: Horseradish peroxidase
Hsp70: Heat shock protein 70
Jab-1: c-Jun activation domain-binding protein 1
kD: Kilodalton
LB: Luria-Bertani
LKB1: Liver kinase B1
MAP: microtubule-associated protein
MAPT: Microtubule-associated protein tau
MARK: Microtubule/MAP affinity regulating kinase
MED24: Mediator complex subunit 24
MEKK2: MAP/ERK kinase kinase-2
MICAL: Molecule interacting with CasL
MTOC: Microtubule organising centre
mRNA: Messenger RNA
MYPT: Myosin binding subunit
nAChR: Nicotinic acetylcholine receptor
NEB: New England Biolabs
NFT: Neurofibrillary tangles
NMDA: N-methyl D-aspartate
NMNAT: Nicotinamide mononucleotide adenylyl transferase
Nup50: Nucleoporin 50kD
PBS: Phosphate-buffered saline
PCR: Polymerase chain reaction
PDF: Pigment dispersing factor
PFA: Paraformaldehyde
PHF: Paired helical filaments
PKA: Protein kinase A
PNS: Peripheral nervous system
Pnut: Peanut
PP2A: Protein phosphatase 2A
PSP: Progressive supranuclear palsy
QED: Quantitative edge detection
RNA: Ribonucleic acid
RNAi: RNA interference
SAD: Synapses of the amphid defective
SDAT: Senile dementia of the Alzheimer's type
SD-NFT: Senile dementia of the neurofibrillary tangle type
SDS-PAGE: Sodium dodecyl sulphate polyacrylamide gel electrophoresis
SEM: Scanning electron microscopy
SFF: Sugar-free frosting
Sgg: Shaggy
SILAC: Stable isotope labelling with amino acids in cell culture
SOD: Superoxide dismutase
Su(dx): Suppressor of deltex
Sut: Sugar transporter
TARGET: Temporal and regional gene expression targeting
TBE: Tris/borate/EDTA
TOR: Target of rapamycin

Tris: Tris(hydroxymethyl)aminomethane
TUNEL: Terminal deoxynucleotidyl transferase mediated dUTP nick end labelling
UAS: Upstream activating sequence
Ubc: Ubiquitin conjugating enzyme
Ublcp1: Ubiquitin-like domain-containing C-terminal domain phosphatase 1
UTP: Uridine triphosphate
UV: Ultraviolet
VDRC: Vienna *Drosophila* RNAi centre
VPS: Vacuolar protein sorting
v/v: volume/volume
WT: wild type
w/v: weight/volume

1| Introduction

The microtubule-associated protein tau is both a key part of the neuronal cytoskeleton, and its dysregulation a common pathological signature of a number of neurodegenerative diseases, the tauopathies. Tauopathies are classified as any disease associated with a build-up of intracellular tau aggregates, known as neurofibrillary tangles (NFT). Most of these conditions present with dementia; indeed tauopathies together account for the majority of dementia cases globally. The most well-known and also most prevalent of these diseases is Alzheimer's disease (AD), although more and more patients are being diagnosed with mixed dementia, with multiple brain pathologies (Schneider et al., 2007). According to the World Alzheimer Report 2010, there were 35.6 million people suffering from dementia globally (Wortmann, 2012), with this number expected to nearly double every 20 years as life expectancy increases. The same report also estimated the economic cost of dementia at US$604 billion, or equivalent to 1% of global gross domestic product. With tau pathology associated with the vast majority of actual cases of dementia, a great deal of research has focused on determining the mechanisms responsible for the apparently pathogenic changes occurring in this cytoskeletal protein, ultimately leading to aggregation and neurodegeneration. This literature review covers the history of research into tau, its normal physiological function and the diseases with which it is associated. It also examines some of the theories attempting to explain tau pathology, with particular attention paid to the history of research into tau phosphorylation and tau kinases, the investigation of which was the primary goal of this work.

1.1 Tau protein

Human tau protein is transcribed from the gene *MAPT* (microtubule-associated protein tau). The gene encodes all six isoforms of tau found in the brain, through alternate splicing of three introns (Goedert et al., 1989a), which vary in length from 352 to 441 amino acids (AA), as shown in Fig 1.1. It functions as a microtubule-stabilising agent (Weingarten et al., 1975), a process which is very strongly regulated by phosphorylation (Lindwall and Cole, 1984). This ability of tau function to be rapidly modulated is likely reflected in the localisation and role of the protein, which is primarily axonal (Binder et al., 1985), where it is involved in the regulation of

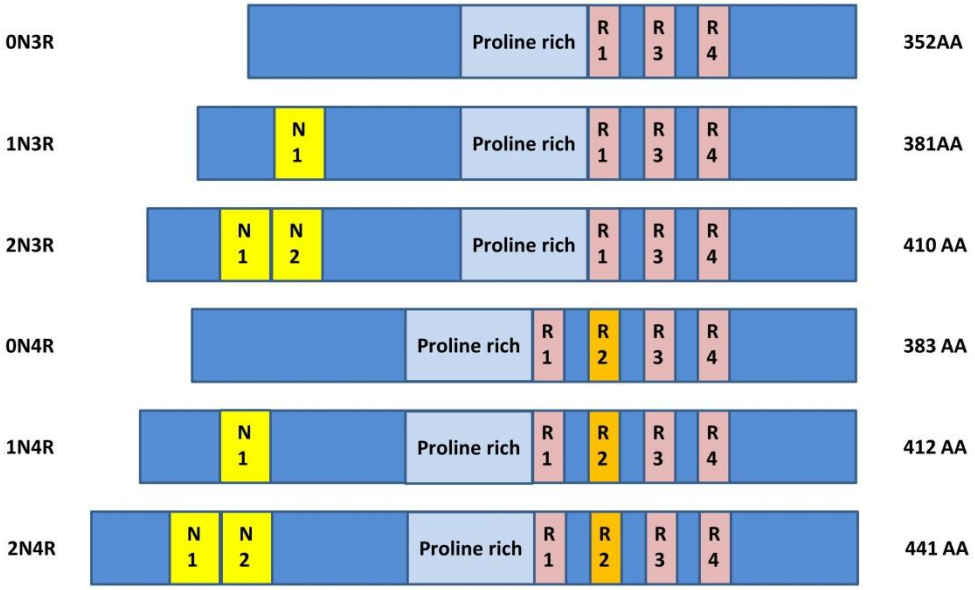

Figure 1.1 The six isoforms of human tau found in the brain
Alternate splicing of the MAPT gene can generate six isoforms of tau of different lengths. Exons 2 and 3 (29AA each) encode the N-terminal inserts labelled here respectively as N1 and N2. Exon 10 (31AA) encodes the second microtubule-binding domain, R2. The proline-rich region is contained within exon 7 and part of exon 9 (Martin et al., 2011), and contains a large number of phosphorylation sites known to influence microtubule-binding and tau aggregation in vitro.

growth cone dynamics (Liu et al., 1999). In mammalian cells and in the fly, the function of tau is thought to be redundant, with no major phenotype recorded in tau null mutants (DiTella et al., 1996; Doerflinger et al., 2003).

1.1.1 The discovery of tau

Tau protein was first isolated in porcine brain in 1975, during relatively early experiments exploiting the then-novel ability to polymerise tubulin *in vitro* (Weingarten et al., 1975). Removal of tau during phosphocellulose chromatography from relatively pure microtubule samples was found to completely remove the ability of tubulin to polymerise *in vitro*. Tau was shown to increase the tendency of tubulin to polymerise stoichiometrically, with greater concentration of tau leading to increased formation of 36S oligomers, the subunits of microtubules composed of αβ-tubulin dimers (Melki et al., 1989). The identification of the *MAPT* gene was completed shortly after the definitive association of tau with the NFT of Alzheimer's disease by a trio of papers appearing in *PNAS* in 1988. Together, two groups form Cambridge managed to overcome the principle impediment to identification of the components of the paired helical filaments (PHF) of NFT, which was their insolubility. This was performed by screening of a cDNA library from the post mortem brain tissue of an Alzheimer's patient using an oligonucleotide probe (Goedert et al., 1988); the probe was generated based on knowledge of a PHF-derived six amino acid fragment(Wischik et al., 1988a; Wischik et al., 1988b). The screen identified the shortest 352AA tau isoform, which was shown to be found within the insoluble PHF core using a monoclonal antibody also generated by these groups. This was the first successful probe of the PHF core, and led to a dramatic increase in interest surrounding tau. Soon after, the number of sequenced mammalian tau proteins dramatically increased (Goedert et al., 1989a).

1.1.2 The multiple isoforms of tau

Prior to the first sequencing of the human tau AA sequence, it was already known that multiple tau isoforms existed (Cleveland et al., 1977a, b). Evidence had been found for only a single human tau gene, located within chromosome 17 (Neve et al.,

1986), indicating the likelihood of alternative splicing leading to multiple tau isoforms. Further tau isoform cDNAs were subsequently isolated by probing with a 17mer oligonucleotide complementary to the tau repeat region, first the 383AA, four microtubule-binding repeat isoform (Goedert et al., 1989b), and finally a comprehensive cDNA library screen revealed there to be six human brain tau isoforms in total (Goedert et al., 1989a). This revealed the presence of two additional N-terminal inserts, of 29AA each, of which the second was never present without the first. Upon complete sequencing of the tau gene, these inserts were shown to be contained within exons 2 and 3, with the additional microtubule-binding repeat in exon 10, placing it second among the four repeats of the longer isoform. Figure 1.2 is a MAPT splicing diagram, indicating the multiple splicing variants of tau found in the brain and peripheral nervous system (PNS). The six brain tau isoforms range in molecular weight from 37 to 46kD. The established nomenclature for the different isoforms is based on the number of N (N-terminal) and R (microtubule-binding repeat) domains, ranging from 0N3R (352 AA) to 2N4R (441 AA). All of the isoforms have been found to migrate abnormally through SDS-PAGE gels, with apparent molecular weights of between 48 and 67kD, even after treatment with alkaline phosphatase to remove phosphate groups (Goedert and Jakes, 1990). In particular, the N-terminal inserts were found to affect migration disproportionately. Four-repeat tau isoforms were found to better stabilise microtubules by a factor of up to 3-fold compared with three-repeat isoforms; the N-terminal inserts were not found to affect microtubule stabilisation (Goedert and Jakes, 1990). In adult brain samples, four major tau bands were found – the number and intensity of these bands did not differ between control and Alzheimer's patients. These bands corresponded in size to the four smallest recombinant tau isoforms, indicating the lack of twin N-terminal repeat isoforms. The mRNA of the largest tau isoform had previously been detected, but in much lower concentrations than these four (Goedert et al., 1989a). In foetal samples, the smallest three-repeat isoform was isolated, along with a second, slightly larger band which was smaller than any other recombinant isoform, indicating the primacy of three-repeat tau in the developing brain. In addition, foetal tau was found to be particularly highly phosphorylated; foetal tau is thus generally less capable of stabilising microtubules.

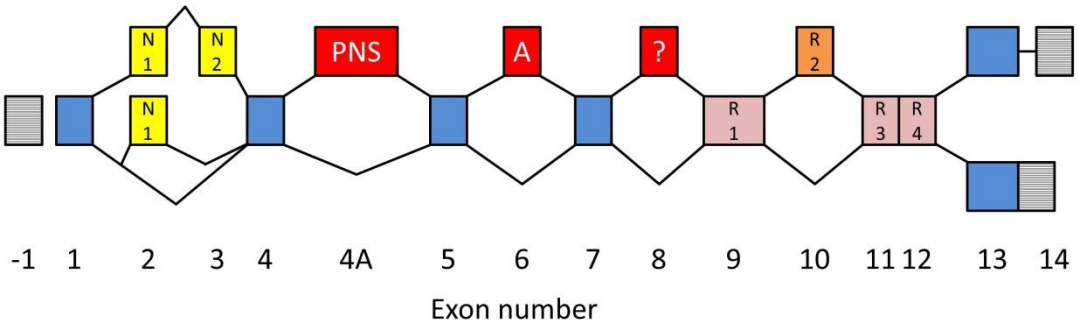

Figure 1.2 Splicing diagram of the* MAPT *gene
Alternative splicing affects exons 2, 3, 4A, 6, 8, 10, 13 and 14 of MAPT. *The N-terminal inserts in exons 2 and 3, and the additional microtubule-binding domain in exon 10, are described above. In addition, three other alternatively spliced exons are more rare or never found in human brain (Liu and Gong, 2008). Inclusion of exon 4A generates an 110kDa tau isoform found only in the peripheral nervous system (PNS). Exon 6 is found only in a minority of axonal tau in the CNS (A), and its inclusion can lead to C-truncated tau molecules with no microtubule-binding domains due to reading frame changes caused by use of two alternative splice sites (Luo et al., 2004). Exon 8 (?) has only been found in bovine tau mRNA (Andreadis, 2005). Murine tau mRNAs have been found which vary in C-terminus length due to excision of the intron between exons 13 and 14.*

The majority of research into tau isoform-specific differences has focused on 3R and 4R tau. These two groups are both roughly equally expressed in the adult brain and cortical neurons specifically, whereas 0N, 1N and 2N isoforms are expressed at a ratio of roughly 37:54:9 (Deshpande et al., 2008). These isoforms are thought to adopt different secondary structures, with each isoform possessing distinct regions of influence over microtubule binding – the 3R isoforms depend on a C-terminal sequence to complement its binding, whereas the 4R isoforms depend solely on the repeat domains (Goode et al., 2000). Recorded differences between 3R and 4R isoforms, as well as altering microtubule stability, include 3R species decreasing taxol affinity for microtubules, either by competition or alteration of microtubule structure (Park et al., 2008); the ability of 3R tau to reduce heparin-induced 4R tau polymerisation, potentially signifying a role for 3R tau in the prevention of aggregation (Adams et al., 2010); and differences in the shapes of fibrils of these isoforms, with 4R tau forming longer, less twisted fibrils, potentially more apt for tangle formation (Furukawa et al., 2011). Each of these differences was found to be independent of the presence or absence of N-terminal inserts.

More recently, some functional differences have been found between isoforms with different numbers of N-terminal inserts. For example, all six isoforms have been shown to possess differing arachidonic acid-induced aggregation kinetics in the presence of heat shock protein 70 (Hsp70), with aggregation of 3R isoforms inhibited at lower Hsp70 concentrations. N-terminal repeats were only consistently found to have an effect when assayed by laser light scattering, indicating reduced sensitivity to the aggregation inhibitor in 4R species containing N-terminal inserts, and the opposite effect in 3R species (Voss et al., 2012). This effect due to the N terminal inserts was less significant than differences between 3R and 4R isoforms, which increased Hsp70 resistance in all cases. The longer N-terminus has an increased negative charge compared to 0N tau isoforms, which has been posited to aid in the correct localisation of tau to the axon (Ittner et al., 2010). In addition, the N-terminal domains lead to an increased negative charge and size of the projection domain of microtubule-bound tau, created by repulsion of the N-terminus of tau by similarly-charged tubulin. This more negative charge has been used to explain the increased kinesin transport speed of microtubules primarily stabilised by 1N or 2N tau – bound tau can act as a “roadblock” for microtubule-based transport, preventing

kinesin from attaching. The negative charge of the projection domain could help redirect the positively-charged kinesin molecules around the intervening MAP, via sidestepping onto neighbouring tubulin (Tarhan et al., 2013). This is perhaps a more likely role for the N-terminal inserts, given that they have a much greater influence on transport dynamics than the extra R domain. The N-terminal inserts could also be of pathogenic interest. The projection domain has been shown to exist along tau fibrils, giving aggregated tau a "coat" of projection domains with a charge dependant on cellular pH and electrolyte concentration (Wegmann et al., 2013). Aggregates could thus be sensitive to cellular conditions (e.g. ionic concentrations), affecting their localisation and growth.

1.1.3 Tau function

Microtubules are composed of 8nm heterodimers of α and β tubulin, assembled into protofilaments, of which 13 can associate to form the cylindrical shape of microtubules (Desai and Mitchison, 1997). They form around microtubule organising centres (MTOCs), and conduct cell division, kinesin-driven transport and cell structure and growth. Tubulin has long been known to rely on guanine nucleotides for its polymerisation (Weisenberg et al., 1968), and the turnover of GTP on polymerised tubulin is at the heart of what is known as the dynamic instability of microtubules (Mitchison and Kirschner, 1984). Microtubules alternate between phases of gradual tubulin addition and rapid dissociation; the transition from microtubule elongation to reduction is termed catastrophe. The collapse of a microtubule is thought to occur once the rate of GTP hydrolysis outpaces that of GTP-tubulin addition; microtubule stability is thus dependent upon the presence of a cap of GTP-tubulin at the plus end, which will be lost without sustained polymerisation (Kirschner and Mitchison, 1986). One complication of this model is that although the growth rate is dependent on tubulin concentration, the frequency of catastrophe is less so, depending primarily on the rate of GTP hydrolysis, as shown by the use of a slow-hydrolysing GTP analogue (Janson et al., 2003). Several models have attempted to account for this, leading to the conclusion that catastrophic events involve multiple steps, likely dependent on binding of MAPs (Holmfeldt et al., 2002) as well as GTP hydrolysis and growth rate (Bowne-Anderson et al., 2013).

Relatively little is known about the precise role or mechanism of action of tau. Its localisation implies a role in axonal growth, steering and transport (Liu et al., 1999), and it has also been shown to play a role in neuronal polarisation (Caceres and Kosik, 1990). The ability of tau to stabilise microtubules is highly modulatable by phosphorylation, a characteristic which would make it more apt for localisation to the distal end of the axon, where greater cytoskeletal flexibility is required (Black et al., 1996). This is perhaps another reason why foetal tau is present in only the 3R isoforms, and in a highly phosphorylated state. This could also explain the existence of multiple isoforms of human tau, as a further method of flexibility. As for the variety of N-terminal projection domains, it is possible that they exist to regulate microtubule spacing, which is smaller in the axon than in dendrites, creating a closer network (Chen et al., 1992). This N-terminal domain also defines the various MAPs, with a far greater degree of variation in the projection domain than in the microtubule-binding region, with tau being particularly small. The spacing of tau on microtubules has been shown to be unusually distant, with one every 60 tubulin dimers, giving the protein a very high efficiency of action and increasing its sensitivity to modulation (Breuzard et al., 2013). Tau was shown to increase microtubule stability through conformational changes in microtubules, causing an increase in the rescue of assembly following microtubule shrinkage.

Normal tau function is associated with correct neuronal polarisation, and the growth and orientation of, and transport along, axons. Tau dysfunction has been linked with a number of neurodegenerative diseases, which together constitute the majority of cases of dementia worldwide. The presence of NFTs in Alzheimer's disease has arguably been the primary motivation behind the majority of research conducted into tau since the late 1980s.

1.2 Alzheimer's disease

The recorded history of senile dementia extends as far back as the classical era. In the 7th century B.C. the ancient Greek physician Pythagoras said of old age, that "the system returns to the imbecility of the first epoch of the infancy" – a mental decline during old age was seen as unremarkable enough to be accounted for in Ancient

Greek law (Berchtold and Cotman, 1998). Much of the early contemplation of dementia centred around the view that it was an inevitable part of the aging process, even if not universal – according to the Roman philosopher Cicero of the 2nd century B.C., "madness or delirium is a characteristic, not of all old men, but only those who are weak in will". The modern medical view of aging-related disease is of course far less fatalistic, and owes much to the onset of study of mental disorders more generally during the 16th century, culminating in the first acceptance of mental disorders as diseases in the early 19th century. It was during the 1800s that post-mortem study of the brains of dementia patients began, revealing the physical changes underlying the loss of mental faculties. It was through such post-mortem examination, using novel histochemical techniques, that Alois Alzheimer first observed the joint characteristic pathologies of the disease which would come to bear his name. In a 1907 paper, Alzheimer described the case of a 51-year-old sufferer of early-onset senile dementia (Auguste Deter), in whose brain he had located two forms of neuropathological lesion (Alzheimer, 1907; Alzheimer et al., 1995). Of these, one was the "miliary focus" which was linked specifically to senile dementia by a competitor of Alzheimer, Oskar Fischer in a separate paper that same year (Fischer, 1907). These were also described as plaques, which are now known to be composed of β-amyloid, or Aβ (Masters et al., 1985). Alzheimer also described a novel characteristic of his case, using the Bielschowsky silver stain: intracellular tangles of neurofibrils, which were capable of surviving the death of the cell in which they had formed. The extent of these lesions, affecting 25% of ganglion cells in this patient "particularly in the upper cell layers" (Alzheimer et al., 1995), and the young age of disease onset were considered distinctive enough to constitute a novel disease, separate from the standard definition of senile dementia. It was described as "Alzheimer's disease" by the revered psychiatrist Emil Kraepelin in 1910, and qualified as a form of pre-senile dementia only, despite the presence of each type of lesion having already been recorded in cases of senile dementia (Berchtold and Cotman, 1998). This distinction came to be widely believed to be an artificial one (Katzman, 1976), with AD and senile dementia eventually being classified together as "senile dementia of the Alzheimer's type" (SDAT), or more commonly simply as Alzheimer's disease.

1.2.1 Symptoms and progression of the disease

Alzheimer's disease is a progressive neurodegenerative condition, characterised by multiple cognitive deficits, initially of memory but in advanced cases of language, reasoning, attention and problem solving skills (Thies and Bleiler, 2011). Memory deficits are the best early indicator of AD, with individuals experiencing difficulties in performing well-known tasks, speaking, writing or orientation. That AD sufferers exhibit reduced levels of acetylcholine (ACh) has long been known, associated with a loss of cholinergic neurons (Davies and Maloney, 1976) and nicotinic receptors, as well as of the neurotransmitter itself, in the cerebral cortex (Quirion et al., 1986; Whitehouse et al., 1986). This preferential loss of cholinergic neurons implies a role for nicotinic ACh receptors (nAChR) in AD pathology. It has been suggested that Aβ functions via direct interaction with α7 nAChRs, leading to activation of the MAPK (microtubule-associated protein kinase) signalling pathway and leading to cell death, possibly involving tau hyperphosphorylation (Buckingham et al., 2009). This process helps to explain the early symptoms of the disease, with primarily hippocampal or para-hippocampal localisation of NFTs, but late-stage AD brains exhibit far wider neurotoxicity, with diffuse cerebral atrophy; the acceleration in brain atrophy in AD sufferers has been shown to be as high as 40 fold greater than control subjects (Fox et al., 1996).

The relentless spread of NFTs over the course of the disease adds a great deal of weight to the idea that tau dysfunction is central to AD. At the same time, it has also been the source of some uncertainty regarding the mechanism by which these intracellular aggregates are spread throughout the cortex in a predictable fashion, apparently radiating from the locus coeruleus and trans-entorhinal region. Evidence has accumulated suggesting "prion-like" propagation of misfolded proteins in AD (Clavaguera et al., 2013b; Frost and Diamond, 2010; Nussbaum et al., 2012), by which pathogenic conformations of both tau and Aβ are capable of acting as templates, initiating toxic transformations of native, healthy proteins. In the case of tau, brain lysates from established mouse models of tauopathy (containing mutated, tangle-forming tau) were found to induce NFT formation in healthy mice following injection (Clavaguera et al., 2009). This catalysis of aggregate formation spread from the site of injection to other brain regions. A similar ability to induce native protein misfolding in mice has also been found in brain homogenates from a variety of

tauopathies (Clavaguera et al., 2013a). As for Aβ, small oligomers of truncated, polyglutamylated Aβ were found to be able to seed oligomerisation in Aβ oligomers through multiple serial dilutions (Nussbaum et al., 2012). An extracellular step in tau transmission, by which toxic tau oligomers are released from affected neurons to be absorbed by neighbouring healthy cells, has also been identified in cultured cells (Frost et al., 2009). Specifically, low molecular weight oligomers, a transitional step as monomers form fibrillar aggregates, were found to be internalised quite avidly by cultured neurons, both axonally and at the soma, via bulk endocytosis (Wu et al., 2013a). The propagation of tau throughout the brain appears thus to have been explained as a system of template misfolding highly comparable to prionopathies.

This progression of the disease, from the hippocampus and trans-entorhinal region into the wider cortical areas, also explains the breadth of psychiatric and behavioural symptoms of late-stage AD. These include depression, aggression, confusion and paranoia, as well as aimless movement, wandering and disruption of diurnal rhythms (Hope et al., 1999). Loss of awareness and confusion combine with deficiencies in communication and normal eating patterns (hypophagia) to increase susceptibility to many secondary conditions, particularly aspiration pneumonia (Kalia, 2003). The exceptional social cost of dementia is also directly attributable to this loss of autonomy and protracted disease course (Thies and Bleiler, 2011).

Effective treatment for AD is not yet available, despite a number of promising breakthroughs and trials. Symptomatic treatments include acetylcholinesterase inhibitors to delay memory loss, particularly Donepezil (Birks and Harvey, 2006), and Memantine, the NMDA receptor antagonist, potentially through reduction of excitotoxic cell death (Areosa Sastre et al., 2004). Given this lack of a cure, much attention has been paid to the risk factors associated with AD.

1.2.2 Alzheimer's disease aetiology

The prevalence of AD in the modern aging population has provided ample motivation for the epidemiological study of the disease. Whereas inroads have been made into mitigating the burden of many other aging-related diseases including many forms of cancer (Jemal et al., 2008), dementia is still considered a public

health “time bomb” (de la Torre, 2013). Although dementia is clearly primarily associated with aging, there are an ever-growing number of additional AD-associated risk factors. Familial Alzheimer’s disease (FAD) describes early-onset AD associated with mutations to the genes for amyloid precursor protein (APP) or the presenilins (Bertram and Tanzi, 2008), but which accounts for less than 4% of cases (Harvey et al., 2003). Late-onset AD has an ever-growing number of associated genetic risk factors, most importantly mutations to apolipoprotein E (ApoE), and twin studies suggest around 60% heritability, making genetics the single most important risk factor for the condition (Bergem et al., 1997). However, that does still leave many cases unaccounted for.

Vascular complications are the principle emerging risk factor of AD, particularly among carriers of the ApoE ε4 allele (Bangen et al., 2013). Midlife exposure to a wide variety of vascular issues, up to and including infarction, increases the probability of cognitive decline and dementia in later life (Kivipelto et al., 2006). That diabetic drugs are also considered a vascular risk factor, and that both diabetes and most circulatory disorders are strongly associated with obesity also raises the likelihood of metabolic stress being relevant to AD, which has even been described by some as “Type 3 diabetes” – a brain-specific form of the metabolic disease (de la Monte and Wands, 2008).

The majority of AD sufferers are female, in some part due to the longer life expectancy of women in the developed world. This is likely not the only cause however – like osteoporosis, it would seem that AD is also associated with decreasing oestrogen levels during menopause, with some protection provided by hormone supplementation (Janicki and Schupf, 2010; Paganini-Hill and Henderson, 1994).

As an aging-associated disease, eliminating many of the risk factors of AD depends on the maintenance of a healthy, moderately active lifestyle (Eggermont et al., 2006); aging well is likely the best protection against environmental factors, but is by no means capable of eliminating the risk completely (Pope et al., 2003). Any chance of curing or preventing AD will likely depend on a superior understanding of the underlying biology of the disease. The brain pathology of sufferers of AD has given research a good place to start.

1.2.3 The protein aggregates of AD

The Alzheimer's brain displays physical characteristics of both cerebral amyloidosis and tauopathy. The presence of two protein aggregates in the disease begs the question of which protein, if either, is primarily responsible for the condition. Increasingly, however, research suggests that it is an interaction between the two which is necessary for the disease, and which defines the condition as separate from the normal aging process.

Amyloid plaques are composed of Aβ, fragments of the highly-conserved APP produced following cleavage by γ-secretase in the amyloidogenic pathway, as detailed in Figure 1.3 (Tharp and Sarkar, 2013). Cleavage of APP can occur at several locations, with the most disease-relevant being at residue 40 ($A\beta_{40}$) or residue 42 ($A\beta_{42}$). The longer form of Aβ is more associated with aggregation; the additional C-terminal peptides have been shown to be critical for nucleation of amyloid peptides, with $A\beta_{42}$ capable of seeding the otherwise soluble $A\beta_{40}$ and leading to aggregation (Jarrett et al., 1993). Formation of the rarer $A\beta_{42}$ has been shown to occur at a distinct intracellular location in neurons, within the endoplasmic reticulum (ER), as opposed to $A\beta_{40}$, generated within the trans-Golgi network (Hartmann et al., 1997). This is consistent with the association of the ER-located presenilins with $A\beta_{42}$ production and familial AD; indeed all well-characterised mutations associated with familial AD occur within genes implicated in Aβ processing. The exact role of Aβ is still unclear, although it appears to be multi-functional, including neuro-protective and cell signalling roles (Lahiri and Maloney, 2010). It has also been implicated in the activation of the tyrosine kinase TrkA pathway, potentially inducing tau phosphorylation (Bulbarelli et al., 2009). The genetic links between APP and familial AD formed the basis of the amyloid cascade hypothesis, which theorised that all AD was dependent on Aβ aggregation, induced by an increase in the $A\beta_{42}$: $A\beta_{40}$ ratio, and which subsequently led to the development of other AD features, i.e. tau pathology. The principle argument in opposition to this hypothesis was based on the much closer association between NFT load and disease progression, compared with the less predictable deposition of plaques.

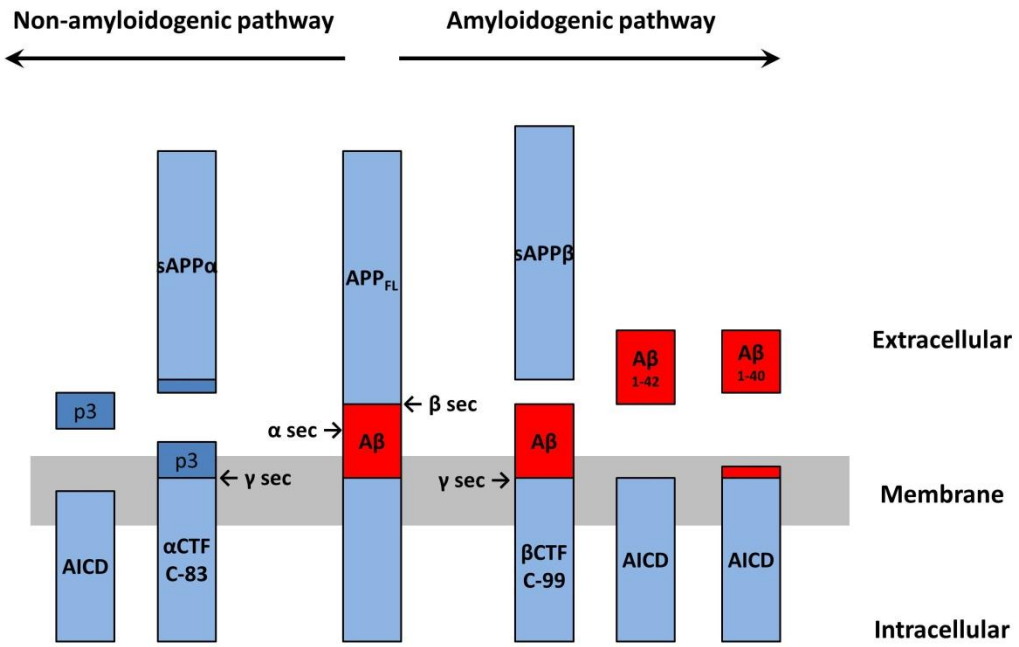

Figure 1.3 Processing the amyloid precursor protein (APP)
Full length APP (APP_{FL}) exists as a trans-membrane protein with an extended ectodomain. In the majority of cell types APP processing follows the non-amyloidogenic pathway in which cleavage by α-secretase generates soluble extracellular APP (sAPPα) and the intracellular, 83AA C-terminal fragment (αCTF or C-83). Further cleavage by γ-secretase releases the C-terminal fragment of Aβ, p3. In neuronal cells, APP more commonly undergoes amyloidogenic cleavage via β-secretase, releasing the smaller soluble APP fragment sAPPβ. This leaves Aβ intact as part of the 99AA βCTF, which can be released via cleavage by γ-secretase at a number of sites; particularly disease relevant is at A42 to release $Aβ_{1-42}$, the normally rare, more aggregation-prone species (Evin et al., 2003; O'Brien and Wong, 2011). In both cases, the APP intracellular domain (AICD) is left membrane-bound.

The progression of hyperphosphorylated tau aggregates from the trans-entorhinal layer, through the hippocampus and into the limbic system and cortex correlates strongly with cognitive symptoms, and only poorly with amyloid deposition (Braak and Braak, 1991), which led to the Braak scale of classification of the disease based on tangle deposition. The ability of amyloid mutation to cause the disease, compared with the apparent necessity of tau pathology for disease progress caused a division of research interest into two camps, dubbed "BAPtist" (for β-amyloid protein) and "Tauist" (Mudher and Lovestone, 2002). Perhaps inevitably, the two ideas have found increasing reasons for a rapprochement as more links between their disease processes have been identified.

Double-transgenic mouse models have shown a relationship between tau and amyloid. By crossing mice overexpressing mutant APP with a separate line overexpressing mutant P301L tau, the presence of mutant APP was shown to enhance both NFT load and distribution, leading to increased toxicity (Lewis et al., 2001). Amyloid deposition has also been shown to be enhanced in similar experiments (Ribé et al., 2005). In the absence of mutant tau overexpression, the spread of NFTs in APP mutant mice is greatly delayed, by around 2.5 months compared with deposition of plaques (Samura et al., 2006), suggesting a compound effect of these two disease processes. That Aβ-induced toxicity is mediated by tau phosphorylation was shown more recently, when tau knockout mice were found to be resistant to memory impairment caused by exposure to $A\beta_{42}$ (Shipton et al., 2011). Inhibition of the tau kinase glycogen synthase kinase 3 (GSK-3) was also found to block the amyloid-induced impairment, reinforcing the idea that the TrkA pathway could be an essential aspect of Aβ-induced toxicity – TrkA is thought to be capable of activating the Akt pathway, of which GSK-3 is a downstream target (Bulbarelli et al., 2009). There is additional evidence that tau dysfunction exacerbates Aβ-induced toxicity. A dendritic function for tau has been established, in the targeting of the Src kinase Fyn to the postsynapse (Ittner et al., 2010). Truncated tau, consisting of only the projection domain of tau, could still interact with Fyn but remained in the soma, reducing Fyn levels in dendrites and phosphorylation and stabilisation of NMDA receptors. It has been hypothesised that tau relocation to dendrites is caused by hyperphosphorylation, leads to higher Fyn levels and more active NMDA receptors, and induces excitotoxicity – tau knockout mice were protected against excitotoxic

seizures. Aβ toxicity is believed to be mediated by interaction with and overstimulation of NMDA receptors on dendritic spines; tau hyperphosphorylation could therefore sensitise neurons to Aβ toxicity (Haass and Mandelkow, 2010). Finally, interactions between tau and Aβ also help to explain the nature of cell death in AD. Aberrant cell cycle re-entry by post-mitotic neurons is the cause of much AD-related cell death (Lee et al., 2009). This process was shown to be induced by exposure of cultured neurons to Aβ, but was prevented by loss of tau or blocking tau phosphorylation at Y18, S409 or S416 (Seward et al., 2013).

That both amyloid plaques and NFTs are associated with neurodegenerative disease separately, but are concomitant in the most common neurodegenerative disorder is an intriguing aspect of this disease. The association of tau phosphorylation with Aβ-induced toxicity further underlines the need to better understand tau phosphorylation in AD, as well as the other tauopathies.

1.3 Tau is implicated in a variety of other diseases

If tau is likely a co-conspirator in the most prevalent form of dementia, there are a number of other tauopathies in which the MAP appears as prime instigator. For as long as none of the genetic evidence for AD implicated *MAPT* as a cause of the disease, and more mutations in elements of the amyloid processing pathway were being found, many believed tau dysfunction to be purely a by-product of other amyloid-dependent disease processes. The isolation of *MAPT* mutation as the cause of the autosomal dominant condition FTDP-17 (frontotemporal dementia and Parkinsonism linked to chromosome 17) provided clear evidence of the ability of mutant tau protein to cause neurodegenerative disease (Hutton et al., 1998). This also had profound implications for the wide range of other tauopathies, such as Pick's disease, progressive supranuclear palsy (PSP), senile dementia of the NFT type (SD-NFT), corticobasal degeneration (CBD) and chronic traumatic encephalopathy (CTE). That these NFT-presenting diseases can be associated with genetics, aging or trauma implies multiple possible pathways leading to tauopathy.

1.3.1 Hereditary tauopathy

The hereditary tauopathy FTDP-17 is a neurodegenerative disease of relatively early onset, with carriers often affected during their 40s or 50s (Wszolek et al., 2006a). It is an extremely rare condition, and relatively polymorphic, with the 100 affected family groups presenting over 35 different tau mutations. Some other symptomatically identical cases present with no tau mutation or NFT build up at all. The tau mutations can be divided into two groups, coding mutants and splicing mutants, with about equal numbers of each group identified. Among the coding mutations, none affect serine, threonine or tyrosine phosphorylation sites and all are located within exons 1, 9, 10, 11, 12 and 13 (see Table 1.1). Those mutations studied have been shown to reduce the microtubule-binding affinity of tau and in many cases to increase the propensity of tau for aggregation – both increasing the pool of unbound tau, and the number of filamentous tau aggregates. The splicing mutations are all within exon 10, or intronic and close to the 5' splicing site of exon 10. These mutations have all been shown to alter the usual 1:1 ratio of 3R and 4R tau isoforms, in most cases increasing the amount of 4R tau (Rodriguez-Martin et al., 2009), although three mutants have been shown to favour 3R tau splicing, one of which has been found in both FTDP-17 sufferers and unaffected individuals (Wszolek et al., 2006a). For an extended summary of these mutations, see Wszolek et al. (2005).

Clinical diagnosis of FTDP-17 is based upon patients presenting with at least two of three characteristic signs, namely behavioural changes (including aggression and loss of inhibition), cognitive deficits (dementia, with later memory loss) and motor disturbance (Parkinsonism). As with the classification of FTDP-17 mutations, there are two broad symptomatic groups, depending on whether the patient presents with more severe dementia or parkinsonism; parkinsonism is potentially associated with relative increases in 4R tau levels (Reed et al., 2001). The discovery of several disease-causing tau mutations has provided research insights into the mechanisms of tau dysfunction, and also one of the most predominant animal models for tauopathy. The P301L tau mutation, common in Western FTDP-17 sufferers (Dumanchin et al., 1998), is contained within the second R domain specific to 4R isoforms, and has been shown to cause tauopathy in a murine model (Lewis et al., 2000). This model was found to develop NFTs of hyperphosphorylated tau and motor impairment; it was this model which was shown to interact with mutant APP (Lewis et al., 2001).

Mutation	Localisation	Type	3R:4R ratio
R5H	E1	Missense	=
R5L	E1	Missense	=
K257T	E9	Missense	=
I260V	E9	Missense	=
L266V	E9	Missense	=
G272V	E9	Missense	=
E9+33	I9	Splicing	N/A
N279K	E10	Missense	>
ΔK280	E10	Deletion	<
L284L	E10	Silent	>
N296H	E10	Missense	>
N296N	E10	Silent	>
ΔN296	E10	Deletion	=
P301L	E10	Missense	=
P301P	E10	Silent	=
P301S	E10	Missense	=
G303V	E10	Missense	>
S305N	E10	Missense	>
S305S	E10	Silent	>
E10+3	I10	Splicing	>
E10+11	I10	Splicing	>
E10+12	I10	Splicing	>
E10+13	I10	Splicing	>
E10+14	I10	Splicing	>
E10+16	I10	Splicing	>
E10+19	I10	Splicing	<
E10+29	I10	Splicing	<
L315R	E11	Missense	=
K317M	E11	Missense	=
S320F	E11	Missense	=
G335V	E12	Missense	N/A
Q336R	E12	Missense	=
V337M	E12	Missense	=
E342V	E12	Missense	=
S352L	E12	Missense	=
K369I	E12	Missense	=
G389R	E13	Missense	=
R406W	E13	Missense	=
T427M	E13	Missense	=

Table 1.1 Tau mutations associated with FTDP-17

FTDP-17-associated tau mutations are listed, alongside location, type and effect on 3R:4R ratio, adapted from Wszolek et al. (2005). There are two broad types of FTDP-17 mutations: those which do not alter the 3R:4R tau balance reduce the ability of tau to bind microtubules (Wszolek et al., 2006b). Mutations with no published data regarding effects on isoform ratios are listed as N/A.

The doxycycline-repressible rTg4510 line is now widely used in research (Ramsden et al., 2005). Interestingly, the P301L mutation has arisen in multiple, unrelated groups of FTDP-17 sufferers with apparently distinct origins and major symptoms (Kobayashi et al., 2002), perhaps indicating a polygenic influence on the disease.

The discovery and study of FTDP-17 in many ways rejuvenated interest in tau in the context of neurodegeneration, though it is a very rare condition which, like all forms of dementia, is often symptomatically indistinct from a number of other diseases. The two groups of FTDP-17 mutation provide evidence for numerous theories of tau toxicity, based around microtubule dissociation, hyperphosphorylation and aggregation, without clearly privileging any individual process. That change in tau isoform ratios can lead to toxicity, and potentially Parkinsonism more specifically, should be of interest to all researchers using animal models for tau which often express single isoforms of tau.

1.3.2 Aging-related tauopathy

Though AD is characterised by the presence of two types of insoluble protein aggregates, variant forms of senile dementia have been identified which privilege one or other lesion in particular. So-called plaque-only Alzheimer's disease was found in a significant minority of sufferers of senile dementia aged over 74 (Terry et al., 1987), and is classified by the total or near-total lack of tangles, though often these are replaced by Lewy bodies, Parkinson's disease-associated aggregates of α-synuclein (Hansen et al., 1993).Similarly, a subset of very elderly senile dementia patients have been found to lack amyloid plaques. Tangle-predominant dementia, or SD-NFT is an extremely rare subtype of senile dementia with an average age of onset of around 80 years, 6 years older than that of AD (Jellinger and Attems, 2007). Compared with plaque-only AD, SD-NFT (senile dementia of the NFT type) or tangle-only dementia (Yamada, 2003) is much less common, with early reports on incidence finding it to account for fewer than 2% of dementia cases (Bancher and Jellinger, 1994). Memory impairment is the predominant symptom of the disease, correlating with high levels of NFT in the hippocampus; other cognitive deficits are much less common (Yamada, 2003).

The genetics of SD-NFT, such as have been determined, further distinguish it from AD – there is no association of the condition with ApoE ε4, very prevalent in cases of sporadic AD. SD-NFT may also provide some insight into the genetics of tau dysfunction. *MAPT* is contained within an inversion polymorphism on chromosome 17 with two haplotypes, H1 and H2. The predominant H1 haplotype has been associated with increased α-synuclein levels in dementia with Lewy bodies (Colom-Cadena et al., 2013), multiple other tauopathies (Pittman et al., 2006) and Parkinson's disease (Skipper et al., 2004). SD-NFT has also been shown to be associated with H1 *MAPT*, as well as polymorphism in the 3' untranslated region (Santa-Maria et al., 2012). That tau protein accumulation can be responsible for dementia in an amyloid-independent, aging-associated manner is significant for the study of tau toxicity. Given that tau accumulation in certain areas of the brain, in particular the locus coeruleus and hippocampus, has been shown to be a normal part of aging even in relatively young persons (Shin et al., 1991), it is possible that some unknown genetic or environmental factors may contribute to a pathological marshalling of the large pool of tau already present in elderly neurons, a process which could be hastened by amyloidosis, pre-existing mutation or trauma.

1.3.3 Physical trauma and tauopathy

In addition to genetics and aging, evidence has accumulated for the potential of physical trauma and inflammation to lead to tauopathy and dementia. Formerly known as *dementia pugilistica* or punch-drunk syndrome, chronic traumatic encephalopathy (CTE) is an early-onset form of dementia most often occurring in full-contact sportspeople. Originally identified in former boxers (Corsellis et al., 1973), the at-risk group has since been expanded to any individuals experiencing repeated head injury, due to sport, profession, seizures or physical abuse (Gavett et al., 2011). This condition has received a recent increase in attention following its association with a number of high-profile suicides involving American sportsmen (Omalu et al., 2010). CTE is associated initially with increased aggression, followed by a wide range of cognitive deficits. Brains of CTE sufferers exhibit extensive atrophy, NFT deposition and (in some cases) amyloid plaques (McKee et al., 2009). That tau should accumulate in response to brain damage, leading to widespread

cortical atrophy, raises some questions. It has been posited that physical trauma leads to a dissociation of tau from microtubules, possibly due to increased kinase activity associated with calcium influx and excitotoxicity (McKee et al., 2013). One hypothesis which has arisen in an attempt to explain the spread of tau pathology throughout the brain in all tauopathies, and which seems especially relevant here (given the presumably localised nature of head trauma), is that tau is capable of spreading between neurons, potentially in a prion-like, misfolded state (Hall and Patuto, 2012). This idea has been bolstered by the discovery of the ability of cytokine release to increase tau phosphorylation and misfolding (Zilka et al., 2012).

The diversity in cause of tauopathies speaks to multiple disease processes being involved in the development of tau pathology. As a consequence, there are a number of theories surrounding the nature of tauopathy which attempt to unite tau dysfunction with neurodegenerative processes.

1.4 Theories of tau pathology

The suggestion that tau dysfunction can be the cause of neurodegenerative disease is now widely accepted. Nonetheless, the processes underlying tau-induced toxicity remain unclear. Debate has surrounded the importance of tau phosphorylation, the toxicity of soluble versus insoluble tau oligomers and the predominant mechanism of cell death in tauopathy. This section explores some of the most widely-held ideas behind tau toxicity.

1.4.1 Tau hyperphosphorylation

Tau phosphorylation has been implicated in tau toxicity for as long as the predominance of tau in NFT has been known. Concurrently with the identification of the *MAPT* gene (Neve et al., 1986), a novel epitope for an apparently unknown protein enriched in Alzheimer's brains was discovered (Wolozin et al., 1986). The antigen was named Alz-50, and the protein, which ran at 68kDa, A68. A68 was originally considered a potentially useful candidate biomarker for AD (Wolozin and Davies, 1987) but in the end was found to be much more significant. Originally

thought to be an additional component of NFTs alongside tau, A68 was eventually revealed as a highly phosphorylated form of tau, with a novel secondary structure but otherwise being identical (Brion et al., 1991; Carmel et al., 1996). This alternative, fixed secondary structure has been described as the "Alz-50 conformation", differing from the transitory "paperclip conformation" that healthy tau is expected to form in that the N-terminus interacts with the microtubule-binding region instead of the C-terminus. This is hypothesised to facilitate tau aggregation (Himmelstein et al., 2012). The association of tau phosphorylation and PHF formation is now integral, with multiple PHF-labelling phospho antibodies in common use, most notably AT8 which recognizes tau phosphorylated at both serine 202 and threonine 205 (Goedert et al., 1995). Tau hyperphosphorylation is now associated with a loss of microtubule affinity and an increase in aggregation, two processes believed to be fundamental in the development of tauopathy.

The extent of potential tau phosphorylation is huge, with 85 candidate phosphorylation sites (see Table 1.2), of which more than half have been found to be phosphorylated in AD (Martin et al., 2011). The majority of these AD-associated sites are located within the P-rich region or at the C-terminus; however, one of the apparently most significant sites is S262, contained within the KXGS motif of the first microtubule-binding domain. Unsurprisingly, this site has been found to alter microtubule binding mechanics (Biernat et al., 1993). It has also been shown to reduce aggregation (Schneider et al., 1999), and yet phosphorylation at this site has been shown to be fundamental for tau toxicity in an animal model (Iijima et al., 2010). The theory of tau hyperphosphorylation has been called into question by experiments attempting to simulate hyper- or hypophosphorylated tau by introduction of multiple phospho-mimetic or non-phosphorylatable tau mutations, creating E14 (containing 14 glutamate mutations) and S11A (containing 11 serine to alanine mutations) mutants, respectively. In separate experiments, S11A tau was found to increase tau toxicity, and E14 tau to alleviate it, leading some to wonder whether the hyperphosphorylated nature of tau in NFTs was merely a byproduct of the disease process (Chatterjee et al., 2009; Wu et al., 2013b). Either the idea that tau hyperphosphorylation leads to toxicity is wrong, or it is incomplete. It is possible

Sites only phosphorylated in AD brain	Sites phosphorylated in AD and control brains	Sites only phosphorylated in non-AD brain	Putative sites without evidence for phosphorylation
Y18	S46	T17	T30
S68	T181	Y29	S61
T69	S198	T39	T63
T71	S199	T50	S64
S113	S202	T52	T76
T123	T205	S56	S129
T153	T212	T95	S137
T175	T217	T101	Y310
T184	T231	T102	T319
S185	S235	T111	T377
S191	S396	S131	
Y197	S400	T135	
S208	S404	T149	
S210	S412	T169	
S214	S413	S195	
S237	S416	T220	
S238		S241	
S258		T245	
S262		T263	
S289		S285	
S356		S293	
Y394		S305	
T403		S316	
S409		S320	
S422		S324	
T427		S341	
S433		S352	
S435		T361	
		T373	
		T386	
		T414	

Table 1.2 A summary of the phosphorylation sites on human 2N4R tau
Of the 85 known or putative sites of phosphorylation on the largest human brain tau isoform, 44 have been found to be phosphorylated in AD brains; 16 of these are also known to undergo phosphorylation in the healthy brain. 31 sites are known to be phosphorylated only in healthy brain. Evidence of phosphorylation at the final 10 sites has not been found (Martin et al., 2013). Yellow: sites contained within the N-terminal inserts of exons 2 and 3. Blue: sites contained within the P-rich region of exons 7 and 9. Red: sites contained within the microtubule-binding region (exons 9, 10, 11 and 12). The majority of additional phosphorylation in disease occurs within the P-rich region; it would appear that there is a reduction in phosphorylation at many of the sites of the microtubule-binding domain in AD brain.

that the creation of such extensively mutated tau was jumping the gun to an extent, based on insufficient knowledge of tau phosphorylation dynamics. Smaller-scale phospho-mutation experiments point to greater complexity, and a possible link between phospho-residue location and role. *In vitro* experiments investigating the microtubule-binding dynamics of tau identify different key residues compared with experiments into tau aggregation dynamics (Chang et al., 2011; Kiris et al., 2011; Necula and Kuret, 2004); in each case however, changes in the phosphorylation state of tau are highly relevant. The cumulative effects of such mutations also appear to be unpredictable, both on microtubule dynamics and toxicity (Alonso et al., 2010; Kiris et al., 2011), perhaps explaining the surprising results of the highly-mutated forms of tau. This particular theory clearly requires further investigation.

1.4.2 Cytoskeletal disruption in tauopathy

A great deal of research into tau neglects to consider the normal, healthy physiological role of tau as a modulator of the microtubule cytoskeleton. In the case of animal models making use of human tau overexpression, this is justifiable, especially given the apparent at least partial dispensability of the protein in mice and the fly (Dawson et al., 2001; Doerflinger et al., 2003). However, the fact remains that cytoskeletal disruption is a feature of AD-affected neurons (Cash et al., 2003). That hyperphosphorylated tau should lose its ability to bind microtubules has long been established *in vitro* (Grundke-Iqbal et al., 1986); this has also been demonstrated in cells (Lovestone et al., 1996). More recently, *Drosophila melanogaster* has been used to effectively demonstrate cytoskeletal disruption *in vivo*. Overexpression of human 0N3R tau in *Drosophila* was shown to lead to a phosphorylation-dependent loss of microtubule stability, with a decidedly sparse microtubule cytoskeleton in transverse sections of larval neurons (Cowan et al., 2010). That this should be caused by overexpression of transgenic tau was explained by the demonstration of resultant impaired microtubule binding by native *Drosophila* tau. Conflicting evidence, indicating a complete lack of effect of human tau on native tau binding in the fly, and zero affinity of human tau for *Drosophila* microtubules, does exist (Feuillette et al., 2010). However, a subsequent demonstration of the link between microtubule disruption and neuronal toxicity as measured by locomotor disruption by Quraishe

and colleagues (2013) is very compelling evidence for the importance of axonal transport in this model. The microtubule-stabilising agent davunetide was shown to rescue the locomotor phenotype caused by expression of human 0N3R tau in fly larvae, without any effect on tau phosphorylation or the sequestration of native tau by the transgenic. The drug was shown to stabilise microtubules in presence of both 0N3R and 0N4R tau.

It would appear that in transgenic animal models hyperphosphorylated human tau exhibits a gain of toxic function, by which it sequesters native tau and disrupts the microtubule cytoskeleton. The hurdle for this hypothesis as it has been established in the fly is the apparent irrelevance of *Drosophila* tau to human tau toxicity in the fly eye – removal of native tau has no effect on the phenotype created by overexpression of human tau (Feuillette et al., 2010). It is still possible that hyperphosphorylated tau is affecting axonal transport in this model, by binding other MAPs or perhaps some entirely separate mechanism of microtubule destabilisation. Alternatively, tissue-specific differences in the nature of tau toxicity are possible. Regardless, such a gain of function has important implications for the role of tau aggregates in the toxic process.

1.4.3 The role of aggregation in tau toxicity

For most of the history of research into AD, the neurotoxic agents of the disease were assumed to be the accumulated, aggregated amyloid plaques and/or NFTs. In the case of NFTs in particular, their presence correlates well with disease progression, as does the total plaque burden. More recently however, this assumption has been challenged from multiple sides, with arguments that toxicity due to insoluble, large aggregates is less likely than from soluble rogue protein. In the case of Aβ, an early plaque-directed vaccine, abandoned due to excessive inflammation (Birmingham and Frantz, 2002), was later shown to have caused an increase in soluble Aβ. This was likely from disrupted plaques and potentially a cause of the encountered toxic side-effects (Lee et al., 2006; Patton et al., 2006). Neuronal impairment in animal models has been found to pre-date the appearance of plaques (Lesne et al., 2006), and to be entirely independent of tangle formation (Wittmann et al., 2001). The idea that insoluble aggregates may be less relevant to

neurodegenerative disease, or even potentially have a protective function, has thus gained traction (Cowan and Mudher, 2013; Spires-Jones et al., 2011). This does of course have profound implications for any putative amyloid or tau-focused treatment strategies, emphasising all the more the importance of early diagnosis and intervention. In the case of tau specifically, the conventional wisdom regarding the toxicity of NFTs has come under growing scrutiny. A large body of evidence now exists to support the idea that NFTs are evidence of a pathological process, rather than the cause of one.

The rationale which places NFTs at the centre of tauopathy is easily understood: NFTs are present at the scene of the crime, and their distribution correlates strongly with disease progression. In the murine P301L tau model, regarded as the animal model which most closely mimics human disease, NFTs form alongside the onset of cell death and motor dysfunction (Gotz et al., 2001). The difficulty here though is that, in all cases in which fibrillar tau aggregates are measured, smaller intermediate tau oligomers will always be present and therefore cannot be ruled out as the source of toxicity; it is therefore likely too simplistic to discuss tau aggregation only in terms of monomeric tau and NFTs. Tau aggregation has been shown to lead to a large number of species of tau, of varying sizes, some of which may be intermediate forms of larger aggregates. As well as the dimers and PHFs mentioned earlier, a variety of small or large, soluble or insoluble, granular or filamentous oligomers have been discovered. Some of these are specific to certain tauopathies; others have been identified in animal models. For a more in-depth discussion of the variety of tau oligomers, see Cowan and Mudher (2013). In general, soluble tau oligomers are more often associated with toxicity than any insoluble oligomers in animal models in which they are sought, and in all cases smaller oligomers are more capable of leading to toxicity, or indeed cell-to-cell transmission of tau pathology as described earlier (Wu et al., 2013a). As an example of the way in which these ideas have changed, expression of the tau repeat domain (Tau_{RD}) with a pro-aggregant FTDP-17 tau mutation (ΔK280) was found to be rendered less toxic by the addition of anti-aggregant proline mutations, which also prevented the rapid tangle formation witnessed in the pro-aggregant construct (Mocanu et al., 2008). Subsequently, this model was found to recover cognitive deficits once Tau_{RD} expression had been turned off, despite persistence of pre-formed aggregates (Sydow et al., 2011):

expression of pro-aggregant tau was the determining factor of toxicity, rather than the presence of large fibrillar aggregates themselves. It is likely that some smaller intermediate tau oligomer was the source of neurodegeneration. This is also not the only example of tau toxicity being rescued without removal of tangles (Santacruz et al., 2005), and in the fly aggregation can be promoted by suppression of tau toxicity (Cowan and Mudher, 2013). These data speak to the gain-of-function hypothesis discussed in the previous section, as smaller or more soluble species are more likely to interact with and disrupt other cellular processes, potentially by sequestering functional tau species. They have also led to a controversial hypothesis regarding the role of NFTs, that they may in fact form as part of a protective response which attempts to reduce soluble protein levels following tau dysfunction, one which is doomed to fail as tau accumulation eventually causes a breakdown in transport and protein degradation (Spires-Jones et al., 2011). Given the apparent increased toxicity of certain tau oligomers, the alternative answer is that NFTs and insoluble aggregates are effectively toxicity neutral, and form as a by-product of toxic aggregation processes.

One factor that unites most theories on the process by which tau leads to toxicity is phosphorylation. This is true when studying the biochemical mechanics of tau aggregation (Iqbal et al., 2013) or microtubule binding (Fischer et al., 2009), just as it is in post-mortem examination of brains of tauopathy sufferers. This has led to multiple attempts to characterise the causes of changes to the phosphorylation balance of tau, the majority of which have focused on tau kinases. In the next section, the importance of tau kinases in toxicity is considered, with particular attention paid to GSK-3β and the AMPK-related kinases.

1.5 Tau kinases and disease

Developmental studies in rats have demonstrated the normal progression of tau phosphorylation levels, which is much higher in developing brain in these animals and coincident with increases in activity in a large number of tau kinases (Yu et al., 2009). This recalls the early demonstration of the hyperphosphorylated status of human foetal tau (Goedert et al., 1993). Is it possible that the increase in tau

phosphorylation in the brains of sufferers of tauopathy is due to similar regulation of kinase activity? No genetic evidence has been found as yet, but a number of tau kinases are known to be enriched or over-activated in the AD brain, and to co-localise with tangles (Jin and Saitoh, 1995; Martin et al., 2013). Given the emerging likelihood of site-specific differences between phospho-residues, the target sites of some of these kinases have been examined, though usually *in vitro* (Liu et al., 2007; Yoshida and Goedert, 2011). In this section some of the major tau kinases are discussed in more detail.

1.5.1 GSK-3β

GSK-3β is perhaps the most widely-studied of the tau kinases. Originally isolated in rabbit skeletal muscle as a Ca^{2+}-independent, highly specific kinase of glycogen synthase (Embi et al., 1980), GSK-3 was first associated with tau phosphorylation in 1992 as part of a search for possible proline-directed kinases of tau (Mandelkow et al., 1992). There are two GSK-3 genes in humans, encoding two isoforms, α and β (Woodgett, 1990). Both were thought to have similar target sites on tau (Mandelkow et al., 1992), but research began to privilege GSK-3β following the demonstration of its enrichment in the AD brain and co-localisation with NFTs (Leroy et al., 2002; Pei et al., 1999). Some differences in substrate preference between the two isoforms have also been recorded (Soutar et al., 2010). The ability of GSK-3β to cause functional changes in tau was demonstrated in cells, in which tau phosphorylated by GSK-3β was shown to lose its ability to bind and stabilise microtubules (Lovestone et al., 1996). Today, GSK-3β is widely held to be a key player in tau-induced toxicity, particularly in AD where it is a prime candidate for the link between amyloid and tau pathology (Hernández et al., 2010; Muyllaert et al., 2008); this has been proposed to occur via either insulin or wnt signalling, both pathways which regulate GSK-3β and with which Aβ is thought to interfere.

One useful characteristic of GSK-3β is its inhibition by lithium ions(Davies et al., 2000; Stambolic et al., 1996), known to function via activation of the GSK-3β-regulating wnt pathway; this was very rapidly used to identify GSK-3-induced tau phosphorylation in cultured neurons (Hong et al., 1997). The pre-eminence of GSK-3β as a controller of tau phosphorylation-induced toxicity has led to a good deal of

interest in the kinase as a therapeutic target (Noh et al., 2013), and is likely the most hopeful candidate for tau phosphorylation-focused AD treatment.

1.5.2 AMPK-related kinases

AMP-activated protein kinase (AMPK) is a key enzyme of energy homeostasis, originally identified as a regulator of lipid metabolism (Hardie et al., 1989). Named for its potent allosteric activation by adenosine monophosphate or AMP (Ferrer et al., 1985), it was later found to be a highly sensitive monitor of the cellular AMP:ATP (adenosine triphosphate) ratio. AMPK is a heterotrimer composed of a catalytic α subunit with kinase function, a regulatory γ subunit (sensitive to increases in the aforementioned AMP:ATP ratio) and a connective β subunit (Carling, 2004; Hardie et al., 2003). Two isoforms of the α activatory subunit have been identified, along with two β and three γ variants. AMPK was found to belong to a subfamily containing 12 other kinases with closely related protein kinase domains (Manning et al., 2002), of which all bar one were found to be regulated by the tumour suppressor liver kinase B1, or LKB1 (Lizcano et al., 2004). Expansion of this family later added one other LKB1-activated kinase, bringing the total number to 14 including both AMPKα isoforms (Alessi et al., 2006), Along with eight LKB1-independent members. Figure 1.4 illustrates the protein taxonomy of the kinase domain of this subfamily.

The first AMPK-related kinase to be identified as a tau kinase was the microtubule/MAP-affinity regulating kinase (MARK), which was shown to phosphorylate tau at S262 and S356 (Drewes et al., 1995; Jenkins and Johnson, 2000). MARK exhibits high specificity for the KXGS motifs of the microtubule-binding domains rather than proline-directed sites, and MARK4 in particular is more prevalent in the brain, where it colocalises with microtubules, particularly in neurites where microtubule dynamics are the most fluid (Drewes, 2004). It is thus highly likely that all four MARKs play a significant role in the healthy regulation of tau/microtubule binding (Gu et al., 2013), and indeed MARK2 has been shown in an *in vitro* model to upregulate neurite outgrowth in a tau-dependent manner (Biernat et al., 2002). The *Drosophila* homologue, PAR-1 also regulates microtubule stability, with PAR-1 mutants exhibiting reduced microtubule stability and defects in follicle

cell polarity (Doerflinger et al., 2003). Unlike in mammalian cells, this influence on microtubule dynamics was shown to be independent of the presence of *Drosophila* tau (dtau); despite being a substrate for PAR-1, dtau was shown to not be phosphorylated at KXGS motifs by the endogenous kinase, and loss of dtau in no way recapitulated the phenotype of PAR-1 mutants.

More recently, AMPK has itself been shown to phosphorylate tau. It was found to be another target of the kinase cascade elicited by Aβ exposure in cultured primary neurons, activated by Ca^{2+}/calmodulin-dependent protein kinase kinase β (CaMKKβ) and phosphorylating tau at KXGS motifs (Thornton et al., 2011). That AMPK is also activated by antidiabetic drugs, including metformin (Zhou et al., 2001) provides a link between treatment for diabetes and tau phosphorylation. This closely-related kinase subfamily is thus of great interest to the study of tau phosphorylation in disease, with increasing effort being made to characterise these enzymes (Yoshida and Goedert, 2011). Other candidate kinases from this family include the BRSKs (brain-selective kinases).

1.5.3 BRSK2 is a brain-specific tau kinase

Originally identified as part of a screen for regulators of synaptic development in *Caenorrhabditis elegans*, *sad-1* (synapses of the amphid defective-1) was implicated in the establishment of neuronal polarity by mislocation of synaptic vesicles in mutants and sequence homology with *par-1* (Crump et al., 2001*)*. SAD-1 was also shown to be primarily localised to synaptic regions of the axon. There are two mammalian homologs, SAD-A and SAD-B, also known respectively as BRSK2 and BRSK1 which is a nomenclature more in keeping with the AMPK-related subfamily. The two mammalian kinases were shown to be redundant, but essential – loss of either kinase individually had no effect, but loss of both was shown to be lethal (Kishi et al., 2005). BRSK double mutants died shortly after birth, and exhibited abnormal development of the central nervous system with a smaller forebrain and disruption of the organisation of cortical sublayers. Loss of neuronal polarity was also a hallmark – failure of axonal growth and targeting was widespread, dendrites were elongated and tau localisation to the axon had failed. BRSKs were shown to be tau kinases, likely controlling neuronal polarity via regulation of tau-microtubule

binding as S262 was shown to be a target site of BRSK2. Later investigation of BRSK activity showed BRSK2 to be more effective at regulating tau-microtubule binding than BRSK1, though still not as potently as MARK1 (Yoshida and Goedert, 2011); this could indicate a separate role for the BRSKs beside regulation of the microtubule cytoskeleton. The proline-directed site T212 was also revealed as a target phosphorylation site for the BRSKs. In common with many of the AMPK-related kinases, BRSK activation is known to require LKB1. Unlike AMPK, however, BRSKs are not phosphorylated by CaMKKβ (Bright et al., 2008); they are however targets for CaMKKα at T189, equivalent to the T172 activation site on AMPK (Fujimoto et al., 2008). Another upstream kinase of BRSK2 is the cyclic AMP-dependent protein kinase A (PKA), via an alternative target site on BRSK, T260 (Guo et al., 2006). The discrepancy between BRSK1 and BRSK2 in terms of tau phosphorylation potency found by Yoshida and Goedert (2011) could also potentially be explained by alternative methods of activation – for example, BRSK1 activity is boosted by association with lipid rafts, unlike BRSK2 (Rodríguez-Asiain et al., 2011). A dependency on the lipid environment could indicate some association of BRSK activity with energy metabolism, potentially in a similar manner to AMPK: BRSK2 has been shown to suppress insulin secretion by pancreatic β cells via PCTAIRE1, related to cyclin-dependent kinase (Chen et al., 2012). Yet another potential function of human BRSK is as a checkpoint kinase – UV-induced DNA damage has been shown to increase BRSK activity, leading to cell cycle arrest (Lu et al., 2004).

The importance of the BRSKs to correct tau-mediated neuronal polarisation, acting via tau phosphorylation as shown by Kishi et al. (2005), was the motivation behind the decision made by the Moffat and Frenguelli labs in 2008 to begin investigating the BRSKs as sources of pathogenic tau phosphorylation. Subsequently, additional evidence accumulated, improving the BRSKs' prospects as pathologically-relevant kinases. The identification of CaMKKα as an upstream kinase of the BRSKs provided a link to calcium metabolism. The BRSKs were even shown to be upregulated in cultured differentiated primary hippocampal neurons following

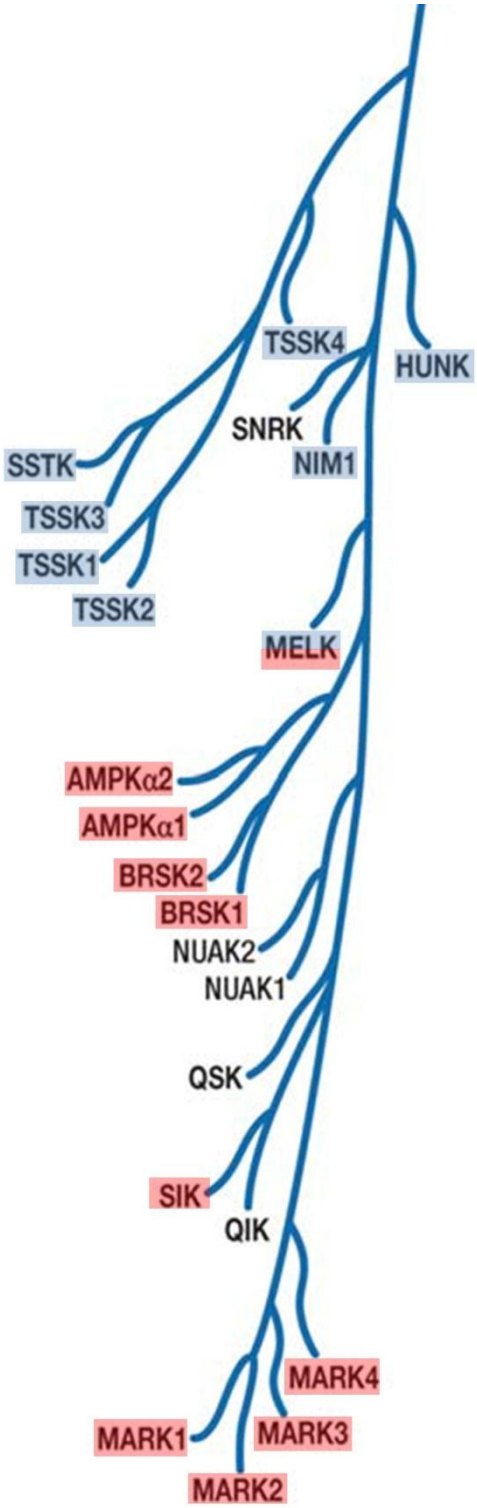

Figure 1.4 The AMPK-related protein kinase family
The phylogeny of AMPK-related protein kinases. Shaded in blue are kinases not activated by LKB1. Known tau kinases are shaded in red. Adapted from Alessi et al. (2006)

exposure to Aβ oligomers, alongside an increase in tau phosphorylation, Ca^{2+} levels and microtubule disruption (Zempel et al., 2010). The association of BRSK2 in particular with tau phosphorylation at two important sites (T212 and S262) by Yoshida and Goedert (2011) raised interesting questions regarding the consequences of BRSK-induced phosphorylation of tau, affecting as it does a proline-directed, aggregation-inducing site in the P-rich region as well as a KXGS motif associated with microtubule dissociation. In sum, BRSK2 is found in the right place to induce tau phosphorylation, its activity is induced by multiple processes associated with AD, and it targets sites on tau believed to be relevant to tau pathology, making it a promising candidate kinase as a cause of pathogenic tau phosphorylation.

1.6 Tau-directed therapies for Alzheimer's disease

The search for disease-modifying treatments for AD has led to a number of promising drug targets. Attempts to develop tau-centric disease therapies have seen increasingly promising results over recent years, in part due to an increase in understanding of the mechanisms of tau dysfunction and renewed interest in tau in the context of disease. Avenues of investigation include immunotherapy-based approaches, as have previously been examined for removal of Aβ. In addition, multiple novel targets have been suggested due to this MAP's supposed disease pathways. Microtubule stabilising agents to combat tau loss-of-function, tau aggregation inhibitors to prevent the assembly of toxic oligomers and modifiers of tau post-translational modification are all under investigation.

1.6.1 Immunotherapy approaches

Immunotherapy has long been considered as a means of Aβ clearance and potentially disease protection, owing to the extracellular localisation of amyloid plaques (Lemere and Masliah, 2010; Schenk et al., 1999). More recently, the emergence of the prion hypothesis of tau propagation has increased interest in anti-tau immunotherapies (Golde et al., 2013); the ability of tau to spread between cells strongly suggests an essential extracellular step in tauopathy progression (Frost et al.,

2009). In addition, the potential for neuronal uptake of antibodies (Mohamed et al., 2002) creates the possibility of some intracellular protection against tau toxicity. Given the ability of Aβ immunotherapy to reduce plaque burden whilst failing to reduce cognitive deficit, or NFT load (Holmes et al., 2008), perhaps tau-directed immunotherapy or even a dual Aβ/tau approach would better combat progression of AD.

An early investigation into the consequences of anti-tau immunisation showed its potential for neurotoxicity: C57BL/6 mice immunised to whole tau protein developed Alzheimer-like histopathological features, axonal damage and behavioural deficits (Rosenmann et al., 2006). This parity between the effects of tau auto-immunity and over-expression implied a role for an anti-tau inflammatory response in the progression of tauopathies, and did not augur well for anti-tau immunotherapy. It is however important to note that this experiment made use of whole recombinant human tau, and as a result did not exploit a major strength of antibody therapies for protein disorders: specificity for the toxic protein conformations (Boimel et al., 2010). Immunisation of mice expressing recombinant mutant P301L/S tau (FTDP-17 P301 mutations) with a number of phospho-tau peptides led to a reduction in tau aggregates with no negative consequences due to inflammation (Asuni et al., 2007; Boimel et al., 2010). The study reported by Asuni et al. (2007) also indicated some improvement in a number of behavioural tasks. Evidence has accumulated over the past five years for the ability of anti-phospho-tau antibodies to mitigate tau toxicity in animal models, including removal of tau aggregates and reversal of behavioural and memory deficits; see Gu and Sigurdsson (2011) for a review of many of these. A recent study has found a correlation between the ability of anti-tau antibodies to prevent seeding *in vitro* and their ability to decrease pathology *in vivo*, again in the P301S tau mouse model (Yanamandra et al., 2013). Three monoclonal tau antibodies were tested, using a bespoke biosensor system, for their ability to prevent seeding of tau repeat domain aggregation in cells exposed to brain lysates from 12-month-old P301S tau mice. The antibody most effective at preventing this seeding was also found to most effectively reduce phospho-tau levels, the seeding abilities of brain lysates of treated animals and associative learning deficits in P301S tau mice. This suggests that anti-tau immunotherapy could be highly effective at preventing transmission of toxic tau between cells, as is hypothesised by the prion-like model of

AD (Clavaguera et al., 2013b). This is unsurprising, given the largely extracellular location of these antibodies following treatment.

Unlike for Aβ, there have yet to be any human trials using anti-tau immunotherapies. Given the disappointing results of the amyloid-focused clinical trials, it is possible that similar tau-focused therapies may also encounter problems involving inflammation or a lack of symptomatic efficacy. It has been speculated that the nature of the trials themselves may have obscured the greatest potential use of AD immunotherapies: as preventative measures (Golde et al., 2011). Clinical trials are conducted using patients already presenting with the major symptoms of AD, at disease stages which may be too far progressed for immunotherapy to be of best use. This could also explain the apparent risk of meningoencephalitis in certain trials (Lemere and Masliah, 2010).

1.6.2 Tau aggregation inhibitors

The nature of tau dysfunction presents several other tau-specific therapeutic targets. Although there may be some dispute over exactly which form of tau aggregate is the most toxic, there is generally a degree of consensus regarding the potential of tau aggregation to be detrimental. Thus, various tau aggregation inhibitors (TAI) have been examined as potential therapeutic candidates. One very well characterised anti-aggregant drug is the phenothiazine methylene blue (MB), an extremely well-categorised drug originally identified as an anti-malarial medication (Wainwright and Amaral, 2005). The discovery that MB can also act as a potent TAI (Wischik et al., 1996) has led to the development of a number of MB-based compounds, taking advantage of its already established safety (Bulic et al., 2013). One MB derivative in particular, Rember, has already passed phase 2 clinical trials. Developed by TauRx, a company established by members of the lab which first discovered MB's TAI properties, Rember was found to significantly reduce the rate of cognitive decline in a trial of 321 patients with mild-to-moderate AD (Bulic et al., 2013).

Aggregation inhibitors have more often been investigated in the context of Aβ and plaque prevention. One notable example is that of tramiprosate, a soluble amyloid-binding glycosaminoglycan mimetic. This drug successfully cleared phase 2 clinical

trials before being cancelled following a lack of efficacy in phase 3. One hypothesis for this failure is particularly intriguing: it has been shown to increase the aggregation of tau (Santa-Maria et al., 2007). Perhaps here again, multidrug therapies could prove particularly effective. A great many Aβ-focused drugs are currently undergoing trials (Anand et al., 2014), aimed at a number of different targets. Aggregation inhibitors are something of a special case however: given the mechanistic overlaps between protein aggregation disorders these trials could also give rise to novel TAIs (Bulic et al., 2013). Indeed, the case of tramiprosate suggests they could well be an essential part of any successful future treatment.

1.6.3 Microtubule-stabilising agents

One obvious avenue of research is to ensure the maintenance of correct tau function in the face of disease by stabilising microtubules. The microtubule-stabilising agent paclitaxel (sold as Taxol) has already been used as a standard cell cycle-blocking treatment for some cancers, particularly breast cancer, where it has also demonstrated the negative consequences of excessive microtubule stabilisation in the form of peripheral neuropathies (Mielke et al., 2006). This is thought to be due to the increased density of microtubules, as well as to a loss of normal MT polarity as MTs are stabilised across their entirety (Baas and Ahmad, 2013). An alternative and rather counter-intuitive option more suited to neurons could be the use of low levels of microtubule destabilising agents, such as nocodazole. At very low levels, these drugs effectively promote microtubule stability by preventing excessive growth and, consequently, catastrophe. In short, if dosed correctly nocodazole can be used to create an equilibrium between rates of tubulin dimer loss and addition, constituting a less-invasive method of MT "kinetic stabilisation" (Baas and Ahmad, 2013).

A major issue with the use of paclitaxel is its low blood-brain barrier penetrance, hence the PNS side-effects. A related drug, epothilone D (EpoD) has been shown to cross the BBB effectively, and to accumulate in brain tissues (Andrieux et al., 2006; Brunden et al., 2010), potentially reducing the risk of PNS damage. EpoD has already been used to treat P301S tau mice, where it has been shown to rescue MT density (Brunden et al., 2010). EpoD was not found to be toxic at the very low concentrations (0.3 mg/kg) required for noticeable improvements to MT

stabilisation, axonal damage and cognitive function in aged mice (Zhang et al., 2012). EpoD was also capable of reducing tau pathology, with a reduction in hyperphosphorylated tau and insoluble tau staining recorded. The exact mechanism responsible for this is unclear, though it has been speculated that fast axonal transport may be improved by the use of paclitaxel and related compounds, a process which has previously been shown to be linked to tau phosphorylation levels (Zhang et al., 2012).

An alternative non-paclitaxel-related MT-stabilising agent, with high BBB permeability and low toxicity, is the octapeptide NAPVSIPQ (NAP), the smallest active element of activity-dependent neuroprotective protein (Gozes et al., 2004). Its mechanism of action was determined to be via interaction with the brain-specific βIII tubulin subunit; this was competitively inhibited by paclitaxel (Divinski et al., 2006). NAP has been shown to reduce tau and even amyloid pathology and to enhance cognitive function in rodent tauopathy models (Matsuoka et al., 2007; Shiryaev et al., 2009). A study in *Drosophila* demonstrated the ability of NAP to reduce the symptom of tauopathy via MT stabilising specifically, though found no reduction in levels of tau hyperphosphorylation (Quraishe et al., 2013). This arguably provides further evidence for the idea that alternative, slower-acting mechanisms were the cause of the reduction in tau pathology found in older mice when treated with EpoD, as detailed above.

The search for brain-specific microtubule-stabilising treatments for tauopathy has yet to progress to clinical trials, but this laboratory evidence is compelling. However, given the comparable early pre-clinical success of TAIs, it will likely still be some time before we know whether MT-focused treatments could be of use in AD.

1.6.4 Modifiers of tau phosphorylation

In each of these successful attempts to reduce tau toxicity in the long term, a reduction in levels of hyperphosphrylated tau was also recorded. Attempts to reduce tau hyperphosphorylation directly via modulation of tau kinases and phosphatases constitute the other major group of tau-targeted drug hopefuls.

As has previously been mentioned, GSK-3β is considered the tau kinase most likely

to play a role in pathogenic phosphorylation in AD, particularly due to its potential to link tau and Aβ dysfunction (Takashima et al., 1996). Thus far, the only tau kinase inhibitors to have been tested in clinical trials have all targeted this kinase, due to the relatively superior specificity of GSK-3β inhibitors compared with other putative target kinases such as CDK5 or MAPK (Yoshiyama et al., 2013). Lithium has been the subject of multiple trials; those conducted for AD failed to show any effect on GSK-3β activity or disease progression in the short term (Hampel et al., 2009). More positive results for the feasibility of lithium-based treatments came from a study focusing on at-risk individuals, specifically suffering from amnestic mild cognitive impairment, a condition believed "to represent the clinical transition between the cognitive changes found in normal aging and those of early Alzheimer disease" (Petersen et al., 2006). After a year's treatment, a significant decrease in hyperphosphorylated CSF tau was witnessed, alongside improvements in performance at AD-classifying cognitive tasks (Forlenza et al., 2011). This suggests, once again, that the greatest likelihood of combating AD is via prevention. Another, more specific GSK-3β inhibitor is NP12, or tideglusib. Administered to a double-transgenic APP/tau mouse, this compound was found to be capable of reducing phosphorylated tau levels, amyloid plaque deposition, cell death and cognitive decline (Serenó et al., 2009). Clinical trials investigating tideglusib have already begun (Yoshiyama et al., 2013).

The alternative route to reduced tau phosphorylation is by upregulation of phosphatases, particularly PP2A, known to be compromised in AD. PP2A accounts for the majority of phosphatase activity in the human brain (Liu et al., 2005); as a result, PP2A over-activation is likely to induce severe side effects and should be focused more on compensating for AD-specific lacunae in PP2A regulation. The NMDA blocker memantine has also been shown to lead to improved PP2A activity (Chohan et al., 2006), for example, perhaps explaining the reduction in tau phosphorylation following a year's treatment (Degerman Gunnarsson et al., 2007).

In sum, our current understanding of tau pathology has provided a number of promising targets for tau-focused therapies for AD and other tauopathies. A consistent theme of the pre-clinical data is the correlation between tau phosphorylation and pathology, reinforcing the need for better understanding of the means by which phosphorylation might determine toxicity.

1.7 *Drosophila melanogaster* and tau research

A great deal of biochemical exploration of the regulation and function of tau has been performed *in vitro*, particularly examination of phospho-mutant tau species. In order to determine whether the recorded effects of tau phosphorylation sites, on microtubule binding or aggregation for example, are relevant to any disease process *in vivo* study in animal models is required. An ideal model for early *in vivo* experimentation is the fruit fly, *Drosophila melanogaster*. The use of *Drosophila* as a model for neuroscience has become more and more commonplace over the past 15 years. There is a perhaps surprising level of homology between fly and mammalian neural development, learning and memory, perhaps best exemplified by the conservation of pathways associated with human learning defects (Guo et al., 2000; Schenck et al., 2003). Neurodegenerative conditions studied in the fly include Alzheimer's disease, other tauopathies, and Huntington's and Parkinson's diseases (Lu and Vogel, 2009).

1.7.1 *Drosophila* tau

Research into tau-induced neurodegeneration in the fly began after the identification of a putative *Drosophila* tau homologue in 2001, also named tau and which will subsequently be referred to here as dtau (Heidary and Fortini, 2001). Initial cDNA prediction was for a 361AA protein, containing five microtubule-binding domain repeats. Subsequently a second, 375AA transcript was also predicted, differing only in its C-terminus (Doerflinger et al., 2003). The 361AA isoform exhibits 46% identity and 66% similarity with the human protein, importantly preserving the four KXGS motifs found in four-repeat isoforms of human tau. Two residues known to be key mutation sites in FTDP-17, V337 and R406, are missing however, along with the aggregation-associated BRSK target site T212 (Figure 1.5). Dtau was shown to bind microtubules by binding assay (dtau pellets almost entirely with microtubules), and GFP-tagging (Doerflinger et al., 2003). However, this same study also demonstrated the dispensability of dtau, both in development and in the adult: no loss in viability or change in behaviour was observed in three different mutants with no detectable tau expression. It is proposed that some other MAP may have redundancy with dtau.

1.7.2 The fruit fly and human neurodegenerative disease

An important early paper in the field demonstrated that human tau (htau) overexpression in the *Drosophila* retina was toxic, leading to reduced adult eye size and a rough, irregular pattern of the compound eye subunits, or ommatidia (Jackson et al., 2002). It also demonstrated exacerbation of this phenotype by the fly homologue of GSK-3β, Shaggy (Sgg) – Sgg loss of function ameliorated the damage, over-expression worsened the phenotype. This paper also presented evidence of filamentous tau aggregates, which were detected with the AT100 antibody for phosphorylation at residues T212 and S214. Neither of these residues is conserved in dtau. Re-confirmation of the ability of htau to form fibrillar aggregates in the fly had to wait until 2013 (Wu et al., 2013), although other forms of htau aggregates have recently been identified in this model (Ali et al., 2012; Cowan and Mudher, 2013). The fly eye has since been used in multiple studies of tau toxicity (Ambegaokar and Jackson, 2011; Shulman and Feany, 2003).

Another *Drosophila* homologue of a human kinase thought to be associated with tau toxicity is PAR-1 (homologous to MARK), which has been shown to phosphorylate human tau in *Drosophila*, also under the control of LKB1 (Iijima-Ando et al., 2010; Nishimura et al., 2004; Wang et al., 2007). Both PAR-1 and Sgg have been shown to cause some neurodegeneration upon overexpression in wild type *Drosophila*, with no extra expression of tau (Chatterjee et al., 2009); this could be due to interaction with dtau. Tau phosphorylation has been shown to strongly influence toxicity in this model, via small and large-scale mutation of phosphorylated residues (Iijima-Ando et al., 2010; Steinhilb et al., 2007).

1.7.3 *Drosophila* and human BRSK

The Moffat and Frenguelli laboratories have begun to study the effect of BRSK2 on human 0N4R tau in *Drosophila*, using the fly eye as a model in a similar fashion to Jackson et al. (2002). Unpublished data from these experiments by Dr Ceri Lyn-Adams showed a strong increase in htau-induced neurodegeneration by BRSK2. Compared with Sgg or PAR-1 overexpression, there was no change in external eye phenotype when expressing BRSK2 alone, indicating a lack of interaction with dtau. Unlike other kinases used in *Drosophila*, the fly BRSK homologue *sugar free frosting* (*sff*), or CG6114 (Baas et al., 2011) has no effect when overexpressed with or without human tau despite retaining important residues, including T189 (unpublished data). This suggests that there is a lack of downstream conservation of this pathway; this could be due to the non-conserved T212 residue in dtau. This phenotype has been partially rescued by RNA inhibition of native LKB1 and the CaMKKα homologue CG17698. Addition of human CaMKKα is also able to compensate for CG17698 suppression, restoring the more severe phenotype. The conservation of the regulatory pathway upstream of BRSK makes it a strong candidate for the examination of phosphorylation-induced toxicity in this model.

As a model organism, the fruit fly presents a number of strengths, not limited to its cost effectiveness and ease of rearing relative to mammalian models or cell culture. The *Drosophila* genetic toolbox allows for in-depth control of transgene insertion and expression. The existence of both spatial and temporal methods of expression control, in the form of the GAL4-UAS system and modifications such as the TARGET temperature-sensitive repression system and drug-inducible promoters including GeneSwitch, enables single transgenes to be tested under a variety of conditions. The rapid reproductive cycle of the fruit fly facilitates screening of large numbers of mutant phenotypes, which has been exploited in the creation of extensive libraries of deficiency mutants. The Moffat and Frenguelli laboratories have exploited the flexibility of this model for several years, examining human tau/BRSK interactions in the fly eye. This thesis describes attempts to improve on this work, testing these interactions in a post-developmental, CNS context, as well as a deficiency screen for other elements of the tau/BRSK pathway. The major part of this project has been exploiting *Drosophila* as a first step in translating *in vitro* work to an *in vivo* setting. Use of site-specific integration in the fly (Groth et al., 2004), as

well as the transgene injection services available to *Drosophila* biologists, enables efficient generation of novel mutant libraries of comparable expression levels. In this thesis, the establishment of such a mutant library is described for the investigation, via site-specific mutation, of phosphorylation sites on tau believed to be relevant to disease. A wide range of genetic tools are used to examine the toxicity of human tau and BRSK across multiple tissues, in both developing and adult flies.

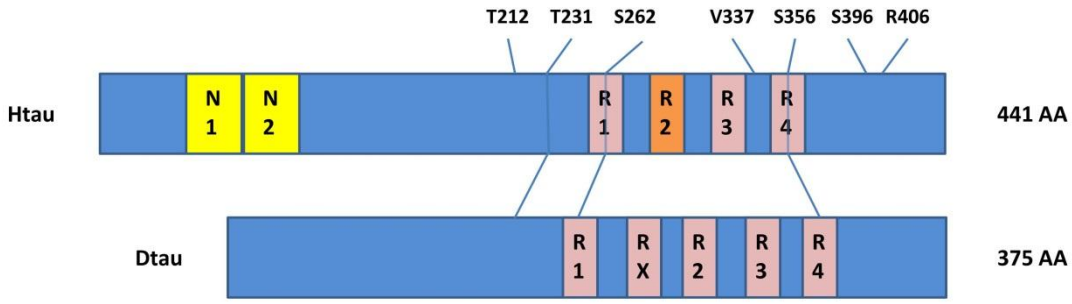

Figure 1.5 Human and* Drosophila *tau
Comparison of the longest human tau isoform (2N4R) with the larger of the two Drosophila *tau isoforms. Conserved residues include T231 and the KXGS motifs. The BRSK2 target site T212 and multiple FTDP-17-related mutations sites are not conserved.*

1.8 Aims of this thesis

The relationship between tau toxicity and phosphorylation is the subject of some controversy, after attempts to create generic hyperphosphorylated or hypophosphorylated tau species by mutation brought the hypothesis into question (Chatterjee et al., 2009). The use of S11A tau, containing 11 serine to alanine mutations, suggested that excessive microtubule binding of hypophosphorylated tau was also a cause of tau toxicity. This has led to speculation that there could be a disconnect between tau phosphorylation and toxicity. In addition to this, *in vitro* studies of individual tau phospho-mutations suggest a more complicated phosphorylation code, with individual sites playing distinct roles (Alonso et al., 2010; Chang et al., 2011; Kiris et al., 2011). This thesis aims to demonstrate the relative importance of these sites to toxicity, using *Drosophila* as a model, enabling the rapid generation and analysis of a library of tau phospho-mutants. In addition, this thesis seeks to expand on previous work examining the potential of human BRSK2 as a tau kinase, using multiple tau isoforms and a deficiency screen.

1. To generate a library of human 2N4R tau phospho-mutants in order to determine the relative toxicity of residues associated with tau aggregation and microtubule binding
2. To use such a library to dissect the importance of phosphorylation to BRSK2-enhanced tau toxicity
3. To develop novel, high-throughput models of tau toxicity in the *Drosophila* central nervous system
4. To expand knowledge of the pathways regulating human BRSK2 in the fly, via a deficiency screen of the fruit fly genome

2| Materials and Methods

All chemicals and reagents were supplied by Sigma Aldrich, UK, unless otherwise stated.

2.1 *Drosophila* husbandry

2.1.1 *Drosophila* stock maintenance

Drosophila stocks were held at 25ºC, 23ºC or 18ºC in bottles or vials containing Sussex fly food (518g corn meal, 471g sucrose, 93g yeast, 28g agar boiled in 5L water, 75ml 10% w/v Nipagen M antifungal added when cool, supplemented with live yeast).

2.1.2 *Drosophila* stocks used

Genotypes and strain labels of stocks used are presented in Appendix 1. Expression of transgenes used the GAL4-UAS expression system, with eye-specific, PDF neuron-specific or pan-neuronal drivers, respectively, GMR (glass multimer reporter), PDF (pigment dispersing factor) and ELAV (embryonic lethal, abnormal vision).

2.2 Deficiency screen

2.2.1 Deficiency kits used

The Bloomington deficiency kits for chromosomes 2 and 3 were acquired from the Bloomington *Drosophila* stock centre (BDSC), consisting of 147 and 179 lines, respectively of *Drosophila* hemizygous for defined chromosomal deletions. Secondary screening used RNAi lines from the Vienna *Drosophila* RNAi Centre (VDRC).

2.2.2 Deficiency crosses

Deficiency lines were crossed at 23ºC with GMR; tau,B2WT5 (human BRSK2 wild type line 5) virgins and the phenotypes of the progeny compared under light microscope for initial screening.

2.3 High resolution imaging and analysis of eye phenotypes

2.3.1 Paraformaldehyde fixation and dehydration

Female flies were fixed in 4% w/v paraformaldehyde (PFA) in phosphate-buffered saline (PBS) at 4ºC overnight, before undergoing dehydration using a series of acetone washes in 30%, 50%, 70% and 90% at room temperature, 20 minutes per cycle. Flies were then kept in 100% acetone at 4ºC for at least 2 days.

2.3.2 Scanning electron microscopy

Eye phenotypes caused by GMR-driven expression of transgenes were imaged using scanning electron microscopy (SEM). Dehydrated flies were attached to metal stubs with double-sided tape and kept on silica gel until imaging. Prior to imaging, flies were coated in gold by a sputter coater, with two coats lasting 60 seconds at 1.5kV, 20 mA. The microscope used was a Zeiss Supra55 VP SEM, magnified 150X.

2.3.3 Analysis of eye phenotypes

High resolution SEM images of fly eyes were analysed using the Quantitative Edge Detection (QED) software for MatLab developed in collaboration with Mr Quentin Caudron and Dr John Aston (Caudron et al., 2013).

QED generates edge sets from greyscale .tif images based on differences in contrast around ommatidia. Manual input is required to optimise the edge set, by tracing the eye outline, and then defining the Gaussian kernel width (determines the expected size in pixels of any edges) and the Sobel threshold (determines the minimum contrast shift over any edges), to make it as accurate a representation as possible of the eye structure (Figure 2.1). QED measures three different parameters for each image. These are ommatidial roundness (a measure of regularity of ommatidial shape), and inter-ommatidial distances and angles (based on the regular hexagonal packing of healthy eyes). Neurodegeneration leads to disruption of ommatidial structure and regularity, and QED measures the level of disruption by generating an "ommatidial distortion coefficient" (DC) for each image, reflecting the increase in variation in the chosen parameters. Roundness was used as the measure in each case as it tests the entire area of the image selected, rather than the centremost seven ommatidia alone.

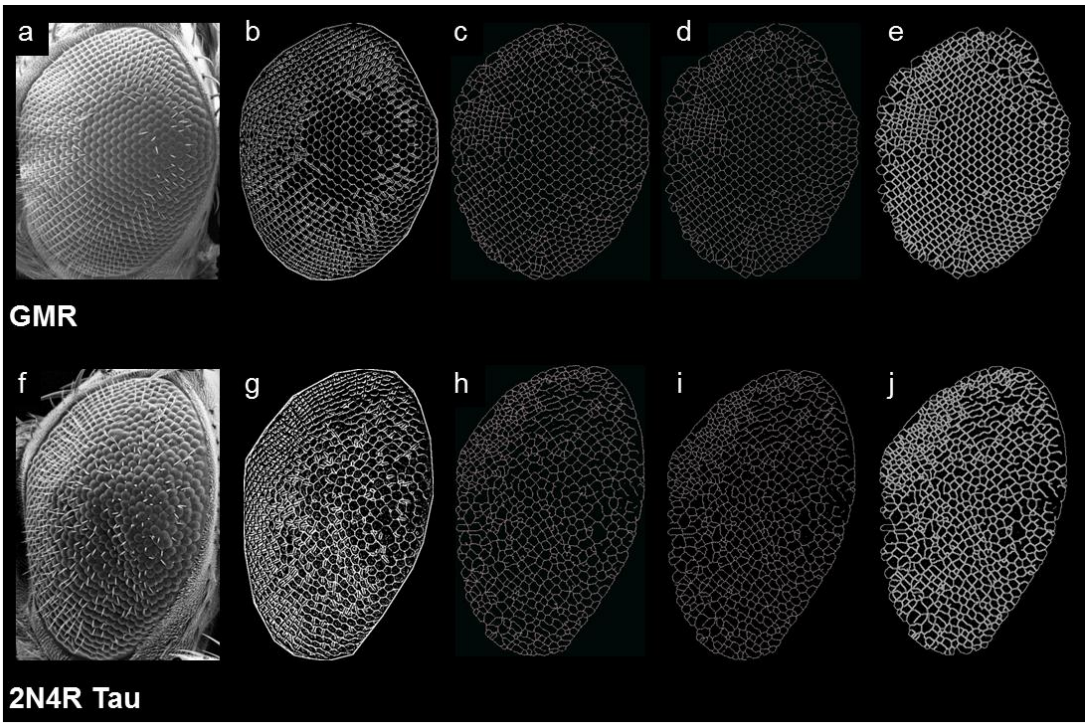

Figure 2.1 QED performs multiple operations to generate ommatidial edge sets
Examples of edge set generation by QED, in both a relatively normal GMR eye (a) and an eye disrupted by expression of 2N4R tau (f). QED initially defines edges by width and luminosity using Marr-Hildreth (b and g) and Sobel algorithms (c and h). The program then attempts to account for the curvature of the eye by perspective transformation, stretching out the edges of the eye (d and i). QED uses this to generate a final edgeset, within which it identifies all complete ommatidia and their centres (e and j).

Origin7 was used for cumulative plots of DCs. Comparisons between populations' DCs were performed using the Mann-Whitney U test

2.4 Analysis of *Drosophila* activity

2.4.1 The *Drosophila* Activity Monitor

The Trikinetics Inc. Drosophila Activity Monitoring (DAM) system, specifically the DAM2 hardware, was used according to manufacturer's instructions. This tracked movement of individual flies, placed in 65mm long capillary tubes, by number of laser beam breaks. Tubes were prepared by filling to around 15mm with food (melted in a microwave and poured into a glass beaker with tubes standing upright) and stoppering below food with a plastic cap. Flies were anaesthetised and added to tubes, plugged with cotton wool. Activity data was recorded by the DAMSystem303 software at pre-set intervals of either 1 or 3 minutes.

2.4.2 Activity experiment crosses

Two promoters were used: ELAV-GAL80^{TS} (a pan-neuronal driver with temperature-sensitive repressor) and PDF (a driver specific for the interneurons of the Drosophila circadian pacemaker). ELAV crosses were performed at 18ºC to prevent expression during development; adults were then placed in DAM vials and placed in DAM2 monitors at 29ºC, the permissive temperature of the GAL80^{TS} repressor. PDF crosses and experiments were performed at 25ºC. A regular light/dark cycle was used for 5 days before switching to constant darkness for the remainder of the experiment, in total lasting at least three weeks.

2.4.3 Activity data analysis

Activity data was analysed in two ways – comparison of average daily activity and analysis of circadian rhythm by summing counts into 30 minute bins using the DAMFileScan107 software. Activity levels were then plotted using Origin7, and actograms made of circadian data using the ImageJ plugin ActogramJ.

2.5 Generation of a library of tau phosphorylation mutants

2.5.1 Mutagenesis and mutagenic PCR

Human 2N4R tau in a pCMV FLAG-1 plasmid underwent mutagenesis of the sites T212, T231 and S262, performed using the Stratagene® QuickChange® mutagenesis kit. Mutagenic primers were designed using the QuikChange primer design program on the Stratagene website. All primers used in this thesis are listed in Appendix 2.

Mutant plasmids were generated from wild type human 2N4R tau inserted into a pCMV Tag3b vector, using mutagenic polymerase chain reaction (PCR). This form of PCR used very long elongation steps to ensure full duplication of the entire plasmid.

50µl mutagenic PCR reaction mix:
5µl 10X *Pfx* Amplification buffer (Invitrogen)
10µl 10X *Pfx* Enhancer solution (Invitrogen)
1µl 50mM $MgSO_4$ (Invitrogen)
1.5µl 10mM dNTPs (Invtrogen)
12.5µl of each mutagenic primer (10µg/ml)
1µl DNA template (5ng/µl)
1µl *Pfx* polymerase (Invitrogen)
10.5 µl H_2O

Reactions were performed in an Eppendorf Mastercycler Gradient thermocycler with the following program:
1. Initial denaturation: 2 minutes, 94°C
2. Denature: 30 seconds, 94°C
3. Primer annealing: 1 minute, 55°C
4. DNA elongation: 6 minutes, 68°C
5. Repeat steps 2-4 for 18 cycles

Pfx Enhancer solution at 2X concentration was found to improve the reaction success rate. Reaction mixes were then digested using Dpn1 restriction enzyme for 2 hours at 37°C in a water bath to remove template DNA.

2.5.2 Transformation in XL-1 Blue cells

Transformation in XL-1 Blue *Escherichia coli* was performed according to manufacturer's instructions. Ampicillin selection plates were used to identify transformed cells.

2.5.3 DNA isolation

Colonies were picked into 5ml of Luria-Bertani (LB) broth and amplified overnight at 37°C in shaking incubator. DNA was isolated using the QIAprep Spin Miniprep Kit (Qiagen) according to manufacturer's instructions.

2.5.4 Agarose gel electrophoresis

Plasmids were checked on a 0.8% agarose gel, using a method based on Maniatis et al. (1982) – book 5, chapter 1, pages 150-162.

DNA solutions were mixed with 5X loading buffer (30% v/v glycerol, 0.1% w/v bromophenol blue, 0.1% w/v xylene cyanol) and loaded onto 0.8% agarose gels (0.4g agarose and 2.5µl RedSafe (iNtRON Biotechnology) in 50ml TBE). Gels were run at 100V until dye had run over halfway down the gel. Gel images were taken using a UV transilluminator.

2.5.5 Determination of DNA concentration

DNA concentration was measured using a NanoDrop ND-1000 spectrophotometer (Thermo Scientific) and Nanodrop 1000 3.6.0 software.

2.5.6 DNA sequencing

Sequencing reactions were in a total volume of 10µl, with 50-500ng of DNA and 5.5pmol of tau sequencing primers. Sequencing was carried out in house by Molecular Biology Services, School of Life Sciences, Warwick University on an ABI Prism Genetic Analyser 3130xl. Sequences were compared and mutations located using the programs Chromas and Clustal X2. This process from 2.5.1 onward was repeated using T212D mutant plasmid and S262D mutagenic primers in order to generate a double mutant.

2.5.7 Subcloning PCR reactions

In order to increase the amount of DNA available for digestion, subcloning PCRs were performed to amplify mutated inserts. Subcloning PCR reactions used primers complementary to regions either side of the insert in the pCMV FLAG-1 plasmid. Reactions used the following 50µl formula:

5µl 10X *Pfx* Amplification buffer (Invitrogen)
1µl 50mM $MgCl_2$ (Invitrogen)
1µl 10mM dNTPs (Invtrogen)
1.5µl of each subcloning primer (100µM)
1µl DNA template (100ng/µl)
0.8µl *Pfx* polymerase (Invitrogen)
38.2 µl H_2O

Reactions were performed in an Eppendorf Mastercycler Gradient thermocycler with the following program:

1. Initial denaturation: 5 minutes, 94°C
2. Denature: 1 minute, 94°C
3. Primer annealing: 30 seconds, 55°C
4. DNA elongation: 90 seconds, 68°C
5. Repeat steps 2-4 for 10 cycles
6. Dentaure: 1 minute, 94°C
7. Primer annealing (selecting for higher complementarity): 30 seconds, 65°C
8. DNA elongation: 90 seconds, 68°C
9. Repeat steps 6-8 for 25 cycles

2.5.8 Gel extraction of DNA

PCR products were run on an agarose gel to purify. The QIAquick Gel Extraction kit (Qiagen) was used according to manufacturer's instructions.

2.5.9 Restriction digestion

The restriction enzymes NotI and EcoRI (Invitrogen) were used to excise mutated 2N4R tau-FLAG from the PCR product with appropriate overhangs. The initial reaction used NotI in a 10µl reaction in REact 3 buffer for 3hrs at 37°C before

addition of EcoRI and further incubation overnight. The same digestion was performed on pUASTattB. Digests underwent a further gel extraction to remove digested ends.

2.5.10 Ligation into pUASTattP2

Ligation reactions used at least 3:2 ratios by weight of insert to vector, depending on available concentration.T4 DNA ligase (Invitrogen) was used in 10µl reactions, kept at room temperature overnight.

2.5.11 Transformation into *Escherichia coli* and colony selection

Ligation mixture was transformed into NEB 5α High or Subcloning Efficiency competent *E. coli* according to manufacturer's instructions. Ampicillin selection plates were used to identify transformed cells.

2.5.12 DNA isolation and injection

Colonies were again amplified in 5ml LB and the QIAprep Spin Miniprep kit used to isolate DNA. This was sequenced a final time to check for any unintended sequence changes, before sufficiently high concentration DNA was sent to the Genetivision Corporation for injection into *Drosophila* at the specific PhiC31 integrase-mediated site P2 on chromosome 3.

2.5.13 Bacterial strains

XL-1 Blue Supercompetent *E. coli* genotype (Agilent): *recA1 endA1 gyrA96 thi-1 hsdR17 supE44 relA1 lac* [F′ *proAB lacI*q*ZΔM15* Tn*10* (Tetr)].

NEB 5α High Efficiency competent *E. coli* genotype (New England Biolabs): *fhuA2Δ(argF-lacZ)U169 phoA glnV44 Φ80 Δ(lacZ)M15 gyrA96 recA1 relA1 endA1 thi-1 hsdR17*

NEB 5α Subcloning Efficiency competent *E. coli* genotype (New England Biolabs): *fhuA2 Δ(argF-lacZ)U169 phoA glnV44 Φ80Δ (lacZ)M15 gyrA96 recA1 relA1 endA1 thi-1 hsdR17*

2.5.14 Media preparation

LB broth: 1% w/v NaCl, 1% w/v tryptone, 0.5% w/v yeast extract, autoclaved. Ampicillin added at 100μg/ml.

LB agar plates: LB broth with 1.5% w/v agar was autoclaved and cooled before pouring into petri dishes to set. Ampicillin added at 100μg/ml.

2.6 Protein manipulations

2.6.1 Protein extraction from *Drosophila melanogaster*

In order to measure transgenic tau levels in the tau phosphorylation mutant library, animals homozygous for wild type or mutant 2N4R tau and hemizygous for the GMR promoter were reared at 25°C until two days post eclosion. Eight females were placed into eppendorfs for each sample and flash frozen in liquid nitrogen. These eppendorfs were vortexed to decapitate the animals. Heads were collected on dry ice then homogenised in 50μl lysis buffer using a mechanical pestle. Samples were then centrifuged at 13,000RPM for 30 minutes at 4°C, supernatant removed and 10μl protein loading dye added before heating at 90°C for 10 minutes and freezing at -20°C until use.

Lysis buffer contained 50mM tris(hydroxymethyl)aminomethane-hydrochloric acid (Tris-HCl pH 7.5), 0.1mM ethylene glycol tetra-acetic acid (EGTA), 1mM ethylene diamine tetra-acetic acid (EDTA), 1% v/v Triton X-100, 1mM sodium orthovanadate (Na_3VO_4), 50mM sodium fluoride (NaF), 5mM sodium pyrophosphate ($Na_4P_2O_7$), 0.27M sucrose, 0.1% v/v β-mercaptoethanol and "complete" protease inhibitor cocktail (Roche, three tablets per 50ml). NaF and $Na_4P_2O_7$ inhibit serine/threonine protein phosphatase activity, Na_3VO_4 that of tyrosine protein phosphatases. EDTA inhibits protein kinase activity as a Mg^{2+} ion chelator. EGTA chelates Ca^{2+} ions. Protease inhibitor cocktail inhibits aspartyl, cysteine, metallo- and serine protease activity. This buffer effectively protected the lysates from the activity of proteases and protein kinases and phosphatases.

2.6.2 Sodium dodecyl sulphate polyacrylamide gel electrophoresis (SDS-PAGE)

SDS-PAGE was performed using the BioRad Mini system. Samples were thawed and heated at 90°C for ten minutes before loading 8µl per lane, alongside ColorPlus prestained protein ladder (New England Biolabs), onto SDS-PAGE gels – 5% stacking gel and 10% resolving gel. Electrophoresis was performed in running buffer (0.1% w/v SDS, 0.3% w/v Tris and 1.44% w/v glycine) at 115V for 1.5-2 hours. Transfer onto nitrocellulose (GE Healthcare) in transfer buffer (0.3% w/v Tris, 1.44% w/v glycine and 20% v/v methanol) lasted 3 hours at a constant current of 200 amps.

2.6.3 Immunoblotting

Membranes were blocked with 5% w/v bovine serum albumin (BSA) in TBS-Tween (0.1% v/v) for 15 minutes at room temperature with agitation. Primary antibodies (listed in Table 2.1) were used at 1:1000 dilutions in 5% w/v BSA in TBS-Tween – membranes were exposed to 3ml of primary solution overnight at 4°C with rotation. Three ten minute washes in PBS-Tween of ten 10 minutes each removed unbound primary before incubation with horseradish peroxidase (HRP)-conjugated secondary antibodies (Thermo Scientific, see Table 2.2), all used at a 1:1000 dilution in 5% w/v dried skimmed milk in PBS-Tween, for 1 hour at room temperature. Three more washes in PBS-Tween removed excess secondary before membranes were dried and incubated with enhanced chemoluminscence (ECL) reagent (GE Healthcare) for three minutes. X-ray film was exposed to the membranes and developed, before being scanned using a CanoScan LiDE 700F scanner (Canon). Band density was measured using ImageJ.

Primary Antibody	Source	Species	Incubation time
T46 tau	Abcam	Mouse	Overnight, 4°C
P262 tau	Abcam	Rabbit	Overnight, 4°C
JL20 actin	Millipore	Mouse	2.5 hours, room temperature
FLAG	Sigma-Aldrich	Mouse	Overnight, 4°C

Table 2.1 Primary antibodies used in this study
Primary antibodies used, their source, species and incubation time and temperature

Secondary Antibody	Source	Species	Incubation time
Anti-rabbit HRP	Thermo Scientific	Goat	1 hour, room temperature
Anti-mouse HRP	Thermo Scientific	Rabbit	1 hour, room temperature

Table 2.2 Secondary antibodies used in this study
Secondary antibodies used, their source, species and incubation time and temperature

3| Characterisation of a library of human tau mutants in the *Drosophila melanogaster* eye

3.1 Introduction

Early attempts to examine neurofibrillary tangles by monoclonal antibody screens led to the discovery of the Alzheimer's-associated protein A68, characterised by immunoreactivity with novel antibodies such as Alz50 (Hyman et al., 1988). Since this was later demonstrated to be a hyper-phosphorylated, tangle-specific form of tau protein (Brion et al., 1991), a significant amount of the research conducted on the nature of tau toxicity has focused on the effects of kinase dysfunction. Early screens for tau kinases associated with PHF formation revealed the proline-directed kinase GSK3 to play an important role (Ishiguro et al., 1993; Mandelkow et al., 1992). Other kinases were found to alter the affinity of tau for microtubules, including the AMPK-related protein kinase MARK, which was shown to phosphorylate tau at S262 in the first KXGS motif (Drewes et al., 1995). Subsequently, this family of kinases has been revisited multiple times in this context. After the two SAD/BRSK kinases were shown to regulate neuronal polarisation in mammals via tau protein phosphorylation at S262 (Kishi et al., 2005), the Moffat and Frenguelli laboratories began to examine BRSK in the context of neurodegeneration. BRSK2 has since been shown to phosphorylate tau *in vitro* at T212 and S262 (Yoshida and Goedert, 2011). This phosphorylation profile was all the more interesting for *in vitro* studies linked these residues to specific processes hypothesised to control tau toxicity. In the case of T212, phospho-mimetic mutation caused enhancement of tau aggregation (Alonso et al., 2010; Chang et al., 2011; Necula and Kuret, 2004). Conversely, a single phospho-mimetic mutation to aspartate at S262 has been shown to reduce tau-microtubule affinity (Kiris et al., 2011). These *in vitro* studies of single or double phospho-mimetic mutations have yet to be replicated *in vivo* – non-phosphorylatable mutations at KXGS motifs have already been shown to mitigate tau toxicity in the fly (Iijima-Ando et al., 2010) – but the use of site-directed mutagenesis to decipher the phosphorylation code of tau has fallen out of favour, since highly-mutated tau genes such as S11A (Chatterjee et al., 2009) were found to produce results described as "uninterpretable" (Goedert, personal communication). These results were perhaps unsurprising, given the apparent compound effects of multiple tau mutations found by Kiris et al. in 2011. Single mutations were found not to be additive in double mutants, but instead to lead to a reversal in effects on microtubule binding.

With this in mind, the tau mutants shown in this chapter were generated to explore the effects of BRSK-induced tau phosphorylation in the fly, in the absence of any human kinase. Phospho-mimetic mutations were made to a wild-type human 2N4R tau gene contained within a pCMV-1 Flag plasmid using the Stratagene® QuickChange® mutagenesis kit. Sites mutated were T212, T231 and S262, with residues replaced with aspartate to simulate part of the negative charge of a phosphorylated residue (Biernat et al., 1993). T212 and S262 were chosen due to their purported phosphorylation by BRSK2; T231 was an alternative microtubule affinity-regulating site, with a similar (but reduced) effect according to Kiris et al. (2010), but external to the microtubule-binding domains which contain S262 and of reduced coverage in the literature. Tau was then spliced into the pUAST attP2 plasmid commonly used for gene insertion into *Drosophila*. This insertion was performed by the Genetivision Corporation at the specific PhiC31 integrase-mediated site P2 on chromosome 3, and resulted in the generation of multiple lines of transgenic flies containing wild-type and mutant, human, flag-tagged 2N4R tau protein, controlled by UAS. These lines together with others containing corresponding non-phosphorylatable mutants created the beginnings of a library of tau phosphorylation mutants. The effects of these mutations when expressed in the fly eye were compared by QED, bespoke software to measure ommatidial distortion caused by developmental transgene toxicity. These lines were also probed for the effects of mutations on phosphorylation at other sites on the protein.

3.2 Results

3.2.1 Generation of a library of human tau phosphorylation mutants in *Drosophila*

One aim of this project was the generation of a library of human tau phosphorylation mutants to be inserted into *Drosophila*. The plasmid source of tau to be mutated and cloned was pCMV-1 2N4R tau Flag (a kind gift of Dr Calum Sutherland, Dundee University), containing the wild type human 2N4R tau gene with attached 1kd Flag tag sequence. Mutations were designed to replace phosphorylatable serine and threonine residues with phospho-mimetic aspartate residues. The sites chosen for mutation were T212 (shown *in vitro* to be involved in promotion of tau aggregation), T231 and S262 (both shown *in vitro* to be involved in regulation of microtubule binding). Both T212 and S262 have also been shown *in vitro* to be phosphorylated by BRSK2. The codon changes were designed to be as small as possible, exploiting the degenerate amino acid code to make two-nucleotide changes in each case. These changes are illustrated in Table 3.1.

Construct	Amino acid change	DNA codon change
T212D	T212D	ACC to GAC
T231D	T231D	ACT to GAT
S262D	S262D	TCC to GAC

Table 3.1 2N4R tau amino acid and codon changes

Phospho-mimetic mutations were generated at sites T212, T231 and S262

The Stratagene® QuickChange® mutagenesis kit was used to insert the mutations into the pCMV-1 2N4R tau Flag vector, which was cloned, excised and ligated into pUAST attP2 for insertion into the *Drosophila* genome, as shown in Figure 3.1. pUAST contains the Upstream Activating Sequence for control of transgenes by the GAL4-UAS expression system, as well as the white gene as a marker for successful integration. The tau gene within the final plasmid (named pUAST 2N4R tau Flag) was sequenced in its entirety to confirm the presence of the mutation as well as the

integrity of the rest of the gene. Sequences showing the successful mutations are shown in Figure 3.2. Minipreps of pUAST 2N4R tau Flag were sent to the Genetivision Corporation, Texas for insertion into *Drosophila* at the specific PhiC31 integrase-mediated site P2 on chromosome 3. This specific insertion was necessary to eliminate variation in transgene expression due to position effect and to make these mutants as comparable as possible. These mutant lines were then combined with previously generated lines containing corresponding non-phosphorylatable 2N4R tau alanine mutants at the same residues, created in-house by Dr Alessia Galasso (in the case of T231A and T262A) or kindly provided by Dr Guy Tear, King's College London (in the case of T212A, with no Flag tag). The lines constituting this library are listed in Table 3.2. Flies were crossed to a 2nd chromosome GMR promoter line and balanced, on the 2nd chromosome with CyO and on the 3rd with MKRS.

Construct	Type of mutation
2N4R WT	Wild type
T212A	Non-phosphorylatable
T231A	Non-phosphorylatable
S262A	Non-phosphorylatable
T212D	Phospho-mimetic
T231D	Phospho-mimetic
S262D	Phospho-mimetic

Table 3.2 The human 2N4R tau mutant library

Mutagenesis of wild type human 2N4R tau was used to complete a library of phosphorylation mutants

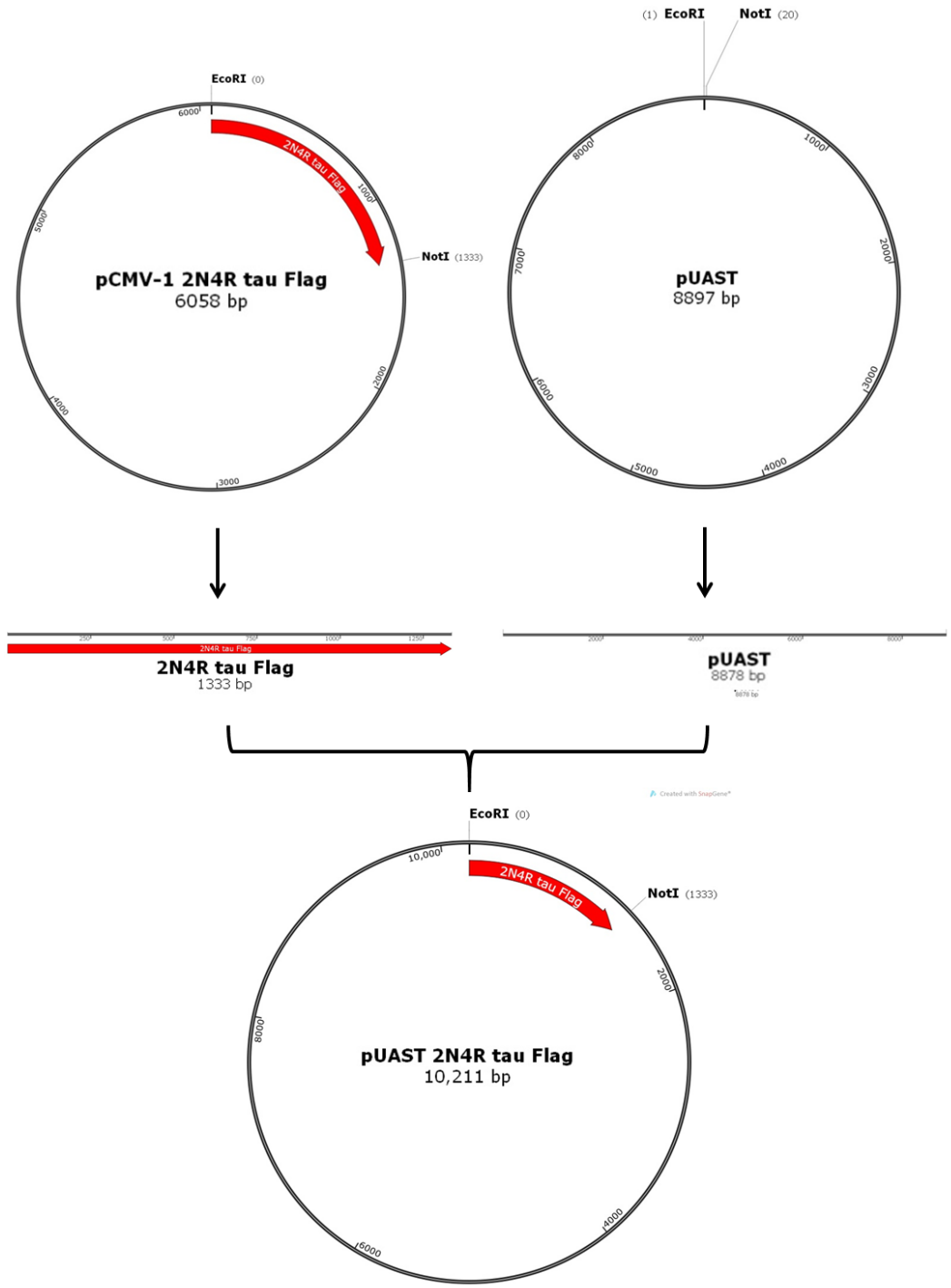

Figure 3.1 2N4R tau cloning schematic
The human 2N4R tau gene (wild type and each mutant) was excised from the pFlag-CMV-1 vector using the restriction enzymes EcoRI and NotI. The pUAST attP2 plasmid (pUAST) was also digested by the same enzymes in preparation for ligation to the 2N4R tau fragments.

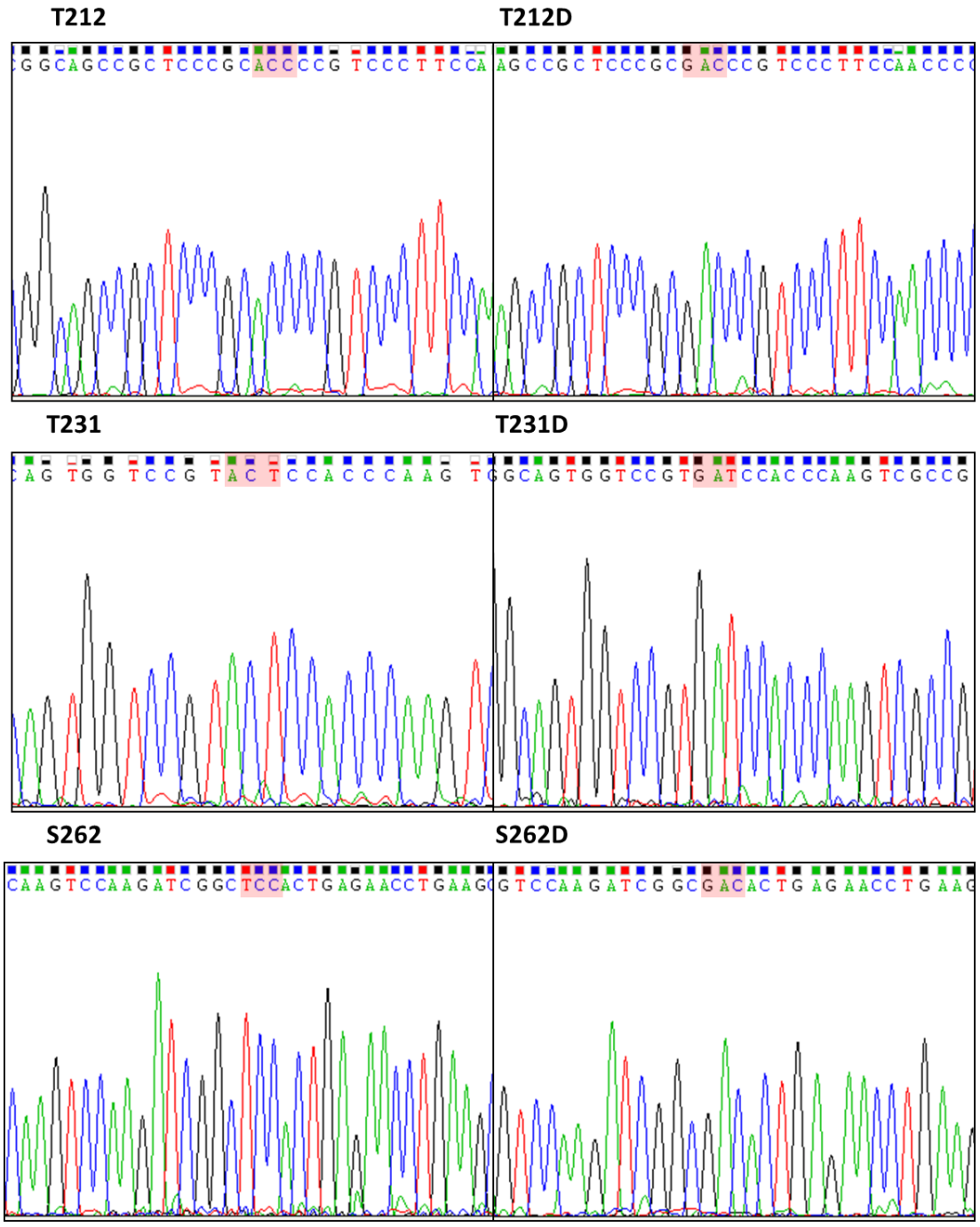

Figure 3.2 2N4R tau mutant genotyping
Sequencing chromatograms showing the codon changes made in each phospho-mimetic mutant. Left (highlighted in red): the codon for the wild type sequence, in descending order threonine 212, threonine 231 and serine 262. Right (highlighted in red): the corresponding change at the same position to generate a mutant aspartate codon.

3.2.2 Quantification of transgene expression levels in *Drosophila*

In order to ascertain whether any phenotypic differences found between these transgenic *Drosophila* lines were due to the introduced mutations, an indication of levels of transgene expression was required. Western blots were performed on flies hemizygous for GMR and homozygous for tau using the total tau T46 antibody and the JL20 actin antibody as loading control (Figure 3.3). Bands were quantified using the Gel Analyser plugin for Fiji, with T46 values normalised to actin and then mutants normalised to the 2N4R WT band of the same blot. No significant differences were found between mutant lines by ANOVA (analysis of variance), though there would appear to be a trend toward relatively reduced expression in T212A and T231A compared with their phospho-mimetic counterparts. (WT n=4, T212A 0.74 ±0.19 n=4, T212D 1.32 ±0.18 n=5, T231A 0.53 ±0.10 n=4, T231D 1.05 ±0.22 n=4, S262A 1.18 ±0.29 n=4, S262D 1.29 ±0.28 n=4)

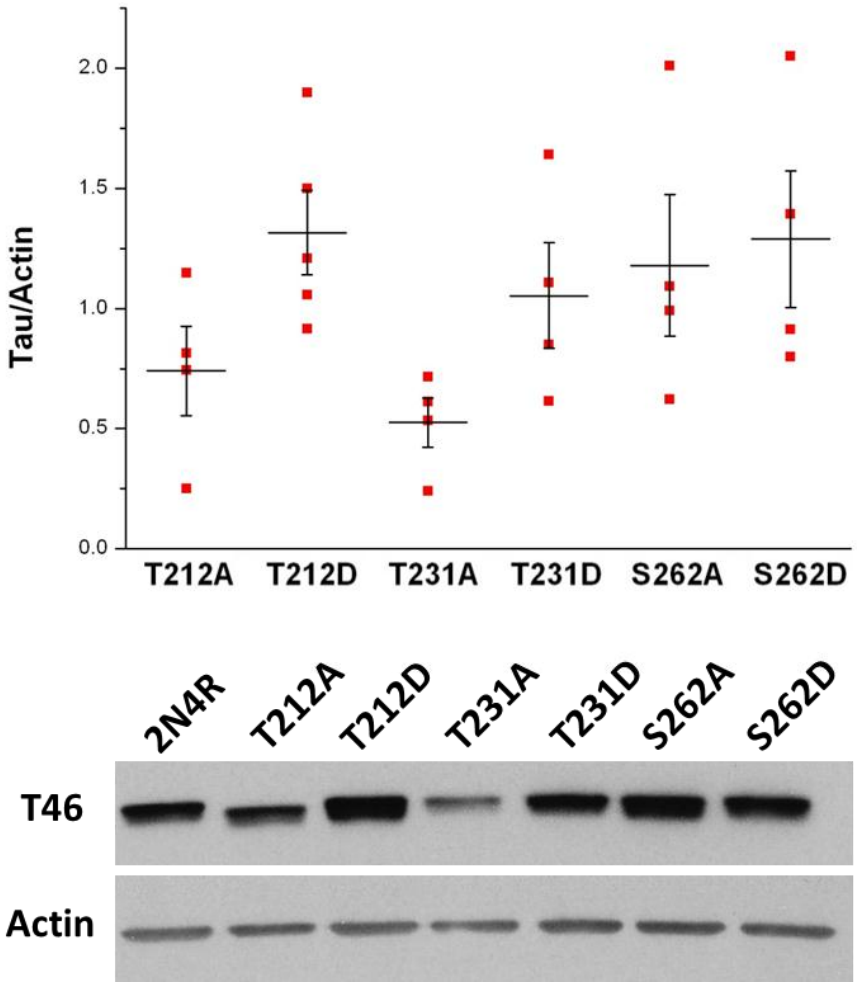

Figure 3.3 Tau mutant expression levels were not found to differ significantly *Total tau expression levels were verified by Western blot using the T46 antibody, with* Drosophila *actin loading control measured using the JL20 antibody. Quantified values were normalised to actin and to wild type tau levels on each corresponding blot. Expression levels of mutants were not found to differ significantly from wild type or from each other by ANOVA. Flies used were hemizygous for the GMR-GAL4 promoter (over CyO balancer) and homozygous for the tau transgene. (WT n=4, T212A 0.74 ±0.19 n=4, T212D 1.32 ±0.18 n=5, T231A 0.53 ±0.10 n=4, T231D 1.05 ±0.22 n=4, S262A 1.18 ±0.29 n=4, S262D 1.29 ±0.28 n=4)*

3.2.3 Quantification of tau mutant phenotypes

Transgenic tau toxicity was measured in the fly eye using the QED program, and samples compared by Mann-Whitney U test. SEM images were taken at 150X magnification of female left eyes, in animals hemizygous for GMR and either hemi- or homozygous for tau transgenes.

3.2.3.1 Wild-type 2N4R tau

Figure 3.4 shows the comparison of 2N4R WT with the GMR promoter alone, which itself causes very little ommatidial disruption in single copies. It demonstrates the establishment of a visible rough-eyed phenotype (Figure 3.4A) and concomitant increase in ommatidial distortion as measured by QED (Figure 3.4B), with a median distortion coefficient (DC) of 0.24 for GMR and 0.29 for hemizygous 2N4R WT ($P<0.0001$). This toxicity is gene dosage dependant – homozygous 2N4R WT presents a significantly different DC of 0.38 ($P<0.0001$). For this reason, all comparisons between mutant 2N4R and WT have been made between samples of equivalent transgene zygosity. Figure 3.5 presents the degree of DC variation within each sample, with the lowest and highest examples as determined by QED shown.

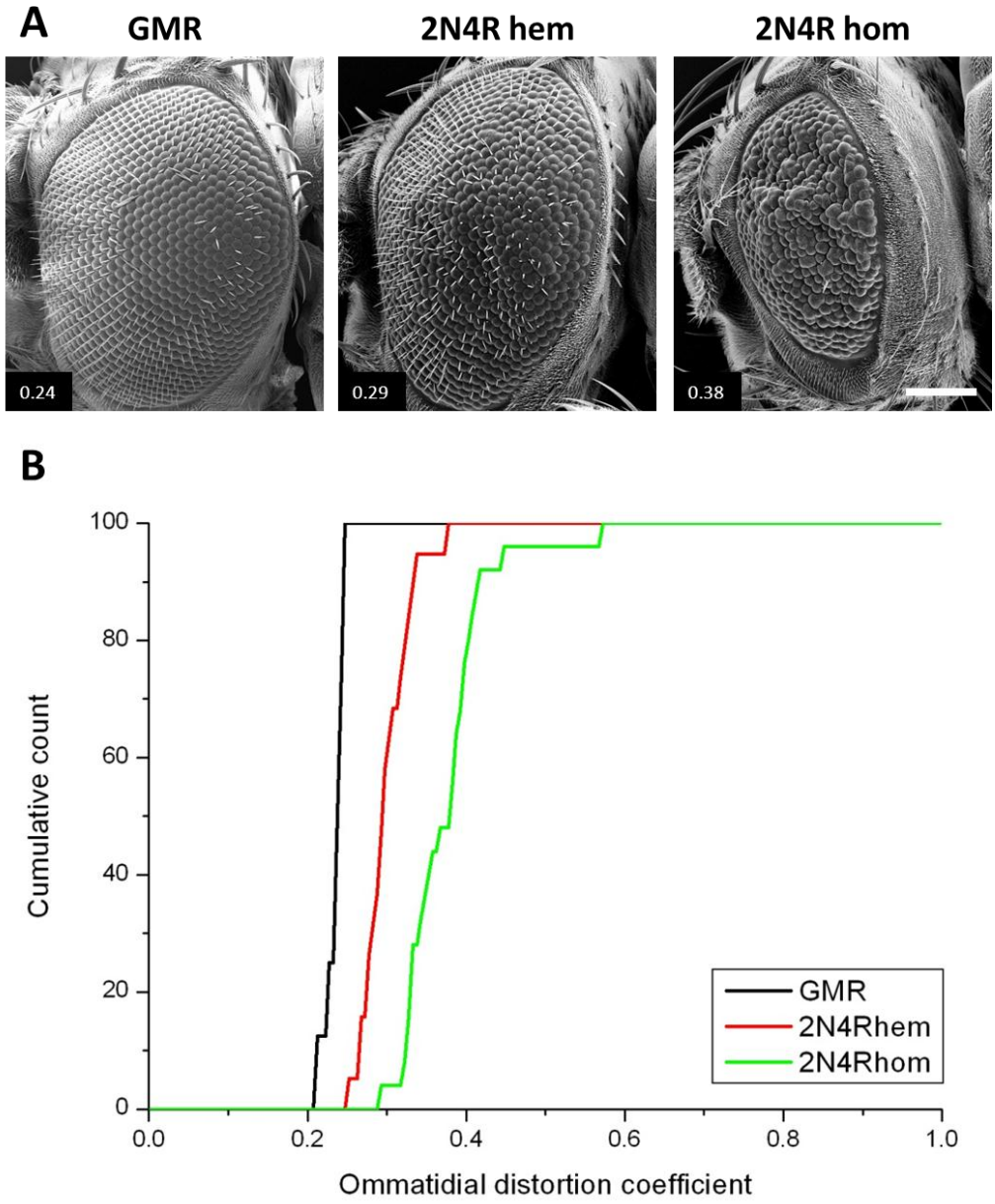

Figure 3.4 Tau expression induces measurable levels of ommatidial distortion
A. Scanning electron microscope images demonstrating the dosage-dependant median toxicity of wild type human 2N4R tau expressed in the fly eye under control of the GMR-GAL4 promoter. Dispersion coefficients shown on images. Genotypes: GMR: GMR-GAL4/CyO;MKRS/TM6B. 2N4R hem: GMR-GAL4/CyO;2N4R WT/MKRS. 2N4R hom: GMR-GAL4/CyO; 2N4R WT/2N4R WT. Scale bar: 100μm.
B. Quantitative analysis of the above phenotypes demonstrated significant difference in ommatidial roundness between GMR and 2N4R hem ($P<0.0001$), between GMR and 2N4R hom ($P<0.0001$) and between 2N4R hem and 2N4R hom ($P<0.0001$). A shift to the right is characteristic of increased toxicity. GMR n=8, 2N4R hem n=23, 2N4R hom n=25.

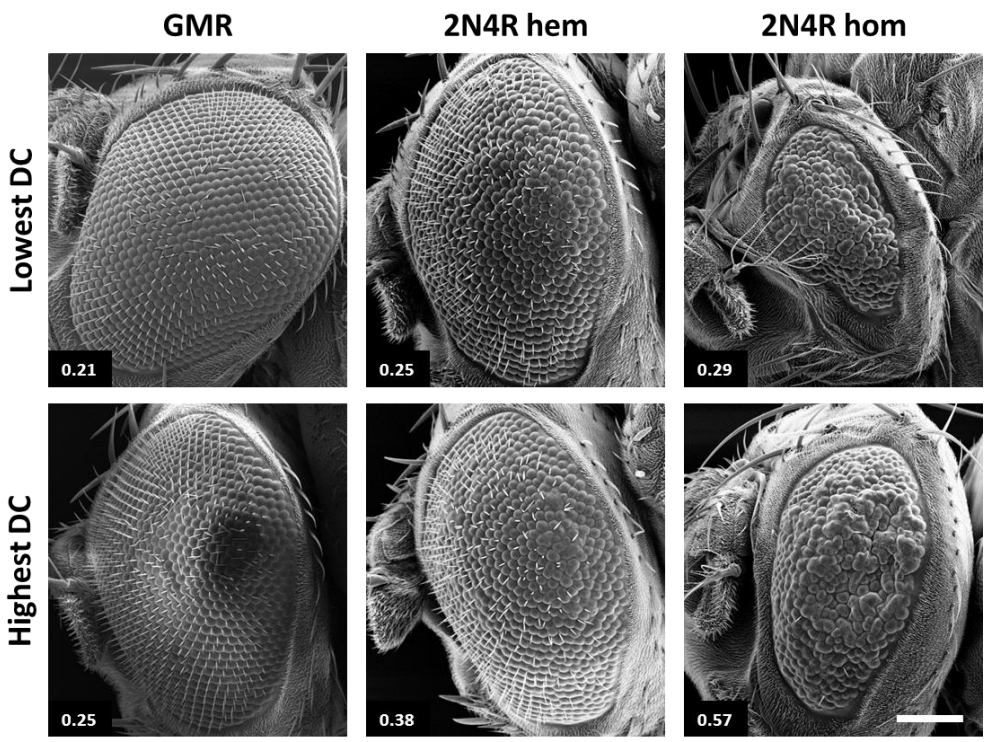

Figure 3.5 The phenotypic extremes of wild type tau flies as measured by QED *Scanning electron microscope images showing the lowest and highest distortion coefficients for roundness in the GMR, 2N4R hem and 2N4R hom samples. Scale bar: 100μm.*

3.2.3.2 Mutations at T212

The effects of mutation to site T212 are shown in Figure 3.6, with median DC images shown for hemi- and homozygous 2N4R T212A (DC of 0.31 and 0.33, respectively) and 2N4R T212D (DC of 0.27 and 0.32, respectively) mutants, along with 2N4R WT for reference. It would appear that the 2N4R T212D mutation in each case reduces tau toxicity. Any effect of 2N4R T212A mutation is less clear. Figure 3.7 shows quantification of these changes, separated by zygosity. Hemizygous T212D had a significantly lower DC than hemizygous T212A ($P=0.035$), but not compared with hemizygous 2N4R ($P=0.081$). Hemizygous T212A and 2N4R WT do not differ ($P=0.61$). Among the homozygous individuals, T212D had a significantly lower DC than 2N4R WT ($P=0.004$). Other comparisons were not significant. Figure 3.8 shows the minimum and maximum DCs for the samples. It would appear that phospho-mimetic T212D mutation does reduce the toxicity of 2N4R tau in this context, and is also less toxic than the non-phosphorylatable T212A mutation, though this is not evident in every case.

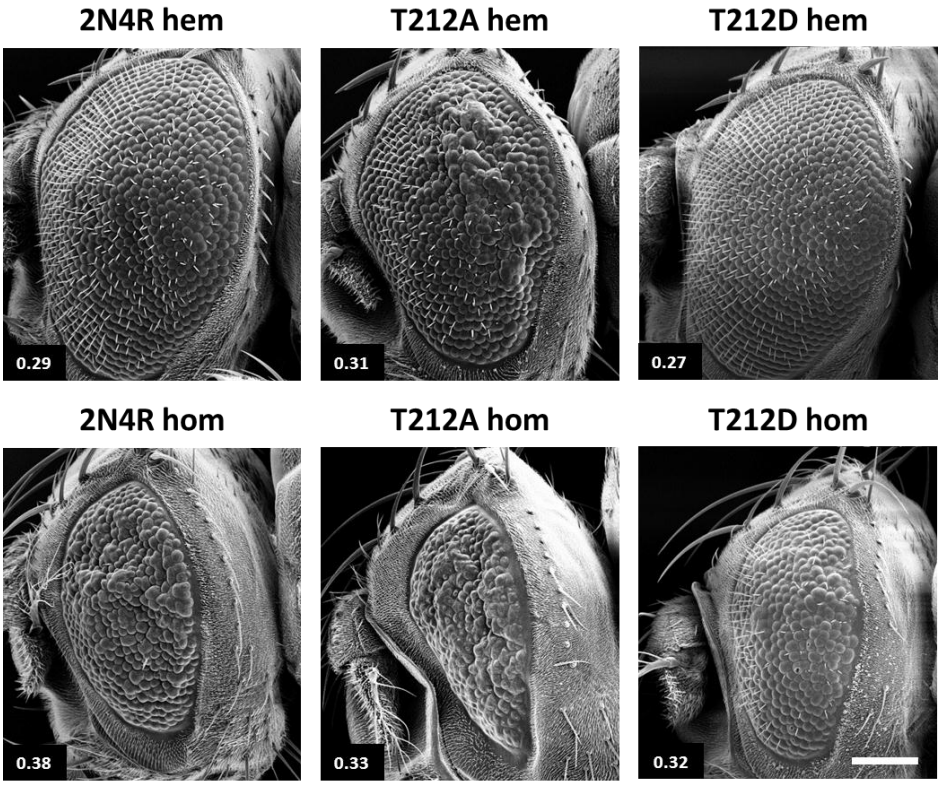

Figure 3.6 Phospho-mimetic T212D mutation leads to reduced toxicity
Scanning electron microscope images demonstrating the dosage-dependant median toxicity of human 2N4R tau, mutated at threonine 212 and expressed in the fly eye under control of the GMR-GAL4 promoter. Dispersion coefficients shown on images. The T212D mutants appear to be less distorted than 2N4R WT or T212A mutants.
Genotypes: T212A hem: GMR-GAL4/CyO;T212A/MKRS. T212D hem: GMR-GAL4/CyO; T212D/MKRS. T212A hom: GMR-GAL4/CyO; T212A/T212A. T212D hom: GMR-GAL4/CyO;T212D/T212D. Scale bar: 100µm.

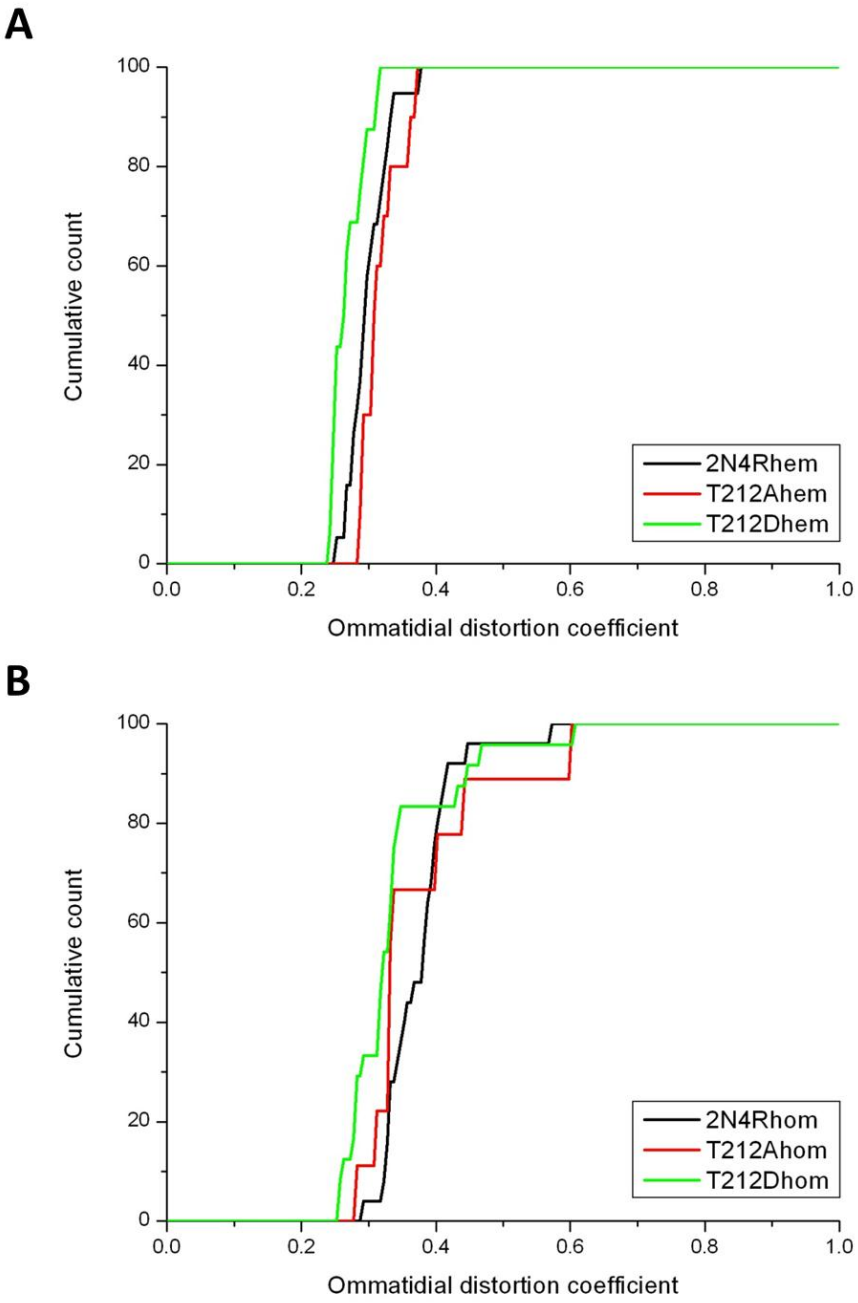

Figure 3.7 Phospho-mimetic T212D mutant tau is less toxic than non-phosphorylatable T212A mutants as measured by QED

Quantitative analysis of the phenotypes of the samples shown in Figure 3.6. T212D hem DC is significantly less than that of T212A hem by Mann-Whitney U test (P=0.035). T212D hom is significantly less distorted than 2N4R hom by the same test (P=0.004).

A: 2N4R hem n=23. T212A hem n=14. T212D hem=18.

B: 2N4R hom n=25. T212A hom n=9. T212D hom n=24.

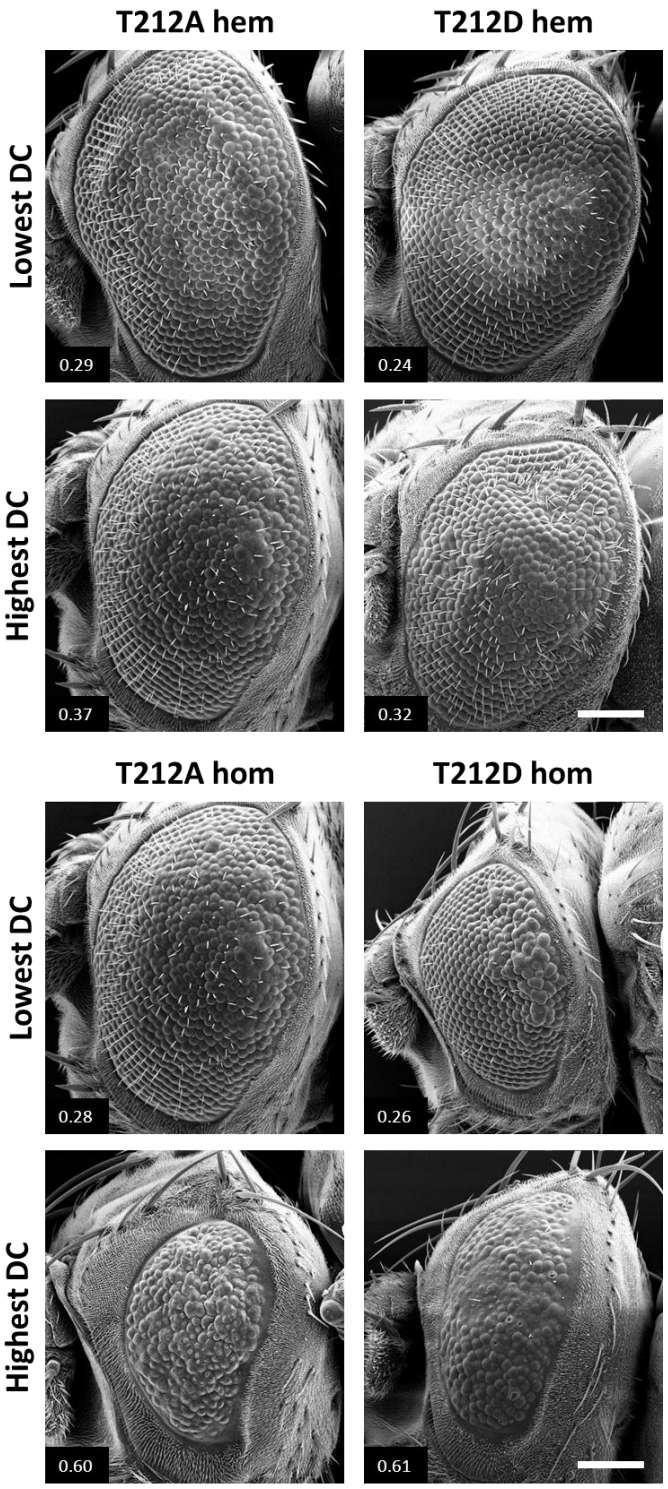

Figure 3.8 Phenotypic extremes of T212 mutants
Scanning electron microscope images showing the lowest and highest distortion coefficients for roundness in the T212A hem, T212D hem, T212A hom and T212D hom samples. Scale bar: 100μm.

3.2.3.3 Mutations at T231

Figure 3.9 shows the median phenotypes among the T231 mutants, with 2N4R WT for reference. T231A mutants were given DC values of 0.30 and 0.37 for hemi- and homozygous respectively; T231D mutants had DC values of 0.35 and 0.40 for hemi- and homozygous respectively. Quantification in Figure 3.10 found a significant increase in DC in the T231D hemizygous individuals compared with both 2N4R WT ($P<0.0001$) and T231A ($P=0.0004$). No change was found among the homozygous samples. Figure 3.11 shows the extremes of DC values for each sample. These data potentially show a slight increase in toxicity of 2N4R tau upon T231D mutation, though are not conclusive. Neither mutation leads to a reduction in toxicity.

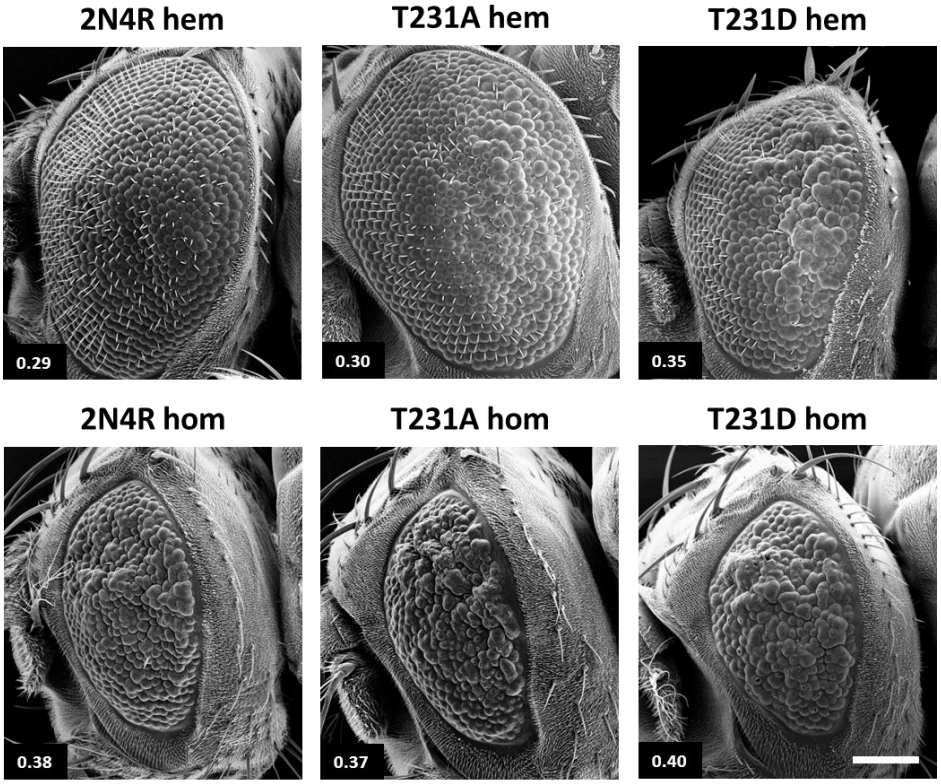

Figure 3.9 T231 mutations do not cause any obvious phenotypic change
Scanning electron microscope images demonstrating the dosage-dependant median toxicity of human 2N4R tau, mutated at threonine 231 and expressed in the fly eye under control of the GMR-GAL4 promoter. Dispersion coefficients shown on images. Any change in distortion is not evident by eye.
Genotypes: T2131A hem: GMR-GAL4/CyO;T231A/MKRS. T231D hem: GMR-GAL4/CyO; T231D/MKRS. T231A hom: GMR-GAL4/CyO; T231A/T231A. T231D hom: GMR-GAL4/CyO;T231D/T231D. Scale bar: 100μm.

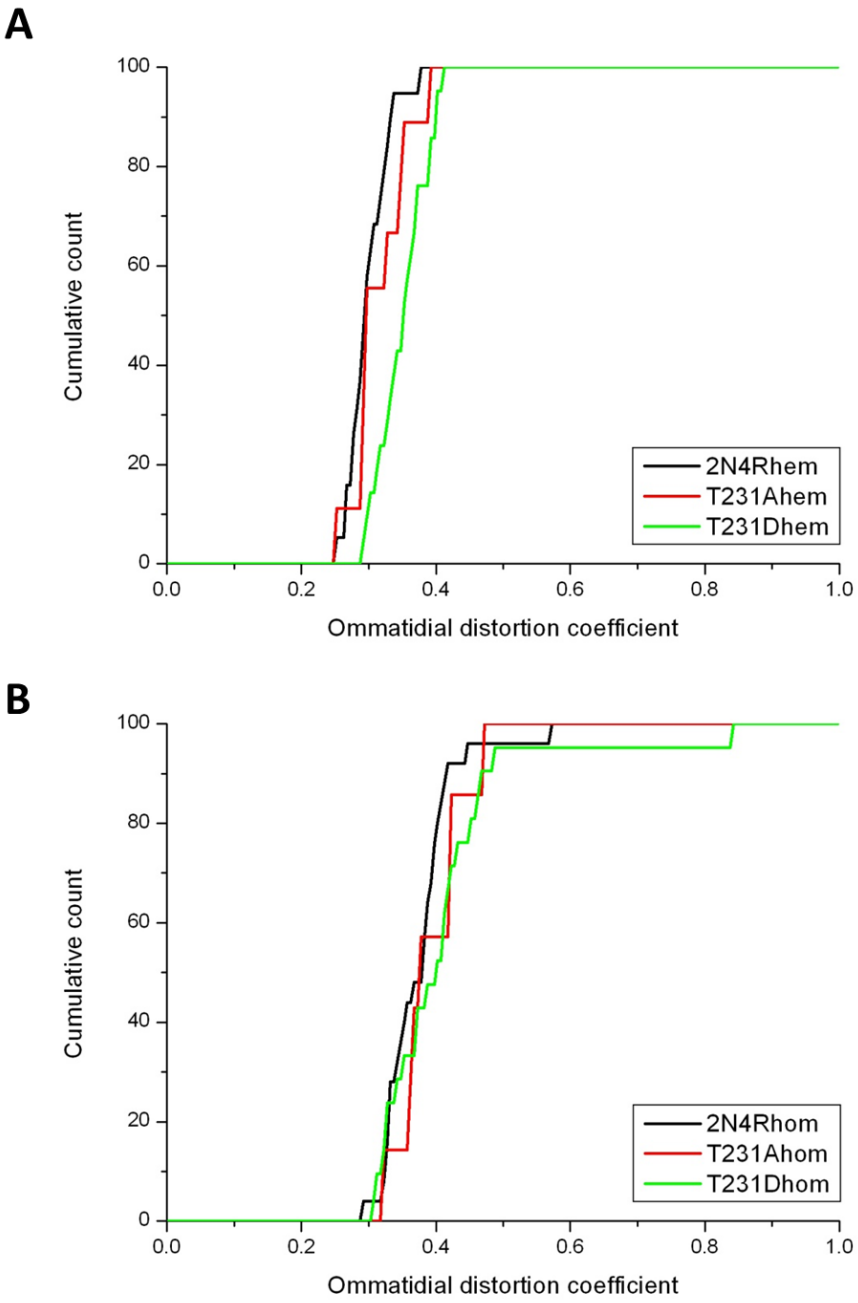

Figure 3.10 T231D mutation increases tau toxicity as measured by QED
Quantitative analysis of the phenotypes of the samples shown in Figure 3.9. The DC of T231D hem is significantly increased compared with 2N4R hem (P<0.0001) and T231A hem (P=0.0004), by Mann-Whitney U test.
A: 2N4R hem n=23. T231A hem=16. T231D hem n=24.
B: 2N4R hom n=25. T231A hom n=10. T231D hom n=21.

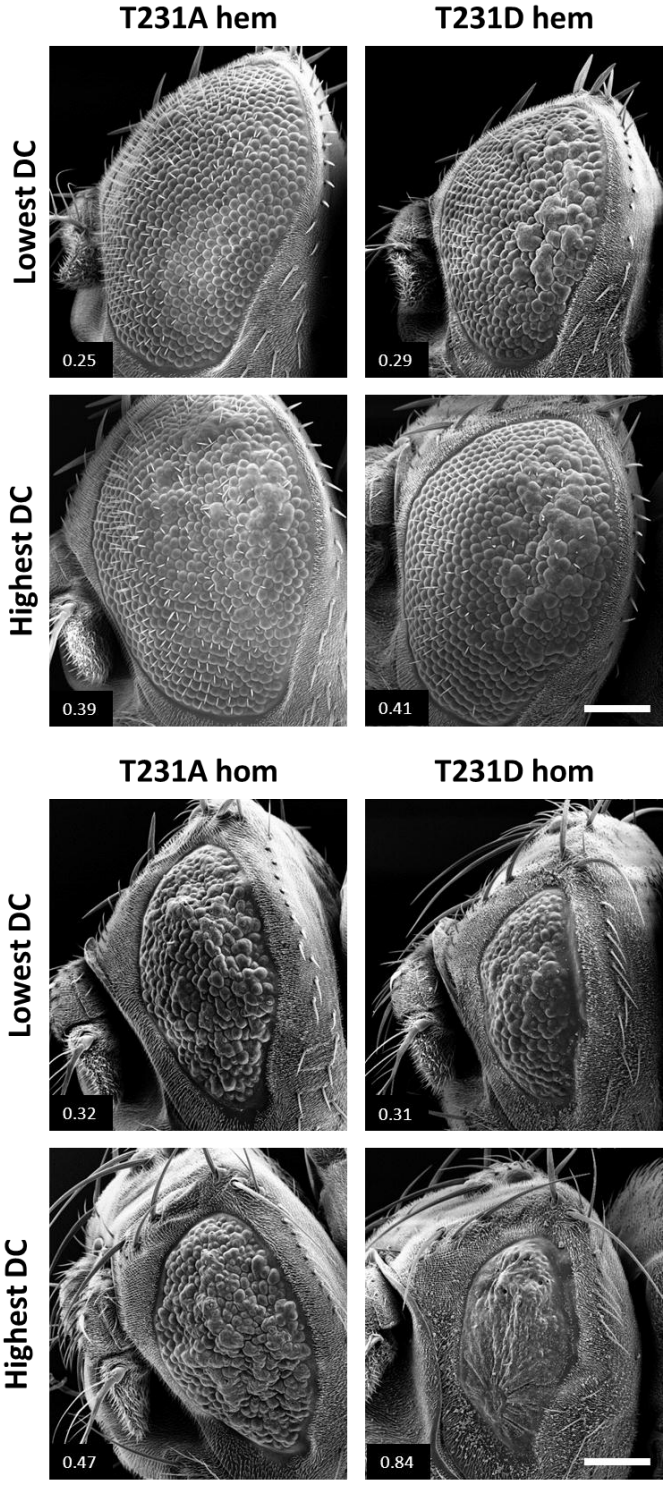

Figure 3.11 Phenotypic extremes of T231 mutants
Scanning electron microscope images showing the lowest and highest distortion coefficients for roundness in the T231A hem, T231D hem, T231A hom and T231D hom samples. Scale bar: 100μm.

3.2.3.4 Mutations at S262

The consequences of mutation of S262 are shown in Figure 3.12, it is possible to see a reduction in median ommatidial distortion in the hemizygous S262A mutant (DC of 0.28) compared with S262D (DC of 0.35), and in homozygous S262A (DC of 0.32) compared with S262D (DC of 0.37). Analysis showed a significant reduction in S262A DC compared with S262D (in hemizygous, $P<0.0001$, and homozygous $P=0.039$ – Figure 3.13). S262A was only significantly reduced compared with 2N4R WT under homozygous conditions ($P=0.004$). Hemizygous S262D was significantly increased compared with 2N4R WT ($P=0.0002$), but not in homozygous conditions. Highest and lowest DC values for S262 mutants are shown in Figure 3.14. It appears that preventing S262 phosphorylation mitigates 2N4R tau toxicity in this model. It is also possible that artificially increasing S262 phosphorylation can lead to an increase in tau toxicity.

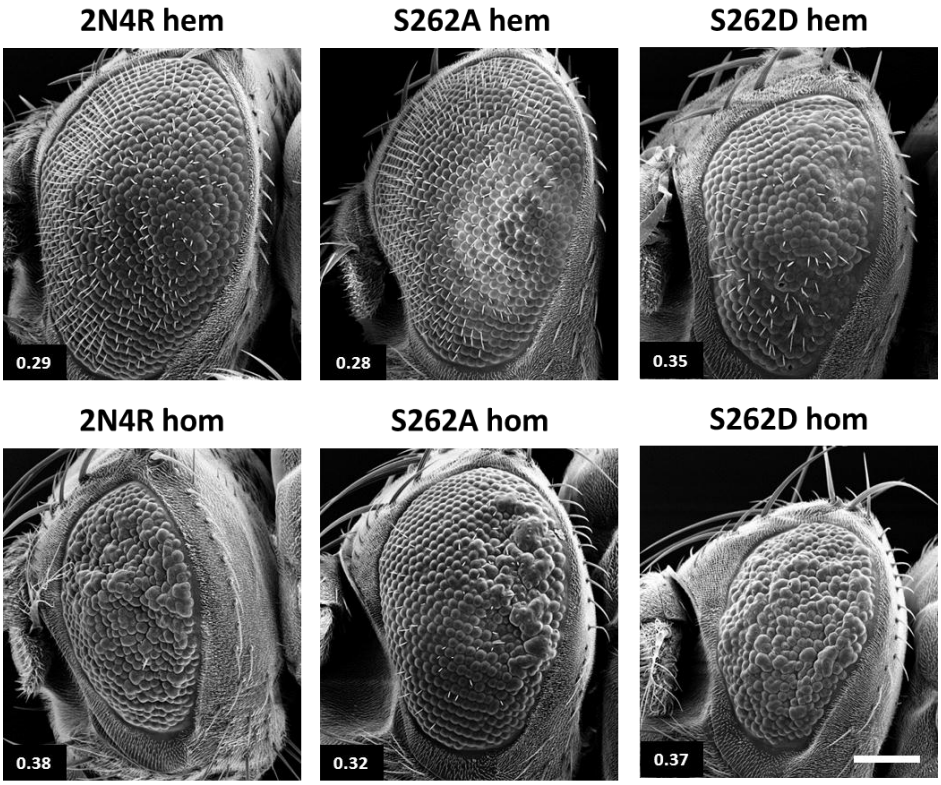

Figure 3.12 Non-phosphorylatable S262A mutation reduces tau toxicity
Scanning electron microscope images demonstrating the dosage-dependant median toxicity of human 2N4R tau, mutated at serine 262 and expressed in the fly eye under control of the GMR-GAL4 promoter. Dispersion coefficients shown on images. S262A mutants appear less distorted than the S262D mutants.
Genotypes: S262A hem: GMR-GAL4/CyO;S262A/MKRS. S262D hem: GMR-GAL4/CyO; S262D/MKRS. S262A hom: GMR-GAL4/CyO; S262A/S262A. S262D hom: GMR-GAL4/CyO;S262D/S262D. Scale bar: 100μm.

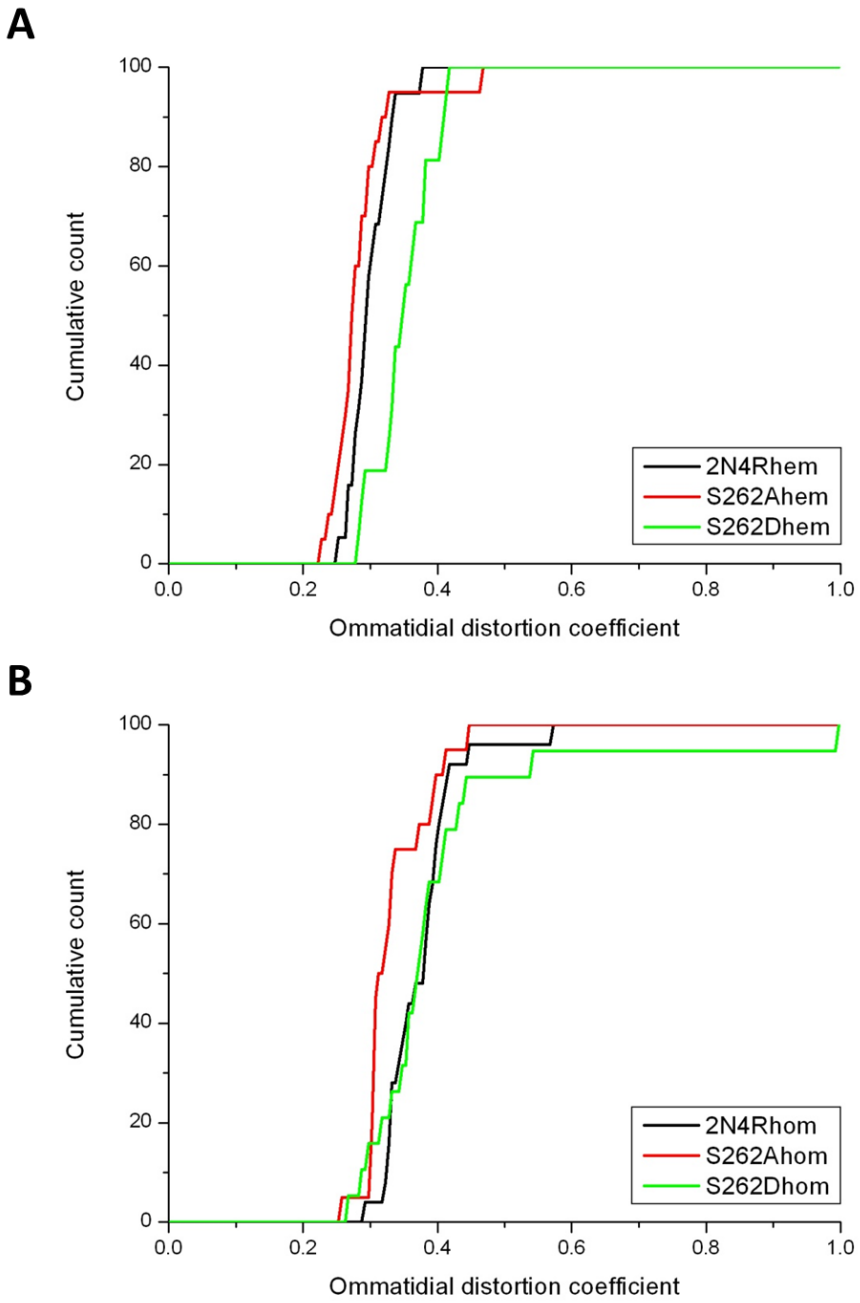

Figure 3.13 Non-phosphorylatable S262A mutants are less toxic than phospho-mimetic S262D mutants, as measured by QED

Quantitative analysis of the phenotypes of the samples shown in Figure 3.12. The DC of S262D hem is significantly increased compared with S262A hem ($P<0.0001$) and 2N4R hem ($P=0.0002$), by Mann-Whitney U test. S262A hom DC is significantly decreased compared with S262D hom DC ($P=0.04$) and 2N4R hom DC ($P=0.004$), by the same test.

A: 2N4R hem n=23. S262A hem n=20. S262D hem n=20.

B: 2N4R hom n=25. S262A hom n=20. S262D hom n=19.

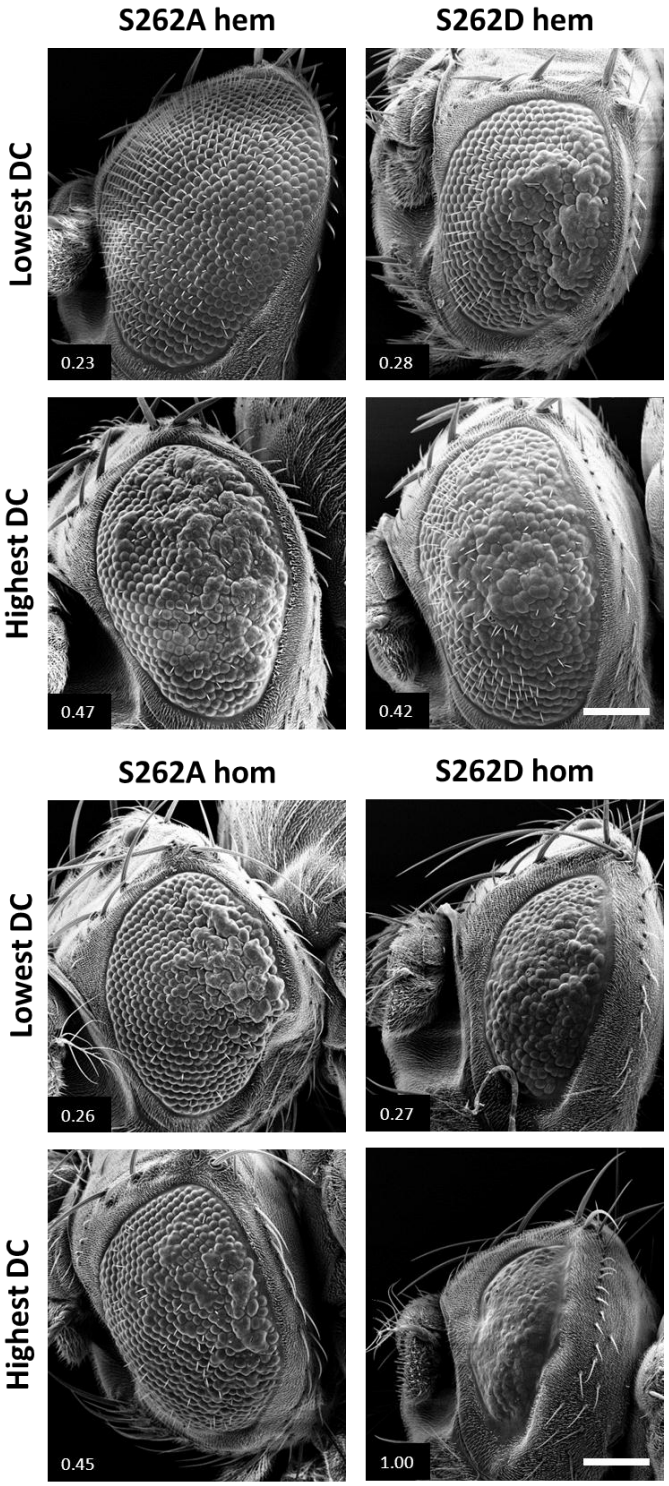

Figure 3.14 Phenotypic extremes of S262 mutants
Scanning electron microscope images showing the lowest and highest distortion coefficients for roundness in the S262A hem, S262D hem, S262A hom and S262D hom samples. Scale bar: 100μm.

3.2.4 Exploring the phosphorylation status of the mutant library

In order to begin to explore the mechanisms behind these mutation-induced changes in 2N4R tau toxicity, Western blots probing for the phosphorylated S262 epitope were performed, using the antibody anti-pS262. Quantification of these blots, performed using the Gel Analyser plugin for Fiji and by normalising the anti-pS262 signal to actin, subsequently to the corresponding T46 signal of the same sample and finally to the 2N4R wild type sample of each series, is shown in Figure 3.15. No significant differences were found between mutants when compared by ANOVA. There are several caveats to this analysis however. Some samples, notably of T231D and S262D exhibited considerable variation. In addition, the specificity of this antibody is questionable given the signal found in both S262 mutants and their variation, which should eliminate the pS262 epitope. This suggests that this antibody finds more than one epitope on 2N4R tau. This also raises an interesting point, considering that both T212D and S262A have a very comparable pS262 signal and are both toxicity-reducing mutations when assessed by eye phenotype (shown in Figure 3.7 and 3.13) – it is possible both of these mutations lower tau toxicity by preventing S262 phopshorylation. (WT n=4, T212A 1.12 ± 0.33 n=4, T212D 0.58 ± 0.17 n=5, T231A 1.03 ± 0.33 n=4, T231D 1.66 ± 0.69 n=4, S262A 0.61 ± 0.17 n=4, S262D 1.32 ± 0.47 n=4)

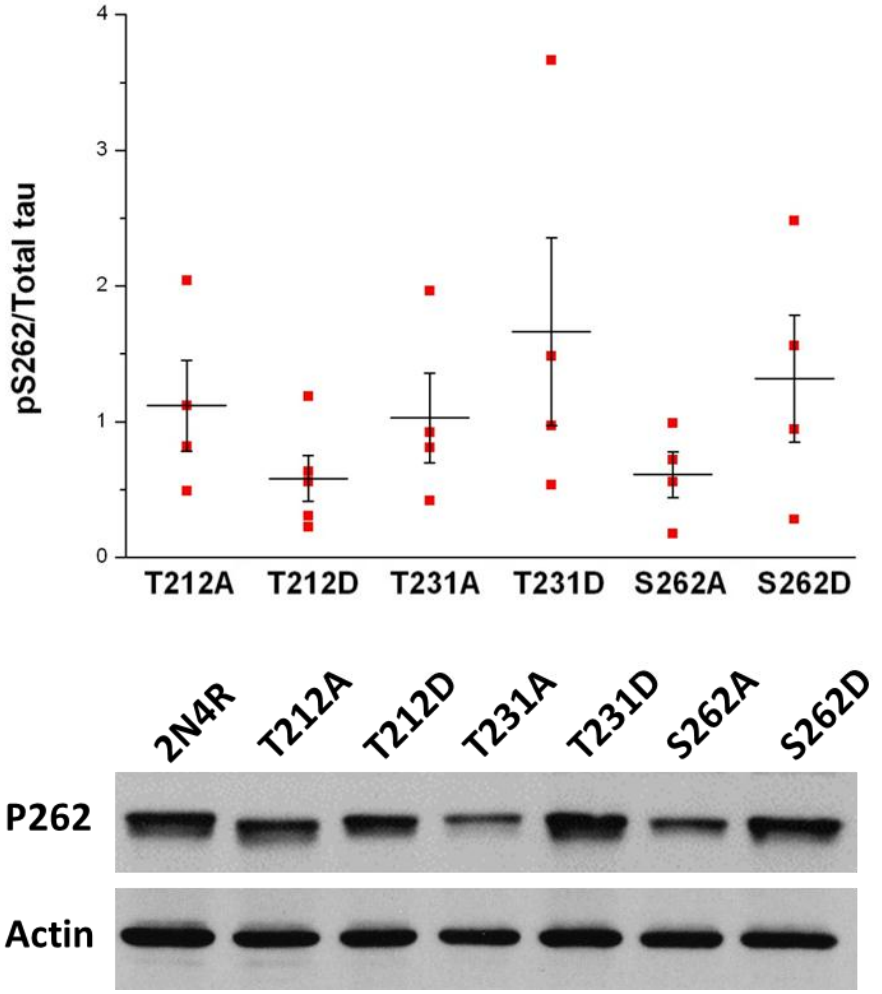

Figure 3.15 No significant differences in levels of S262 phosphorylation were found among the tau mutants

Levels of pS262 immunoreactivity were verified by Western blot using the pS262 antibody, with Drosophila actin loading control measured using the JL20 antibody. Quantified values were normalised to actin, to the total tau blot of the same sample and to wild type tau levels on each corresponding blot. pS262 immunoreactivity of mutants was not found to differ significantly from wild type or from each other by ANOVA. Flies used were hemizygous for the GMR-GAL4 promoter (over CyO balancer) and homozygous for the tau transgene. (WT n=4, T212A 1.12 ± 0.33 n=4, T212D 0.58 ± 0.17 n=5, T231A 1.03 ± 0.33 n=4, T231D 1.66 ± 0.69 n=4, S262A 0.61 ± 0.17 n=4, S262D 1.32 ± 0.47 n=4)

3.3 Discussion

Phenotypic analysis by QED was the heart of the initial screening process of this mutant library. By combining measurement of eye damage with that of transgenic protein levels, we obtain an indicator of tau toxicity, and how it can be changed by mutation.

3.3.1 Wild-type 2N4R tau

The hemizygous GMR line has been used as the initial baseline to demonstrate 2N4R tau toxicity, as the GMR promoter has previously been shown to have a minor disruptive effect (unpublished data) and was present in all subsequent tested lines in this chapter. Hemizygous and homozygous 2N4R tau lines are both more distorted than this control. The homozygous 2N4R line exhibits significantly more distortion than the single-copy line, demonstrating the dosage-dependant nature of this toxicity and the need to factor in gene expression and protein levels in any discussion of mutation-controlled modulation of tau toxicity *in vivo*. Subsequent mutant comparisons were conducted in both hemi- and homozygous conditions, in the hope that the extra information provided by these two conditions would provide greater sensitivity in differentiating phosphorylation-dependant effects.

3.3.2 Mutations of T212

The phosphorylation site T212 has been shown to be the site most prone to BRSK2-induced phosphorylation (Yoshida and Goedert, 2011), as well as heavily implicated in modulation of tau aggregation (Chang et al., 2011). This led us to propose that a major part of BRSK2-induced tau toxicity, as demonstrated previously using 0N4R tau, could be due to a change in tau aggregation kinetics induced by the kinase. Our 2N4R T212D mutant was generated in order to test this hypothesis. As it transpired, levels of toxicity in the T212D mutant appeared to be less than in 2N4R WT and in T212A by eye, differences which were corroborated by QED analysis of the hemizygous individuals. It was also significantly less than 2N4R WT among the homozygous samples, but not when compared with homozygous T212A. This is potentially due to multiple factors: the extent of phenotypic variation within populations, variation in the quality of coating before SEM imaging or the method of ommatidial measurement by QED. Another possible cause could be the apparent trend in the quantified Western blot data toward higher levels of protein in the

T212D line. This could potentially explain the lack of a difference in the homozygous comparison between T212A and T212D. These findings were initially difficult to reconcile with the effects of BRSK in 0N4R tau, but were eventually better explained by tau isoform-specific effects (see Chapter 4). These data would imply a protective role for this aggregation-inducing mutation. The lack of change caused by the T212A mutation suggests a lack of T212 phosphorylation by endogenous *Drosophila* kinases.

3.3.3 Mutations of T231

As a site implicated in modulation of tau-microtubule binding, T231 was chosen as it had previously been shown to be phosphorylated by the prototypical AMPK-related kinase, AMPK (Thornton et al., 2011) but was not addressed in the study by Yoshida and Goedert (2011) demonstrating tau phosphorylation by this family of kinases. This mutant was designed as a second example of one affecting microtubule dissociation, alongside the better-studied and more widely-implicated S262. T231's location within the proline-rich region also differentiated it from the microtubule-binding domain KXGS motif site. The SEM images obtained were not strongly indicative of any change in toxicity from these mutations, but QED testing found a significant increase in distortion in the hemizygous T231D mutant, from both 2N4R WT and T231A. This increase was not found among the homozygous phenotypes. This change is potentially due to differences in protein levels which, although again not significant, appear to exhibit a trend of reduced T231A levels. It is possible that this difference in protein levels leads to phenotypic changes at lower expression values in the hemizygous examples. Why there should be such a difference in protein levels in the first place is intriguing – expression could differ, though this should be minimised or eliminated by PhiC31 integration. It is possible that the T231A mutation has a destabilising effect on tau, targeting it for removal by endogenous mechanisms of protein clearance. The ubiquitin-proteasome system (UPS) has been proposed to play some role in tau clearance in disease models (Tseng et al., 2008) and autophagy has been heavily implicated in mitigation of tau toxicity, including in *Drosophila* (Berger et al., 2006). Autophagy has recently taken the ascendancy due to its potential for removing tau aggregates (Schaeffer et al., 2012). Such aggregates are regarded as being too large for degradation by proteasomes, and instead removed by a system of specific macroautophagy, known as aggrephagy (Overbye et al.,

2007), in which accumulated abnormal tau is sequestered into large, insoluble aggregates known as aggresomes. These aggresomes prevent free misfolded protein from forming other, potentially more toxic aggregates and are subsequently cleared by autophagy. Histone deacetylase 6 (HDAC6) has been shown to play a role in aggresome targeting, particularly following accumulation of misfolded protein due to proteasomal inhibition (Guthrie and Kraemer, 2011). Whether T231A mutant tau is more prone to degradation by autophagosomes, in a soluble or insoluble form, could be examined for example by probing for lysosome accumulation (Scott et al., 2004). Another method would be to probe for the autophagic substrate p62 (Bjorkoy et al., 2005; Pankiv et al., 2007), the abundance of which is inversely related to stimulation of autophagy (Komatsu et al., 2007). The fly p62 orthologue, Ref(2)p has also been used in this way (Nezis et al., 2008). The slight changes in phenotype of T231D flies could be due to changes in microtubule affinity, which would be expected to be less severe than changes to S262 phosphorylation according to the *in vitro* work or Kiris et al (2011).

3.3.4 Mutations of S262

The tau phosphorylation site most strongly linked to microtubule binding is S262, often singled out as a key residue for tau toxicity (Iijima-Ando et al., 2010), including amyloid β-dependant toxicity (Iijima et al., 2010). It is a target of many non-proline-directed tau kinases including MARK (Biernat et al., 1993; Drewes et al., 1995) and protein kinase A (Liu et al., 2007). In the present study, S262A mutation appeared to reduce tau toxicity when examined by eye. Quantification of hemizygous samples instead revealed a significant increase in toxicity in the S262D mutants compared with 2N4R WT or S262A; S262A hemizygous was not significantly different to 2N4R WT. In the homozygous tests, S262A was found to be significantly less toxic than 2N4R WT and S262D. This correlates well with the SEM images, in which homozygous S262A flies demonstrate much smaller eyes with much less well-defined ommatidia than in S262D or 2N4R WT-expressing animals. This is consistent with previous data from Iijima-Ando et al (2010). Multiple sources have reported S262 phosphorylation or phospho-mimetic mutants to reduce tau-microtubule binding (Fischer et al., 2009; Kiris et al., 2011; Schneider et al., 1999), so we can hypothesise that this reduction in toxicity caused by S262A mutation could be due to higher affinity of the mutant human tau for *Drosophila*

microtubules. This also demonstrates a level of S262 phosphorylation by endogenous kinases. No differences between levels of transgenic tau in the S262 lines were detected.

3.3.5 Potential mechanisms of regulation of tau toxicity by phospho-mutation

This partial human tau phospho-mutation library would seem to suggest that increasing both the affinity of human tau for *Drosophila* microtubules and the propensity of human tau for aggregation in the *Drosophila* eye protect against tau toxicity. Both of these results would support the idea that an excess of free tau is the principle driver of tau toxicity. However, there are caveats surrounding each of these proposed disease processes due to the use of *Drosophila* as a model.

In the case of tau aggregation, for a long time there was simply not much cause to expect this to happen in the fruit fly. An early study showing suspected neurofibrillary pathology with AT100 immunoreactivity (the antibody used to probe for dual T212/S214 phosphorylation, a marker for PHF formation) in the fly eye, caused by overexpression of human tau and the fly GSK3 orthologue *shaggy* (Jackson et al., 2002), was not followed by other reported sightings for a decade. The author has since downplayed the likelihood of any tangle-like pathology playing a role in *Drosophila* models of tauopathy (Dr George R. Jackson, personal communication). It was argued that fruit fly models of tauopathy were something of a coup for the now prevailing view that larger tau aggregates are less important for toxicity than soluble aggregates and PHF formation (Wittmann et al., 2001), ideas which were later backed by work in mammals (Andorfer et al., 2005). Given the much longer timescales involved in progression to tangle-positive tauopathy in humans or mammalian models, it is perhaps unsurprising that evidence for the existence of the *Drosophila* tangle was unforthcoming. More recently however, some evidence for tau aggregation has been uncovered by different groups, with differing implications for oligomeric tau toxicity. One study demonstrated the ability of wild-type human 0N4R tau to form large oligomers (>400kDa) in aged fly dopaminergic neurons, strongly resembling PHF-like filaments under electron microscope (Wu et al., 2013b). These were strongly associated with tau toxicity, with motor and learning deficits. Other insoluble granular tau oligomers (GTOs) have also been identified in fly models, and associated with a rescue of tau toxicity, either by inhibition of GSK-

3β (Cowan and Mudher, 2013) or expression of nicotinamide mononucleotide adenylyl transferase (NMNAT), a known neuroprotectant (Ali et al., 2012). In each of these cases, reduction in toxicity was associated with a loss of tau monomers and the appearance of insoluble oligomers. This leads to two possibilities surrounding the change in phenotype caused by T212D tau. One is that the mutation does indeed lead to an increase in tau-tau binding (which could potentially go no further than PHF formation or perhaps GTOs (Maeda et al., 2007)). The other is that the change in toxicity is due to another mechanism, perhaps a structural change caused by the mutation or even microtubule-binding and potentially leading to a reduction in tau phosphorylation at other sites, for example S262.

The binding of human tau to *Drosophila* microtubules has been studied using specific assays based around the ability of taxol to stabilise microtubules with their associated proteins. In some cases, human tau has been shown to bind comparably to *Drosophila* tau (and even be capable of displacing it), and this binding to be modulated by phosphorylation status or mutation (Chatterjee et al., 2009; Cowan et al., 2010). However, a separate study showed very poor binding of human tau to fly microtubules and no reduction in binding rate of endogenous tau (Feuillette et al., 2010). The same study also demonstrated a lack of improvement of human tau binding in a *Drosophila* tau null background, and an improvement in both binding and eye-specific toxicity of human tau when subject to multiple non-phosphorylatable mutations (tau-AP, lacking in most proline-directed phosphorylation sites). The methods used by Cowan et al. (2010) and Feuillette et al. (2010) use the same taxol concentration, but differ in the tau isoform used: the former used 0N3R, the latter, 0N4R. If this is what accounts for the difference then it is surprising that the isoform with more microtubule-binding repeats has lower affinity, especially given its closer similarity to five-repeat endogenous fly tau. Ultimately however, the second study does not rule out the possibility that human tau can bind to microtubules, especially following non-phosphorylatable mutation. An increase in microtubule-binding could indeed explain the reduction in toxicity of 2N4R tau following S262A mutation.

3.3.6 Examining the phosphorylation status of mutant tau

In order to further examine the mechanisms underlying our ability to manipulate tau toxicity in this way, we began to explore the phosphorylation status of the tau mutants in our library. There were initially some assumptions we could verify based on our mutation-induced phenotypic changes – T212 would be unphosphorylated, S262 phosphorylated on wild-type human tau by endogenous *Drosophila* kinases. The first phospho-blot performed was a probe of S262 phosphorylation using the antibody anti-pS262, which label all of the tau species tested. This antibody was found to lack specificity – even in S262 mutant isoforms, immunoreactivity was found. This could be due to binding at other KXGS motifs in four-repeat tau isoforms. No significant changes in phosphorylation at this site were found between mutant isoforms, possibly due to this non-specific binding generating noise, but there did appear to be a trend toward reduced immunoreactivity in the S262A mutant compared with the S262D mutant. It is unlikely that the antibody recognised the aspartate mutant, which could indicate increased binding elsewhere, potentially at other KXGS motifs. Interestingly, this trend was also found between the T212 mutants, with T212D (the less toxic isoform) exhibiting relatively reduced immunoreactivity. This is potential evidence for an association between tau toxicity and S262 phosphorylation. In order to test this, it would be useful to employ other KXGS-directed antibodies, for example pS356 or the dual S262/S356 phospho-antibody 12E8 (Wittmann et al., 2001), which would also help determine the other pS262 epitopes. This leads back to one of the possible causes of T212-induced changes in toxicity – that it potentially controls S262 phosphorylation. This could be a normal structural change upon phosphorylation or an artifact induced by the aspartate mutation. In order to verify changes in tau aggregation, PHF-recognising antibodies would also be a useful next step. Although the classical AT100 antibody would not be suitable due to the mutation of part of its epitope, other PHF antibodies do exist, targeted against other phospho-residues in the proline-rich region and elsewhere on tau. These include AT8 (Goedert et al., 1995) and PHF-1 (Otvos et al., 1994), both of which effectively label neurofibrillary deposits. Any increase in immunoreactivity would be cause to consider the possibility of an increase in PHF formation caused by T212 mutation. If not, the possibility for changes in tau secondary structure is real. The Alz50 antibody, which used been used to probe for

tangles was demonstrated to recognise a specific conformational epitope (Carmel et al., 1996). This involved a change from the so-called “paperclip” conformation of healthy tau, in which the C-terminus fold brings it close to the microtubule-binding domain (Jeganathan et al., 2006), to an Alz50 conformation in which the N-terminus holds this position (Himmelstein et al., 2012). This has been hypothesised to facilitate the stacking of tau into aggregates, but could potentially prevent phosphorylation of S262 by endogenous kinases.

These data demonstrate the potential to change toxicity caused by transgenic human 2N4R tau in the fly eye by single residue mutation. They show the lack of equivalence between phosphorylation sites, speaking to specific roles for sites potentially based on aggregation or microtubule-binding kinetics. In the next chapter, the relationship between the ability of the human kinase BRSK2 to modulate tau toxicity in this model is explored, demonstrating the effects of multiple tau mutation to mimic kinase activity and the importance of tau isoform-specific effects on toxicity.

4| Exploring the effects of BRSK-induced tau phosphorylation

4.1 Introduction

The AMPK-related protein kinases BRSK1 and BRSK2 are closely related to the tau kinase MARK. The *Caenorhabditis elegans* orthologue of the BRSKs was discovered in a screen for mutations affecting presynaptic development (Crump et al., 2001) and was named SAD-1 (for synapses of the amphid defective). Subsequently the mouse orthologues SAD-B and SAD-A (along with the respective human BRSKs) were identified by sequence homology and were characterised as expressing predominantly in the murine central nervous system, and were shown to be integral to the correct polarisation of neurons, potentially via tau phosphorylation (Kishi et al., 2005). SAD-B has also been shown to be localised presynaptically and to be associated with regulation of neurotransmitter release (Inoue et al., 2006). The pathway leading to BRSK phosphorylation and activation has also been explored, with LKB1 (Barnes et al., 2007) and CaMKKα (Fujimoto et al., 2008) both revealed to include BRSKs among their substrates. More recently, the phosphorylation of tau by BRSKs has been better characterised, demonstrating the ability of the kinases to phosphorylate tau at T212 and S262 (Yoshida and Goedert, 2011).

Previous unpublished work here at Warwick has shown that the toxicity of human 0N4R tau in a *Drosophila* model is greatly exacerbated by co-expression of BRSK2, in an LKB1 and CaMKK-dependant manner, with an increase in phosphorylation at S262. These data are all consistent with BRSK2 activity as it is understood in mammalian systems. However, whether these effects on transgenic tau toxicity in the fly are a direct result of phosphorylation by this kinase has not yet been shown.

The characterisation of BRSK2-induced phosphorylation of 1N4R tau *in vitro* by Yoshida and Goedert (2011), though not definitive, demonstrates a particularly interesting phosphorylation profile for this kinase – it was shown to target both the aggregation-associated residue T212 and the modulator of microtubule binding, S262. The consequences of individual phospho-mutations at both of the BRSK2-targeted residues (the aggregation-implicated T212 and microtubule binding-associated S262) were explored in the human 2N4R tau isoform in the previous chapter, and shown to have opposing effects on tau toxicity. That BRSK2 should have a particularly drastic effect on 0N4R tau toxicity as a result of phosphorylation at each of these sites is unintuitive. However, as was demonstrated by Kiris et al.

(2011), the consequences of tau phospho-mimetic mutation (i.e. pseudo-phosphorylation) are not necessarily additive. I therefore attempted to recapitulate the effect of BRSK2 phosphorylation by mutation, with the addition of an extra S262D mutation to the previously-generated 2N4R tau T212D mutant. By simulating putative BRSK2 phosphorylation of human tau without the presence of the additional transgene, the T212D S262D tau double mutant might potentially demonstrate the precise role played by changes to tau phosphorylation in the tau/BRSK2 phenotype, eliminating any secondary effects of the kinase due to possible interactions with other endogenous substrates. The mutant library of Chapter 3 has also allowed further exploration of the nature of the tau/BRSK2 interaction, as well as raising questions regarding the differences between tau isoforms as relates to toxicity.

4.2 Results

The GMR promoter and QED software were again used to evaluate the effect of BRSK2 on tau toxicity and the toxicity of BRSK2 phosphorylation-mimicking mutation.

4.2.1 Tau isoform-specific effects of BRSK2

In order to determine the effect of human BRSK2 on the 2N4R tau phenotype, *Drosophila* containing wild type BRSK2 on the third chromosome (named B2WT5) were crossed to the 2N4R WT tau line and also to a line containing 0N4R WT tau. In Figure 4.1, median DC images are shown for GMR (0.24), B2WT5 (0.22), 0N4R WT (0.50) and 2N4R WT tau (0.29), as well as flies containing either tau isoform alongside B2WT5 (0.78 for 0N4R/B2WT5, 0.25 for 2N4R/B2WT5). 0N4R/B2WT5 recombinants shown were reared at 23°C due to lethality at 25°C. The drastic increase in toxicity in the 0N4R/B2WT5 recombinant line is clearly visible by eye. Analysis by QED (Figure 4.2) indicated a slight but significant reduction in DC of the GMR distribution when expressing B2WT5 alone ($P=0.0017$). The two different hemizygous tau isoform samples, of which 0N4R was not generated by specific insertion, have significantly differing DCs ($P<0.0001$). 0N4R tau toxicity is drastically increased in the recombinant 0N4R/B2WT5 line ($P=0.0002$), in contrast to 2N4R tau toxicity, which is reduced in the non-recombinant 2N4R/B2WT5 line ($P=0.0002$). Eyes displaying minimum and maximum DC values for each genotype are shown in Figure 4.3.

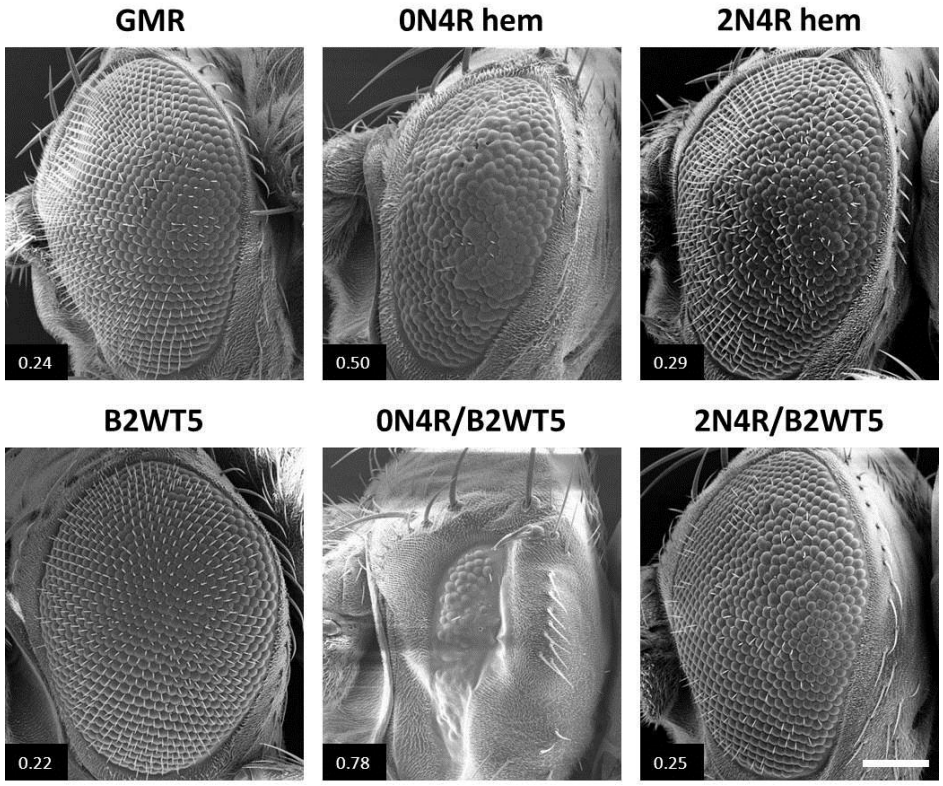

Figure 4.1: Co-expression of BRSK2 with 0N4R tau increases tau-induced toxicity; co-expression with 2N4R tau does not

Scanning electron microscope images demonstrating the lack of phenotype caused by expression of human BRSK2 in the fly eye, the disruption caused by human 0N4R or 2N4R tau, and the change in phenotype caused by co-expression of BRSK2 with the different tau isoforms. Images used were of sample median DC values, shown on images.

Genotypes: GMR: GMR-GAL4/CyO;MKRS/TM6B. B2WT5: GMR-GAL4/CyO; BRSK2 WT5/TM6B. 0N4R hem: GMR-GAL4/CyO; 0N4R WT/TM6B. 0N4R/B2WT5: GMR-GAL4/CyO; 0N4R WT, BRSK2 WT5/TM6B. 2N4R hem: GMR-GAL4/CyO;2N4R WT/MKRS. 2N4R/B2WT5: GMR-GAL4/CyO; 2N4R WT/BRSK2 WT5. Scale bar: 100μm.

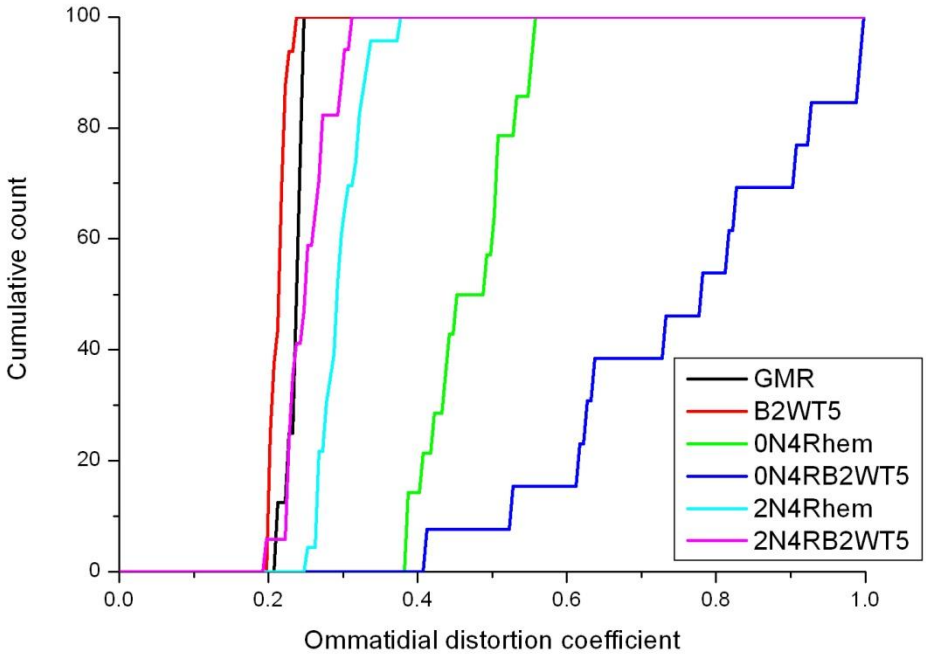

Figure 4.2 BRSK2 dramatically increases 0N4R tau toxicity; in contrast, BRSK2 reduces 2N4R tau-induced toxicity as measured by QED

Quantitative analysis of the phenotypes of the populations shown in Figure 4.1. B2WT5 has significantly lower DCs than GMR (P=0.0017) by Mann-Whitney U test. DCs of 0N4R/B2WT5 recombinants are significantly higher than 0N4R hem, also by Mann-Whitney U test (P=0.0002). DCs of 2N4R/B2WT5 are significantly less than 2N4R hem by the same test (P=0.0002).

GMR n=8. B2WT5 n=16. 0N4R hem n=14. 0N4R/B2WT5 n=13. 2N4R hem n=23. 2N4R/B2WT5 n=17.

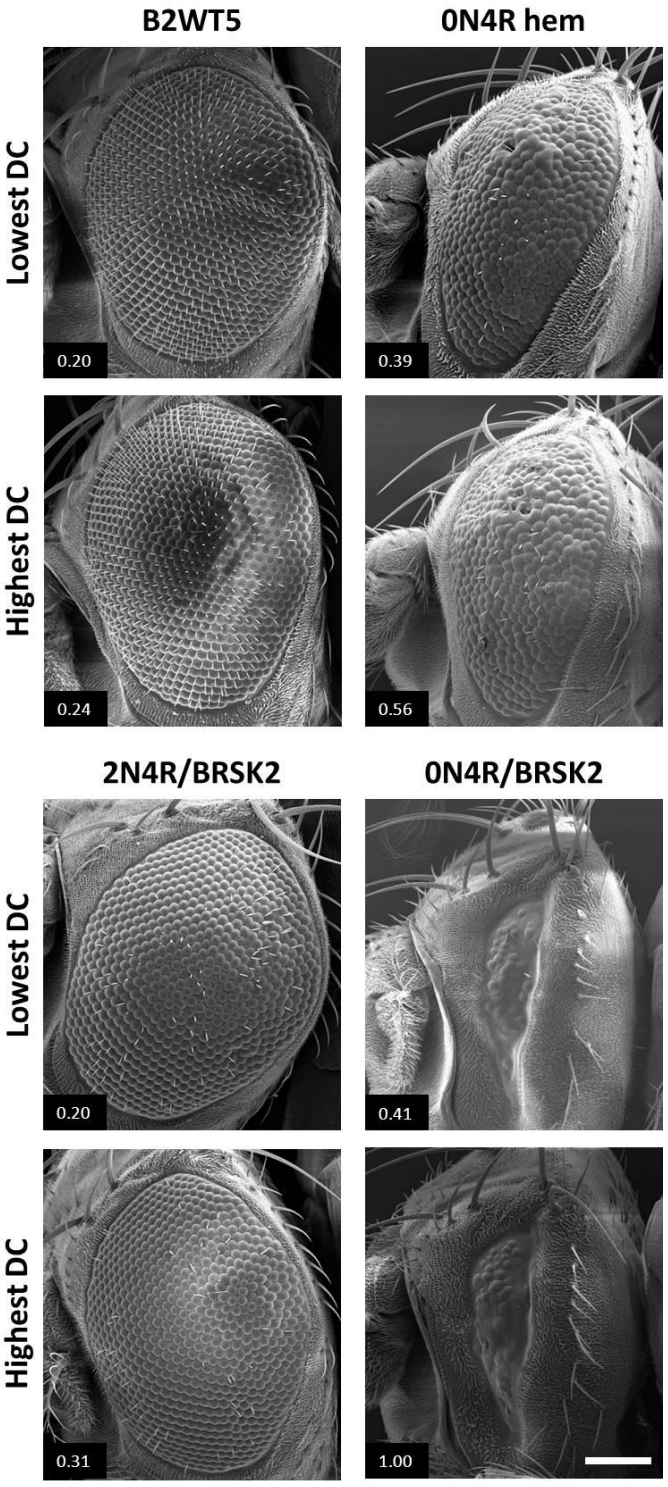

Figure 4.3 Phenotypic extremes of BRSK2-expressing flies
Scanning electron microscope images showing the lowest and highest distortion coefficients for roundness among the 0N4R hem, 0N4R/B2WT5, 2N4R hem and 2N4R/B2WT5 samples. DC values shown on images. Scale bar: 100µm.

4.2.2 Recapitulation of the tau/BRSK2 phenotype by phospho-mimetic mutation

A double phospho-mimetic mutant, T212D/S262D was generated by site-directed mutagenesis in order to mimic tau phosphorylation by BRSK2 as described by Yoshida and Goedert (2011). The previously generated T212D mutant plasmid underwent further mutagenesis to add the S262D mutation. The resulting double mutant was then subcloned and inserted at the P2 PhiC3 integrase site as already described (Section 3.2.1). The median DC value images of this genotype are compared with 2N4R WT and 2N4R/B2WT5 in Figure 4.4. The double mutant exhibits visibly reduced toxicity compared with hemizygous 2N4R WT. QED analysis of these samples is shown in Figure 4.5. Hemi- and homozygous 2N4R tau DC values were found to be reduced significantly by introduction of these two mutations (P values of 0.0008 and <0.0001, respectively). T212D S262D hem DC values were not found to differ significantly from those of 2N4R/B2WT5 (P=0.41). Eyes showing minimum and maximum DC values for the double mutant phenotypes are shown in Figure 4.6.

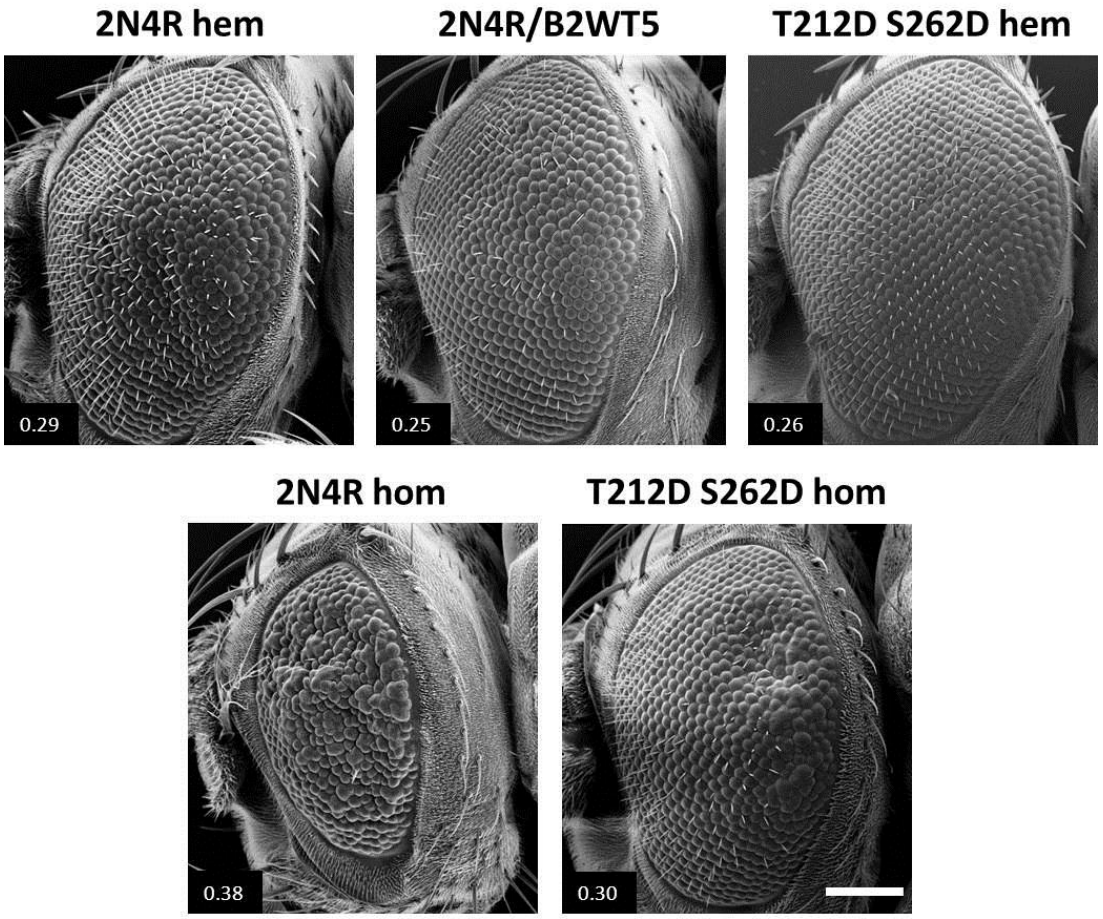

Figure 4.4 Double phospho-mimetic T212D S262D mutation reduces tau toxicity *Scanning electron microscope images. Dispersion coefficients shown on images. Genotypes: 2N4R hem: GMR-GAL4/CyO; 2N4R WT/MKRS. 2N4R/B2WT5: GMR-GAL4/CyO; 2N4R WT/BRSK2 WT5. T212D S262D hem: GMR-GAL4/CyO; T212D S262D/MKRS. 2N4R hom: GMR-GAL4/CyO; 2N4R WT/2N4R WT. T212D S262D hom: GMR-GAL4/CyO; T212D S262D/ T212D S262D. Scale bar: 100μm.*

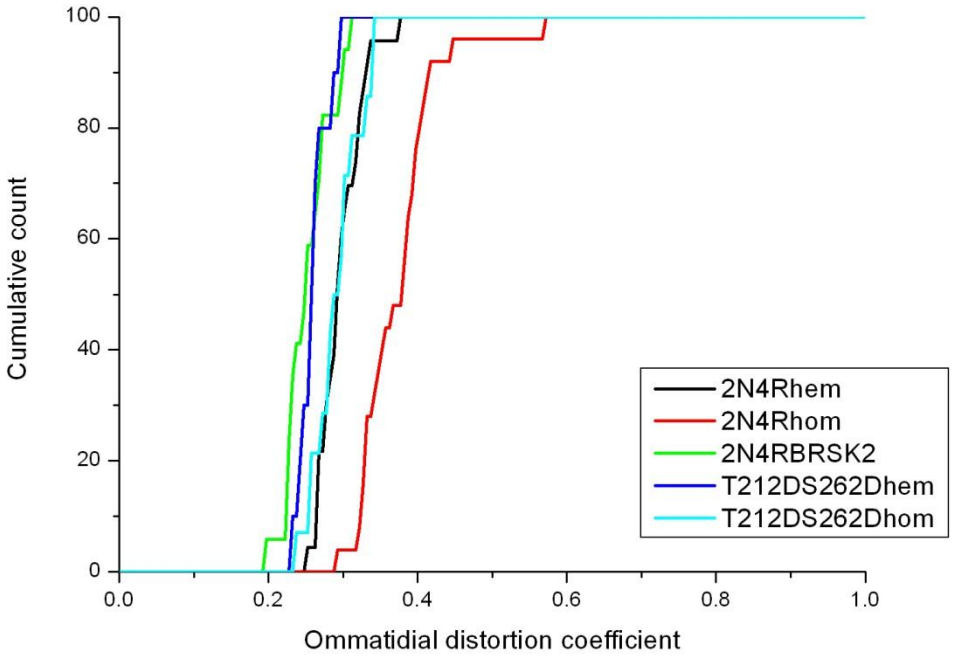

Figure 4.5 The phospho-mimetic double tau mutant exhibits a phenotype very similar to that of wild type 2N4R tau co-expressed with BRSK2, as measured by QED

Quantitative analysis of the phenotypes of the samples shown in Figure 4.4. The DC of T212D S262D hem is significantly less than that of 2N4R hem (P=0.0008), by Mann-Whitney U test. The DC of T212D S262D hom is significantly less than that of 2N4R hom (P<0.0001), by the same test.
2N4R hem n=23. 2N4R hom n=25. 2N4R/B2WT5 n=17. T212D S262D hem n=10. T212D S262D hom n=14.

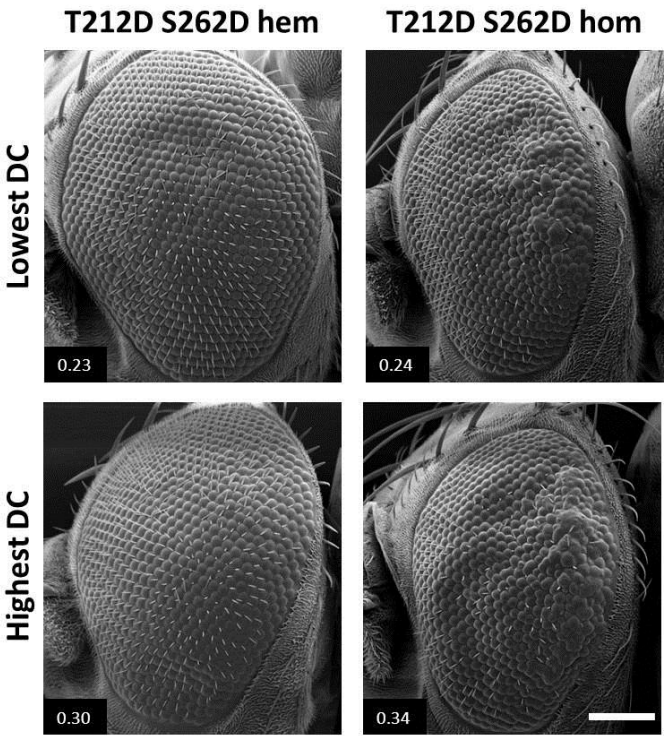

Figure 4.6 Phenotypic extremes of T212D S262D tau-expressing flies
Scanning electron microscope images showing the lowest and highest distortion coefficients for roundness among the T212D S262D hem and hom samples. DC values shown on images. Scale bar: 100μm.

4.2.3 The effect of single-residue tau mutation on the tau/BRSK2 phenotype

The double phospho-mimetic 2N4R tau mutations caused a very comparable change in phenotype to BRSK2, suggesting that phosphorylation at T212 and S262 constituted the major part of tau phenotypic modulation by the kinase. However, this did not definitively prove that the effect of BRSK2 was solely due to these phosphorylation sites; indeed, the phenotypic correlation between the two could have been coincidental, with very similar phenotypes arising from different mechanisms in each case. Another possibility is that a larger number of phosphorylation sites are targeted by BRSK2, with a combined effect very similar to the double mutant.

The 2N4R tau mutant library provided an opportunity to explore the interaction between 2N4R tau and BRSK2 further. Non-phosphorylatable mutation at T212 or S262 should have predictable effects on BRSK2 phenotypic modulation, blocking its activity provided these sites are essential to this interaction. A similar experiment has previously been performed in 0N4R tau, in which an S262A mutation blocked exacerbation of toxicity by BRSK2 (Dr. Ceri Lyn-Adams, unpublished data). The T231 mutants were also tested as phosphorylation at this site by BRSK2 has not been examined previously.

4.2.3.1 T212 mutation and BRSK2

T212 mutant lines were crossed with B2WT5 to determine any change in the ability of BRSK2 to mitigate 2N4R tau toxicity in these mutants. Figure 4.7 shows the median DC value images for T212A hem (0.31) and T212D hem (0.27), alongside lines co-expressing BRSK2 on the third chromosome (0.24 And 0.27, respectively). Toxicity caused by T212A hem appears to be reduced by BRSK2. There is no clear reduction in phenotype in the T212D/B2WT5 sample compared with T212D hem. According to QED in Figure 4.8, BRSK2 significantly reduced T212A tau-induced ommatidial distortion ($P<0.0001$). There is no significant change between T212D hem and T212D/B2WT5 ($P=0.19$). Figure 4.9 contains eyes showing the lowest and highest DC values for the samples introduced in Figure 4.7.

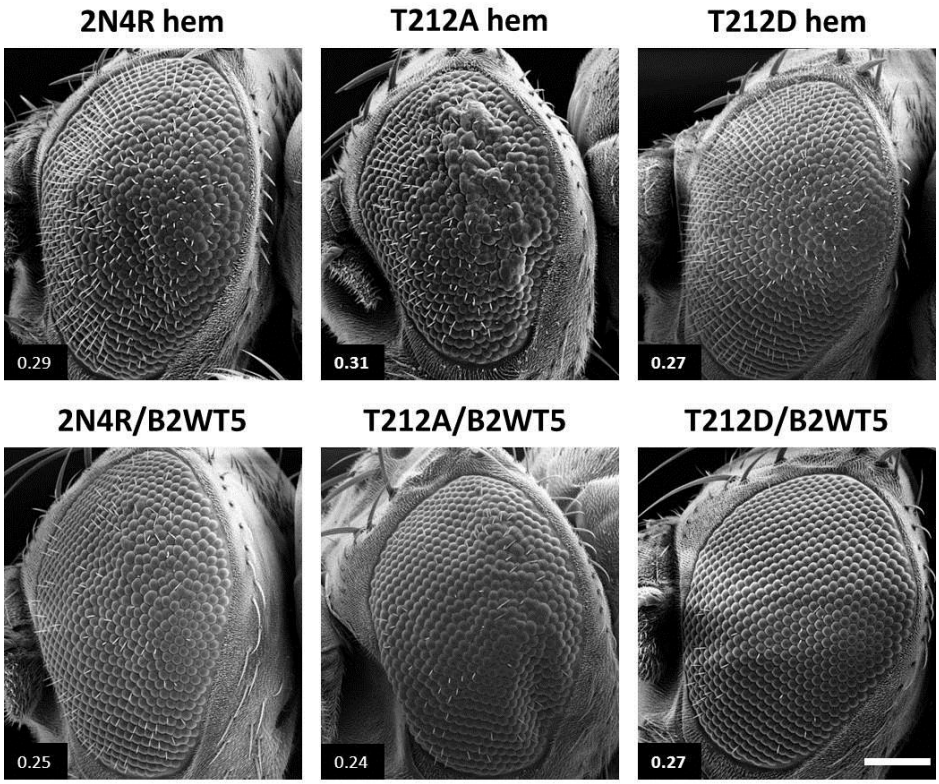

Figure 4.7 Co-expression of BRSK2 alongside T212 mutant tau appears to reduce tau toxicity

Scanning electron microscope images demonstrating the median toxicity of human 2N4R tau, mutated at threonine 212, with or without BRSK2 co-expression and expressed in the fly eye under control of the GMR-GAL4 promoter. Dispersion coefficients shown on images. BRSK2 appears capable of reducing tau toxicity caused by T212A tau.

Genotypes: T212A hem: GMR-GAL4/CyO; T212A/MKRS. T212D hem: GMR-GAL4/CyO; T212D/MKRS. T212A/B2WT5: GMR-GAL4/CyO; T212A/BRSK2 WT5. T212D/B2WT5: GMR-GAL4/CyO; T212D/BRSK2 WT5. Scale bar: 100μm.

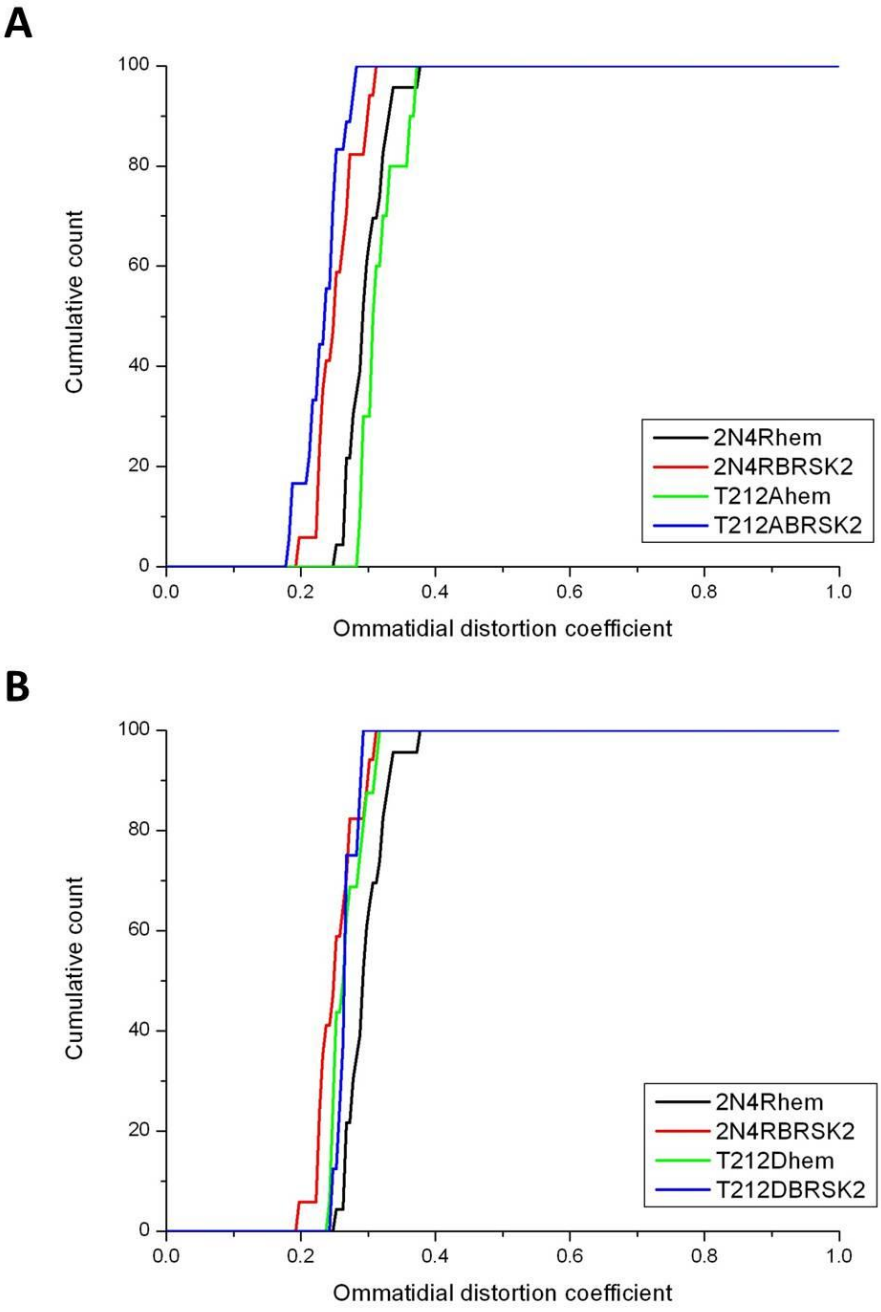

Figure 4.8 The ability of BRSK2 to mitigate 2N4R tau-induced toxicity is unaffected by T212 mutation

Quantitative analysis of the phenotypes of the samples shown in Figure 4.7. The DC of T212A hem is significantly more than that of T212A/BRSK2 ($P<0.0001$), by Mann-Whitney U test.

A: 2N4R hem n=23. 2N4R/B2WT5 n=17. T212A hem n=14. T212A/B2WT5 n=18.

B: 2N4R hem n=23. 2N4R/B2WT5 n=17. T212D hem n=18. T212D/B2WT5 n=8.

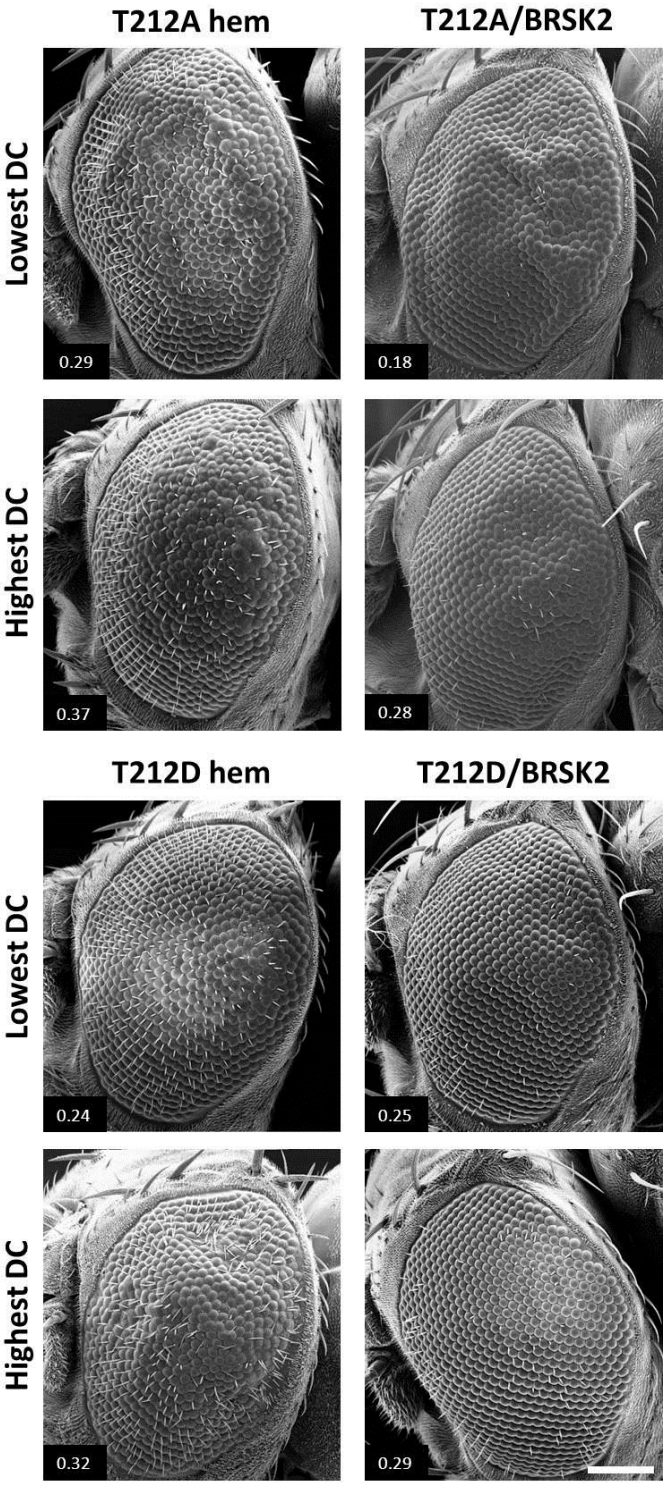

Figure 4.9 Phenotypic extremes of flies co-expressing BRSK2 and T212 mutant tau

Scanning electron microscope images showing the lowest and highest distortion coefficients for roundness in the T212A hem, T212A/B2WT5, T212D hem and T212D/B2WT5 samples. Scale bar: 100μm.

4.2.3.2 T231 mutation and BRSK2

Figure 4.10 shows median DC value images for T231 mutants with (T231A hem DC=0.30, T231D hem DC=0.35) or without (T231A/B2WT5 DC=0.31, T231D/B2WT5 DC=0.27) BRSK2 co-expression. Visually, T231A/B2WT5 appears similar to T231A hem. T231D/B2WT5 appears to exhibit reduced toxicity. Analysis by QED (Figure 4.11) shows the inability of BRSK2 to reduce T231A toxicity ($P=0.84$). T231D/B2WT5 DC values are significantly reduced compared with T231D hem ($P<0.0001$). Figure 4.12 shows the lowest and highest DC value individual for each.

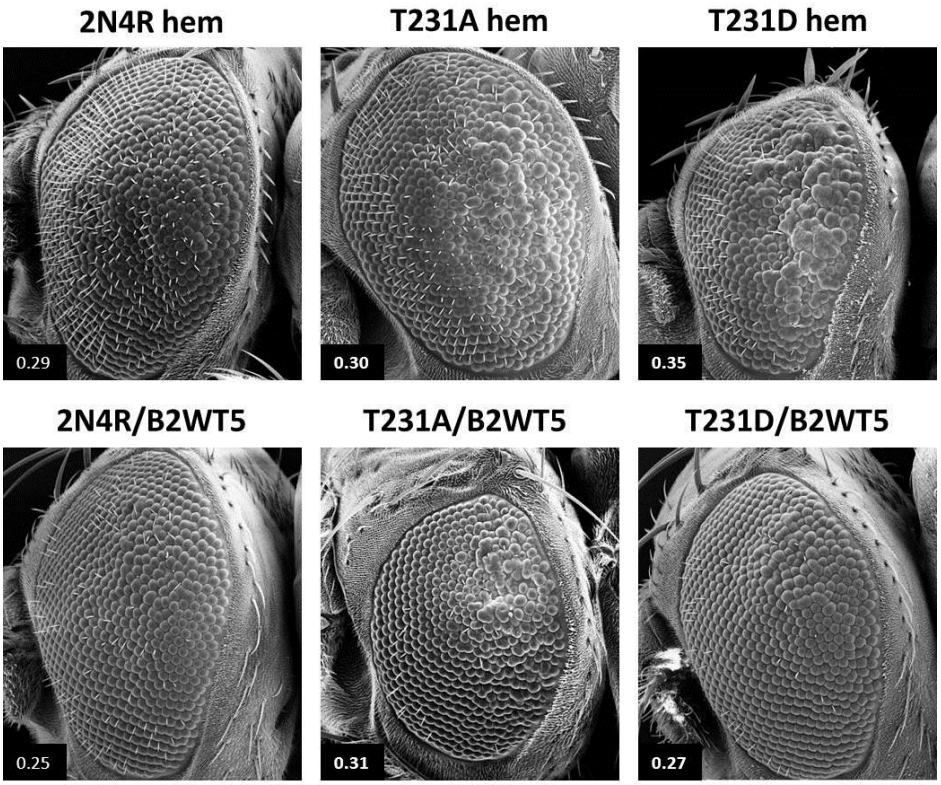

Figure 4.10 Co-expression of BRSK2 with T231A tau has no obvious phenotypic effect, unlike with T231D tau, in which a reduction in toxicity is noticeable
Scanning electron microscope images demonstrating the median toxicity of human 2N4R tau, mutated at threonine 231, with or without BRSK2 co-expression and expressed in the fly eye under control of the GMR-GAL4 promoter. Dispersion coefficients shown on images. BRSK2 appears unable to reduce toxicity caused by T231A.
Genotypes: T231A hem: GMR-GAL4/CyO; T231A/MKRS. T231D hem: GMR-GAL4/CyO; T231D/MKRS. T231A/B2WT5: GMR-GAL4/CyO; T231A/BRSK2 WT5. T231D/B2WT5: GMR-GAL4/CyO; T231D/BRSK2 WT5. Scale bar: 100μm.

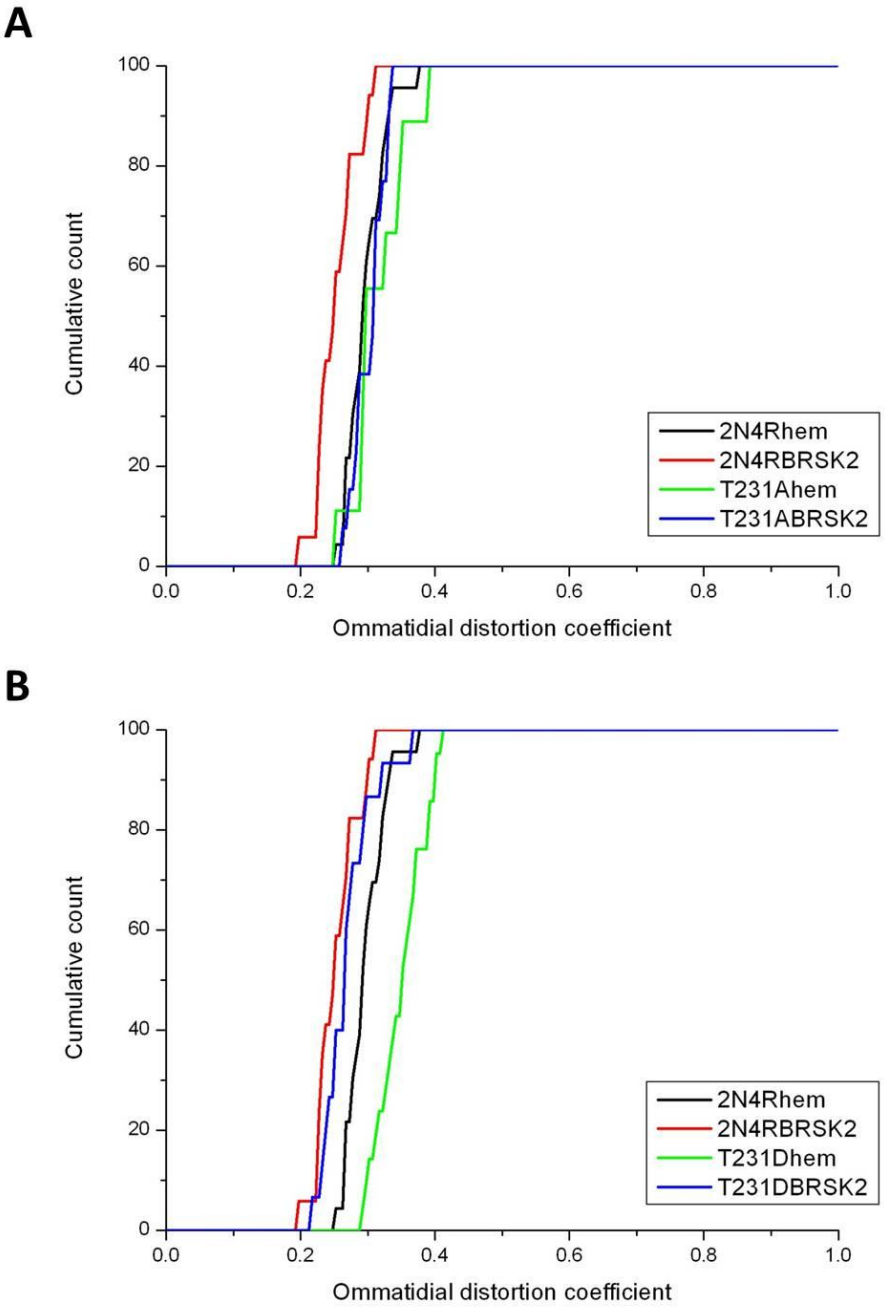

Figure 4.11 The ability of BRSK2 to reduce 2N4R tau-induced toxicity is blocked by T231A mutation

Quantitative analysis of the phenotypes of the samples shown in Figure 4.10. T231D hem DC is significantly more than that of T231D/B2WT5 by Mann-Whitney U test ($P<0.0001$).

A: 2N4R hem n=23. 2N4R/B2WT5 n=17. T231A hem n=16. T231A/B2WT5 n=13.

B: 2N4R hem n=23. 2N4R/B2WT5 n=17. T231D hem n=24. T231D/B2WT5 n=15.

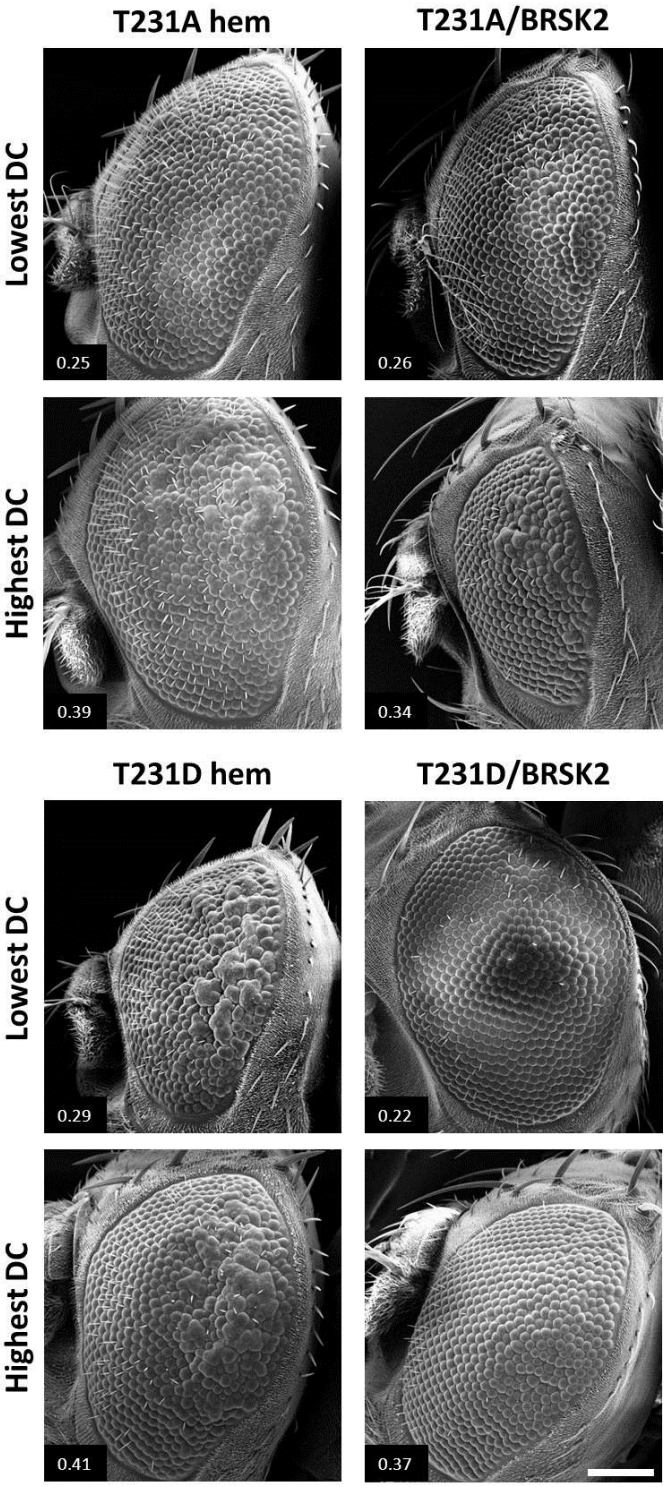

Figure 4.12 Phenotypic extremes of flies co-expressingBRSK2 and T231 mutant tau

Scanning electron microscope images showing the lowest and highest distortion coefficients for roundness in the T231A hem, T231A/B2WT5, T231D hem and T231D/B2WT5 samples. Scale bar: 100μm.

4.2.3.3 S262 mutation and BRSK2

The effect of S262 mutation on the 2N4R tau/BRSK2 interaction was examined in the same way. Figure 4.13 shows the median DC values for S262A hem (0.28), S262A/B2WT5 (0.20), S262D hem (0.35) and S262D/B2WT5 (0.24). In each case it would appear that BRSK2 retains its capacity for reducing 2N4R tau toxicity. Analysis by QED (Figure 4.14) shows both S262A and S262D toxicity can be reduced by BRSK2 ($P<0.0001$ for S262A, $P=0.0003$ for S262D). Images with extreme DC values are shown in Figure 4.15.

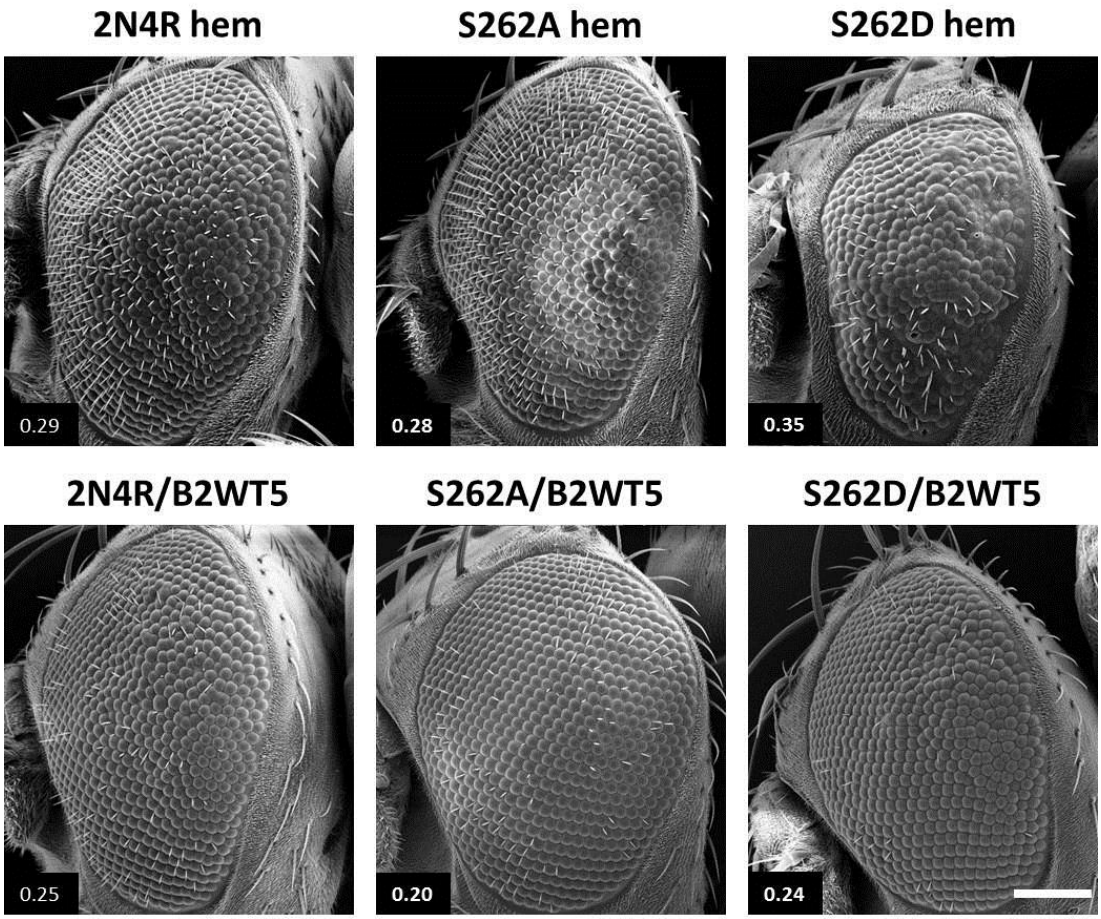

Figure 4.13 Co-expression of BRSK2 with S262 mutant tau leads to a reduction in tau toxicity

Scanning electron microscope images demonstrating the median toxicity of human 2N4R tau, mutated at serine 262, with or without BRSK2 co-expression and expressed in the fly eye under control of the GMR-GAL4 promoter. Dispersion coefficients shown on images. BRSK2 appears capable of reducing tau toxicity in each case.

Genotypes: S262A hem: GMR-GAL4/CyO ; S262A/MKRS. S262D hem: GMR-GAL4/CyO; S262D/MKRS. S262A/B2WT5: GMR-GAL4/CyO; S262A/BRSK2 WT5. S262D/B2WT5: GMR-GAL4/CyO; S262D/BRSK2 WT5. Scale bar: 100μm.

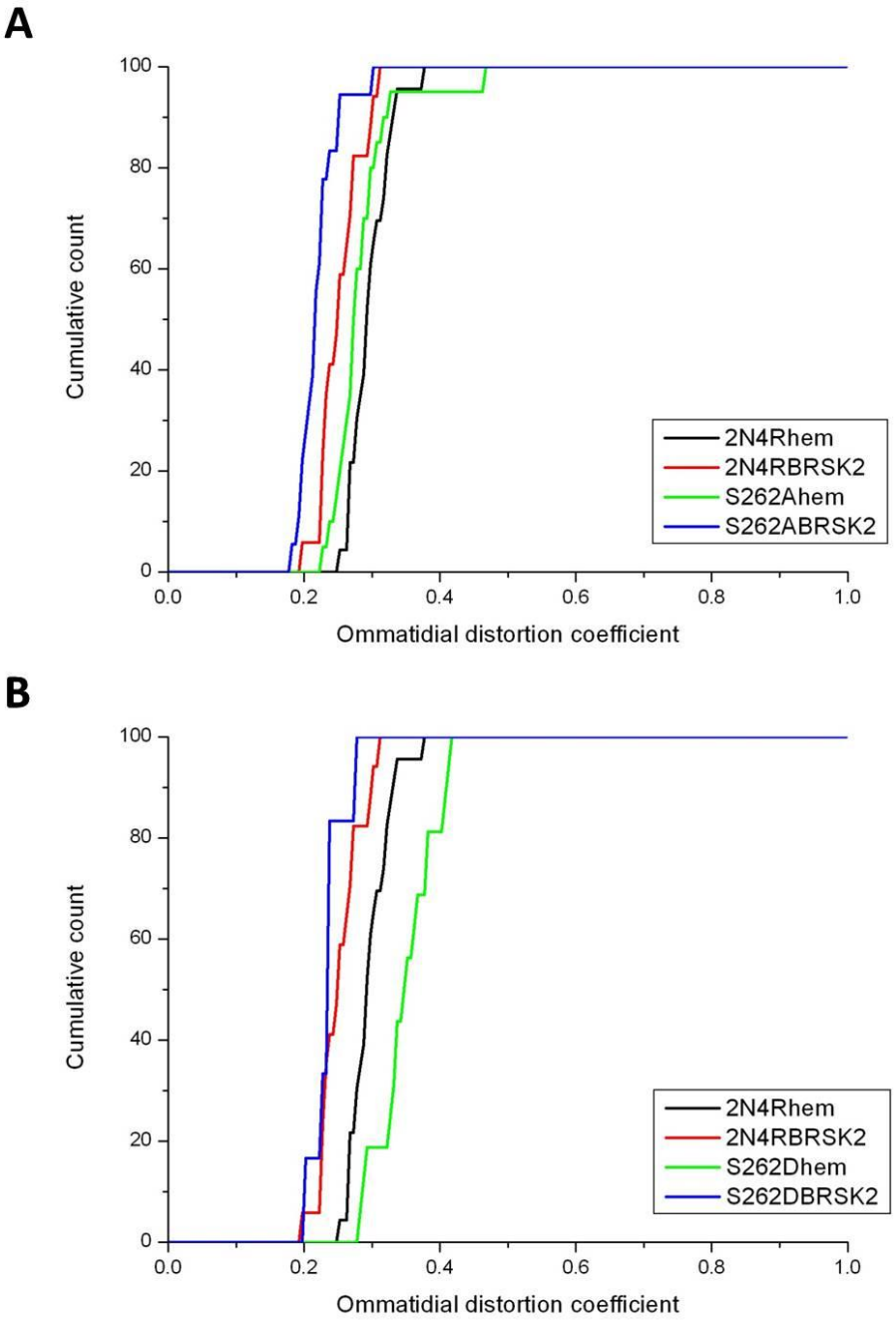

Figure 4.14 The ability of BRSK2 to reduce 2N4R tau-induced toxicity is unaffected by S262 mutation

Quantitative analysis of the phenotypes of the samples shown in Figure 4.10. S262A hem DC is significantly more than that of S262A/B2WT5 by Mann-Whitney U test ($P<0.0001$). S262D hem DC is significantly more than that of S262D/B2WT5 by the same test ($P=0.0003$).

A: 2N4R hem n=23. 2N4R/B2WT5 n=17. S262A hem n=20. S262A/B2WT5 n=18.

B: 2N4R hem n=23. 2N4R/B2WT5 n=17. S262D hem n=20. S262D/B2WT5 n=6.

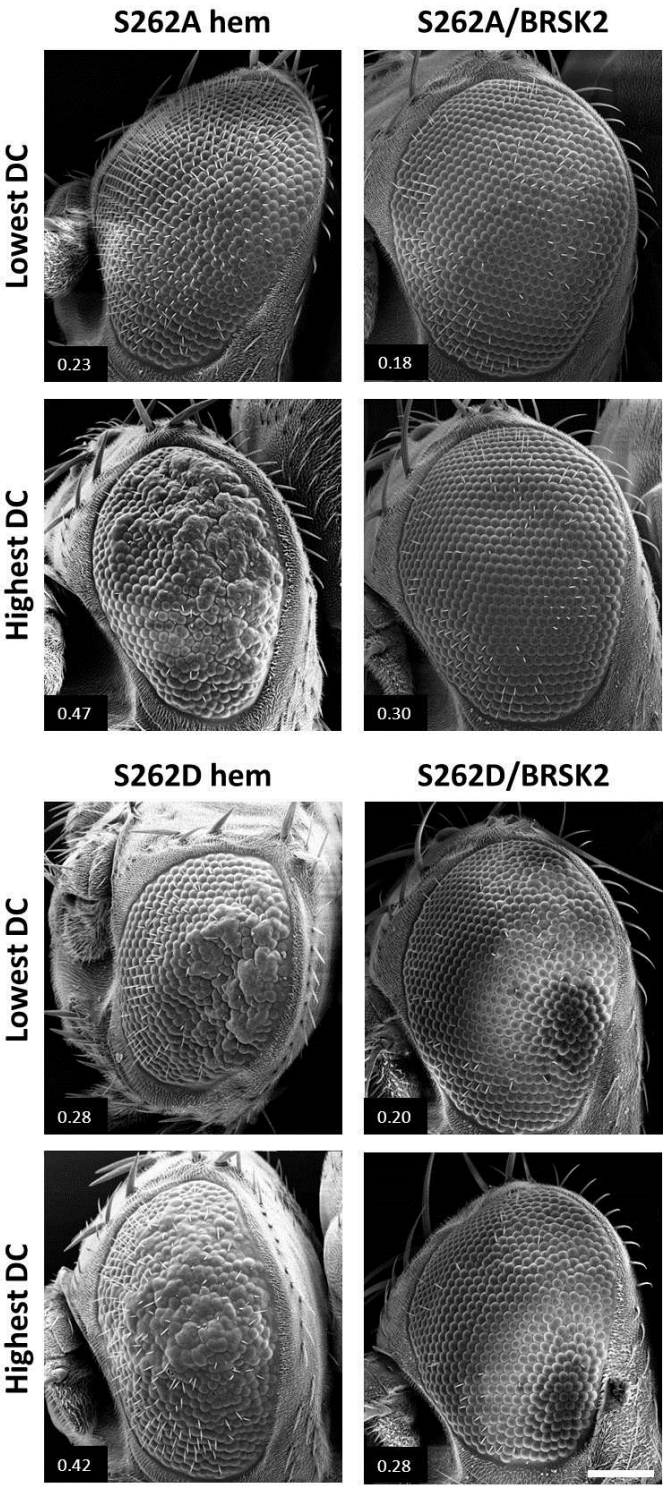

Figure 4.15 Phenotypic extremes of flies co-expressing BRSK2 and S262 mutant tau

Scanning electron microscope images showing the lowest and highest distortion coefficients for roundness in the S262A hem, S262A/B2WT5, S262D hem and S262D/B2WT5 samples. Scale bar: 100µm.

4.3 Discussion

This chapter has continued the exploration of the role of phosphorylation in human toxicity in a *Drosophila* model by examining the effect of the human kinase BRSK2. By expanding previous work by the Moffat and Frenguelli labs, demonstrating the ability of BRSK2 to exacerbate toxicity caused by the 0N4R isoform of human tau, this has revealed clear differences between tau isoforms in phenotypic changes caused by BRSK2.

4.3.1 BRSK2 influences tau toxicity in an isoform-dependent manner

Previous, unpublished data on the transgenic *Drosophila* lines expressing BRSK2 (B2WT5) and human 0N4R tau (0N4R) had demonstrated a severely neurotoxic interaction between the two human transgenes in the fly eye. Expression of BRSK2 alone, controlled by GMR led to no detectable increase in eye phenotype. Indeed QED analysis indicated a slight reduction in distortion compared with the GMR line, due either to variation in image quality leading to slight changes in edgeset integrity, or potentially a rescue of the minor changes previously recorded in the GMR line. This BRSK2-expressing line was generated by random insertion; the transgene was located on the third chromosome. The same was also true of the 0N4R line. These lines were generated prior to the decision being taken to generate all subsequent lines using the PhiC31 integrase-mediated specific insertion system which led to the generation of the 2N4R library. As a result, expression levels of these transgenes are dependent on positional effects relating to the insertion point which complicates direct comparison of the potency of the two wild type tau isoforms. This could explain the significantly more severe DC values of the 0N4R samples, compared with those of the 2N4R WT line. Regardless, it is clear that both 0N4R and 2N4R tau are capable of driving neurotoxicity in the fly eye. It is in their response to BRSK2 co-expression that the two isoforms differ dramatically.

Previous work on the 0N4R tau/BRSK2 interaction demonstrated the ability of BRSK2 to dramatically increase 0N4R tau-induced toxicity. Indeed, the toxicity of the recombinant 0N4R/B2WT5 line shown in Figure 4.1 is such that it cannot be reared to eclosion at 25°C, likely due to a certain amount of leakiness in the GMR promoter, as has been described in some other studies (Mondal et al., 2007; Xu et al.,

2003). To combat this, the 0N4R/B2WT5 samples analysed were reared at 23°C. This interaction was shown to be based upon conserved pathways of BRSK2 induction, with suppression of LKB1 or the CaMKK homologue CG17698 by RNAi both capable of reducing BRSK2-induced exacerbation of the tau phenotype. This work also outlined a pathway leading from Ca^{2+} to tau toxicity; via the fly Ca^{2+} channel α subunit cac1, through CaMKK and BRSK2, to tau. This work was unusual in *Drosophila* as it introduced a human kinase alongside transgenic human tau, but this served to demonstrate the conservation of the pathway in *Drosophila*. The fly BRSK homologue, CG6114 or *SFF* (Baas et al., 2011) was not found to have any effect on toxicity caused by human tau, and the lack of phenotype caused by BRSK2 in the fly eye alone would indicate that the reverse is also true. Kinase dead and non-phosphorylatable, uninducible BRSK2 mutants were both incapable of altering tau toxicity.

With this information in hand, the expectation was for 2N4R tau to behave similarly to 0N4R tau in response to BRSK2, especially given the similar S262-dependant nature of toxicity in each isoform. On the contrary, there is a dramatic reversal in phenotype, with a significant reduction as measured by ommatidial distortion. This came as a surprise, given that these two tau isoforms differ only by number of N-terminal inserts, the rather more neglected alternative splicing products of the tau gene. All previously-identified target residues of AMPK-related kinases on tau have been contained with the proline-rich region, microtubule-binding domains or carboxy-terminal region. This contrasting response could raise important questions regarding the roles of different tau isoforms in disease; it certainly poses a challenge to any attempt to draw definitive conclusions based upon data obtained in single-isoform animal models.

4.3.2 2N4R tau mutation can mimic the BRSK2 phenotype

One goal of this project had always been to examine the precise role of tau phosphorylation in the tau/BRSK phenotype, by eliminating the possibility of BRSK2 acting via other substrates or altering tau metabolism. This goal was still relevant after the discovery of the importance of tau isoform to this interaction. To this end, a double phospho-mimetic aspartate mutant was generated, T212D S262D tau, based on the study of AMPK-related kinases by Yoshida and Goedert (2011).

Given the study of the 2N4R mutant library in Chapter 3, wherein T212D mutation was found to be protective and S262D mutation toxic, and the demonstration of non-additive effects of phosphorylation in the context of microtubule binding (Kiris et al., 2011), it was difficult to make a prediction. This more recent discovery of BRSK2 having a protective role when co-expressed alongside 2N4R tau in the fly eye was considered a better indicator of the effect of this double mutation.

In Figures 4.4 through 4.6, the phenotype and DC values of the T212D S262D double mutants are shown and compared with 2N4R WT and 2N4R/B2WT5. There is a significant reduction in ommatidial distortion compared with wild type 2N4R tau, in both hemi- and homozygous cases. When hemizygous T212D S262D is compared with 2N4R/B2WT5 (containing a single copy of 2N4R tau) based on DC values, there is no significant change; the double mutant seems capable of recapitulating the effect of BRSK2 on 2N4R tau in the absence of transgenic kinase. This is a potential indication of conservation of BRSK2 phosphorylation targets across isoforms, with the two sites indicated by a study on 1N4R tau (Yoshida and Goedert, 2011) capable alone of reproducing the phenotype caused by the kinase with 2N4R tau. Additionally, it is helpful in demonstrating that the lack of BRSK2-induced exacerbation of neurotoxicity in this isoform is not necessarily due to a loss of affinity, but can be reproduced by targeted phospho-mimetic mutation. It is also another indication of the difficulty in predicting the phenotypic consequences of multiple, individually contrasting phospho-mutations.

This does not mean, however that the interaction between 2N4R tau and BRSK2 has been fully explained. The novel tau phospho-mutant library was used to further explore this relationship, and to determine whether mutant tau would respond to BRSK2 as predicted.

4.3.3 BRSK2 and the 2N4R phosphorylation mutant library

Crossing mutant 2N4R tau lines with B2WT5 demonstrated the importance of phosphorylation at T212, T231 and S262 to the 2N4R/BRSK2 phenotype, as demonstrated by Figures 3.7 through 3.15.

At T212, DC values for the non-phosphorylatable alanine mutant were significantly reduced by BRSK2 co-expression, whereas those of the T212D mutant were not. The

T212D/BRSK2 result can be explained if we posit that the reduction in toxicity caused by the T212D mutant, which should be mimicking part of the phosphorylation caused by BRSK2, represents the major part of the effect of BRSK2. This is reinforced by the lack of difference between 2N4R WT/BRSK2 and T212D/BRSK2 when compared by Mann Whitney U test (P=0.23). The ability of BRSK2 to reduce toxicity in the T212A mutant however, especially in this light, is surprising – if T212D is essential for BRSK2-induced protection, how can it still have had such an effect on this non-phosphorylatable mutant? Indeed, if we assume that T212 and S262 are the only important residues affected by this kinase, the effect of BRSK2 would be reversed if S262 was its sole target, as shown by the S262D mutant in Chapter 3. This contradiction is perhaps partially explained by T231.

The T231D mutant is predictably affected by BRSK2, with a significant reduction in DC values upon co-expression. However, any effect of BRSK2 is apparently entirely eliminated by T231A mutation. This could be due to a reduction in affinity for BRSK2 caused by this mutation, removing any interaction completely. Alternatively, this could be evidence of yet another target residue of BRSK2. As has previously been observed, the proline-directed T231 was not investigated in the only major screen of tau phosphorylation by AMPK-related kinases (Yoshida and Goedert, 2011), and has been shown to be phosphorylated by AMPK itself (Thornton et al., 2011). Given the complexity of the tau phosphorylation code, it is possible that some level of T231 phosphorylation is a prerequisite of the reduction in tau toxicity observed upon introduction of BRSK2, potentially even (at endogenous levels) of the T212D S262D double mutation. Endogenous levels of T231 phosphorylation are clearly not sufficient alongside S262D pseudo-phosphorylation to produce such protection, otherwise the S262D mutant would exhibit such an effect alone; thus, it can only explain the ability of BRSK2 to reduce toxicity in the T212A mutant if the kinase increases phosphorylation at this site beyond endogenous levels. One additional possibility is that there is at least one other target of BRSK2 on 2N4R tau, which together with T212 (and potentially T231) creates some redundancy.

Toxicity caused by both S262 mutants can be reduced significantly by BRSK2, which would indicate a lack of importance of this residue in the BRSK2 phenotypic changes. This is perhaps supported by the similarity in phenotype between the T212D mutant and the T212D S262D double mutant. However, direct comparison of

hemizygous DC values between these two do show a significant reduction in the double mutant (P=0.026), which is eliminated after addition of BRSK2 to T212D (P=0.27) so there would appear to be some extra effect in the double mutant.

Together, these studies suggest a much more complex phosphorylation profile underlying the 2N4R tau/BRSK2 phenotype than that represented by the double phospho-mimetic mutant already generated. To summarise, BRSK2 leads to a phenotype suggestive of T212 pseudophosphorylation and recapitulated by a T212D/S262D mutant, but which is independent of T212 and S262 phosphorylation status, whilst being dependant on T231 phosphorylation. These data suggest that the similarity between the T212D S262D phenotype and that of 2N4R WT/BRSK2 is not evidence of these mutations representing the entirety of the effect of BRSK2. Perhaps inevitably given the complex system being investigated, there appear to be multiple paths to reaching the same result (and degree) of reduced toxicity, with far more combinations than measurable potential outcomes. If the effect of BRSK2 is indeed due to phosphorylation, and if the 1N4R tau phosphorylation data *in vitro* are applicable to this 2N4R model *in vivo*, then at the very least there must be some redundancy in this phosphorylation code. This would require phosphorylation of tau at other residues, likely T231 and others. A simple initial set of experiments would be to probe for changes in phosphorylation at T212, T231 and S262 in 2N4R tau in samples from flies co-expressing BRSK2. This would give an indication of relevance of the *in vitro* work as well as examining the relationship between T231 and BRSK2. Ultimately though, such small scale screens are likely to lead to uncertain conclusions given the number of potential residues of interest. Equally, expansion of the tau mutant library can only be effective with enough information to direct targeted mutation of residues of interest – the process is too slow and costly to explore every possible combination, even among the few sites listed here. This is rendered all the more pressing by the unearthed differences between tau isoforms and potential interest in replicating the library in 0N4R tau. One potential method of exploring BRSK2-induced phosphorylation could come from phosphoproteomics. Advances in the field of mass spectrometry over the past decade have begun to allow quantitative evaluation of the phosphorylation state of proteins. For example, SILAC (stable isotope labelling with amino acids in cell culture) is a method which uses heavy isotope-labelled growth media to differentiate between cell populations,

before aligning cleaved peptides by liquid chromatography prior to analysis (Ong et al., 2002). This method has been used proteome-wide to explore Cdk1(cyclin-dependent kinase 1) phosphorylation (Holt et al., 2009). Less expensive stable isotope labelling methods have also been developed, in which deuterium labelling occurs at the peptide level, following digestion which would likely be more practical for study of a single protein (Boersema et al., 2009). Given the number of post-translational modifications tau is subject to, such comprehensive data would be very useful for informing any future addition to the phosphorylation library or phospho-antibody collection.

The other possible explanation for the discrepancy between the predicted importance of BRSK2 phosphorylation and the apparent reality would be for the kinase to play an entirely different role in determining tau toxicity.

4.3.4 An alternative hypothesis for the tau/BRSK phenotype

The phosphorylation mutants have demonstrated a previously unknown importance for T231 in the 2N4R tau/BRSK interaction, which is completely prevented in the T231A mutant. This is also the only mutation shown to be capable of preventing this phenotypic suppression, despite other BRSK2 target residues being studied. The T231A mutant was also shown to present the lowest protein levels in Figure 3.3, which, it was hypothesised, could be caused by changes in tau stability. Previous work on BRSK2, using 0N4R tau found evidence of a drastic increase in autophagic activity in the developing eye disc (as measured by lysotracker stain) in samples co-expressing both human transgenes (unpublished data). The severe eye phenotype was also found in preliminary experiments to respond to modulation of two elements of autophagic machinery, Atg1 and TorTED. One possibility is that the observed ability of BRSK2 to modulate tau toxicity in the fly eye is due to changes in transgene removal. In the highly toxic 0N4R tau/BRSK2, it is possible that the high lysotracker stain was due to either a massive upregulation of autophagy in response to changes in tau post-translational modification, or to a blockage in autophagic flux leading to an accumulation of unused lysosomes. Potentially, in the context of the fly eye, it is tau removal which is most important in determining toxicity, rather than levels of microtubule binding or aggregation. Indeed, the innocuous nature of

BRSK2 in the eye in the absence of tau has been shown to be tissue-dependant, with BRSK2 expression lethal in the fly when driven by the pan-neuronal ELAV driver (unpublished data), indicating that this model may not be able to tell the full story of neurotoxicity. It is also possible that changes in tau clearance could help explain the isoform-specific differences in the effect of BRSK2.

The roles of the six tau isoforms in disease remain unclear. In particular, the significance of the N terminal inserts in disease has historically received little attention. In this work, two tau isoforms each with four microtubule-binding repeats have been found to demonstrate remarkably different responses to the AMPK-related kinase BRSK2. The current understanding of the role of exons 2 and 3 provides no clear answers. Whereas the effect of an extra microtubule-binding domain on cytoskeletal dynamics has fairly intuitive consequences (Goode et al., 2000), variation in tau projection domain length is a less obvious potential contributor to disease. Quantitative analysis has shown the importance of the N-terminal domain in balancing out kinesin-based transport velocity (Tarhan et al., 2013), with the increased negative charge of the projection domain helping the kinesin to sidestep intervening tau "roadblocks", a charge which could also help tau maintain its healthy axonal localisation (Haass and Mandelkow, 2010; Ittner et al., 2010). This could point to a potential link between transgenic tau and microtubule-based transport disruption, with an overabundance of 0N4R tau impeding kinesin passage. The projection domain has also been shown to be responsible for creating a negatively-charged "polyelectrolyte brush" around tau aggregates (Wegmann et al., 2013), which would presumably be larger and of even greater charge if predominantly composed of 2N tau. This does seem unlikely to be relevant to the fly model given the short developmental period for the formation of large aggregates. One area of interest in which the tau N terminal domain may be of interest is in the link between conformational changes of tau and disease.

Alz-50, one of the first antibodies to be discovered for pathological tau (Wolozin et al., 1986) evaded easy classification for several years owing to its complex epitope, furthering the mystery surrounding the A68 antigen which was later discovered to be hyperphosphorylated tau (Brion et al., 1991). This conformational antibody would in fact only recognise tau possessed of a specific secondary structure (Carmel et al., 1996), enriched in cases of neurodegenerative disease, in which the extreme N

terminus was brought into proximity with the microtubule-binding region. This Alz50 conformation differs from the normal "paperclip" conformation (Himmelstein et al., 2012) and has been hypothesised to greatly increase the likelihood of tau aggregation. Further studies have indicated the potential of conformational control for reducing tau aggregation (Akoury et al., 2013) and microtubule dissociation (Fischer et al., 2009). Isoform-specific differences in secondary structure have not been found, and in the case of Alz-50 all isoforms are capable of exhibiting reactivity. Nonetheless, conformational changes could potentially underlie the different responses to BRSK2 between 0N4R and 2N4R tau, or even some phospho-mutant phenotypes. Phosphorylation-induced tau conformational changes have been recorded, particularly in proline-rich regions (Bielska and Zondlo, 2006). The additional charge of the projection domain could also lead to an increased likelihood of binding to the microtubule-binding region in an Alz50 conformation. This leads to one possible explanation of BRSK2's isoform-specific effects: that there may be no direct (or relevant) interaction between BRSK2 and 2N4R tau. The apparent ability, according to QED, of BRSK2 to reduce slight GMR-induced ommatidial distortion could be evidence of the same mechanism causing a rescue of 2N4R tau toxicity. This could again implicate BRSK2 as a regulator of protein clearance, but also in the absence of any tau protein. BRSK2 could directly effect changes to 0N4R tau which it cannot in the longer isoform, or each isoform could provoke entirely different autophagic responses, with 0N4R tau leading to an extreme cytotoxic response. Differences in secondary structure could underlie this distinction. Any such change in tau clearance should lead to a change in total tau levels, detectable by Western blot with a total tau antibody such as the T46 used in the previous Chapter. Whether this is due to changes in the autophagic process could be examined using Lysotracker or Ref(2)P stain (Nezis et al., 2008). The Alz-50 antibody could also be one method of examining the secondary structure of human tau in this model, although there is no guarantee that this conformation can arise in the fly eye.

This chapter has demonstrated the isoform-specific effects of the tau kinase BRSK2. It has begun to show the complexity of the phosphorylation code of tau, with a double mutant phenotype and unexpected resistance to BRSK2 activity. The fly eye could play host to a great deal more experiments to explore the tau/BRSK2

interaction further, including further forays into phosphorylation, autophagy and tau secondary structure. One drawback has been underlined by comparison of eye phenotypes: the low resolution of quantification in this unusual tissue. In the next chapter, the potential of other expression systems in *Drosophila* is explored.

5| Establishing a *Drosophila* CNS model of progressive, tau-dependent functional impairment

5.1 Introduction

The *Drosophila* eye has been used as a model for the study of tau-induced neurodegeneration for more than ten years (Jackson et al., 2002; Wittmann et al., 2001). The regular nature of ommatidial organisation is determined by the Ras signalling pathway (Wassarman et al., 1995), with correct development of each of the eight photoreceptors present per ommatidium dependent upon specific genes; for example, differentiation of the R7 photoreceptor is regulated by the receptor tyrosine kinase Sevenless (Tomlinson et al., 1987). Another example of using the fly eye as a model is in the study of cell death pathways (Hay et al., 1994; Ollmann et al., 2000). As a measure of neurotoxicity, ommatidial disruption has ample sensitivity for differentiating individual tau mutations, whether of phosphorylation sites, as shown in this work, or FTDP-17 mutations such as R406W (Wittmann et al., 2001). However, the commonly-used eye-specific promoter GMR has a limitation when studying particularly toxic genotypes: leakiness in control of expression (Mondal et al., 2007; Xu et al., 2003), which can lead to lethality, as found in the previous Chapter. This necessitated a change in the rearing temperature for the recombinant 0N4R tau/BRSK2 line. In addition, a limitation of this model is that it bases its quantification of toxicity on developmental cell death, with the adult eye essentially formed following eclosion. Alternative methods of studying and quantifying tau-induced toxicity were thus sought.

In order to move beyond the study of developmental toxicity, a mechanism of transgene expression control was required. This would also allow the study of toxicity in essential tissues of the CNS without developmental lethality, as had been found in the case of constitutive expression of BRSK2 by the ELAV pan-neuronal promoter (unpublished observation). This was considered desirable as it would allow quantification of toxicity by more varied means and in contexts more comparable to the tissues affected by tauopathy. Helpfully, multiple methods allowing temporal control of expression exist, involving pharmacological and environmental factors. The first system tested, known as the TARGET system (temporal and regional gene expression targeting) was based around temperature-dependent control of expression (McGuire et al., 2004a). This system uses a temperature-sensitive mutant of GAL80, the repressor of GAL4 activity to allow repression of transgene expression at 18°C

and de-repression at 29°C. An ELAV promoter line under the control of this GAL4-GAL80^{TS} was kindly provided by Dr. Kyung-An Han of the University of Texas at El Paso. This repressor was shown to function effectively in a study on the dopamine receptor dDA1 and its role in aversive and appetitive learning in the mushroom body (Kim et al., 2007). This system would allow the examination of the consequences of adult-onset transgene expression throughout the CNS, with the possibility of multiple behavioural and activity-based measures of morbidity and mortality.

Initially, a simple mortality curve experiment was attempted, but the high experimental temperature resulted in very rapid desiccation of food and led to many early deaths as animals became trapped in cracks in their food. In order to increase the amount of data obtained and to create a more stable environment, the TriKinetics Inc. *Drosophila* Activity Monitor, or DAM2 System was used to record activity and survival over long time periods. This also reduced the danger of animals becoming trapped on food as the small vials are held horizontally within the machines. This system was also designed for the study of circadian rhythm analysis and as such was ideal for the study of transgene expression within the PDF (pigment dispersing factor) neurons which act as the fly circadian pacemaker (Helfrich-Forster et al., 2000; Park and Hall, 1998; Park et al., 2000).

5.2 Results

5.2.1 Effects of ELAV-GAL4 GAL80^{TS}-controlled transgene expression on activity and survival

In order to explore the post-developmental toxicity of tau in neuronal tissue other than the eye, a recombinant ELAV-GAL4 GAL80^{TS} line (hereafter referred to as ELAV) was crossed with transgenes described in the previous two Chapters. These crosses were performed and the progeny maintained at 18°C in order to suppress transgene expression. Adults of up to one week of age were then transferred to the DAM2 monitoring system at 29°C for transgene induction and activity recording. These experiments were performed under conditions suitable for study of a free-running period to enable retrospective examination of circadian rhythm changes, and were consequently exposed to equal light/dark cycles for 5 full days before onset of constant darkness for the remainder of the experiment.

5.2.1.1 0N4R tau and BRSK2

The first experiments performed were attempts to examine the effect of 0N4R tau and BRSK2 transgenes on behavioural activity. It was expected that expression of these transgenes would lead to measurable effects on total activity due to morbidity or mortality if they had any toxic effect in the CNS. Crosses were thus performed between the ELAV line and the 0N4R and B2WT5 lines, as well as the recombinant 0N4R/B2WT5 line introduced in Section 4.2.1. Recording by the DAM2 system sorted data into 1 minute bins which, upon completion of the recording, could be re-binned into 30 minute intervals, using the software DAM Filescan 1.07. These bins were then summed into values for each 24 hours of activity, using a simple spreadsheet in Origin 7. All measurements of total daily activity in this Chapter underwent this re-binning procedure. In Figure 5.1, the average daily activity over a three week time course of each of these lines, as well as ELAV controls, is plotted. Data from individuals were discarded if they did not survive past the first week in order to remove particularly sickly animals from the analysis. In order to determine whether the activity levels of each of the genotypes evolved differently over the period studied, a two-way ANOVA with repeated measures was performed in

GraphPad Prism 6. Both the genotype (P=0.0062) and day (P<0.0001) were found to be significant sources of variation in total daily activity. In addition, the interaction of these two variables was also found to be significant (P<0.0001), indicating that the rate of change in daily activity is dependent on the genotype. This was still found to be significant if the first week of data was removed from the analysis to avoid taking into account the early acclimatisation period and any possible increase in variance it may have caused: this was the case for genotype (P=0.0048), day (P<0.0001) and their interaction (P<0.0001). This also removes the earliest periods of expression, likely with the lowest transgenic protein levels of the experiment. When compared individually, 0N4R tau was not found to lead to a significant change in activity over the final two weeks of data (genotype/day interaction P=0.1231). BRSK2 expression was found to cause significant changes in activity (P=0.0271 under the same conditions), as was the recombinant 0N4R/B2WT5 line (P=0.001). Both B2WT5 and 0N4R/B2WT5 differed significantly from 0N4R tau alone (P=0.0007 and P=0.0011, respectively). 0N4R/B2WT5 differed significantly from B2WT5 if all three weeks of data were compared (interaction P=0.0025), but not if the first week was omitted (P=0.12). Flies expressing both 0N4R tau and BRSK2 die off earliest, with 100% lethality by day 12. There is an increase in 0N4R-induced activity decline compared with ELAV after day 11, but there are still some survivors after 21 days. As had been suspected after previous unpublished data revealed the lethality of ELAV-controlled developmental BRSK2 expression, the offspring of the ELAV cross to B2WT5 exhibit a severe decline in activity, with 100% lethality by day 20. It would seem that BRSK2 is toxic in at least some vital tissues of the CNS. It was also noted that the high temperatures used here were having an effect on behaviour, with animals becoming predominantly nocturnal in response – this was not surprising given recorded effects of temperature on periodicity (Sawyer et al., 1997) diurnal activity levels (Tomioka et al., 1998). It was also likely responsible for the shortened lifespan of control animals (Miquel et al., 1976).

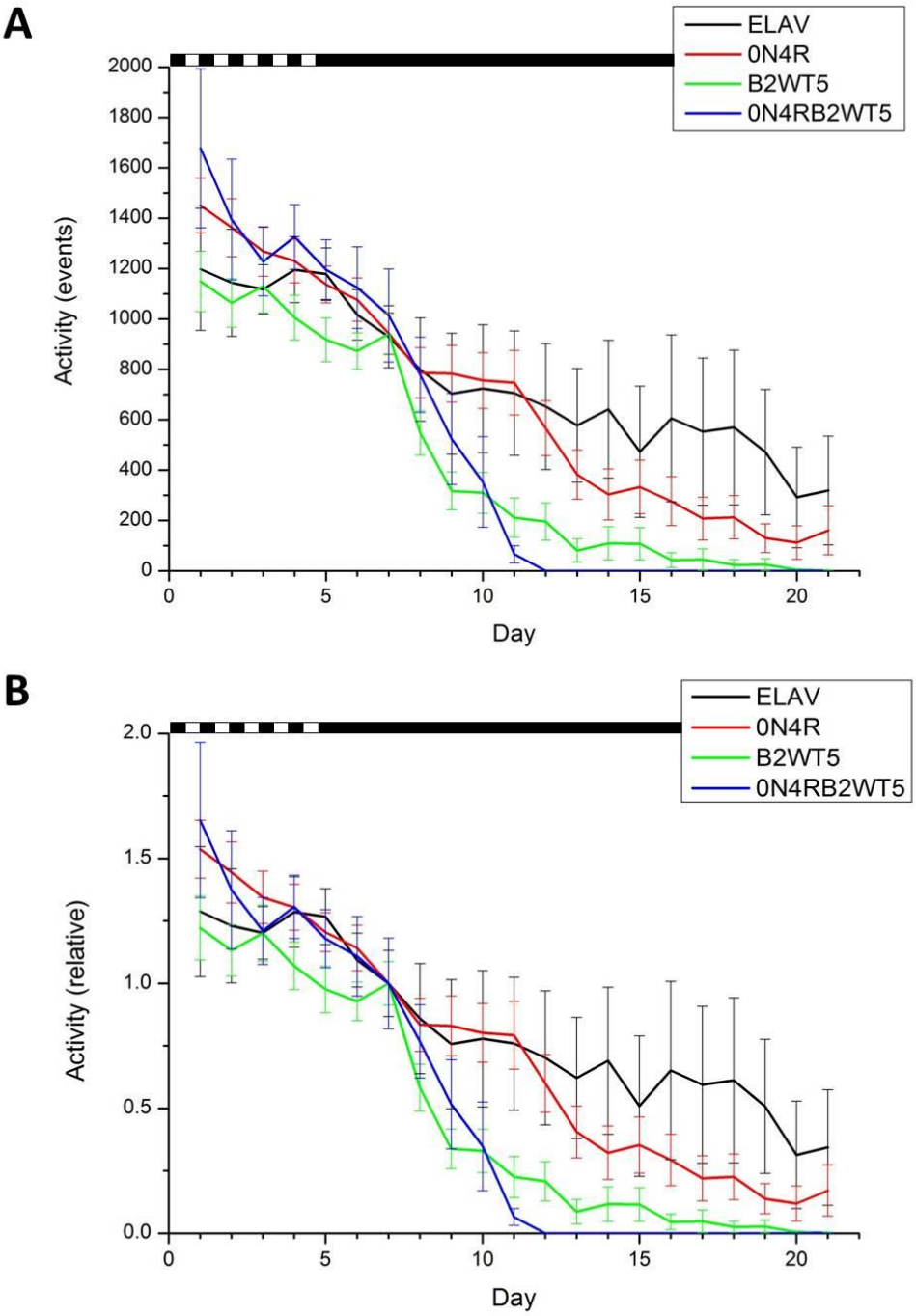

Figure 5.1: BRSK2 expression in the CNS, with or without 0N4R tau, reduces lifespan

A: Total daily activity measured in number of beam break events. Genotype was shown to control rate of decrease over time by two-way repeated measures ANOVA ($P<0.0001$). Error bars represent standard error. The black and white bar above the plot indicates the duration of alternating light/dark.

B: Total values normalised to readings of day 7, in order to reduce line-specific differences in baseline activity, and to avoid exaggeration caused by light/dark change. ELAV n=10. 0N4R n=18. B2WT5 n=23. 0N4R/B2WT5 n=10.

5.2.1.2 2N4R tau and mutants

The 2N4R tau mutant library was also crossed with the ELAV line to determine whether the differences in toxicity found in the eye upon GMR-controlled expression could also be reproduced in the CNS of adults. The 2N4R WT line and all single tau mutations were crossed with ELAV and the progeny studied using the DAM2 system, this time for a longer period of 33 days. Figure 5.2 shows total activity, Figure 5.3 activity relative to day 7. Animals not surviving after the first week were again disregarded from analysis. Two-way repeated measures ANOVA initially indicated a significant interaction between genotype and time point ($P<0.0001$), but re-analysis of the data obtained under constant dark (after day 7) failed to find a significant relationship ($P=0.097$). Given that acclimatisation to the conditions of the experiment is likely to lead to increased variation between all individuals over the first week, and that transgene levels would be expected to be lowest during this period, it seems appropriate to consider the latter measure more applicable. It is possible to speculate on some trends, for example comparing S262A to S262D the phospho-mimetic mutant consistently exhibits lower activity levels than its non-phosphorylatable counterpart. The T212A mutant exhibited a long period of hyper-activity before a sharp decline, with maximum lifespan comparable with all other lines. Indeed, upon normalisation of the data in Figure 5.3, it would appear that a certain level of hyperactivity is witnessed in all 2N4R tau and mutant lines. The two T231 mutants produced curves which are particularly close to 2N4R WT, also in line with the smaller range of eye phenotypes produced by mutation at this site.

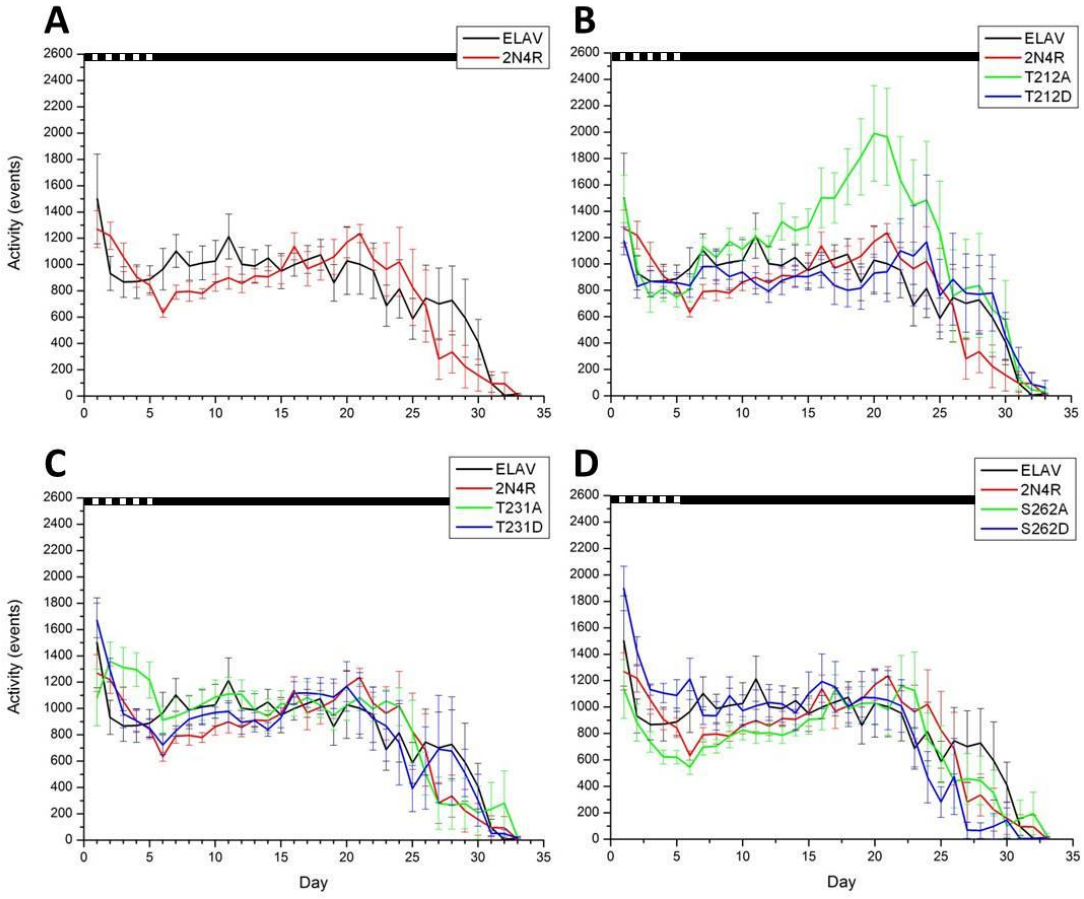

Figure 5.2: Absolute activity levels over 33 days do not reveal any 2N4R tau-induced reduction in lifespan

Data from flies expressing 2N4R tau was recorded for 33 days. No significant difference was found between the curves by two-way ANOVA with repeated measures (P=0.097). The black and white bars above the plots indicate the duration of alternating light/dark.

A: Data from ELAV controls and WT 2N4R tau-expressing individuals.

B: Data from controls and WT 2N4R, overlaid with data from individuals expressing T212A or T212D mutant tau.

C: Data from controls and WT 2N4R, overlaid with data from individuals expressing T231A or T231D mutant tau.

D: Data from controls and WT 2N4R, overlaid with data from individuals expressing S262A or S262D mutant tau.

ELAV n=9. 2N4R n=9. T212A n=9. T212D n=10. T231A n=8. T231D n=9. S262A n=10. S262D n=10.

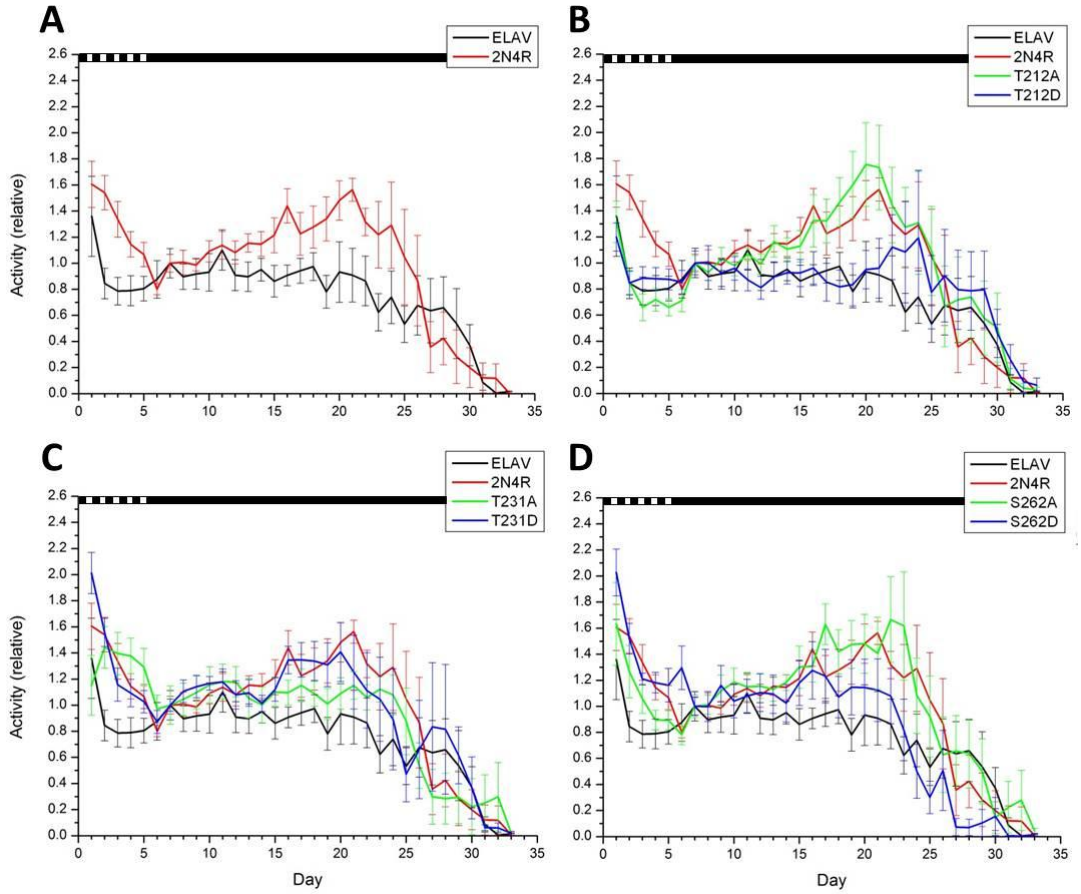

Figure 5.3: Normalised data from Figure 5.2 reveals consistently higher levels of activity after three weeks in 2N4R tau-expressing lines

Data from flies expressing 2N4R tau was recorded for 33 days. Data has been normalised to day 7 values to remove line-specific differences in baseline activity and to avoid additional variation caused by light/dark acclimatisation. The black and white bars above the plots indicate the duration of alternating light/dark.

A: Data from ELAV controls and WT 2N4R tau-expressing individuals.

B: Data from controls and WT 2N4R, overlaid with data from individuals expressing T212A or T212D mutant tau.

C: Data from controls and WT 2N4R, overlaid with data from individuals expressing T231A or T231D mutant tau.

D: Data from controls and WT 2N4R, overlaid with data from individuals expressing S262A or S262D mutant tau.

ELAV n=9. 2N4R n=9. T212A n=9. T212D n=10. T231A n=8. T231D n=9. S262A n=10. S262D n=10.

5.2.2 Effects of PDF-GAL4-controlled transgene expression on activity and survival

In the search for novel methods of quantification of neurotoxicity in the fly, it was hoped that the diverse array of techniques developed for the study of circadian rhythmicity could be of use. To this end, we set out to determine whether expression of human tau under the control of the PDF promoter, driving expression of the transgenes within the interneurons of the *Drosophila* circadian pacemaker, could have any destabilising effect on periodicity. Flies were generated by crossing all of the transgenic lines described in Section 5.2.1 with the PDF promoter line rather than with the ELAV line. Crosses were performed at 25°C in order to maximise transgene exposure; this temperature was kept constant throughout the experiment. Animals were exposed to an alternating 12 hours of light, 12 hours of darkness cycle for the first five full days of recording.

5.2.2.1 PDF expression and survival

One expected advantage of using the PDF promoter over ELAV is the non-essential nature of the target tissues. As a result, it was possible to cross flies without any attempt to suppress expression during development. In order to verify that there was no additional morbidity or mortality associated with transgene expression, total daily activity levels were monitored for each individual. Figure 5.4 presents the total activity curves for all 11 genotypes tested. The same data is shown normalised to day 7 activity values in Figure 5.5. Animals were again disregarded if they did not survive past the first week. Under these more conventional conditions of temperature, there was a marked decrease in activity upon entry into constant darkness. Analysis of the curves by two-way ANOVA with repeated measures showed no significant variation due to genotype alone ($P=0.082$), but highly significant variation with interaction ($P<0.0001$). This could be removed by reducing the period of analysis to the final 10 days (interaction $P=0.12$). The statistical differences in activity levels are concentrated within the first week of recording, suggesting any variation is due to early differences in acclimatisation, rather than toxicity due to leaky expression elsewhere in the nervous system, which would presumably become more pronounced over time. For example, 0N4R/B2WT5 is initially found to differ in activity levels to all other genotypes except WT 2N4R tau,

as measured by Turkey's multiple comparisons test; by day 7, no significant difference remains. 2N4R tau is found to differ from both T212 mutants and S262D until day 5. Some initial differences were also found between 0N4R tau and T212A mutant 2N4R tau. Turkey's multiple comparisons test ceases to find any significant differences between genotypes by day 7. After this time, repeated measures ANOVA continues to find significant variation with interaction until day 11. Again, this reduction in variation over time is consistent with a lack of transgene-induced toxicity, suggesting expression is limited to non-essential regions. Visually, the data indicated T231D exhibited reduced activity for the duration of the phase of constant darkness. The only genotype which appeared to have had an effect on the rate of decline in activity is 0N4R/B2WT5. The majority of 2N4R lines do not exhibit any obvious differences in their total activity levels under constant darkness.

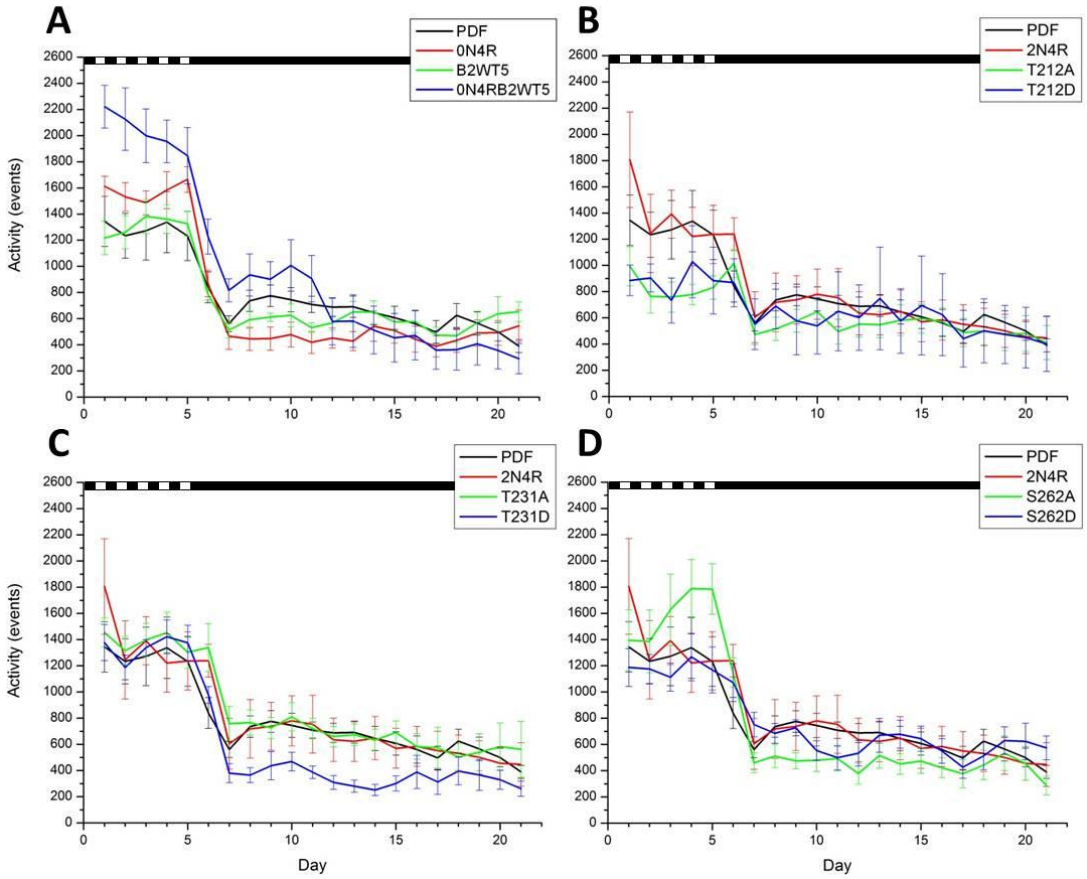

Figure 5.4: Absolute activity levels do not reveal any effect of tau or BRSK2 expression on lifespan

Data was recorded for 21 days. Two-way ANOVA with repeated measures showed significant variation in activity curves between genotypes from 7 days ($P<0.0001$) but not from 12 days ($P=0.12$). The black and white bars above the plots indicate the duration of alternating light/dark.

A: Data from PDF controls and individuals expressing 0N4R tau, BRSK2 and 0N4R tau and BRSK2 together.

B: Data from controls, WT 2N4R and both T212 tau mutants.

C: Data from controls, WT 2N4R and both T231 tau mutants.

D: Data from controls, WT 2N4R and both S262 tau mutants.

PDF n=9. 0N4R n=8. B2WT5 n=7. 0N4R/B2WT5 n=9. 2N4R n=8. T212A n=10. T212D n=4. T231A n=9.T231D n=8. S262A n=8. S262D n=9.

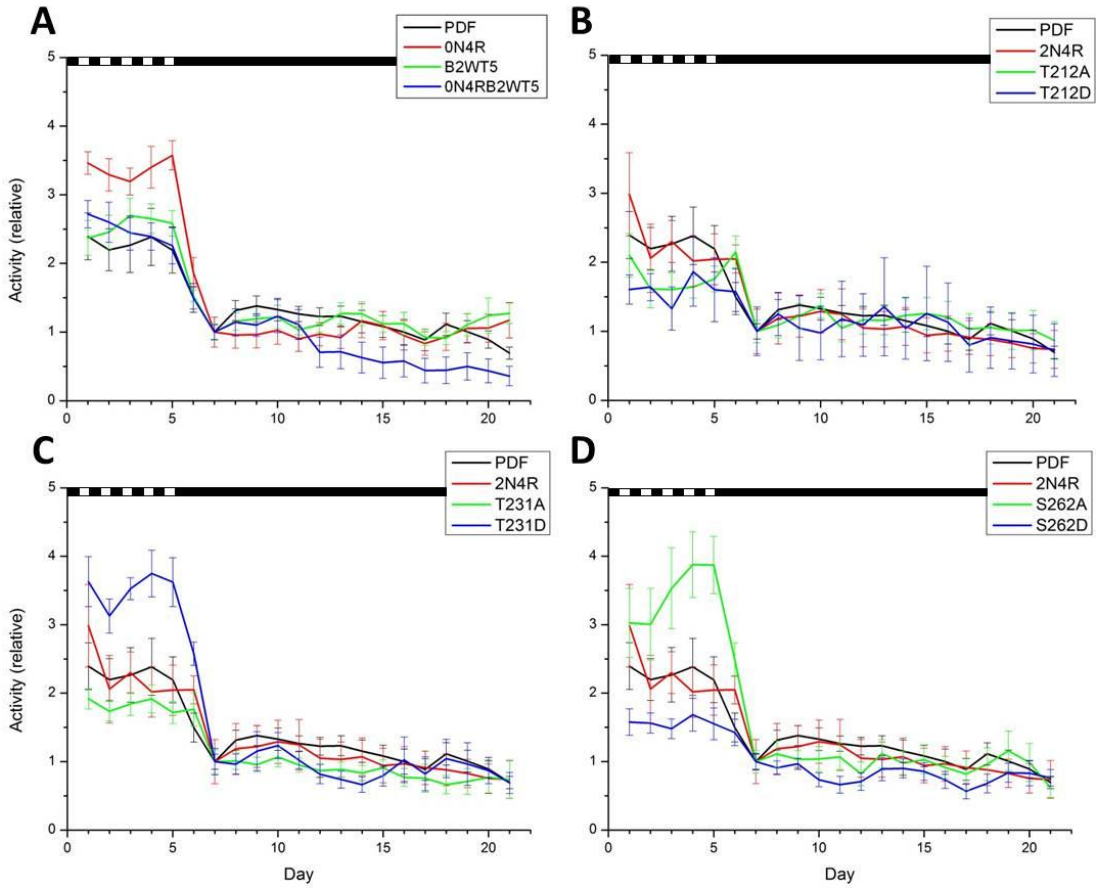

Figure 5.5: Normalised data from Figure 5.4. No significant effects on lifespan caused by PDF-controlled transgene expression were found

Data was recorded for 21 days. Data has been normalised to day 7 values to remove line-specific differences in baseline activity and to avoid additional variation caused by light/dark acclimatisation. The black and white bars above the plots indicate the duration of alternating light/dark.

A: Data from PDF controls and individuals expressing 0N4R tau, BRSK2 and 0N4R tau and BRSK2 together.

B: Data from controls, WT 2N4R and both T212 tau mutants.

C: Data from controls, WT 2N4R and both T231 tau mutants.

D: Data from controls, WT 2N4R and both S262 tau mutants.

PDF n=9. 0N4R n=8. B2WT5 n=7. 0N4R/B2WT5 n=9. 2N4R n=8. T212A n=10. T212D n=4. T231A n=9.T231D n=8. S262A n=8. S262D n=9.

5.2.2.2 PDF expression and circadian periodicity

In order to determine whether human tau isoforms or BRSK2 were toxic to PDF neurons, the DAM2 activity data was also analysed to compare periodicity. Where previous analysis was based around total values for each 24 hours of activity, for analysis of circadian rhythms the data were kept in 30 minute bins. These were suitable for analysis by the ImageJ plugin Actogram J. This program provided multiple methods of analysing periodicity. The most effective of these are Chi square and Lomb-Scargle. As the Chi square method requires at least 10 cycles of data to be accurate, and we were only interested in the free running period of these flies, all individuals with fewer than 10 days of data in constant darkness were discarded.

Figure 5.6 demonstrates the spread and mean of the periods for each sample. In Figure 5.6A, the periods are based on chi square periodograms; in Figure 5.6B, they are based on Lomb-Scargle periodograms. Comparison of the data by Kruskal-Wallis test (non-parametric one-way ANOVA) revealed a significant difference between genotypes (P=0.011), due to some variation in T231A and B2WT5. The Lomb-Scargle data did not reveal any significant differences by the same test (P=0.079). Comparing the two spreads of data, the only genotypes which contained consistently high levels of variation were the two lines expressing BRSK2, with T231A only differing due to a single sample in the chi square test, and PDF and T231D by single readings in the Lomb-Scargle data. It appears unlikely based on these data that human tau is having any severe effect on PDF neurons in these animals. It is possible however, that BRSK2 is causing some disruption.

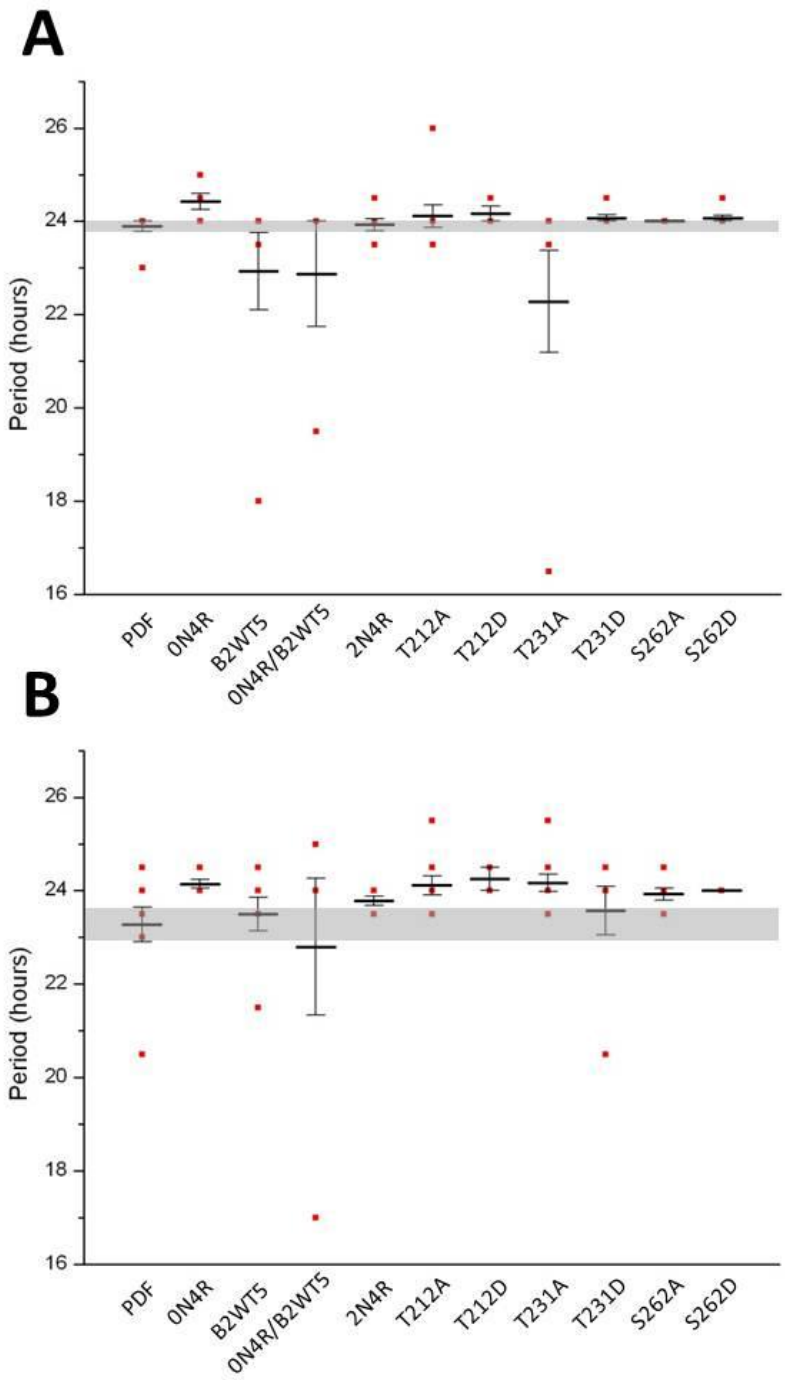

Figure 5.6: BRSK2 expression was found to have a greater effect on periodicity than 0N4R or 2N4R tau

A: Mean and spread of period of each genotype, by chi square periodogram. Variances were found to differ significantly by Kruskal-Wallis test (P=0.011).
B: Mean and spread of period of each genotype, by Lomb-Scargle periodogram. Variances were not found to differ significantly by the same test (P=0.079).
Grey bars represent mean +/- standard error of the PDF control line. PDF n=9. 0N4R n=8. B2WT5 n=7. 0N4R/B2WT5 n=9. 2N4R n=8. T212A n=10. T212D n=4. T231A n=9.T231D n=8. S262A n=8. S262D n=9.

5.3 Discussion

This chapter has documented the attempts made to complement the *Drosophila* eye-based model used in Chapters 3 and 4 with alternative, CNS expression-based functional assays. The primary goal was to determine whether the fruit fly could effectively become a useful model for the demonstration of progressive, adult-onset neurotoxicity due to expression of human proteins implicated in disease. In addition, we sought to establish alternative methods of quantification, in order to help distinguish between the many genotypes already screened in the eye.

5.3.1 Inducible CNS expression using the TARGET system

The *Drosophila* eye is a useful model for tau toxicity as it provides a sensitive, visible, non-lethal and quantifiable platform for neurotoxicity. However, this model is reliant on developmental transgene expression disrupting the formation of the eye, and consequently provided no information on the toxicity of these transgenes in the adult. Since the ommatidia, once developed, are no longer capable of reporting strong external signs of neurotoxicity, the CNS was considered an apt target for adult-onset toxicity experiments. Given that previous attempts to express BRSK2 under the control of ELAV had failed, due to apparent developmental lethality, a powerful method of transgene repression was required for the experiment. The use of the TARGET system of expression control meant the experiments had to be performed at unusual temperatures (18°C during development, 29°C during monitoring), which caused behavioural changes in the animals studied as their activity patterns shifted to nocturnal. As a result, the decision was made to limit analysis of DAM2 data of $GAL80^{TS}$-controlled subjects to sums of daily activity, to look for differences in morbidity, mortality or gross activity changes.

The recombinant 0N4R/B2WT5 line was used in an experiment to test whether this interaction would exhibit comparably toxic effects in the CNS to those witnessed in the eye. When plotted in Figure 5.1, the daily activity levels of each genotype do seem to differ, particularly when normalised to account for initial differences in activity for each genotype in Figure 5.1B. What is most clear is the drastic reduction in lifespan in both lines expressing BRSK2, with 100% mortality of B2WT5 at day 20, and of 0N4R/B2WT5 at day 12. Neither ELAV nor 0N4R alone reached 100%

mortality within three weeks. Comparison of these activity data by two-way ANOVA with repeated measures did not find any significant change between these latter two samples. This is potentially due to the large degree of error in the ELAV samples, caused by the accumulation of dead animals among other healthy, relatively very active individuals and the smaller sample size. However, what is clear is that 0N4R tau alone did not have as much of an effect as did expression of BRSK2 alone. This result makes sense in the light of the earlier finding of the developmental toxicity of ELAV-driven BRSK2. There would appear to be some additional toxicity in the recombinant line when comparing mortality rate, but differences in activity were not found to be significant. These data differ remarkably from those of eye-based experiments, which find BRSK2 alone to be completely benign (Section 4.2.1). This certainly begs questions of other tau kinases previously studied in the fly eye, particularly the AMPK-related kinases. This tissue-specific toxicity could offer some potential insight into BRSK2's mechanism of action on human tau in the fly eye. In Section 4.3.4, it was speculated that BRSK2 could play some role in the removal of the transgenes involved in the eye experiments, as the kinase appeared to mitigate the low-level disruption caused by the GMR promoter; hypothetically, this could also be the cause of the reduction in toxicity of 2N4R tau when co-expressed with BRSK2. It is possible that among the wider array of tissues being exposed to BRSK2 by ELAV, this hypothetical increase in degradation could affect a number of essential, endogenous proteins. A potential first candidate to investigate is *Drosophila* tau. The existence of a d-tau null allele (Doerflinger et al., 2003), and the success of experiments using homozygous d-tau -/- flies (Feuillette et al., 2010) make this a testable possibility. Equally however, given that d-tau is clearly not an essential component of the fly microtubule cytoskeleton, likely due to some element of redundancy with other MAPs (Doerflinger et al., 2003), it is unlikely that removal of d-tau would be a significant contributor to toxicity. BRSK2-induced dysfunction could be an alternative hypothesis, and one with a more manageable number of potential research targets. Given the growing number of BRSK substrates, including the cell cycle regulators Cdc25-C and Wee1 (Lu et al., 2004; Muller et al., 2010), the synaptic vesicle-priming factor RIM1 (Inoue et al., 2006) and γ-tubulin directly (Alvarado-Kristensson et al., 2009), there are many mechanisms potentially being misregulated. Any and all of these processes could play essential roles as BRSKs emerge as conductors of axonal morphogenesis (Lilley et al., 2013). *Drosophila*

homologues of Wee1 (Campbell et al., 1995) and Cdc25 (Edgar and O'Farrell, 1989) are well-documented and could be useful avenues of research into this novel BRSK2-induced toxic effect.

As for 0N4R tau, it is tempting to see a trend toward reduced activity among the older surviving flies, or perhaps reduced survival compared with the ELAV controls. Expanding the size of the experiment to enable a proper analysis of survival would perhaps be one avenue of further inquiry. Another simple next step would be to use homozygous 0N4R tau transgenics, which would likely emphasise any effect of 0N4R tau. It would be interesting to be able to examine individuals of different ages more closely, perhaps with transverse paraffin sections (Kucherenko et al., 2010) of the heads of aged flies. This would enable visual determination of the nature of neuronal damage in these individuals, which if severe should lead to visible lesions, and would also be the best indication of whether this model is capable of representing progressive neurodegenerative conditions over a relatively short time period.

Given the lack of significant change in activity levels between the ELAV controls and 0N4R tau flies, it is unsurprising that none of the 2N4R mutants exhibit a significant change compared with controls in Figures 5.2 and 5.3. The trends in both average daily activity and maximum lifespan are very similar in virtually every case, with only activity of the T212A line standing out as having changed differently over the course of the experiment. Over the second and third weeks of monitoring, a consistent increase in activity was recorded among the majority of T212A individuals, before dropping down to control levels at day 26. It does not appear as though this increase in activity led to any deleterious effect, as the maximum lifespan for this genotype was in line with all others. It is interesting to note that the increase coincides with the onset of the phase of constant darkness – it is possible that T212A tau was causing disruption of a subset of neurons responsible for regulating behavioural responses to light. However, this trend becomes common to several other 2N4R lines upon normalisation of the data, including 2N4R WT, T231D and S262A. Such normalisation somewhat exaggerates the difference between S262A and S262D in the final days of the experiment, with S262D appearing to drop off more quickly, a possible indicator of increased toxicity though not to any statistically significant degree.

The primary drawback of the TARGET system in this experiment is the high temperature required for derepression, leading to reduced lifespan and changes in behaviour. In order to validate more in-depth study of activity patterns and survival curves, it would be desirable to consider alternative methods of temporal transgene control. One possibility is the GeneSwitch system, a pharmacological method of regulating gene expression. The system makes use of a mutated progesterone receptor ligand-binding domain in a GAL-4 chimera, and allows induction of transgene expression in the presence of RU486 (Burcin et al., 1998; McGuire et al., 2004b), the progesterone receptor antagonist and abortifacient commercialised as Mifepristone. It has been used effectively in *Drosophila*, including inducing ELAV-controlled expression (Osterwalder et al., 2001). The system boasts high levels of transcriptional control through modulation of RU486 concentration in food and little leakiness, ideal characteristics for these experiments.

These experiments studying transgene expression throughout the CNS raised the possibility of tissue-dependent tau kinase toxicity but were unable to effectively demonstrate human tau toxicity. More specific experiments were then designed, using the PDF promoter to drive expression within the 16 interneurons of the fly circadian pacemaker to attempt to quantify human tau toxicity through circadian rhythm defects.

5.3.2 Quantification of transgene toxicity in the PDF neurons

In order to demonstrate the non-essential nature of the PDF neurons, the total daily activity levels of all 10 test lines and PDF controls were compared, as was performed for the ELAV crosses in Section 5.2.1. The expectation was for no significant changes in activity decline. Although no significant differences in variance were recorded between genotypes across any individual days, the change in activity levels over time was found to exhibit significant differences unless only the final 10 days of data were compared. This could be due to changes in activity from PDF neuron disruption, though if that were the case it would seem logical for the differences to become more pronounced as the duration of free running increased. It is possible that these differences are primarily due to basal activity level discrepancies. The 0N4R/B2WT5 recombinant line exhibited a steeper decline in total activity, made marginally clearer in the normalised data of Figure 5.5, perhaps evidence of

transgene leak, though this was not the case in the B2WT5 line which was found to be similarly toxic when controlled by ELAV. The T231D line had consistently lower average activity under constant darkness.

Expression of toxic transgenes within the PDF neurons would have been expected to lead to disruption of circadian rhythmicity. This was measured by evaluation of periodicity using the ActogramJ program. This software provided multiple methods of analysis of period. In Figure 5.6, both the chi square and Lomb-Scargle methods were used to generate periods for each individual surviving at least 15 days. Both methods were used in order to provide greater certainty in cases of highly unusual periods. The nature of the analysis meant that every individual received a value, regardless of the strength of rhythmicity. In some cases, this led to extremely unlikely scores (such as the 16.5 hour period of one individual in Figure 5.6A), which can be considered as examples of arrhythmicity. No genotype was found to be consistently arrhythmic, though both BRSK2-expressing lines contained one arrhythmic individual according to each method. The chi square method finds significant variation between both BRSK2-expressing lines and the PDF control, whereas the Lomb-Scargle method does not. The strength of the Lomb-Scargle method lies in analysis of unequally-spaced time series (Van Dongen et al., 1999), which is of no benefit in this case, and it is based on the older, now less used Fourier analysis, initially developed for analysis of short-term rhythmic bioluminescence (Plautz et al., 1997). The chi square method (Sokolove and Bushell, 1978) is much more commonly used, and its requirement of at least 10 cycles of data for effective analysis (Refinetti et al., 2007) was considered a useful quality control guideline among these samples. Consequently, it is possible to say that BRSK2 has again been shown to have neurotoxic effects in the *Drosophila* CNS, including in the PDF neurons. It would appear however that this model is not sensitive enough to detect toxicity caused by human tau expression, using both 0N4R and 2N4R tau. Again, it would be interesting to examine whether tau homozygotes exhibited any detectable changes. Anti-PDF antibody has also been widely used to stain dissected adult fly brains (Park et al., 2000; Peng et al., 2003; Shang et al., 2008), allowing visualisation of the well-characterised PDF-expressing interneurons, including eight each of the large and small lateral ventral neurons (Helfrich-Förster, 1995). The highly specific number and structure of these neurons means they are extremely well suited for

probing in this manner, and could provide visual verification of transgene expression and neuronal damage.

So far, these attempts to exploit the DAM2 activity monitoring system to explore neurotoxicity in *Drosophila* have had limited success. Though they may well have led to several future lines of inquiry regarding the consequences of BRSK2 expression in the fly, so far they have not been shown to be sensitive enough to provide useful insights into tau toxicity. There is still potential for further examination, to determine whether increased expression or visual examination could demonstrate and quantify human tau-induced CNS toxicity in the fly. The demonstration of BRSK2-induced toxicity adds an intriguing extra dimension to the role played by BRSK2 in exacerbating tau-induced neurodegeneration in the fly eye. In the next chapter, this interaction has been explored further, using a *Drosophila* deficiency screen to explore the pathways surrounding the tau/BRSK interaction.

6| A deficiency screen to isolate novel regulators of the 0N4R tau/BRSK2 eye phenotype

6.1 Introduction

The clear eye phenotype of 0N4R-B2WT5 flies has previously been shown to be dependent on two endogenous *Drosophila* kinases (unpublished data). These were LKB1 and CG17698, the fly CaMKKα homologue. The kinase domain of *Drosophila* LKB1 displays 66% amino acid identity with that of its mammalian homologue (Martin and St Johnston, 2003). This serine/threonine kinase was shown to be required for several cellular processes, including establishment of cell polarity in the fly (Martin and St Johnston, 2003) and in mammals (Baas et al., 2004). After LKB1 had been shown to regulate 13 members of the AMPK-related kinase family (Lizcano et al., 2004), the BRSKs, as substrates of LKB1, were revealed to be essential for neuronal polarisation (Kishi et al., 2005). That the BRSKs were also shown to be tau kinases, and also activated by the calcium-dependent CaMKKα (Fujimoto et al., 2008), made them suitable targets for research into tauopathies, particularly given the well-established links between calcium homeostasis and Alzheimer's disease (Berridge, 2011; Grynspan et al., 1997; Murray et al., 1992). That the pathways regulating human BRSK2 activation were conserved in *Drosophila* raised the possibility of discovering other BRSK2 modulators by virtue of the extensive screening methods available to *Drosophila* biologists. Once the tau isoform-specific nature of the BRSK2-induced eye phenotype became apparent, it was also hoped that such a screen would unearth an explanation for this specificity. The more detailed study of the relationship between modulation of tau toxicity by BRSK2 and the phosphorylation status of tau has given cause to look beyond phosphorylation pathways to help solve the questions surrounding tau isoform-specific BRSK2-induced toxicity.

Arguably the greatest strength of *Drosophila* as a model organism is its extensive genetic toolkit, allowing multiple methods of exogenous gene insertion and expression control. Deficiency screens are also important elements of modern *Drosophila* research. Deficiency lines lack a discrete, defined chromosomal region (Bridges, 1917), effectively generating null alleles for multiple genes without need for random mutagenesis (Roote and Russell, 2012). The modern deficiency kits, including the DrosDel and Bloomington projects, consist of libraries of hundreds of categorised deficiency lines. This was made possible by an adaptation of yeast FLP

recombinase (Golic and Lindquist, 1989), placed under control of the heat-sensitive hsp70 promoter. This could be inserted in transposable P elements alongside FLP recombination target (FRT) sequences; heat shock treatment activates recombination which can then be identified thanks to the location of FRT within a copy of the *white* gene, for eye pigmentation (Golic and Golic, 1996). Thanks in particular to the large-scale Bloomington project, deficiency screens have become increasingly comprehensive, now covering 98.4% of the fly genome (Cook et al., 2012). One established use of such kits is for pathway-expansion experiments, allowing chosen phenotypic analysis in hemizygous deficiency backgrounds, thus potentially uncovering likely upstream or downstream pathway components. Multiple genomic screens for modifiers of tauopathy have already been carried out in *Drosophila*, using alternative screening libraries or in conjunction with mouse microarray analysis (Ambegaokar and Jackson, 2011; Karsten et al., 2006; Shulman and Feany, 2003). In this Chapter, a screen making use of the Bloomington and Exelixis deficiency stocks is described. These deficiency libraries together boast extremely comprehensive coverage. As they constitute the major part of the fly genome, chromosomes 2 and 3 were investigated in the screen as extensively as time allowed, with over 300 stocks obtained through the Bloomington stock centre. The screen made use of the 0N4R-BRSK2 recombinant line described in Chapter 4, facilitating examination of the interaction between the two transgenes. This line had already been used in experiments demonstrating the ability of its phenotype to be both enhanced and suppressed, a necessary characteristic for a deficiency screen. Suppression of the phenotype was witnessed upon RNAi of the fly CaMKKα homologue, enhancement upon overexpression of the Ca^{2+} channel Cacophony (unpublished data). In addition, this recombinant line has been found to exhibit a more consistent phenotype than that generate by crossing of 0N4R tau and BRSK2 lines, likely due to its origin as a result of a single recombination event. This indicates the ability of variation at other loci to modulate the phenotype, precisely what a deficiency screen seeks to demonstrate. The screen was initially as high-throughput as possible, attempting merely to highlight genomic regions of interest which could then be examined for putative modulators of BRSK2 activity or tau toxicity. Likely candidates included kinases, phosphatases, regulators of calcium homeostasis or cell death pathways, and cytoskeletal proteins.

6.2 Results

The Bloomington deficiency stocks for chromosomes 2 and 3 were acquired in order to perform screens of the majority of the fly genome for modulators of the 0N4R tau/BRSK2 eye phenotype. The chromosome 2 kit was obtained in October 2010, at the time containing 142 stocks. The chromosome 3 kit obtained in February 2013 contained 178 stocks. Stock males were crossed with 0N4R-B2WT5 virgins at 23°C and screened under light microscope for phenotype-suppressing or enhancing deletions. These were then screened for their effect on 0N4R tau alone, in order to avoid duplication of previous tau studies and to focus on the BRSK2-induced phenotype. Where possible, once the primary screen using the predefined kit was finished, areas of interest were shortened using additional overlapping deficiency stocks, before potential genes of interest were examined using mutant or RNAi lines.

6.2.1 Chromosome 2

6.2.1.1 Primary screen of chromosome 2

The initial chromosome 2 screen using the 142 lines which comprised the older deficiency kit revealed eleven regions of interest. Of these, one was isolated to a single gene, thanks to overlapping deficiencies – this was *chickadee*, encoding the *Drosophila* homologue of Profilin, the actin-binding protein. Of the remaining ten chromosomal regions, nine led to a suppression of the phenotype and one to an enhancement (as defined by visual inspection). In order to reduce the number of candidate genes in these regions, a further 35 overlapping lines were ordered. Following evaluation of these deficiencies, three of the regions were eliminated entirely from the study due to complete coverage by deficiencies which were not found to alter the phenotype. These included the only phenotype-enhancing region. Overlapping lines within three other regions were found to lead to suppression, while the remaining four had no phenotype-changing, overlapping deficiencies but were not ruled out due to a lack of complete coverage. The remaining regions of interest on chromosome 2 are shown in Figure 6.1.

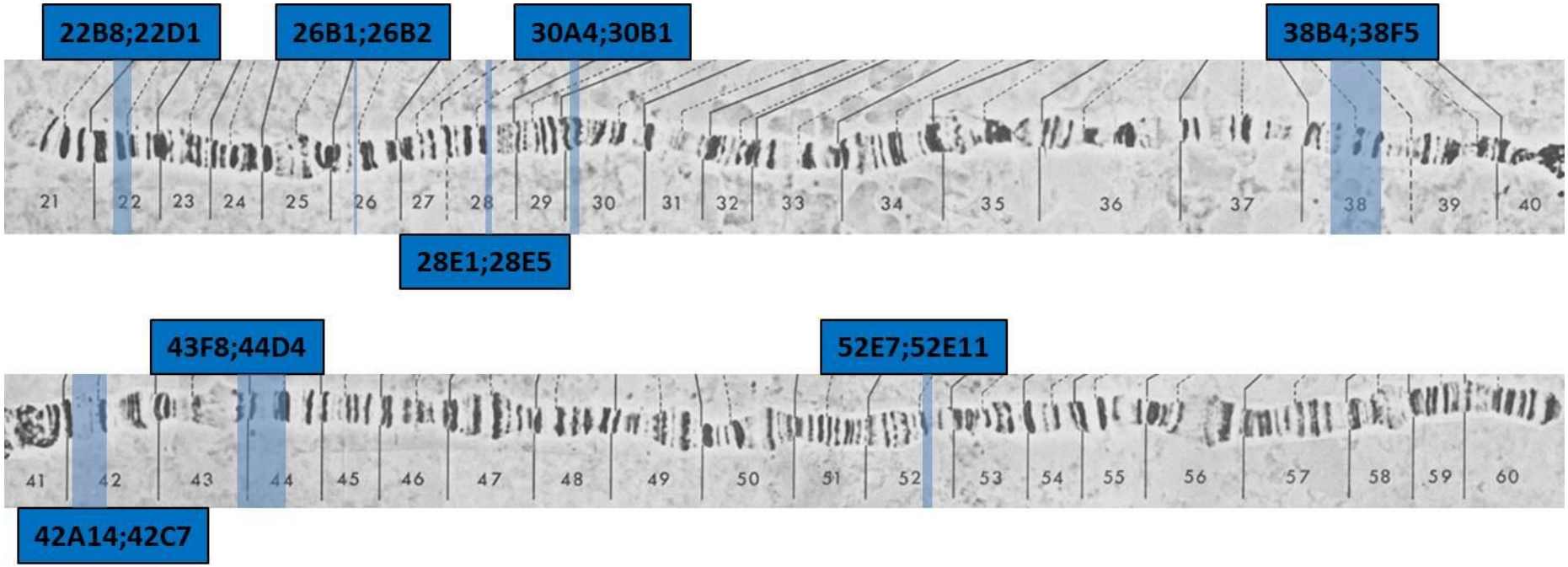

Figure 6.1: Chromosome 2 polytene maps annotated with regions associated with phenotypic change
Regions associated with phenotypic suppression listed in blue boxes. The region 26B1;26B2 is contained entirely within the gene chickadee. *All other regions are polygenic. Polytene chromosome (Balbiani, 1881) photographs adapted from Schaeffer et al. (2008)*

6.2.1.2 Secondary screen of chromosome 2

The secondary screen began with the search for putative BRSK2-affecting genes within these regions. A number of mechanisms were considered, including kinase activity, cell death mechanisms, proteolytic processing, calcium homeostasis, neurogenesis, energy metabolism and cytoskeletal association. Eighteen RNAi lines were obtained, suppressing individual genes within four of the target areas. These lines are listed in Table 6.1, together with any phenotypic effect they were found to exhibit.

Among the four regions studied using RNAi lines, two were found to contain genes with a phenotypic effect upon inhibition. These were also the two regions with the most lines examined. In each case, two genes were found, perhaps demonstrating the greater sensitivity of RNAi screening; this could also imply some propensity for false positives in the screen. Time constraints prevented any further investigation of these genes, or of any of the other regions of interest on chromosome 2.

Gene	Location	Target Region	Phenotype	Associated with
CG4238	22B8-22C1	22B8;22D1	No change	Ubiquitination
Su(dx)	22C1	22B8;22D1	Suppression	Notch binding
DPR3	22C1-22C3	22B8;22D1	No change	Calcium metabolism
GlyP	22C3-22D1	22B8;22D1	No change	Glycogen catabolism
CG7261	22D1	22B8;22D1	No change	Tubulin binding
AIF	22D1	22B8;22D1	Suppression	Apoptosis
Spire	38C5	38B4;38F5	No change	Cytoskeleton
Arpc2	38C6	38B4;38F5	No change	Actin binding
Debcl	42B2-42C1	42A14;42C7	No change	Apoptosis
CG8726	43F9	43F8;44D4	No change	Protein kinase
CG14763	43F9	43F8;44D4	Suppression	Cytoskeleton
CSN4	43F9-44A1	43F8;44D4	No change	Ubiquitination
Hey	44A2	43F8;44D4	No change	Notch binding
Sut3	44A4	43F8;44D4	No change	Sugar metabolism
Sut2	44A4	43F8;44D4	No change	Sugar metabolism
Sut1	44A4	43F8;44D4	Suppression	Sugar metabolism
Nup50	44B2-44B3	43F8;44D4	No change	Neurogenesis
Pnut	44C2	43F8;44D4	No change	Apoptosis

Table 6.1: RNAi lines used in the chromosome 2 secondary screen
Information on the genes studied using RNAi, including location, proposed function and any effect on phenotype. Changes were recorded for four lines (blue), located within two regions of the chromosome.

6.2.1.3 Chickadee

Four suppressing deficiencies were found to overlap a 737 bp region, located entirely within the gene *chickadee*. Chickadee is an actin-binding protein, the *Drosophila* homologue for Profilin. Given the deficiency data and the cytoskeleton-associated target, *chickadee* mutants were obtained and studied further. These lines were numbered Bl. 4891, carrying a loss-of-function allele generated by P-element insertion, and Bl. 4892, with an amorphic $chic^{221}$ allele encoding a shorter transcription product (Verheyen and Cooley, 1994). These will be referred to as 4891 and 4892, respectively from here on. Stock 4891 was sickly, with few progeny. Each line was crossed with 0N4R-B2WT5 and evaluated as with the deficiencies. Figure 6.2 shows scanning electron micrographs of progeny from the cross using 4892. Images shown were those given the highest, lowest and median DC values by QED. Cumulative distribution plots for the progeny are shown in Figure 6.3.

Purely visual examination of the SEM images appears to show a consistently larger surface area for the eye in individuals possessed of the $chic^{221}$ allele. This is visible at both extremes of DC values, with an attenuation of the inverted teardrop shape characteristic of 0N4R-B2WT5 flies. The DC values themselves do not register any difference due to *chic* mutation when compared by Mann-Whitney U test (P=0.95). It is important to remember however that QED does not measure eye size and so is insensitive to any change in this metric; it is possible that ommatidial disruption is very similar in each sample in spite of the change in size, leading to similar DC values. QED values are low across all samples when compared with those recorded for 0N4R-B2WT5 in Chapter 4, perhaps evidence of a difference in incubator temperature or genetic background in the 4892 line, demonstrating the importance of repeating controls for each experiment.

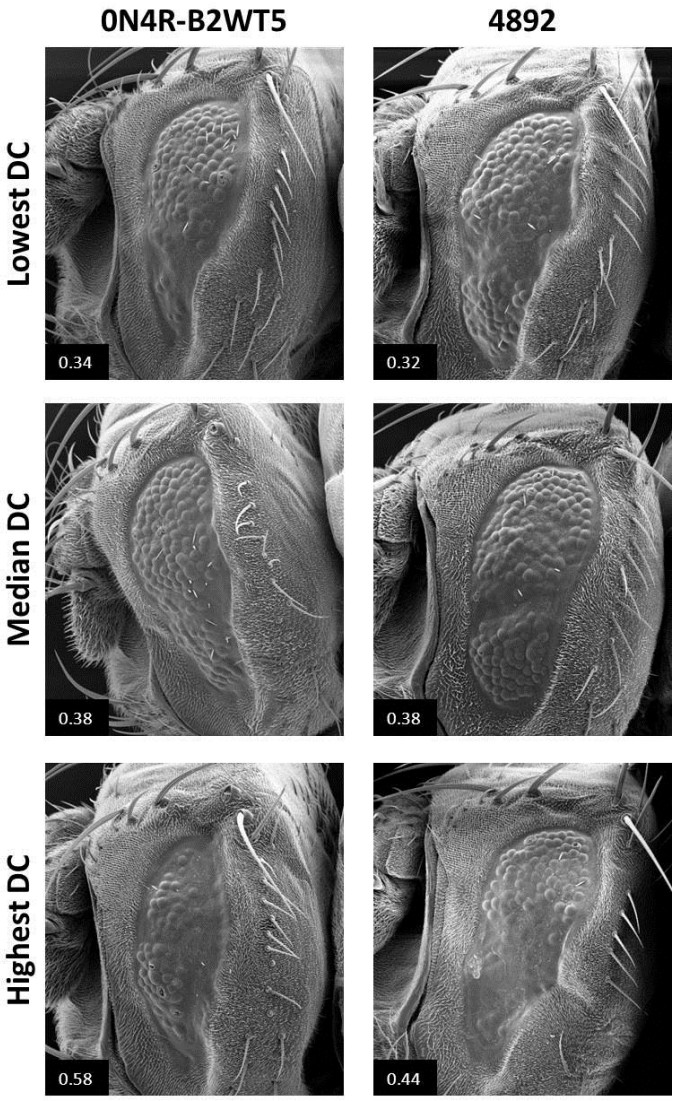

Figure 6.2: Chic mutation increases eye size of 0N4R-BRSK2 flies
SEM images of 0N4R-B2WT5 flies without or with the 4892 chic mutation. Lowest, highest and median DC values are shown. The chic *mutation appears to lead to an increase in eye size across the sample. This is not accompanied by a suppression of ommatidial distortion when measured by QED.*
*Genotypes: 0N4R-B2WT5: GMR/CyO; 0N4R, B2WT5/+. 4892: GMR/*chic*221; 0N4R, B2WT5/+.*

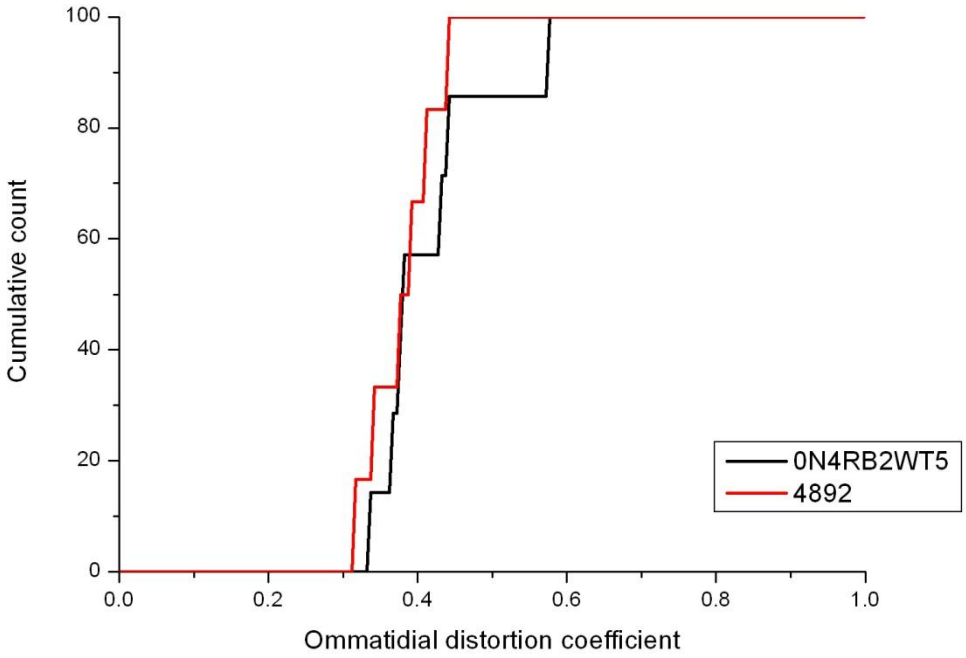

Figure 6.3: QED analysis does not reveal any effect of Chic mutation on ommatidial distortion

Cumulative distribution plot of DC values of the samples shown in Figure 6.2. Quantitative analysis of the phenotypes shown in Figure 6.2. There was no significant difference found between DC values of each genotype when compared by Mann-Whitney U test (P=0.95).
0N4R-B2WT5 n=7. 4892 n=6.

6.2.2 Chromosome 3

The Bloomington deficiency kit for chromosome 3 was also examined for modulators of the 0N4R-BRSK2 phenotype. This kit contained 178 deficiencies at the time of ordering. Study of these lines was less comprehensive due to time constraints but initial screening isolated fourteen chromosomal regions of interest, eight identified as phenotypic suppressors and six as enhancers. These regions are represented on the chromosome 3 polytene map in Figure 6.4.

These regions have not yet undergone any further analysis to reduce their size through the study of overlapping deficiencies not contained within the kit and as a result are still generally very large, with too many potential genes of interest for RNAi screening. The exception is 92F13;93A1, which contains only the gene *syncrip*, associated with neurogenesis. Some candidates are listed in Table 6.2, based on recorded gene function in the literature and prioritising association with the mechanisms listed in Section 6.2.1.2.

Both of the known BRSK2 modulators in *Drosophila*, LKB1 and CG17698 are located within chromosome 3, though neither is contained within standard deficiencies of the Bloomington kit. CG17698 is not covered by any deficiency stock, as it is extremely proximal to the centromere at 80F9, and so could not be examined in this screen. LKB1 (at 87F7-87F9) is covered by a single stock in the entire Bloomington library, numbered 7648 (covering 87F2-87F10). No phenotypic change was recorded upon crossing this stock.

Gene	Location	Target Region	Associated with
MED24	66B11-66B12	66B11;66C3	Apoptosis
Ubc12	66B12	66B11;66C3	Ubiquitination
UbcD4	67C5	67C5;67D1	Ubiquitination
CDK8	67C10	67C5;67D1	Protein kinase
Inhibitor-2	67C10	67C5;67D1	Phosphatase regulation
Calpain-B	67D1	67C5;67D1	Calcium metabolism
CG11261	69F5	69E6;69F6	Ubiquitination
MICAL-like	69F5	69E6;69F6	Actin-binding
Reaper	75C6	75B11;75E4	Apoptosis
MYPT-75D	75D4-D4	75B11;75E4	Phosphatase regulation
Canoe	82F4-82F6	82E7;82F8	Eye development
Katanin 60	82F6	82E7;82F8	Microtubule severing
Retinophilin	82F6	82E7;82F8	Apoptosis
CG12163	82F6-82F7	82E7;82F8	Autophagy
Unc-115A	85E4-85E5	85E5;85E9	Actin-binding
Hyperplastic discs	85E5-85E5	85E5;85E9	Ubiquitination
Whamy	85E8-85E8	85E5;85E9	Microtubule formation
CG31391	86C4	86B1;86C7	Phosphatase regulation
Cadherin 86C	86C7	86B1;86C7	Calcium ion binding
Heartless	90E2-90E2	90E2;90F4	Protein kinase
PP2A-B'	90F4-90F5	90E2;90F4	Phosphatase regulation
Frayed	91B4-91B5	91A5;91F1	Protein kinase
MEKK1	91C5	91A5;91F1	Protein kinase
Syncrip	92F12;93A1	92F13;93A1	Neurogenesis
Ublcp1	94D10	94D10;94E7	Protein phosphatase
CG13830	94D12-94D13	94D10;94E7	Calcium ion binding
Unkempt	94E1-94E2	94D10;94E7	Eye development
Cadherin 96Ca	96C4-96C5	96C3;96C8	Calcium ion binding
Cadherin 96Cb	96C7	96C3;96C8	Calcium ion binding

Table 6.2: Putative modulators of the 0N4R-BRSK2 phenotype on chromosome 3
Information on potential candidate genes, including location and proposed function.

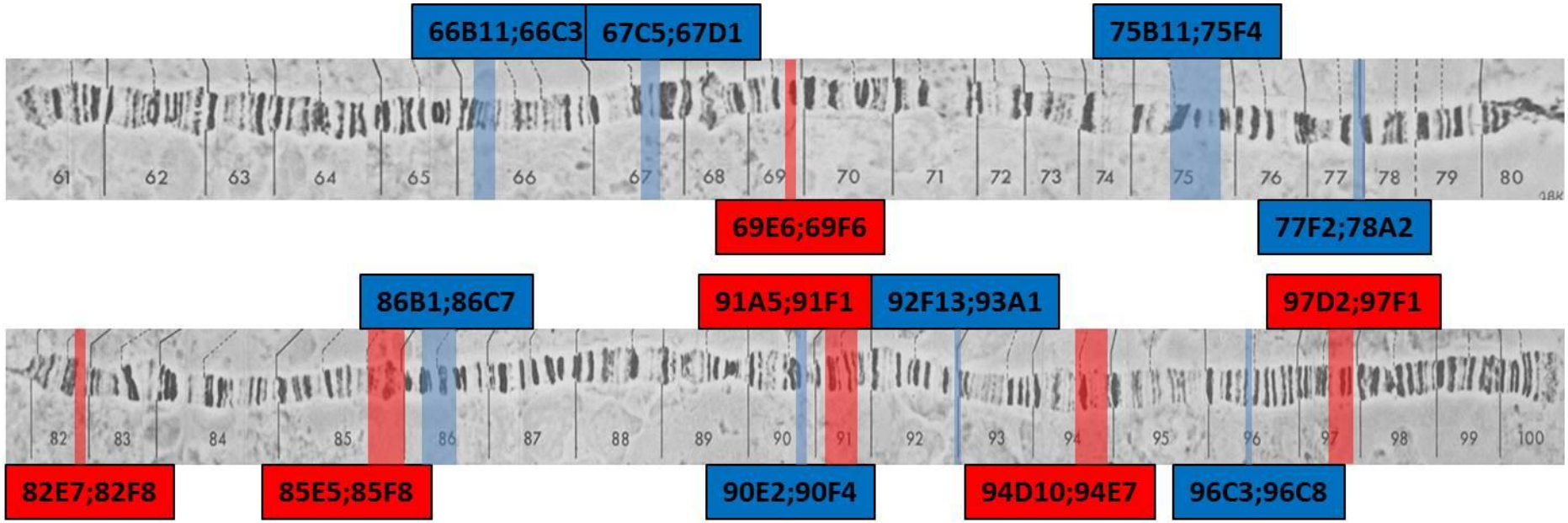

Figure 6.4: Chromosome 3 polytene maps annotated with regions associated with phenotypic change
Regions associated with phenotypic suppression listed in blue boxes and phenotypic enhancement in red boxes. All regions are polygenic except for 92F13;93A1, which overlaps only the gene syncrip. *Polytene chromosome photographs adapted from Schaeffer et al. (2008)*

6.3 Discussion

The deficiency screen is a very powerful method of pathway expansion. Now that coverage of the fruit fly genome is relatively comprehensive, deficiency kits are very useful as a first step in isolating novel research targets. In this case, the possibility of finding novel elements modulating the 0N4R-BRSK2 pathway was improved by the prior knowledge of the conserved BRSK kinases LKB1 and the CaMKKα homologue CG17698, and their importance to the eye phenotype. This method cannot guarantee to uncover the entirety of any given pathway, as evidenced by the inability of the screen to identify CG17698 or LKB1. Nonetheless, in the case of an obvious phenotype such as that seen here in the eye it allows relatively rapid screening of the majority of the genome by a single individual. Given the diverse aetiology of the tauopathies, this screen has unearthed a large number of candidate genes across 22 regions of the two largest *Drosophila* chromosomes.

6.3.1 Candidate genes on chromosome 2

The screen of chromosome 2 isolated eight regions of phenotypic suppression and began to examine these regions at the level of individual genes. The use of additional deficiencies to reduce the size of these regions greatly reduced the number of candidate genes. In the case of tau toxicity, there are a great many associated cellular processes, as has been revealed by past screens (Ambegaokar and Jackson, 2011). For BRSK2-associated modulation of tau toxicity, I decided to focus on potential components of the pathway, and on processes with which BRSK2 has previously been implicated. Among the former, protein kinases and phosphatases were obvious candidates. For the latter, the potential of calcium as a BRSK modulator, as well as the potential of BRSK2 to alter cell death or protein clearance mechanisms (autophagy in particular) gave some obvious target categories. Some genes associated with sugar metabolism were also considered, given the similarity between the BRSKs and AMPK. Additionally, cytoskeleton-associated proteins were included as potential indicators of BRSK2's effect on tau function, and genes associated with neurogenesis or eye development were included.

6.3.1.1 RNAi-based silencing of candidate genes

Among the polygenic phenotype-suppressing regions, eighteen genes were screened with RNAi, with another seven also considered candidates. As shown in table 6.1, four RNAi lines were found to lead to suppression of toxicity. These were contained within only two regions, and although it is possible for multiple BRSK2 modulators to be found within the same small chromosomal area, there is also the potential for false positives when performing a visual screen, given the subjective nature of the classification and the potential for phenotypic variation in the model. It is also possible that multiple deletions of relevant genes were responsible for the loss of phenotype seen in the deficiency, whereas suppression by RNAi tends to be stronger and could thus amplify the effect of individual genes. Six genes were tested within the approximately 163kb region of 22B8;22D1, containing 54 genes in total. RNAi against two of these genes was found to lead to phenotypic suppression: *su(dx)* (suppressor of Deltex) and *AIF* (apoptosis-inducing factor). *Su(dx)* was chosen as a potential candidate owing to the various recorded functions of the Notch signalling-associated *deltex* (Xu and Artavanis-Tsakonas, 1990), located on the X chromosome. These include influencing eye morphology (Gorman and Girton, 1992). An alternative hypothesis is based on Deltex acting in a similar manner to the tau kinase Shaggy, the GSK3 homologue and tau kinase which is also heavily implicated in regulation of Notch signalling. Indeed, mutations in these two proteins have the same ability to suppress specific Notch mutants (Ramain et al., 2001), leading to the possibility of an important role for Notch in BRSK2-mediated toxicity. Multiple components of the Notch signalling pathway have been implicated in tau toxicity in this model (Ambegaokar and Jackson, 2011). Su(dx) is itself a ubiquitin ligase of which Deltex is not presumed to be the sole target (Cornell et al., 1999), with a putative proline-rich binding site potentially found within other components of the 0N4R-BRSK2 pathway. The other possibility is that loss of Su(dx) leads to changes downstream of BRSK2, with loss of the ubiquitin ligase, proteasome-targeting activity of Su(dx) (Ramain et al., 2001) mitigating the dramatic upregulation of autophagy and potentially of protein turnover seen in 0N4R-B2WT5 fly eyes (Dr Alessia Galasso, unpublished data).

The alternative gene within this region is *AIF*, regulator of programmed cell death during development (Joza et al., 2008). Given that no increase in apoptosis was

observed in the eye disc in 0N4R-B2WT5 larvae as measured by TUNEL stain (Dr Alessia Galasso, unpublished data), it seems unlikely that a reduction in apoptosis could lead to a reduction in BRSK2-induced toxicity. However, it is still possible that apoptosis has an important role to play at a later developmental stage than that studied, or that a reduction in programmed cell death could lead to an appearance of larger eyes in these individuals when screened. One untested candidate in this region was *kebab*, a microtubule-associated protein which has been shown to play a role in mitosis, though an apparently dispensable one (Meireles et al., 2011).

The second region successfully probed using RNAi was much larger, covering over 600kb and 127 genes (43F8;44D4). Seven genes were studied, of which RNAi of two, CG14763 and *sut1* (sugar transporter 1), was reported to lead to phenotypic suppression. CG14763 has yet to be studied in depth. Its function is predicted to be involved in microtubule-based transport, with an ATPase domain and a TCTEX1 dynein light chain domain associated with cargo binding, as well as actin dynamics during neurite outgrowth (Chuang et al., 2005). This associates this gene with two possible mechanisms of interest to this screen – it is both microtubule-associated and potentially involved in neuronal development. The second gene, *sut1* was the only glucose transporter of the three within this region studied to be identified by the screen. The decision to study the sugar transporters was speculative, based on the links between sugar metabolism, diabetes and Alzheimer's disease as well as AMPK's more recent classification as a tau kinase (Thornton et al., 2011). It is perhaps more likely than CG14763 to be the result of a false positive, given that neither of the other *sut* genes exhibited any proclivity for BRSK2 phenotypic modulation. If not, then it is potential evidence for a metabolic influence on 0N4R-BRSK2-induced neurodegeneration. Besides the seven genes tested, other candidates for this region included four genes involved in eye development and neurogenesis (*vps28*, *pabp2*, *nito* and *optix*) and an ubiquitin ligase (*cul-4*).

Outside of these two regions, no other candidate genes have been successfully shown to have an effect on our phenotype by RNAi. Other potential genes to be tested are *spinster*, *basigin*, CG31687, *anterior open*, *eyes shut* and *decapentaplegic*. Mutations in *spinster* lead to a reduction in programmed cell death in the developing nervous system (Nakano et al., 2001). It is also implicated in autophagy – specifically, in reactivation of mTOR and autophagic inhibition following starvation

(Rong et al., 2011). If silencing *spinster* were found to lead to suppression of the 0N4R-BRSK2 phenotype, this would be evidence of a protective role for autophagy in this context. CG31687 has been implicated in cell polarity, though only in planar cells (Weber et al., 2012). The other four genes listed are all implicated in eye development.

6.3.1.2 Chickadee as a regulator of BRSK

The actin-binding protein Chickadee (Chic) is the *Drosophila* Profilin homologue, a protein family of highly conserved structure but only weakly conserved amino acid sequence (Cooley et al., 1992), thought to be ubiquitous among eukaryotes (Reichstein and Korn, 1979). It was originally thought to reduce actin polymerisation through sequestering actin monomers (Carlsson et al., 1977), though at physiological concentrations actually performs the opposite function. Profilin promotes the replenishment of ATP on actin filaments by decreasing the affinity of actin for its bound nucleotide, allowing replacement of ADP with ATP, in excess in the cell (Pantaloni and Carlier, 1993; Theriot and Mitchison, 1993). Its importance to the dynamics of the actin cytoskeleton is thus well characterised – what relevance could it have for the MAP-associated neurotoxicity studied here?

Although QED did not register any effect on ommatidial distortion in *chic* mutants, there appeared to be a consistent increase in eye size which could be evidence of an amelioration of 0N4R tau/BRSK2-induced neurodegeneration. The method of analysis of QED involves use of the edge set to recreate ommatidia as complete circles, eliminating any circle differing too severely from the expected size. As a result, there is no measure based on changes in whole eye size or shape. It would appear that a reduction in Chickadee function is capable of mitigating some aspects of 0N4R-BRSK2 toxicity. I would like to propose two hypotheses regarding the influence this actin-binding protein could have on tau-induced neurodegeneration.

One possibility stems from research performed specifically on Chickadee. In the fly, Chic is heavily involved in the transport (dumping) of cytoplasm from nurse cells into oocytes. Loss of *chic* has been shown to reduce dumping by 25 to 50% (Cooley et al., 1992), indicating a role for actin in this process. The actin cytoskeleton is involved in the establishment and maintenance of the ring canals connecting the cells, through which cytoplasm is transported via cytoplasmic microfilaments

(Mahajan-Miklos and Cooley, 1994). Interestingly, this process is also dependant on the microtubule-based cytoskeleton, which controls the rapid cytoplasmic streaming – loss of the microtubule-associated proteins Cappuccino and Spire leads to a very similar phenotype to that of *chic* mutants. In each case, disruption of streaming occurs due to a premature bundling of microtubules prior to streaming and ring canal formation (Manseau et al., 1996). Here then, Chic is involved in the synchronisation of the actin- and microtubule-based cytoskeletons and it has been hypothesised that these proteins could form the interface between them. Although Chic mutant phenotypes have not been recorded within neural tissues, this idea remains a tantalising prospect for its implications regarding the importance of both cytoskeletons in this model of tauopathy. It should be noted however that *spir* was tested in the RNAi screen, and was not found to lead to a change in phenotype.

An alternative hypothesis for the role of Chic returns to the idea of autophagic cell death being the cause of the phenotypes observed here. As was already noted in Chapter 3, HDAC6 has been shown to be important in aggresome targeting (Guthrie and Kraemer, 2011). This deacetylase has been shown to control microtubule-dependent cell motility via deacetylation of tubulin (Hubbert et al., 2002), some of the first evidence for the importance of acetylation in processes more diverse than control of gene transcription via histones. The deacetylase has also been shown to interact with the actin cytoskeleton (Gao et al., 2007). Subsequently, the first evidence was found for HDAC6 controlling selective autophagy via actin, and ubiquitin-dependent aggrephagy specifically (Lee et al., 2010). This study demonstrated that aggrephagy was dependent upon both HDAC6 and the actin cytoskeleton, both of which were entirely dispensable for conventional, starvation-induced autophagy. HDAC6 was shown to be necessary for autophagosome-lysosome fusion, but again only in quality-control aggrephagy, with this effect reversed under other conditions of autophagy. Finally, the study showed that this function of HDAC6 was F-actin dependent. The fly HDAC6 homologue is located within the X chromosome and was not covered by this screen. It is possible that loss of Chic could disrupt F-actin, leading to a reduction in aggresome formation. This would imply a cytotoxic role for autophagy in this model, with cell death caused by an overzealous upregulation of the process in response to 0N4R tau and BRSK2. This could be investigated via study of autophagy levels in *chic* mutants, via probing

for lysosomes or p62 as described in Chapter 3.

Profilin has previously been implicated in neurodegenerative disease, specifically as a genetic risk factor in amyotrophic lateral sclerosis (Wu et al., 2012). Though speculative, this screen may indicate a link between this protein and tau-induced neurodegeneration.

6.3.2 Candidate genes on chromosome 3

The screen of chromosome 3 was not pursued in as much detail as that of chromosome 2 due to time constraints. As a result, only the 178 lines of the standard Bloomington deficiency kit were examined, with no extra lines acquired to reduce the regions of interest, or RNAi screening performed. In addition, the lines have not yet been screened to remove deficiencies altering the phonotype of tau alone. Consequently, the majority of the 14 regions of interest are extensive, with a large list of potential candidate genes, as listed in Table 6.2.

It was hoped that the knowledge of modulators of BRSK2-induced toxicity would allow the use of deficiencies containing CG17698 or LKB1 as positive controls for the screen. With CG17698 not contained within any deficiency line, and the LKB1-containing deficiency not identified by screening, this was not the case. That hemizygosity for LKB1 should not noticeably alter the phenotype is ultimately not wholly unexpected – two copies of LKB1 RNAi were required for effective suppression of BRSK2-induced toxicity, likely reducing LKB1 activity far more than loss of a single gene copy. This illustrates one shortcoming of the deficiency screen when compared with RNAi as a method of gene suppression – it is generally less sensitive.

The only region containing a single gene is 92F13;93A1, which overlaps *syncrip* (synaptotagmin-binding, cytoplasmic RNA-interacting protein), encoding a protein originally isolated in mouse brain lysate (Mizutani et al., 2000). In the fly, this mRNA-binding protein has been shown to bind and localise multiple transcripts in the oocyte (McDermott et al., 2012). It was also shown to be highly expressed in the larval nervous system, though precisely which tissues require SYNCRIP for correct development has yet to be determined. A developmental role for the gene puts it at the right time to influence our phenotype; whether it is also in the right place has yet

to be seen. The same group, led by Professor Ilan Davis at Oxford, also claims to have evidence for the control of some synaptic kinase transcripts by SYNCRIP, including those of CamKII and Discs large (DLG). Loss of DLG in particular has been shown to cause disruption of the cytoskeleton and cell polarity (Woods et al., 1996).

Multiple calcium-dependent proteins are also found by the screen, across three regions, including the protease Calpain-B and three Cadherins. There are a number of genes associated with protein turnover, including multiple ubiquitin-protein ligases (*hyperplastic discs* and *CG11261*), regulators of apoptosis (*MED24* and *reaper*) and a single gene associated with autophagy (*CG12163*). *Hyperplastic discs* in particular is associated with differentiation of the photoreceptor cells of the eye imaginal disc (Lee et al., 2002). Among the regulators of phosphorylation found by the screen, the stress response-associated mitogen-activated protein kinase kinase kinase MEKK1 (Inoue et al., 2001) is unsurprising given that it was also found in the screen by Ambegaokar and Jackson (2011). Cyclin-dependent kinase 8 (CDK8) has not yet been implicated in tau phosphorylation, neither have the serine-threonine kinase Frayed or the tyrosine kinase Heartless. Among the other genes in Table 6.2, *MYPT*, *canoe* and *unkempt* are associated with development of the eye and likely of limited interest. Further screening of the chromosome would be necessary before committing to further study of any of these genes, as was performed for chromosome 2. The majority of these candidate genes would likely be eliminated by additional screening with overlapping deficiencies and RNAi lines.

The complex, tau isoform-dependent nature of the effect of BRSK2 on tau-induced neurotoxicity was revealed in Chapter 4 of this work, and the tissue-specific toxicity of BRSK2 in Chapter 5. This chapter has described attempts to uncover the endogenous pathways responsible. This screen was incomplete but has uncovered some promising leads, particularly the potential of *chic* to help explain the nature of the toxicity observed in the eye, or the role of the cytoskeleton in this model of tauopathy. Completion of the chromosome 3 screen is an obvious next step in the search for 0N4R tau-BRSK2 modulators.

7| General Discussion

The work described in this thesis has been an attempt to expand current understanding of the relationship between tau phosphorylation and toxicity. This work began with the goal to further characterise the tau kinase BRSK2, which had already been examined in some detail by the Moffat and Frenguelli labs, and was thus firmly in the domain of examining the consequences of tau hyperphosphorylation. This was at a time when several laboratories had begun to express frustration with the term "hyperphosphorylation", which had become something of a catch-all for any and all instances of recorded tau dysfunction. One of the most vocal critics of the term was Guy Lippens, of Lille University, whose dissatisfaction with the broad definition of tau hyperphosphorylation was perhaps spurred on by a background in chemistry and nuclear magnetic resonance (NMR) spectroscopy (Lippens et al., 2012; Lippens et al., 2007). That tau hyperphosphorylation can only be defined stoichiometrically (as an increase in the number of phosphate groups per molecule of tau) due to the overlap between healthy and diseased phosphorylation patterns speaks to a complex code of tau phosphorylation, if indeed phosphorylation is the primary mechanism of tau dysfunction. That tau hyperphosphorylation as a concept may be overly simplistic is perhaps best illustrated by studies involving tau species bearing large numbers of phospho-mutations. Hypo-phosphorylated S11A tau was shown to exhibit increased toxicity in the fly retina (Chatterjee et al., 2009); in contrast E14 tau, supposed to simulate a hyper-phosphorylated state, was found to be less toxic to dopaminergic neurons than wild-type (Wu et al., 2013b). Clearly, these data do not sit well with the idea that tau phosphorylation should correlate directly with toxicity. Interpretation of these results, based on wholesale mutation of large numbers of residues on tau, is extremely difficult without better understanding of the importance of individual phosphorylation sites, or smaller combinations of them.

In vitro studies of mutant tau species have demonstrated the ability of individual phosphorylatable residues on tau to alter both normal tau function (microtubule stabilisation) and disease-associated processes (tau aggregation), testament to their relevance to disease. These *in vitro* experiments also hinted at a tau phosphorylation "bar code" (Lippens et al., 2007), establishing hierarchies of importance to specific processes among residues. For example, a 2N4R tau S262D mutant was shown to be particularly inefficient in stabilising microtubules, with a greater loss of function

than a T231D mutant (Kiris et al., 2011). On the other hand, a study of tau aggregation found a 2N4R tau T212E mutant to be far more prone to fibrillisation than an S262E mutant, which was found to be no different to WT 2N4R tau (Chang et al., 2011; Necula and Kuret, 2004). Such mutants have also been shown to demonstrate unexpected combinatorial effects; mutants were found to not exhibit additive effects on microtubule stability (Kiris et al., 2011). In contrast exponential increases in apoptosis were witnessed in cell culture models transfected with poly-E mutants, as measured by TUNEL stain (Alonso et al., 2010).

The relevance of these experiments to our study of BRSK2 was underlined by the study of tau phosphorylation by a number of AMPK-related kinases, including BRSK2, by Yoshida and Goedert (2011). This study demonstrated the phosphorylation profile of recombinant 1N4R tau in the presence of BRSK2 *in vitro*, which was shown to include both T212 and S262. BRSK2 had already been shown by our lab to induce an unusually strong eye phenotype upon co-expression with 0N4R tau in the fly eye (see Figure 4.1 for an example), much stronger than observed with MARK-induced phenotypes (Chatterjee et al., 2009). Given that BRSK2 was shown to be apparently less potent a tau kinase than MARK1 *in vitro* (Yoshida and Goedert, 2011) but more able to phosphorylate T212, this suggested the possibility of T212 phosphorylation being the primary determinant of tau-induced neurotoxicity in this model. The tau mutants examined in Chapters 3, 4 and 5 of this thesis were created as a result, and the reality was found to be more complicated.

This project has attempted to transplant *in vitro* studies into the effects of phosphorylation mutants into an *in vivo* model, in order to gain insights into the fundamental mechanisms and functional consequences of tau toxicity, including microtubule binding, tau aggregation and kinase activity. At the close of the project, I would like to consider the most interesting aspects of the data presented herein with regard to current ideas of tauopathy.

7.1 Tau aggregation and neurotoxicity

When planning the tau mutations which would later be inserted into *Drosophila*, one aspect of interest was the relative importance of tau aggregation versus microtubule binding. The T212A and T212D mutations were considered most likely to alter tau aggregation (Necula and Kuret, 2004), if indeed aggregation was a relevant phenomenon to tau toxicity in *Drosophila* models given the apparent dispensability of large tau aggregates to toxicity in the fly (Wittmann et al., 2001). Thus, the phenotypic expectation of T212D animals was for either a lack of effect (with an aggregation-inducing mutation of no consequence in the fly) or for a partial recapitulation of the increase in toxicity witnessed in flies co-expressing BRSK2 and 0N4R tau. That the T212D mutant phenotype was less severe than that of 2N4R WT, or the S262D mutant, was consequently seen as the most important discovery of the individual 2N4R tau mutant library, particularly given the concurrent upsurge in evidence for the formation of insoluble tau aggregates in fruit fly tauopathy models.

Colodner and Feany (2010) were able to demonstrate the accumulation of insoluble, hyperphosphorylated 0N4R tau in glia of aged flies (evident at 20 days old), after aging at 30°C to boost expression. One interesting aspect of their experiments was the demonstration of a disconnection between insoluble tau levels and toxicity – reducing the temperature from 30°C to 17°C was shown to reduce both tau expression and cellular toxicity (as measured by apoptosis using TUNEL stain), with no concomitant drop in insoluble tau levels. Other studies have since associated the formation of insoluble tau oligomers in *Drosophila* with a suppression of toxicity, via inhibition of GSK-3β (Cowan and Mudher, 2013) or upregulation of NMNAT (Ali et al., 2012). In each of these cases, the mitigation of human tau-induced behavioural phenotypes was accompanied by an increase in the formation of insoluble oligomers. In another case, in which fibrillar tau aggregates were witnessed in neurons, no indication of the relative levels of oligomer formation in WT or E14 mutant tau was given, though the E14 mutant was found to be less toxic (Wu et al., 2013b). Conversely, highly mutated S11A tau was found to exhibit increased toxicity in the fly eye compared with wild-type or S2A tau; this increase in toxicity was not accompanied by any increase in insoluble tau levels, but rather by radically improved microtubule binding (Chatterjee et al., 2009). In the fly, it would seem that

tau toxicity is heavily dependent upon solubility, with smaller, soluble oligomers present in two of these studies (Ali et al., 2012; Wu et al., 2013b).

I hypothesise that the reduction in toxicity of tau following T212D mutation is due to a change in its aggregation kinetics, leading to a decrease in levels of soluble tau in animals expressing this mutant. With the recent examples of tau aggregation in *Drosophila* all involving neuronal expression, the eye may not be the best target tissue to demonstrate this. It is likely that ELAV would constitute a better driver, although Chau et al. (2006) appear to have had some success in demonstrating tau-immunoreactive aggregates in the eye. The temperature-sensitive GAL80 repressor could be used to ensure healthy development, before driving high levels of expression at 30°C, as in Colodner and Feany (2010). Insoluble tau appears to accumulate and be stable over time, facilitating comparison between different tau species after aging the animals. Western blotting would allow quantification, with visualisation of oligomers possible using electron microscopy as used by Wu et al. (2013). If it is the case that aggregation can be protective, potentially by sequestering soluble, toxic tau, then this could explain why the T212D S262D double mutant exhibited a phenotype extremely close to that of T212D. This would make any aggregation-increasing mutation effectively dominant in the panoply of tau phospho-mutations. In this context, any change of microtubule-binding or other effect caused by S262 mutation would be effectively silenced. That S262A mutation also reduces toxicity is potentially further evidence for the benefits associated with binding tau either in insoluble oligomers or to microtubules, again preventing soluble tau from initiating neurodegeneration. Such a hypothesis certainly depends upon soluble tau exhibiting some gain of function; perhaps, as suggested by Cowan et al. (2010), such species are capable of disrupting the microtubule cytoskeleton by sequestration of native tau and other MAPs, leading to axonal transport defects. Tau phosphorylated at serines 199 and 202 has been shown to sequester MAPs 1 and 2 (Alonso et al., 1997), which could help to explain the additional effect of transgenic tau in this model beyond simply the loss of native dtau, given that toxicity is still evident in a dtau null background (Feuillette et al., 2010). Figure 7.1 provides an overview of this hypothesis. Further assays in order to classify tau solubility and microtubule-binding in each of these mutants would be required to support this model of tau toxicity.

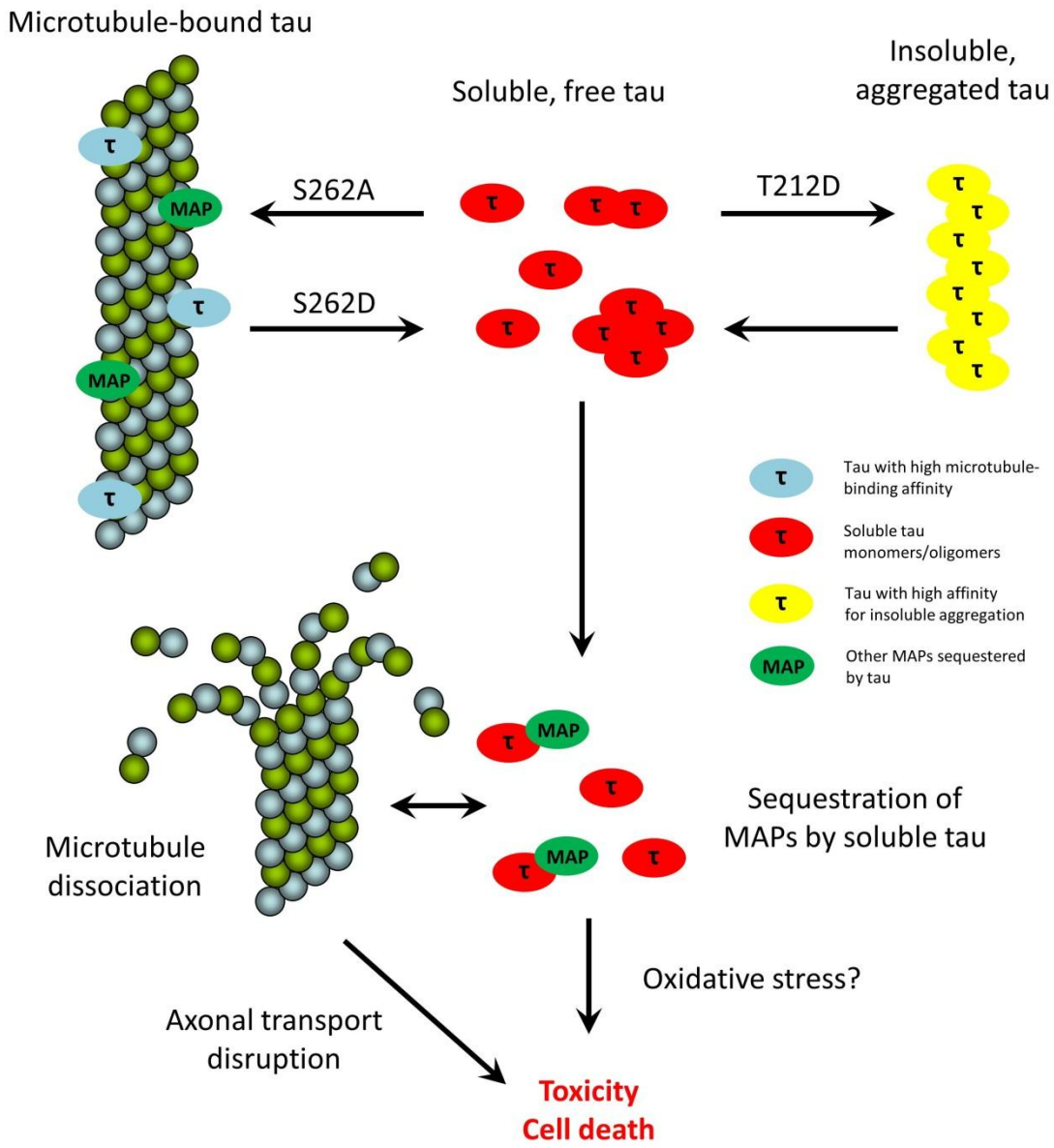

Figure 7.1 Hypothetical effects of tau phospho-mutation on toxicity
Observations from this work in vivo *combined with* in vitro *data from other sources (Kiris et al., 2011; Necula and Kuret, 2004) suggest the ability of S262A mutation to increase microtubule binding and T212D to increase aggregation. Both of these mutations led to decreased toxicity the fly eye, potentially by reducing the pool of soluble tau. This soluble tau appears to exhibit some toxic gain of function, including disruption of the microtubule cytoskeleton, likely via sequestration of other MAPs. It may also lead to cell death via oxidative stress, DNA damage and apoptosis (see below).*

In all, the results of this screen of the tau phospho-mutant library conform well to ideas privileging tau solubility over tangle formation as the cause of neurodegeneration in tauopathy. It is with regards to BRSK2 that this work has raised the most challenging questions, particularly that of the relationship between tau isoform and disease.

7.2 The prospects for BRSK2 as a tau kinase

The unusually strong eye phenotype of 0N4R tau/BRSK2 flies was the principal motivation for further study of this kinase. That 2N4R tau would not respond in the same way was unexpected, and not easily explained. It may also serve to provide some insight into the effect of BRSK2 expression in the fly eye.

The previously observed, S262-dependent toxicity of 0N4R tau/BRSK2 animals (unpublished data) bears significant resemblance to the interaction between 0N4R tau and *Drosophila* checkpoint kinase 2 (Chk2) shown by Iijima-Ando et al. (2010). Chk2 was shown to exhibit no external eye toxicity when overexpressed without tau, but to drastically increase toxicity caused by 0N4R tau. Chk2 overexpression had no effect on an S262A mutant, or on toxicity caused by PAR-1 in the absence of tau. The eye phenotype caused by co-expression of 0N4R tau and Chk2 is reminiscent of our recombinant 0N4R/B2WT5 line and is more severe than recorded phenotypes for co-expression of 0N4R tau and either Sgg or PAR-1 (Jackson et al., 2002; Nishimura et al., 2004). Such a similarity in effect between BRSK2 and Chk2 is perhaps to be expected, given the existing evidence for BRSK2 itself being a checkpoint kinase. SAD1 kinase was shown to relocate to the nucleus following UV treatment and be activated specifically following UV-induced DNA damage, leading to cell cycle arrest at G_2/M (Lu et al., 2004). This is likely due to phosphorylation and downregulation of the checkpoint kinase Wee1 by both of the BRSKs, an essential step in the establishment of neuronal polarity (Muller et al., 2010). It is interesting to note that this last step appears to not involve microtubule regulation and is thus presumably tau-independent, indicating a dual role for the BRSKs in neuronal differentiation. This distinction between tau-dependent and tau-independent functions of BRSKs could be relevant to our model. Indeed, regulation of cell cycle

progression has been shown to influence tau toxicity in *Drosophila*, with cell cycle interference reducing toxicity and tau-induced apoptosis (Khurana et al., 2006).

One possible explanation for the increase in 0N4R tau toxicity due to BRSK2 is that the kinase serves to amplify cell death during development in response to a threshold level of tau-induced DNA damage, potentially via oxidative stress (Dias-Santagata et al., 2007) or cytoskeletal disruption (Cowan et al., 2010). In this case, our WT 0N4R tau transgenic line (which has been shown to lead to greater distortion of the eye in the absence of BRSK2 than any of the 2N4R lines or S262A/S2A mutant 0N4R tau) passes this threshold leading to activation of BRSK2-induced cell cycle arrest and cell death. This would all take place during development in our model, leading to the shrunken eyes found in the 0N4R/B2WT5 line. This process would effectively sideline any phosphorylation of tau by BRSK2 (the assumed primary function of BRSKs) unless the threshold of damage for initiation of cell cycle arrest was reached; this could explain the reduction of 2N4R tau toxicity in the presence of BRSK2, in line with the double phospho-mimetic mutant shown in Chapter 4. The other possible explanation for this reduction would be an induction of DNA repair by the kinase in response to a lower level of DNA damage. One potential complication for this hypothesis is the lack of apoptosis witnessed in the developing larval eye of these flies (as measured by TUNEL stain – Dr Alessia Galasso, personal communication), and the increase in lysosomal numbers (as measured by LysoTracker stain – Dr Alessia Galasso, personal communication). It is possible that apoptosis does occur, at a later stage of development to that observed, via expected apoptotic pathways involving Chk2 and p53 (Hirao et al., 2000). As for the upregulation of lysosomal activity, this could be protective, in an attempt to forestall cell death via apoptosis, as has been observed in cancer (Abedin et al., 2007; Katayama et al., 2007). This would situate autophagy as an antecedent to apoptotic cell death. The other possibility is that in this case BRSKs induce cell death via an overactivation of autophagy alone (Rodriguez-Rocha et al., 2011). Overall, this explanation for the discrepancy between tau isoforms in their response to BRSK2 appears to be the most straightforward, and is outlined in Figure 7.2. Examination of levels of cell death and autophagy in 2N4R tau-expressing larvae would be the obvious first step in investigating this theory, as was performed previously. As has already been performed in the fly, modification of antioxidant pathways in order to

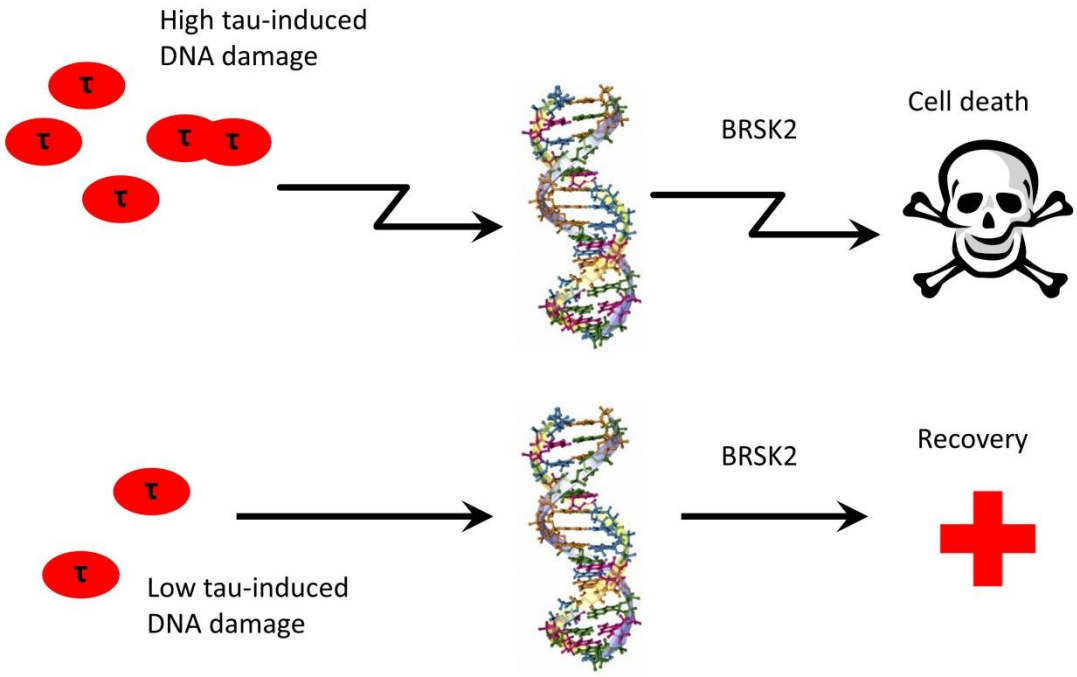

Figure 7.2 Level of tau-induced toxicity appears to determine the consequences of BRSK2 co-expression

A potential role for the checkpoint kinase function of BRSK2 in our model. Putative DNA damage caused by transgenic tau expression activates BRSK2, causing cell cycle arrest. The severity of tau-induced toxicity then determines whether BRSK2 activity leads to either cell death or DNA repair and cell survival.

determine their effect on the tau/BRSK interaction could be very informative (Dias-Santagata et al., 2007). Superoxide dismutase (SOD) downregulation, for example, has been shown to increase tau neurotoxicity, leading to an increase in apoptosis. Would such modification activate BRSK2 if performed on 2N4R tau-expressing flies? Conversely, would SOD overexpression eliminate the 0N4R tau/BRSK2 interaction? Indeed, simply increasing levels of 2N4R tau expression could be an alternative method of investigation; given the genetics of the flies we have generated, it would be necessary to generate a recombinant 2N4R/B2WT5 line to pursue this. Another question would be whether this interaction was tau-specific, or whether it could be activated in response to other sources of DNA damage. Iijima-Ando et al. (2010) tested this in their study of Chk2 using Aβ42 peptide and found no effect due to the kinase. However, it is worth noting that the apparent level of external eye disruption caused by Aβ42

alone was less than that witnessed in their 0N4R tau-expressing fly, perhaps creating a similar situation to our 2N4R tau model. On the other hand, this could be due to differing mechanisms of cellular toxicity between tau and Aβ.

Were such experiments not able to increase 2N4R/BRSK2-induced toxicity, then the implication would be that the interaction was tau isoform-dependent. Although very little work has been performed directly comparing the effective differences between 0N4R and 2N4R tau in disease, some comparisons have already been made (Papanikolopoulou and Skoulakis, 2011). The presence of two amino-terminal inserts in the S11A tau used by Chatterjee et al. (2009) was postulated to result in its increased toxicity relative to a previously-studied 0N4R S14A construct (Steinhilb et al., 2007), though it is also worth noting that only eight of residues were similarly altered in both constructs. A simpler and stronger comparison was made by Kosmidis et al. (2010), who demonstrated that 2N4R tau was more toxic to mushroom body neurons than 0N4R tau, even when expressed at lower levels. Although this differs from the relative toxicity we have found in the retina, this is likely due to more drastic differences in expression levels due to their respective insertion sites, or potentially tissue-specific differences in toxicity (Grammenoudi et al., 2006). I have already speculated about potential mechanisms of N-domain-dependent changes in tau toxicity in Section 4.3. BRSK2-induced changes in tau levels would be relatively easily detectable via Western blotting. In addition, the possibility of N-domain-

determined secondary structure changes could be an interesting avenue of investigation, given the ability of the amino terminus to alter tau polymerisation kinetics (Gamblin et al., 2003). The increased negative charge of the projection domain in the 2N4R isoforms could conceivably lead to an increase in the Alz50 conformation, in which the microtubule-binding domains exhibit affinity for the N terminus, rather than tubulin (also negatively charged). Whether BRSK2-induced phosphorylation is capable of increasing the likelihood of such a conformational change, particularly in an isoform-specific manner, is admittedly speculative. That this conformation has been particularly associated with neurofibrillary tangles, and thus insoluble tau aggregation, does make it consistent with a reduction in toxicity in this model. Alternatively, it is possible that some change in tau secondary structure caused by amino-terminal differences could alter the ability of BRSK2 to interact with 2N4R tau. Thorough quantification of BRSK2-induced tau phosphorylation, ideally via mass spectrometry, would likely be a good source of leads in such an investigation. Alternatively, replication of the phospho-mutant library in 0N4R tau would provide an indication of whether any phosphorylation-induced changes were isoform-specific. Given that 0N4R S262A mutants have already been studied and shown to exhibit reduced toxicity (Iijima-Ando et al., 2010), the most interesting mutation to replicate would be T212D, the toxicity-reducing, putative aggregation-increasing mutation.

7.3 Concluding remarks

Two observations of this work are likely consequential to tauopathy studies in animal models more generally. For any tau isoform-specific effects to be observable highlights the importance of looking beyond single isoforms or transgenes, as has been suggested by the study of FTDP-17 mutations, which alter 3R:4R expression ratios, and other tauopathies (Hong et al., 1998; Majounie et al., 2013). If N-terminal domains are also relevant to disease, then potentially all six isoforms could play different roles. The second observation is that of tissue-specific effects of the tau kinase BRSK2. That human tau undergoes differential phosphorylation in the fly in a tissue-dependent manner, and that this leads to different cellular outcomes has already been noted by the laboratory of Efthimios Skoulakis (Grammenoudi et al.,

2006; Kosmidis et al., 2010). Specifically, tau driven by ELAV was shown to be phosphorylated at T212 and S214, whereas tau driven in the retina was not. That BRSK2 overexpression alone leads to toxicity in the fly CNS, indeed significantly more than does tau, suggests that tissue-specific studies would be useful in any investigation of tau kinases. I have already speculated that this could be due to additional targets of BRSK2 in the brain (see Chapter 5). Given the hypothesis raised earlier regarding the role of BRSKs as checkpoint kinases, disruption of cell cycle mechanics seems a likely cause. Both upstream and downstream components of the BRSK2 cell cycle pathway are conserved in *Drosophila*, including its target Wee1 (Campbell et al., 1995) and the regulator of BRSK2, c-Jun activation domain-binding protein 1 or Jab1 (Gemmill et al., 2002; Zhou et al., 2012). Neither of these elements of the cell cycle pathway was revealed by the deficiency screen of Chapter 6, perhaps because of its use of the eye as an expression system (in which BRSK2 exhibits no toxicity alone), or due to the relative insensitivity of the deficiency screen. It is possible that the CNS is more sensitive than cells of the *Drosophila* retina to disruption of the cell cycle or indeed of neuronal polarisation by BRSK2.

In attempting to demonstrate the nature of BRSK2 as a conventional tau kinase, as well as a regulator of tau toxicity via phosphorylation, this project has generated evidence of a far more complex phosphorylation code. BRSK2 appears to modulate tau toxicity in an isoform-, or potentially a concentration-dependent manner, and via at least three phosphorylation sites on tau (T212, T231 and S262). I have shown the inequivalence between tau phosphorylation and toxicity, and provided evidence supporting the idea that individual phosphorylation sites play specific roles in the regulation of tau function and dysfunction. Future examination of the nature of tau phosphorylation *in vivo* would benefit from expansion of this work, and further attempts are required to link residues and regions of tau to the different processes of microtubule binding, aggregation and toxicity.

8| References

Abedin, M. J., D. Wang, M. A. McDonnell, U. Lehmann, and A. Kelekar, 2007, Autophagy delays apoptotic death in breast cancer cells following DNA damage: Cell Death Differ, v. 14, p. 500-10.
Adams, S. J., M. A. DeTure, M. McBride, D. W. Dickson, and L. Petrucelli, 2010, Three repeat isoforms of tau inhibit assembly of four repeat tau filaments: PLoS One, v. 5, p. e10810.
Akoury, E., M. Gajda, M. Pickhardt, J. Biernat, P. Soraya, C. Griesinger, E. Mandelkow, and M. Zweckstetter, 2013, Inhibition of tau filament formation by conformational modulation: J Am Chem Soc, v. 135, p. 2853-62.
Alessi, D. R., K. Sakamoto, and J. R. Bayascas, 2006, LKB1-dependent signaling pathways: Annu Rev Biochem, v. 75, p. 137-63.
Ali, Y. O., K. Ruan, and R. G. Zhai, 2012, NMNAT suppresses tau-induced neurodegeneration by promoting clearance of hyperphosphorylated tau oligomers in a Drosophila model of tauopathy: Hum Mol Genet, v. 21, p. 237-50.
Alonso, A. D., J. Di Clerico, B. Li, C. P. Corbo, M. E. Alaniz, I. Grundke-Iqbal, and K. Iqbal, 2010, Phosphorylation of tau at Thr212, Thr231, and Ser262 combined causes neurodegeneration: J Biol Chem, v. 285, p. 30851-60.
Alonso, A. D., I. Grundke-Iqbal, H. S. Barra, and K. Iqbal, 1997, Abnormal phosphorylation of tau and the mechanism of Alzheimer neurofibrillary degeneration: sequestration of microtubule-associated proteins 1 and 2 and the disassembly of microtubules by the abnormal tau: Proc Natl Acad Sci U S A, v. 94, p. 298-303.
Alvarado-Kristensson, M., M. J. Rodriguez, V. Silio, J. M. Valpuesta, and A. C. Carrera, 2009, SADB phosphorylation of gamma-tubulin regulates centrosome duplication: Nat Cell Biol, v. 11, p. 1081-92.
Alzheimer, A., 1907, Uber eine eigenartige Erkrankung der Hirnrinde: Allgemeine Zeitschrife Psychiatrie, v. 64, p. 146-148.
Alzheimer, A., R. A. Stelzmann, H. N. Schnitzlein, and F. R. Murtagh, 1995, An English translation of Alzheimer's 1907 paper, "Uber eine eigenartige Erkankung der Hirnrinde": Clin Anat, v. 8, p. 429-31.
Ambegaokar, S. S., and G. R. Jackson, 2011, Functional genomic screen and network analysis reveal novel modifiers of tauopathy dissociated from tau phosphorylation: Hum Mol Genet.
Anand, R., K. D. Gill, and A. A. Mahdi, 2014, Therapeutics of Alzheimer's disease: Past, present and future: Neuropharmacology, v. 76 Pt A, p. 27-50.
Andorfer, C., C. M. Acker, Y. Kress, P. R. Hof, K. Duff, and P. Davies, 2005, Cell-cycle reentry and cell death in transgenic mice expressing nonmutant human tau isoforms: J Neurosci, v. 25, p. 5446-54.
Andreadis, A., 2005, Tau gene alternative splicing: expression patterns, regulation and modulation of function in normal brain and neurodegenerative diseases: Biochimica et Biophysica Acta (BBA) - Molecular Basis of Disease, v. 1739, p. 91-103.
Andrieux, A., P. Salin, A. Schweitzer, M. Bégou, B. Pachoud, P. Brun, S. Gory-Fauré, P. Kujala, M.-F. Suaud-Chagny, G. Höfle, and D. Job, 2006, Microtubule Stabilizer Ameliorates Synaptic Function and Behavior in a Mouse Model for Schizophrenia: Biological Psychiatry, v. 60, p. 1224-1230.

Areosa Sastre, A., R. McShane, and F. Sherriff, 2004, Memantine for dementia: Cochrane Database Syst Rev, p. Cd003154.
Asuni, A. A., A. Boutajangout, D. Quartermain, and E. M. Sigurdsson, 2007, Immunotherapy targeting pathological tau conformers in a tangle mouse model reduces brain pathology with associated functional improvements: J Neurosci, v. 27, p. 9115-29.
Baas, A. F., L. Smit, and H. Clevers, 2004, LKB1 tumor suppressor protein: PARtaker in cell polarity: Trends Cell Biol, v. 14, p. 312-9.
Baas, P. W., and F. J. Ahmad, 2013, Beyond taxol: microtubule-based treatment of disease and injury of the nervous system: Brain, v. 136, p. 2937-51.
Baas, S., M. Sharrow, V. Kotu, M. Middleton, K. Nguyen, H. Flanagan-Steet, K. Aoki, and M. Tiemeyer, 2011, Sugar-free frosting, a homolog of SAD kinase, drives neural-specific glycan expression in the Drosophila embryo: Development, v. 138, p. 553-63.
Balbiani, E. G., 1881, Sur le structure du noyau des cellules salivaires chez les larves de Chironomus: Zoologische Anzeiger, v. 4, p. 637-641.
Bancher, C., and K. A. Jellinger, 1994, Neurofibrillary tangle predominant form of senile dementia of Alzheimer type: a rare subtype in very old subjects: Acta Neuropathol, v. 88, p. 565-70.
Bangen, K. J., A. Beiser, L. Delano-Wood, D. A. Nation, M. Lamar, D. J. Libon, M. W. Bondi, S. Seshadri, P. A. Wolf, and R. Au, 2013, APOE Genotype Modifies the Relationship between Midlife Vascular Risk Factors and Later Cognitive Decline: J Stroke Cerebrovasc Dis.
Barnes, A. P., B. N. Lilley, Y. A. Pan, L. J. Plummer, A. W. Powell, A. N. Raines, J. R. Sanes, and F. Polleux, 2007, LKB1 and SAD kinases define a pathway required for the polarization of cortical neurons: Cell, v. 129, p. 549-63.
Berchtold, N. C., and C. W. Cotman, 1998, Evolution in the conceptualization of dementia and Alzheimer's disease: Greco-Roman period to the 1960s: Neurobiol Aging, v. 19, p. 173-89.
Bergem, A. L., K. Engedal, and E. Kringlen, 1997, The role of heredity in late-onset Alzheimer disease and vascular dementia. A twin study: Arch Gen Psychiatry, v. 54, p. 264-70.
Berger, Z., B. Ravikumar, F. M. Menzies, L. G. Oroz, B. R. Underwood, M. N. Pangalos, I. Schmitt, U. Wullner, B. O. Evert, C. J. O'Kane, and D. C. Rubinsztein, 2006, Rapamycin alleviates toxicity of different aggregate-prone proteins: Hum Mol Genet, v. 15, p. 433-42.
Berridge, M. J., 2011, Calcium signalling and Alzheimer's disease: Neurochem Res, v. 36, p. 1149-56.
Bertram, L., and R. E. Tanzi, 2008, Thirty years of Alzheimer's disease genetics: the implications of systematic meta-analyses: Nat Rev Neurosci, v. 9, p. 768-78.
Bielska, A. A., and N. J. Zondlo, 2006, Hyperphosphorylation of tau induces local polyproline II helix: Biochemistry, v. 45, p. 5527-37.
Biernat, J., N. Gustke, G. Drewes, E. M. Mandelkow, and E. Mandelkow, 1993, Phosphorylation of Ser262 strongly reduces binding of tau to microtubules: distinction between PHF-like immunoreactivity and microtubule binding: Neuron, v. 11, p. 153-63.
Biernat, J., Y.-Z. Wu, T. Timm, Q. Zheng-Fischhöfer, E. Mandelkow, L. Meijer, and E.-M. Mandelkow, 2002, Protein Kinase MARK/PAR-1 Is Required for Neurite Outgrowth and Establishment of Neuronal Polarity: Molecular Biology of the Cell, v. 13, p. 4013-4028.

Binder, L. I., A. Frankfurter, and L. I. Rebhun, 1985, The distribution of tau in the mammalian central nervous system: J Cell Biol, v. 101, p. 1371-8.
Birks, J., and R. J. Harvey, 2006, Donepezil for dementia due to Alzheimer's disease: Cochrane Database Syst Rev, p. Cd001190.
Birmingham, K., and S. Frantz, 2002, Set back to Alzheimer vaccine studies, Nat Med, v. 8: United States, p. 199-200.
Bjorkoy, G., T. Lamark, A. Brech, H. Outzen, M. Perander, A. Overvatn, H. Stenmark, and T. Johansen, 2005, p62/SQSTM1 forms protein aggregates degraded by autophagy and has a protective effect on huntingtin-induced cell death: J Cell Biol, v. 171, p. 603-14.
Black, M. M., T. Slaughter, S. Moshiach, M. Obrocka, and I. Fischer, 1996, Tau is enriched on dynamic microtubules in the distal region of growing axons: J Neurosci, v. 16, p. 3601-19.
Boersema, P. J., R. Raijmakers, S. Lemeer, S. Mohammed, and A. J. Heck, 2009, Multiplex peptide stable isotope dimethyl labeling for quantitative proteomics: Nat Protoc, v. 4, p. 484-94.
Boimel, M., N. Grigoriadis, A. Lourbopoulos, E. Haber, O. Abramsky, and H. Rosenmann, 2010, Efficacy and safety of immunization with phosphorylated tau against neurofibrillary tangles in mice: Exp Neurol, v. 224, p. 472-85.
Bowne-Anderson, H., M. Zanic, M. Kauer, and J. Howard, 2013, Microtubule dynamic instability: a new model with coupled GTP hydrolysis and multistep catastrophe: Bioessays, v. 35, p. 452-61.
Braak, H., and E. Braak, 1991, Neuropathological stageing of Alzheimer-related changes: Acta Neuropathol, v. 82, p. 239-59.
Breuzard, G., P. Hubert, R. Nouar, T. De Bessa, F. Devred, P. Barbier, J. N. Sturgis, and V. Peyrot, 2013, Molecular Mechanisms of Tau Binding to Microtubule and its Role in Microtubule Dynamics in Live Cells: Journal of Cell Science.
Bridges, C. B., 1917, Deficiency: Genetics, v. 2, p. 445-65.
Bright, N. J., D. Carling, and C. Thornton, 2008, Investigating the regulation of brain-specific kinases 1 and 2 by phosphorylation: J Biol Chem, v. 283, p. 14946-54.
Brion, J. P., D. P. Hanger, A. M. Couck, and B. H. Anderton, 1991, A68 proteins in Alzheimer's disease are composed of several tau isoforms in a phosphorylated state which affects their electrophoretic mobilities: Biochem J, v. 279 (Pt 3), p. 831-6.
Brunden, K. R., B. Zhang, J. Carroll, Y. Yao, J. S. Potuzak, A. M. Hogan, M. Iba, M. J. James, S. X. Xie, C. Ballatore, A. B. Smith, 3rd, V. M. Lee, and J. Q. Trojanowski, 2010, Epothilone D improves microtubule density, axonal integrity, and cognition in a transgenic mouse model of tauopathy: J Neurosci, v. 30, p. 13861-6.
Buckingham, S. D., A. K. Jones, L. A. Brown, and D. B. Sattelle, 2009, Nicotinic Acetylcholine Receptor Signalling: Roles in Alzheimer's Disease and Amyloid Neuroprotection: Pharmacological Reviews, v. 61, p. 39-61.
Bulbarelli, A., E. Lonati, E. Cazzaniga, F. Re, S. Sesana, D. Barisani, G. Sancini, T. Mutoh, and M. Masserini, 2009, TrkA pathway activation induced by amyloid-beta (Abeta): Mol Cell Neurosci, v. 40, p. 365-73.
Bulic, B., M. Pickhardt, and E. Mandelkow, 2013, Progress and Developments in Tau Aggregation Inhibitors for Alzheimer Disease: Journal of Medicinal Chemistry, v. 56, p. 4135-4155.

Burcin, M. M., B. W. O'Malley, and S. Y. Tsai, 1998, A regulatory system for target gene expression: Front Biosci, v. 3, p. c1-7.
Caceres, A., and K. S. Kosik, 1990, Inhibition of neurite polarity by tau antisense oligonucleotides in primary cerebellar neurons: Nature, v. 343, p. 461-3.
Campbell, S. D., F. Sprenger, B. A. Edgar, and P. H. O'Farrell, 1995, Drosophila Wee1 kinase rescues fission yeast from mitotic catastrophe and phosphorylates Drosophila Cdc2 in vitro: Mol Biol Cell, v. 6, p. 1333-47.
Carling, D., 2004, The AMP-activated protein kinase cascade--a unifying system for energy control: Trends Biochem Sci, v. 29, p. 18-24.
Carlsson, L., L. E. Nystrom, I. Sundkvist, F. Markey, and U. Lindberg, 1977, Actin polymerizability is influenced by profilin, a low molecular weight protein in non-muscle cells: J Mol Biol, v. 115, p. 465-83.
Carmel, G., E. M. Mager, L. I. Binder, and J. Kuret, 1996, The structural basis of monoclonal antibody Alz50's selectivity for Alzheimer's disease pathology: J Biol Chem, v. 271, p. 32789-95.
Cash, A. D., G. Aliev, S. L. Siedlak, A. Nunomura, H. Fujioka, X. Zhu, A. K. Raina, H. V. Vinters, M. Tabaton, A. B. Johnson, M. Paula-Barbosa, J. Avíla, P. K. Jones, R. J. Castellani, M. A. Smith, and G. Perry, 2003, Microtubule Reduction in Alzheimer's Disease and Aging Is Independent of τ Filament Formation: The American Journal of Pathology, v. 162, p. 1623-1627.
Caudron, Q., C. Lyn-Adams, J. A. D. Aston, B. G. Frenguelli, and K. G. Moffat, 2013, Quantitative assessment of ommatidial distortion in Drosophila melanogaster: *Drosophila* Information Services, v. 96, p. 136-144.
Chang, E., S. Kim, K. N. Schafer, and J. Kuret, 2011, Pseudophosphorylation of tau protein directly modulates its aggregation kinetics: Biochim Biophys Acta, v. 1814, p. 388-95.
Chatterjee, S., T. K. Sang, G. M. Lawless, and G. R. Jackson, 2009, Dissociation of tau toxicity and phosphorylation: role of GSK-3beta, MARK and Cdk5 in a Drosophila model: Hum Mol Genet, v. 18, p. 164-77.
Chau, K. W., W. Y. Chan, P. C. Shaw, and H. Y. Chan, 2006, Biochemical investigation of Tau protein phosphorylation status and its solubility properties in Drosophila: Biochem Biophys Res Commun, v. 346, p. 150-9.
Chen, J., Y. Kanai, N. J. Cowan, and N. Hirokawa, 1992, Projection domains of MAP2 and tau determine spacings between microtubules in dendrites and axons: Nature, v. 360, p. 674-7.
Chen, X. Y., X. T. Gu, H. Saiyin, B. Wan, Y. J. Zhang, J. Li, Y. L. Wang, R. Gao, Y. F. Wang, W. P. Dong, S. M. Najjar, C. Y. Zhang, H. F. Ding, J. O. Liu, and L. Yu, 2012, Brain-selective kinase 2 (BRSK2) phosphorylation on PCTAIRE1 negatively regulates glucose-stimulated insulin secretion in pancreatic β-cells: J Biol Chem, v. 287, p. 30368-75.
Chohan, M. O., S. Khatoon, I.-G. Iqbal, and K. Iqbal, 2006, Involvement of in the abnormal hyperphosphorylation of tau and its reversal by Memantine: FEBS Letters, v. 580, p. 3973-3979.
Chuang, J. Z., T. Y. Yeh, F. Bollati, C. Conde, F. Canavosio, A. Caceres, and C. H. Sung, 2005, The dynein light chain Tctex-1 has a dynein-independent role in actin remodeling during neurite outgrowth: Dev Cell, v. 9, p. 75-86.
Clavaguera, F., H. Akatsu, G. Fraser, R. A. Crowther, S. Frank, J. Hench, A. Probst, D. T. Winkler, J. Reichwald, M. Staufenbiel, B. Ghetti, M. Goedert, and M. Tolnay, 2013a, Brain homogenates from human tauopathies induce tau inclusions in mouse brain: Proc Natl Acad Sci U S A, v. 110, p. 9535-40.

Clavaguera, F., T. Bolmont, R. A. Crowther, D. Abramowski, S. Frank, A. Probst, G. Fraser, A. K. Stalder, M. Beibel, M. Staufenbiel, M. Jucker, M. Goedert, and M. Tolnay, 2009, Transmission and spreading of tauopathy in transgenic mouse brain: Nat Cell Biol, v. 11, p. 909-13.

Clavaguera, F., I. Lavenir, B. Falcon, S. Frank, M. Goedert, and M. Tolnay, 2013b, "Prion-like" templated misfolding in tauopathies: Brain Pathol, v. 23, p. 342-9.

Cleveland, D. W., S. Y. Hwo, and M. W. Kirschner, 1977a, Physical and chemical properties of purified tau factor and the role of tau in microtubule assembly: J Mol Biol, v. 116, p. 227-47.

Cleveland, D. W., S. Y. Hwo, and M. W. Kirschner, 1977b, Purification of tau, a microtubule-associated protein that induces assembly of microtubules from purified tubulin: J Mol Biol, v. 116, p. 207-25.

Colodner, K. J., and M. B. Feany, 2010, Glial fibrillary tangles and JAK/STAT-mediated glial and neuronal cell death in a Drosophila model of glial tauopathy: J Neurosci, v. 30, p. 16102-13.

Colom-Cadena, M., E. Gelpi, M. J. Martí, S. Charif, O. Dols-Icardo, R. Blesa, J. Clarimón, and A. Lleó, 2013, MAPT H1 haplotype is associated with enhanced α-synuclein deposition in dementia with Lewy bodies: Neurobiology of Aging, v. 34, p. 936-942.

Cook, R. K., S. J. Christensen, J. A. Deal, R. A. Coburn, M. E. Deal, J. M. Gresens, T. C. Kaufman, and K. R. Cook, 2012, The generation of chromosomal deletions to provide extensive coverage and subdivision of the Drosophila melanogaster genome: Genome Biol, v. 13, p. R21.

Cooley, L., E. Verheyen, and K. Ayers, 1992, chickadee encodes a profilin required for intercellular cytoplasm transport during Drosophila oogenesis: Cell, v. 69, p. 173-84.

Cornell, M., D. A. Evans, R. Mann, M. Fostier, M. Flasza, M. Monthatong, S. Artavanis-Tsakonas, and M. Baron, 1999, The Drosophila melanogaster Suppressor of deltex gene, a regulator of the Notch receptor signaling pathway, is an E3 class ubiquitin ligase: Genetics, v. 152, p. 567-76.

Corsellis, J. A., C. J. Bruton, and D. Freeman-Browne, 1973, The aftermath of boxing: Psychol Med, v. 3, p. 270-303.

Cowan, C. M., T. Bossing, A. Page, D. Shepherd, and A. Mudher, 2010, Soluble hyper-phosphorylated tau causes microtubule breakdown and functionally compromises normal tau in vivo: Acta Neuropathol.

Cowan, C. M., and A. Mudher, 2013, Are tau aggregates toxic or protective in tauopathies?: Frontiers in Neurology, v. 4.

Crump, J. G., M. Zhen, Y. Jin, and C. I. Bargmann, 2001, The SAD-1 kinase regulates presynaptic vesicle clustering and axon termination: Neuron, v. 29, p. 115-129.

Davies, P., and A. J. Maloney, 1976, Selective loss of central cholinergic neurons in Alzheimer's disease: Lancet, v. 2, p. 1403.

Davies, S. P., H. Reddy, M. Caivano, and P. Cohen, 2000, Specificity and mechanism of action of some commonly used protein kinase inhibitors: Biochem J, v. 351, p. 95-105.

Dawson, H. N., A. Ferreira, M. V. Eyster, N. Ghoshal, L. I. Binder, and M. P. Vitek, 2001, Inhibition of neuronal maturation in primary hippocampal neurons from τ deficient mice: Journal of Cell Science, v. 114, p. 1179-1187.

de la Monte, S. M., and J. R. Wands, 2008, Alzheimer's disease is type 3 diabetes-evidence reviewed: J Diabetes Sci Technol, v. 2, p. 1101-13.
de la Torre, J. C., 2013, Vascular Risk Factors: A Ticking Time Bomb to Alzheimer's Disease: Am J Alzheimers Dis Other Demen.
Degerman Gunnarsson, M., L. Kilander, H. Basun, and L. Lannfelt, 2007, Reduction of phosphorylated tau during memantine treatment of Alzheimer's disease: Dement Geriatr Cogn Disord, v. 24, p. 247-52.
Desai, A., and T. J. Mitchison, 1997, Microtubule polymerization dynamics: Annu Rev Cell Dev Biol, v. 13, p. 83-117.
Deshpande, A., K. M. Win, and J. Busciglio, 2008, Tau isoform expression and regulation in human cortical neurons: The FASEB Journal, v. 22, p. 2357-2367.
Dias-Santagata, D., T. A. Fulga, A. Duttaroy, and M. B. Feany, 2007, Oxidative stress mediates tau-induced neurodegeneration in Drosophila: J Clin Invest, v. 117, p. 236-45.
DiTella, M. C., F. Feiguin, N. Carri, K. S. Kosik, and A. Cáceres, 1996, MAP-1B/TAU functional redundancy during laminin-enhanced axonal growth: J Cell Sci, v. 109 (Pt 2), p. 467-77.
Divinski, I., M. Holtser-Cochav, I. Vulih-Schultzman, R. A. Steingart, and I. Gozes, 2006, Peptide neuroprotection through specific interaction with brain tubulin: J Neurochem, v. 98, p. 973-84.
Doerflinger, H., R. Benton, J. M. Shulman, and D. St Johnston, 2003, The role of PAR-1 in regulating the polarised microtubule cytoskeleton in the Drosophila follicular epithelium: Development, v. 130, p. 3965-75.
Drewes, G., 2004, MARKing tau for tangles and toxicity: Trends Biochem Sci, v. 29, p. 548-55.
Drewes, G., B. Trinczek, S. Illenberger, J. Biernat, G. Schmitt-Ulms, H. E. Meyer, E. M. Mandelkow, and E. Mandelkow, 1995, Microtubule-associated protein/microtubule affinity-regulating kinase (p110mark). A novel protein kinase that regulates tau-microtubule interactions and dynamic instability by phosphorylation at the Alzheimer-specific site serine 262: J Biol Chem, v. 270, p. 7679-88.
Dumanchin, C., A. Camuzat, D. Campion, P. Verpillat, D. Hannequin, B. Dubois, P. Saugier-Veber, C. Martin, C. Penet, F. Charbonnier, Y. Agid, T. Frebourg, and A. Brice, 1998, Segregation of a missense mutation in the microtubule-associated protein tau gene with familial frontotemporal dementia and parkinsonism: Hum Mol Genet, v. 7, p. 1825-9.
Edgar, B. A., and P. H. O'Farrell, 1989, Genetic control of cell division patterns in the Drosophila embryo: Cell, v. 57, p. 177-87.
Eggermont, L., D. Swaab, P. Luiten, and E. Scherder, 2006, Exercise, cognition and Alzheimer's disease: More is not necessarily better: Neuroscience & Biobehavioral Reviews, v. 30, p. 562-575.
Embi, N., D. B. Rylatt, and P. Cohen, 1980, Glycogen synthase kinase-3 from rabbit skeletal muscle. Separation from cyclic-AMP-dependent protein kinase and phosphorylase kinase: Eur J Biochem, v. 107, p. 519-27.
Evin, G., A. Zhu, R. M. Holsinger, C. L. Masters, and Q. X. Li, 2003, Proteolytic processing of the Alzheimer's disease amyloid precursor protein in brain and platelets: J Neurosci Res, v. 74, p. 386-92.
Ferrer, A., C. Caelles, N. Massot, and F. G. Hegardt, 1985, Activation of rat liver cytosolic 3-hydroxy-3-methylglutaryl coenzyme A reductase kinase by

adenosine 5'-monophosphate: Biochem Biophys Res Commun, v. 132, p. 497-504.
Feuillette, S., L. Miguel, T. Frebourg, D. Campion, and M. Lecourtois, 2010, Drosophila models of human tauopathies indicate that Tau protein toxicity in vivo is mediated by soluble cytosolic phosphorylated forms of the protein: J Neurochem, v. 113, p. 895-903.
Fischer, D., M. D. Mukrasch, J. Biernat, S. Bibow, M. Blackledge, C. Griesinger, E. Mandelkow, and M. Zweckstetter, 2009, Conformational changes specific for pseudophosphorylation at serine 262 selectively impair binding of tau to microtubules: Biochemistry, v. 48, p. 10047-55.
Fischer, P. D. D. O., 1907, Miliare Nekrosen mit drusigen Wucherungen der Neurofibrillen, eine regelmässige Veränderung der Hirnrinde bei seniler Demenz: European Neurology, v. 22, p. 361-372.
Forlenza, O. V., B. S. Diniz, M. Radanovic, F. S. Santos, L. L. Talib, and W. F. Gattaz, 2011, Disease-modifying properties of long-term lithium treatment for amnestic mild cognitive impairment: randomised controlled trial: The British Journal of Psychiatry, v. 198, p. 351-356.
Fox, N. C., P. A. Freeborough, and M. N. Rossor, 1996, Visualisation and quantification of rates of atrophy in Alzheimer's disease: Lancet, v. 348, p. 94-7.
Frost, B., and M. I. Diamond, 2010, Prion-like mechanisms in neurodegenerative diseases: Nature Reviews Neuroscience, v. 11, p. 155-159.
Frost, B., R. L. Jacks, and M. I. Diamond, 2009, Propagation of Tau Misfolding from the Outside to the Inside of a Cell: Journal of Biological Chemistry, v. 284, p. 12845-12852.
Fujimoto, T., S. Yurimoto, N. Hatano, N. Nozaki, N. Sueyoshi, I. Kameshita, A. Mizutani, K. Mikoshiba, R. Kobayashi, and H. Tokumitsu, 2008, Activation of SAD kinase by Ca2+/calmodulin-dependent protein kinase kinase: Biochemistry, v. 47, p. 4151-4159.
Furukawa, Y., K. Kaneko, and N. Nukina, 2011, Tau Protein Assembles into Isoform- and Disulfide-dependent Polymorphic Fibrils with Distinct Structural Properties: Journal of Biological Chemistry, v. 286, p. 27236-27246.
Gamblin, T. C., R. W. Berry, and L. I. Binder, 2003, Tau polymerization: role of the amino terminus: Biochemistry, v. 42, p. 2252-7.
Gao, Y. S., C. C. Hubbert, J. Lu, Y. S. Lee, J. Y. Lee, and T. P. Yao, 2007, Histone deacetylase 6 regulates growth factor-induced actin remodeling and endocytosis: Mol Cell Biol, v. 27, p. 8637-47.
Gavett, B. E., R. A. Stern, and A. C. McKee, 2011, Chronic traumatic encephalopathy: a potential late effect of sport-related concussive and subconcussive head trauma: Clin Sports Med, v. 30, p. 179-88, xi.
Gemmill, R. M., L. T. Bemis, J. P. Lee, M. A. Sozen, A. Baron, C. Zeng, P. F. Erickson, J. E. Hooper, and H. A. Drabkin, 2002, The TRC8 hereditary kidney cancer gene suppresses growth and functions with VHL in a common pathway: Oncogene, v. 21, p. 3507-3516.
Goedert, M., and R. Jakes, 1990, Expression of separate isoforms of human tau protein: correlation with the tau pattern in brain and effects on tubulin polymerization: EMBO J, v. 9, p. 4225-30.
Goedert, M., R. Jakes, R. A. Crowther, J. Six, U. Lubke, M. Vandermeeren, P. Cras, J. Q. Trojanowski, and V. M. Lee, 1993, The abnormal phosphorylation of

tau protein at Ser-202 in Alzheimer disease recapitulates phosphorylation during development: Proc Natl Acad Sci U S A, v. 90, p. 5066-70.
Goedert, M., R. Jakes, and E. Vanmechelen, 1995, Monoclonal antibody AT8 recognises tau protein phosphorylated at both serine 202 and threonine 205: Neurosci Lett, v. 189, p. 167-9.
Goedert, M., M. G. Spillantini, R. Jakes, D. Rutherford, and R. A. Crowther, 1989a, Multiple isoforms of human microtubule-associated protein tau: sequences and localization in neurofibrillary tangles of Alzheimer's disease: Neuron, v. 3, p. 519-26.
Goedert, M., M. G. Spillantini, M. C. Potier, J. Ulrich, and R. A. Crowther, 1989b, Cloning and sequencing of the cDNA encoding an isoform of microtubule-associated protein tau containing four tandem repeats: differential expression of tau protein mRNAs in human brain: EMBO J, v. 8, p. 393-9.
Goedert, M., C. M. Wischik, R. A. Crowther, J. E. Walker, and A. Klug, 1988, Cloning and sequencing of the cDNA encoding a core protein of the paired helical filament of Alzheimer disease: identification as the microtubule-associated protein tau: Proc Natl Acad Sci U S A, v. 85, p. 4051-5.
Golde, T. E., J. Lewis, and N. R. McFarland, 2013, Anti-tau antibodies: hitting the target: Neuron, v. 80, p. 254-6.
Golde, T. E., L. S. Schneider, and E. H. Koo, 2011, Anti-Aβ therapeutics in alzheimer's disease: The need for a paradigm shift: Neuron, v. 69, p. 203-213.
Golic, K. G., and M. M. Golic, 1996, Engineering the Drosophila genome: chromosome rearrangements by design: Genetics, v. 144, p. 1693-711.
Golic, K. G., and S. Lindquist, 1989, The FLP recombinase of yeast catalyzes site-specific recombination in the Drosophila genome: Cell, v. 59, p. 499-509.
Goode, B. L., M. Chau, P. E. Denis, and S. C. Feinstein, 2000, Structural and Functional Differences between 3-Repeat and 4-Repeat Tau Isoforms: IMPLICATIONS FOR NORMAL TAU FUNCTION AND THE ONSET OF NEURODEGENERATIVE DISEASE: Journal of Biological Chemistry, v. 275, p. 38182-38189.
Gorman, M. J., and J. R. Girton, 1992, A genetic analysis of deltex and its interaction with the Notch locus in Drosophila melanogaster: Genetics, v. 131, p. 99-112.
Gotz, J., F. Chen, R. Barmettler, and R. M. Nitsch, 2001, Tau filament formation in transgenic mice expressing P301L tau: J Biol Chem, v. 276, p. 529-34.
Gozes, I., R. A. Steingart, and A. D. Spier, 2004, NAP mechanisms of neuroprotection: J Mol Neurosci, v. 24, p. 67-72.
Grammenoudi, S., S. Kosmidis, and E. M. Skoulakis, 2006, Cell type-specific processing of human Tau proteins in Drosophila: FEBS Lett, v. 580, p. 4602-6.
Groth, A. C., M. Fish, R. Nusse, and M. P. Calos, 2004, Construction of Transgenic Drosophila by Using the Site-Specific Integrase From Phage φC31: Genetics, v. 166, p. 1775-1782.
Grundke-Iqbal, I., K. Iqbal, Y. C. Tung, M. Quinlan, H. M. Wisniewski, and L. I. Binder, 1986, Abnormal phosphorylation of the microtubule-associated protein tau (tau) in Alzheimer cytoskeletal pathology: Proc Natl Acad Sci U S A, v. 83, p. 4913-7.
Grynspan, F., W. R. Griffin, A. Cataldo, S. Katayama, and R. A. Nixon, 1997, Active site-directed antibodies identify calpain II as an early-appearing and

pervasive component of neurofibrillary pathology in Alzheimer's disease: Brain Res, v. 763, p. 145-58.
Gu, G. J., H. Lund, D. Wu, A. Blokzijl, C. Classon, G. von Euler, U. Landegren, D. Sunnemark, and M. Kamali-Moghaddam, 2013, Role of Individual MARK Isoforms in Phosphorylation of Tau at Ser(262) in Alzheimer's Disease: Neuromolecular Med, v. 15, p. 458-69.
Gu, J., and E. M. Sigurdsson, 2011, Immunotherapy for tauopathies: J Mol Neurosci, v. 45, p. 690-5.
Guo, H. F., J. Tong, F. Hannan, L. Luo, and Y. Zhong, 2000, A neurofibromatosis-1-regulated pathway is required for learning in Drosophila: Nature, v. 403, p. 895-8.
Guo, Z., W. Tang, J. Yuan, X. Chen, B. Wan, X. Gu, K. Luo, Y. Wang, and L. Yu, 2006, BRSK2 is activated by cyclic AMP-dependent protein kinase A through phosphorylation at Thr260: Biochemical and Biophysical Research Communications, v. 347, p. 867-871.
Guthrie, C. R., and B. C. Kraemer, 2011, Proteasome inhibition drives HDAC6-dependent recruitment of tau to aggresomes: J Mol Neurosci, v. 45, p. 32-41.
Haass, C., and E. Mandelkow, 2010, Fyn-tau-amyloid: a toxic triad: Cell, v. 142, p. 356-8.
Hall, G. F., and B. A. Patuto, 2012, Is tau ready for admission to the prion club?: Prion, v. 6, p. 223-33.
Hampel, H., M. Ewers, K. Burger, P. Annas, A. Mortberg, A. Bogstedt, L. Frolich, J. Schroder, P. Schonknecht, M. W. Riepe, I. Kraft, T. Gasser, T. Leyhe, H. J. Moller, A. Kurz, and H. Basun, 2009, Lithium trial in Alzheimer's disease: a randomized, single-blind, placebo-controlled, multicenter 10-week study: J Clin Psychiatry, v. 70, p. 922-31.
Hansen, L. A., E. Masliah, D. Galasko, and R. D. Terry, 1993, Plaque-only Alzheimer disease is usually the lewy body variant, and vice versa: J Neuropathol Exp Neurol, v. 52, p. 648-54.
Hardie, D. G., D. Carling, and A. T. R. Sim, 1989, The AMP-activated protein kinase: a multisubstrate regulator of lipid metabolism: Trends in Biochemical Sciences, v. 14, p. 20-23.
Hardie, D. G., J. W. Scott, D. A. Pan, and E. R. Hudson, 2003, Management of cellular energy by the AMP-activated protein kinase system: FEBS Letters, v. 546, p. 113-120.
Hartmann, T., S. C. Bieger, B. Bruhl, P. J. Tienari, N. Ida, D. Allsop, G. W. Roberts, C. L. Masters, C. G. Dotti, K. Unsicker, and K. Beyreuther, 1997, Distinct sites of intracellular production for Alzheimer's disease A beta40/42 amyloid peptides: Nat Med, v. 3, p. 1016-20.
Harvey, R. J., M. Skelton-Robinson, and M. N. Rossor, 2003, The prevalence and causes of dementia in people under the age of 65 years: J Neurol Neurosurg Psychiatry, v. 74, p. 1206-9.
Hay, B. A., T. Wolff, and G. M. Rubin, 1994, Expression of baculovirus P35 prevents cell death in Drosophila: Development, v. 120, p. 2121-9.
Heidary, G., and M. E. Fortini, 2001, Identification and characterization of the Drosophila tau homolog: Mech Dev, v. 108, p. 171-8.
Helfrich-Forster, C., M. Tauber, J. H. Park, M. Muhlig-Versen, S. Schneuwly, and A. Hofbauer, 2000, Ectopic expression of the neuropeptide pigment-dispersing factor alters behavioral rhythms in Drosophila melanogaster: J Neurosci, v. 20, p. 3339-53.

Helfrich-Förster, C., 1995, The period clock gene is expressed in central nervous system neurons which also produce a neuropeptide that reveals the projections of circadian pacemaker cells within the brain of Drosophila melanogaster: Proceedings of the National Academy of Sciences, v. 92, p. 612-616.

Hernández, F., E. Gómez de Barreda, A. Fuster-Matanzo, J. J. Lucas, and J. Avila, 2010, GSK3: a possible link between beta amyloid peptide and tau protein: Exp Neurol, v. 223, p. 322-5.

Himmelstein, D. S., S. M. Ward, J. K. Lancia, K. R. Patterson, and L. I. Binder, 2012, Tau as a therapeutic target in neurodegenerative disease: Pharmacol Ther, v. 136, p. 8-22.

Hirao, A., Y.-Y. Kong, S. Matsuoka, A. Wakeham, J. Ruland, H. Yoshida, D. Liu, S. J. Elledge, and T. W. Mak, 2000, DNA Damage-Induced Activation of p53 by the Checkpoint Kinase Chk2: Science, v. 287, p. 1824-1827.

Holmes, C., D. Boche, D. Wilkinson, G. Yadegarfar, V. Hopkins, A. Bayer, R. W. Jones, R. Bullock, S. Love, J. W. Neal, E. Zotova, and J. A. Nicoll, 2008, Long-term effects of Abeta42 immunisation in Alzheimer's disease: follow-up of a randomised, placebo-controlled phase I trial: Lancet, v. 372, p. 216-23.

Holmfeldt, P., G. Brattsand, and M. Gullberg, 2002, MAP4 Counteracts Microtubule Catastrophe Promotion but Not Tubulin-Sequestering Activity in Intact Cells: Current Biology, v. 12, p. 1034-1039.

Holt, L. J., B. B. Tuch, J. Villen, A. D. Johnson, S. P. Gygi, and D. O. Morgan, 2009, Global analysis of Cdk1 substrate phosphorylation sites provides insights into evolution: Science, v. 325, p. 1682-6.

Hong, M., D. C. Chen, P. S. Klein, and V. M. Lee, 1997, Lithium reduces tau phosphorylation by inhibition of glycogen synthase kinase-3: J Biol Chem, v. 272, p. 25326-32.

Hong, M., V. Zhukareva, V. Vogelsberg-Ragaglia, Z. Wszolek, L. Reed, B. I. Miller, D. H. Geschwind, T. D. Bird, D. McKeel, A. Goate, J. C. Morris, K. C. Wilhelmsen, G. D. Schellenberg, J. Q. Trojanowski, and V. M. Lee, 1998, Mutation-specific functional impairments in distinct tau isoforms of hereditary FTDP-17: Science, v. 282, p. 1914-7.

Hope, T., J. Keene, C. G. Fairburn, R. Jacoby, and R. McShane, 1999, Natural history of behavioural changes and psychiatric symptoms in Alzheimer's disease. A longitudinal study: Br J Psychiatry, v. 174, p. 39-44.

Hubbert, C., A. Guardiola, R. Shao, Y. Kawaguchi, A. Ito, A. Nixon, M. Yoshida, X. F. Wang, and T. P. Yao, 2002, HDAC6 is a microtubule-associated deacetylase: Nature, v. 417, p. 455-8.

Hutton, M., C. L. Lendon, P. Rizzu, M. Baker, S. Froelich, H. Houlden, S. Pickering-Brown, S. Chakraverty, A. Isaacs, A. Grover, J. Hackett, J. Adamson, S. Lincoln, D. Dickson, P. Davies, R. C. Petersen, M. Stevens, E. de Graaff, E. Wauters, J. van Baren, M. Hillebrand, M. Joosse, J. M. Kwon, P. Nowotny, L. K. Che, J. Norton, J. C. Morris, L. A. Reed, J. Trojanowski, H. Basun, L. Lannfelt, M. Neystat, S. Fahn, F. Dark, T. Tannenberg, P. R. Dodd, N. Hayward, J. B. Kwok, P. R. Schofield, A. Andreadis, J. Snowden, D. Craufurd, D. Neary, F. Owen, B. A. Oostra, J. Hardy, A. Goate, J. van Swieten, D. Mann, T. Lynch, and P. Heutink, 1998, Association of missense and 5'-splice-site mutations in tau with the inherited dementia FTDP-17: Nature, v. 393, p. 702-5.

Hyman, B. T., G. W. Van Hoesen, B. L. Wolozin, P. Davies, L. J. Kromer, and A. R. Damasio, 1988, Alz-50 antibody recognizes Alzheimer-related neuronal changes: Ann Neurol, v. 23, p. 371-9.

Iijima, K., A. Gatt, and K. Iijima-Ando, 2010, Tau Ser262 phosphorylation is critical for Abeta42-induced tau toxicity in a transgenic Drosophila model of Alzheimer's disease: Hum Mol Genet, v. 19, p. 2947-57.

Iijima-Ando, K., L. Zhao, A. Gatt, C. Shenton, and K. Iijima, 2010, A DNA damage-activated checkpoint kinase phosphorylates tau and enhances tau-induced neurodegeneration: Human Molecular Genetics, v. 19, p. 1930-1938.

Inoue, E., S. Mochida, H. Takagi, S. Higa, M. Deguchi-Tawarada, E. Takao-Rikitsu, M. Inoue, I. Yao, K. Takeuchi, I. Kitajima, M. Setou, T. Ohtsuka, and Y. Takai, 2006, SAD: a presynaptic kinase associated with synaptic vesicles and the active zone cytomatrix that regulates neurotransmitter release: Neuron, v. 50, p. 261-75.

Inoue, H., M. Tateno, K. Fujimura-Kamada, G. Takaesu, T. Adachi-Yamada, J. Ninomiya-Tsuji, K. Irie, Y. Nishida, and K. Matsumoto, 2001, A Drosophila MAPKKK, D-MEKK1, mediates stress responses through activation of p38 MAPK: Embo j, v. 20, p. 5421-30.

Iqbal, K., C.-X. Gong, and F. Liu, 2013, Hyperphosphorylation-induced tau oligomers: Frontiers in Neurology, v. 4.

Ishiguro, K., A. Shiratsuchi, S. Sato, A. Omori, M. Arioka, S. Kobayashi, T. Uchida, and K. Imahori, 1993, Glycogen synthase kinase 3 beta is identical to tau protein kinase I generating several epitopes of paired helical filaments: FEBS Lett, v. 325, p. 167-72.

Ittner, L. M., Y. D. Ke, F. Delerue, M. Bi, A. Gladbach, J. van Eersel, H. Wolfing, B. C. Chieng, M. J. Christie, I. A. Napier, A. Eckert, M. Staufenbiel, E. Hardeman, and J. Gotz, 2010, Dendritic function of tau mediates amyloid-beta toxicity in Alzheimer's disease mouse models: Cell, v. 142, p. 387-97.

Jackson, G. R., M. Wiedau-Pazos, T. K. Sang, N. Wagle, C. A. Brown, S. Massachi, and D. H. Geschwind, 2002, Human wild-type tau interacts with wingless pathway components and produces neurofibrillary pathology in Drosophila: Neuron, v. 34, p. 509-19.

Janicki, S. C., and N. Schupf, 2010, Hormonal influences on cognition and risk for Alzheimer's disease: Curr Neurol Neurosci Rep, v. 10, p. 359-66.

Janson, M. E., M. E. de Dood, and M. Dogterom, 2003, Dynamic instability of microtubules is regulated by force: J Cell Biol, v. 161, p. 1029-34.

Jarrett, J. T., E. P. Berger, and P. T. Lansbury, 1993, The carboxy terminus of the beta amyloid protein is critical for the seeding of amyloid formation: implications for the pathogenesis of Alzheimer's disease: Biochemistry, v. 32, p. 4693-7.

Jeganathan, S., M. von Bergen, H. Brutlach, H. J. Steinhoff, and E. Mandelkow, 2006, Global hairpin folding of tau in solution: Biochemistry, v. 45, p. 2283-93.

Jellinger, K. A., and J. Attems, 2007, Neurofibrillary tangle-predominant dementia: comparison with classical Alzheimer disease: Acta Neuropathol, v. 113, p. 107-17.

Jemal, A., R. Siegel, E. Ward, Y. Hao, J. Xu, T. Murray, and M. J. Thun, 2008, Cancer Statistics, 2008: CA: A Cancer Journal for Clinicians, v. 58, p. 71-96.

Jenkins, S. M., and G. V. W. Johnson, 2000, Microtubule/MAP-Affinity Regulating Kinase (MARK) Is Activated by Phenylarsine Oxide In Situ and

Phosphorylates Tau Within Its Microtubule-Binding Domain: Journal of Neurochemistry, v. 74, p. 1463-1468.
Jin, L. W., and T. Saitoh, 1995, Changes in protein kinases in brain aging and Alzheimer's disease. Implications for drug therapy: Drugs Aging, v. 6, p. 136-49.
Joza, N., K. Galindo, J. A. Pospisilik, P. Benit, M. Rangachari, E. E. Kanitz, Y. Nakashima, G. G. Neely, P. Rustin, J. M. Abrams, G. Kroemer, and J. M. Penninger, 2008, The molecular archaeology of a mitochondrial death effector: AIF in Drosophila: Cell Death Differ, v. 15, p. 1009-18.
Kalia, M., 2003, Dysphagia and aspiration pneumonia in patients with Alzheimer's disease: Metabolism, v. 52, p. 36-8.
Karsten, S. L., T. K. Sang, L. T. Gehman, S. Chatterjee, J. Liu, G. M. Lawless, S. Sengupta, R. W. Berry, J. Pomakian, H. S. Oh, C. Schulz, K. S. Hui, M. Wiedau-Pazos, H. V. Vinters, L. I. Binder, D. H. Geschwind, and G. R. Jackson, 2006, A genomic screen for modifiers of tauopathy identifies puromycin-sensitive aminopeptidase as an inhibitor of tau-induced neurodegeneration: Neuron, v. 51, p. 549-60.
Katayama, M., T. Kawaguchi, M. S. Berger, and R. O. Pieper, 2007, DNA damaging agent-induced autophagy produces a cytoprotective adenosine triphosphate surge in malignant glioma cells: Cell Death Differ, v. 14, p. 548-58.
Katzman, R., 1976, Editorial: The prevalence and malignancy of Alzheimer disease. A major killer: Arch Neurol, v. 33, p. 217-8.
Khurana, V., Y. Lu, M. L. Steinhilb, S. Oldham, J. M. Shulman, and M. B. Feany, 2006, TOR-mediated cell-cycle activation causes neurodegeneration in a Drosophila tauopathy model: Curr Biol, v. 16, p. 230-41.
Kim, Y. C., H. G. Lee, and K. A. Han, 2007, D1 dopamine receptor dDA1 is required in the mushroom body neurons for aversive and appetitive learning in Drosophila: J Neurosci, v. 27, p. 7640-7.
Kiris, E., D. Ventimiglia, M. E. Sargin, M. R. Gaylord, A. Altinok, K. Rose, B. S. Manjunath, M. A. Jordan, L. Wilson, and S. C. Feinstein, 2011, Combinatorial Tau pseudophosphorylation: markedly different regulatory effects on microtubule assembly and dynamic instability than the sum of the individual parts: J Biol Chem, v. 286, p. 14257-70.
Kirschner, M., and T. Mitchison, 1986, Beyond self-assembly: from microtubules to morphogenesis: Cell, v. 45, p. 329-42.
Kishi, M., Y. A. Pan, J. G. Crump, and J. R. Sanes, 2005, Mammalian SAD kinases are required for neuronal polarization: Science, v. 307, p. 929-32.
Kivipelto, M., T. Ngandu, T. Laatikainen, B. Winblad, H. Soininen, and J. Tuomilehto, 2006, Risk score for the prediction of dementia risk in 20 years among middle aged people: a longitudinal, population-based study: Lancet Neurol, v. 5, p. 735-41.
Kobayashi, T., H. Mori, Y. Okuma, D. W. Dickson, N. Cookson, Y. Tsuboi, Y. Motoi, R. Tanaka, N. Miyashita, M. Anno, H. Narabayashi, and Y. Mizuno, 2002, Contrasting genotypes of the tau gene in two phenotypically distinct patients with P301L mutation of frontotemporal dementia and parkinsonism linked to chromosome 17: J Neurol, v. 249, p. 669-75.
Komatsu, M., S. Waguri, M. Koike, Y. S. Sou, T. Ueno, T. Hara, N. Mizushima, J. Iwata, J. Ezaki, S. Murata, J. Hamazaki, Y. Nishito, S. Iemura, T. Natsume, T. Yanagawa, J. Uwayama, E. Warabi, H. Yoshida, T. Ishii, A. Kobayashi, M. Yamamoto, Z. Yue, Y. Uchiyama, E. Kominami, and K. Tanaka, 2007,

Homeostatic levels of p62 control cytoplasmic inclusion body formation in autophagy-deficient mice: Cell, v. 131, p. 1149-63.
Kosmidis, S., S. Grammenoudi, K. Papanikolopoulou, and E. M. Skoulakis, 2010, Differential effects of Tau on the integrity and function of neurons essential for learning in Drosophila: J Neurosci, v. 30, p. 464-77.
Kucherenko, M. M., A. K. Marrone, V. M. Rishko, A. S. Yatsenko, A. Klepzig, and H. R. Shcherbata, 2010, Paraffin-Embedded and Frozen Sections of Drosophila Adult Muscles, p. e2438.
Lahiri, D. K., and B. Maloney, 2010, Beyond the signaling effect role of amyloid-ss42 on the processing of APP, and its clinical implications: Exp Neurol, v. 225, p. 51-4.
Lee, H. G., G. Casadesus, X. Zhu, R. J. Castellani, A. McShea, G. Perry, R. B. Petersen, V. Bajic, and M. A. Smith, 2009, Cell cycle re-entry mediated neurodegeneration and its treatment role in the pathogenesis of Alzheimer's disease: Neurochem Int, v. 54, p. 84-8.
Lee, H. G., X. Zhu, A. Nunomura, G. Perry, and M. A. Smith, 2006, Amyloid-beta vaccination: testing the amyloid hypothesis?: heads we win, tails you lose!: Am J Pathol, v. 169, p. 738-9.
Lee, J. D., K. Amanai, A. Shearn, and J. E. Treisman, 2002, The ubiquitin ligase Hyperplastic discs negatively regulates hedgehog and decapentaplegic expression by independent mechanisms: Development, v. 129, p. 5697-706.
Lee, J. Y., H. Koga, Y. Kawaguchi, W. Tang, E. Wong, Y. S. Gao, U. B. Pandey, S. Kaushik, E. Tresse, J. Lu, J. P. Taylor, A. M. Cuervo, and T. P. Yao, 2010, HDAC6 controls autophagosome maturation essential for ubiquitin-selective quality-control autophagy: Embo j, v. 29, p. 969-80.
Lemere, C. A., and E. Masliah, 2010, Can Alzheimer disease be prevented by amyloid-beta immunotherapy?: Nat Rev Neurol, v. 6, p. 108-19.
Leroy, K., A. Boutajangout, M. Authelet, J. R. Woodgett, B. H. Anderton, and J. P. Brion, 2002, The active form of glycogen synthase kinase-3beta is associated with granulovacuolar degeneration in neurons in Alzheimer's disease: Acta Neuropathol, v. 103, p. 91-9.
Lesne, S., M. T. Koh, L. Kotilinek, R. Kayed, C. G. Glabe, A. Yang, M. Gallagher, and K. H. Ashe, 2006, A specific amyloid-beta protein assembly in the brain impairs memory: Nature, v. 440, p. 352-7.
Lewis, J., D. W. Dickson, W. L. Lin, L. Chisholm, A. Corral, G. Jones, S. H. Yen, N. Sahara, L. Skipper, D. Yager, C. Eckman, J. Hardy, M. Hutton, and E. McGowan, 2001, Enhanced neurofibrillary degeneration in transgenic mice expressing mutant tau and APP: Science, v. 293, p. 1487-91.
Lewis, J., E. McGowan, J. Rockwood, H. Melrose, P. Nacharaju, M. Van Slegtenhorst, K. Gwinn-Hardy, M. Paul Murphy, M. Baker, X. Yu, K. Duff, J. Hardy, A. Corral, W. L. Lin, S. H. Yen, D. W. Dickson, P. Davies, and M. Hutton, 2000, Neurofibrillary tangles, amyotrophy and progressive motor disturbance in mice expressing mutant (P301L) tau protein: Nat Genet, v. 25, p. 402-5.
Lilley, B. N., Y. A. Pan, and J. R. Sanes, 2013, SAD Kinases Sculpt Axonal Arbors of Sensory Neurons through Long- and Short-Term Responses to Neurotrophin Signals: Neuron.
Lindwall, G., and R. D. Cole, 1984, Phosphorylation affects the ability of tau protein to promote microtubule assembly: J Biol Chem, v. 259, p. 5301-5.

Lippens, G., L. Amniai, J. M. Wieruszeski, A. Sillen, A. Leroy, and I. Landrieu, 2012, Towards understanding the phosphorylation code of tau: Biochem Soc Trans, v. 40, p. 698-703.
Lippens, G., A. Sillen, I. Landrieu, L. Amniai, N. Sibille, P. Barbier, A. Leroy, X. Hanoulle, and J. M. Wieruszeski, 2007, Tau aggregation in Alzheimer's disease: what role for phosphorylation?: Prion, v. 1, p. 21-5.
Liu, C. W., G. Lee, and D. G. Jay, 1999, Tau is required for neurite outgrowth and growth cone motility of chick sensory neurons: Cell Motil Cytoskeleton, v. 43, p. 232-42.
Liu, F., and C. X. Gong, 2008, Tau exon 10 alternative splicing and tauopathies: Mol Neurodegener, v. 3, p. 8.
Liu, F., I. Grundke-Iqbal, K. Iqbal, and C.-X. Gong, 2005, Contributions of protein phosphatases PP1, PP2A, PP2B and PP5 to the regulation of tau phosphorylation: European Journal of Neuroscience, v. 22, p. 1942-1950.
Liu, F., B. Li, E. J. Tung, I. Grundke-Iqbal, K. Iqbal, and C. X. Gong, 2007, Site-specific effects of tau phosphorylation on its microtubule assembly activity and self-aggregation: Eur J Neurosci, v. 26, p. 3429-36.
Lizcano, J. M., O. Goransson, R. Toth, M. Deak, N. A. Morrice, J. Boudeau, S. A. Hawley, L. Udd, T. P. Makela, D. G. Hardie, and D. R. Alessi, 2004, LKB1 is a master kinase that activates 13 kinases of the AMPK subfamily, including MARK/PAR-1: Embo j, v. 23, p. 833-43.
Lovestone, S., C. L. Hartley, J. Pearce, and B. H. Anderton, 1996, Phosphorylation of tau by glycogen synthase kinase-3 beta in intact mammalian cells: the effects on the organization and stability of microtubules: Neuroscience, v. 73, p. 1145-57.
Lu, B., and H. Vogel, 2009, Drosophila models of neurodegenerative diseases: Annu Rev Pathol, v. 4, p. 315-42.
Lu, R., H. Niida, and M. Nakanishi, 2004, Human SAD1 kinase is involved in UV-induced DNA damage checkpoint function: J Biol Chem, v. 279, p. 31164-70.
Luo, M.-h., S.-W. Tse, J. Memmott, and A. Andreadis, 2004, Novel isoforms of tau that lack the microtubule-binding domain: Journal of Neurochemistry, v. 90, p. 340-351.
Maeda, S., N. Sahara, Y. Saito, M. Murayama, Y. Yoshiike, H. Kim, T. Miyasaka, S. Murayama, A. Ikai, and A. Takashima, 2007, Granular tau oligomers as intermediates of tau filaments: Biochemistry, v. 46, p. 3856-61.
Mahajan-Miklos, S., and L. Cooley, 1994, Intercellular cytoplasm transport during Drosophila oogenesis: Dev Biol, v. 165, p. 336-51.
Majounie, E., W. Cross, V. Newsway, A. Dillman, J. Vandrovcova, C. M. Morris, M. A. Nalls, L. Ferrucci, M. J. Owen, M. C. O'Donovan, M. R. Cookson, A. B. Singleton, R. de Silva, and H. R. Morris, 2013, Variation in tau isoform expression in different brain regions and disease states: Neurobiol Aging, v. 34, p. 1922.e7-1922.e12.
Mandelkow, E. M., G. Drewes, J. Biernat, N. Gustke, J. Van Lint, J. R. Vandenheede, and E. Mandelkow, 1992, Glycogen synthase kinase-3 and the Alzheimer-like state of microtubule-associated protein tau: FEBS Lett, v. 314, p. 315-21.
Maniatis, T., E. Fritsch, and J. Sambrook, 1982, Molecular Cloning, a laboratory approach, Cold Spring Harbor Laboratory Press.

Manning, G., D. B. Whyte, R. Martinez, T. Hunter, and S. Sudarsanam, 2002, The protein kinase complement of the human genome: Science, v. 298, p. 1912-34.
Manseau, L., J. Calley, and H. Phan, 1996, Profilin is required for posterior patterning of the Drosophila oocyte: Development, v. 122, p. 2109-16.
Martin, L., X. Latypova, and F. Terro, 2011, Post-translational modifications of tau protein: implications for Alzheimer's disease: Neurochem Int, v. 58, p. 458-71.
Martin, L., X. Latypova, C. M. Wilson, A. Magnaudeix, M.-L. Perrin, C. Yardin, and F. Terro, 2013, Tau protein kinases: Involvement in Alzheimer's disease: Ageing Research Reviews, v. 12, p. 289-309.
Martin, S. G., and D. St Johnston, 2003, A role for Drosophila LKB1 in anterior-posterior axis formation and epithelial polarity: Nature, v. 421, p. 379-84.
Masters, C. L., G. Simms, N. A. Weinman, G. Multhaup, B. L. McDonald, and K. Beyreuther, 1985, Amyloid plaque core protein in Alzheimer disease and Down syndrome: Proc Natl Acad Sci U S A, v. 82, p. 4245-9.
Matsuoka, Y., A. J. Gray, C. Hirata-Fukae, S. S. Minami, E. G. Waterhouse, M. P. Mattson, F. M. LaFerla, I. Gozes, and P. S. Aisen, 2007, Intranasal NAP administration reduces accumulation of amyloid peptide and tau hyperphosphorylation in a transgenic mouse model of Alzheimer's disease at early pathological stage: J Mol Neurosci, v. 31, p. 165-70.
McDermott, S. M., C. Meignin, J. Rappsilber, and I. Davis, 2012, Drosophila Syncrip binds the gurken mRNA localisation signal and regulates localised transcripts during axis specification: Biology Open, v. 1, p. 488-497.
McGuire, S. E., Z. Mao, and R. L. Davis, 2004a, Spatiotemporal gene expression targeting with the TARGET and gene-switch systems in Drosophila: Sci STKE, v. 2004, p. pl6.
McGuire, S. E., G. Roman, and R. L. Davis, 2004b, Gene expression systems in Drosophila: a synthesis of time and space: Trends Genet, v. 20, p. 384-91.
McKee, A. C., R. C. Cantu, C. J. Nowinski, E. T. Hedley-Whyte, B. E. Gavett, A. E. Budson, V. E. Santini, H. S. Lee, C. A. Kubilus, and R. A. Stern, 2009, Chronic traumatic encephalopathy in athletes: progressive tauopathy after repetitive head injury: J Neuropathol Exp Neurol, v. 68, p. 709-35.
McKee, A. C., T. D. Stein, C. J. Nowinski, R. A. Stern, D. H. Daneshvar, V. E. Alvarez, H.-S. Lee, G. Hall, S. M. Wojtowicz, C. M. Baugh, D. O. Riley, C. A. Kubilus, K. A. Cormier, M. A. Jacobs, B. R. Martin, C. R. Abraham, T. Ikezu, R. R. Reichard, B. L. Wolozin, A. E. Budson, L. E. Goldstein, N. W. Kowall, and R. C. Cantu, 2013, The spectrum of disease in chronic traumatic encephalopathy: Brain, v. 136, p. 43-64.
Meireles, A. M., N. S. Dzhindzhev, and H. Ohkura, 2011, Kebab: kinetochore and EB1 associated basic protein that dynamically changes its localisation during Drosophila mitosis: PLoS One, v. 6, p. e24174.
Melki, R., M. F. Carlier, D. Pantaloni, and S. N. Timasheff, 1989, Cold depolymerization of microtubules to double rings: geometric stabilization of assemblies: Biochemistry, v. 28, p. 9143-52.
Mielke, S., A. Sparreboom, and K. Mross, 2006, Peripheral neuropathy: a persisting challenge in paclitaxel-based regimes: Eur J Cancer, v. 42, p. 24-30.
Miquel, J., P. R. Lundgren, K. G. Bensch, and H. Atlan, 1976, Effects of temperature on the life span, vitality and fine structure of Drosophila melanogaster: Mechanisms of Ageing and Development, v. 5, p. 347-370.

Mitchison, T., and M. Kirschner, 1984, Dynamic instability of microtubule growth: Nature, v. 312, p. 237-42.
Mizutani, A., M. Fukuda, K. Ibata, Y. Shiraishi, and K. Mikoshiba, 2000, SYNCRIP, a Cytoplasmic Counterpart of Heterogeneous Nuclear Ribonucleoprotein R, Interacts with Ubiquitous Synaptotagmin Isoforms: Journal of Biological Chemistry, v. 275, p. 9823-9831.
Mocanu, M. M., A. Nissen, K. Eckermann, I. Khlistunova, J. Biernat, D. Drexler, O. Petrova, K. Schonig, H. Bujard, E. Mandelkow, L. Zhou, G. Rune, and E. M. Mandelkow, 2008, The potential for beta-structure in the repeat domain of tau protein determines aggregation, synaptic decay, neuronal loss, and coassembly with endogenous Tau in inducible mouse models of tauopathy: J Neurosci, v. 28, p. 737-48.
Mohamed, H. A., D. R. Mosier, L. L. Zou, L. Siklós, M. E. Alexianu, J. I. Engelhardt, D. R. Beers, W. D. Le, and S. H. Appel, 2002, Immunoglobulin Fc gamma receptor promotes immunoglobulin uptake, immunoglobulin-mediated calcium increase, and neurotransmitter release in motor neurons: J Neurosci Res, v. 69, p. 110-6.
Mondal, K., A. G. Dastidar, G. Singh, S. Madhusudhanan, S. L. Gande, K. VijayRaghavan, and R. Varadarajan, 2007, Design and isolation of temperature-sensitive mutants of Gal4 in yeast and Drosophila: J Mol Biol, v. 370, p. 939-50.
Mudher, A., and S. Lovestone, 2002, Alzheimer's disease-do tauists and baptists finally shake hands?: Trends Neurosci, v. 25, p. 22-6.
Muller, M., D. Lutter, and A. W. Puschel, 2010, Persistence of the cell-cycle checkpoint kinase Wee1 in SadA- and SadB-deficient neurons disrupts neuronal polarity: J Cell Sci, v. 123, p. 286-94.
Murray, F. E., J. P. Landsberg, R. J. Williams, M. M. Esiri, and F. Watt, 1992, Elemental analysis of neurofibrillary tangles in Alzheimer's disease using proton-induced X-ray analysis: Ciba Found Symp, v. 169, p. 201-10; discussion 210-6.
Muyllaert, D., A. Kremer, T. Jaworski, P. Borghgraef, H. Devijver, S. Croes, I. Dewachter, and F. Van Leuven, 2008, Glycogen synthase kinase-3beta, or a link between amyloid and tau pathology?: Genes Brain Behav, v. 7 Suppl 1, p. 57-66.
Nakano, Y., K. Fujitani, J. Kurihara, J. Ragan, K. Usui-Aoki, L. Shimoda, T. Lukacsovich, K. Suzuki, M. Sezaki, Y. Sano, R. Ueda, W. Awano, M. Kaneda, M. Umeda, and D. Yamamoto, 2001, Mutations in the novel membrane protein spinster interfere with programmed cell death and cause neural degeneration in Drosophila melanogaster: Mol Cell Biol, v. 21, p. 3775-88.
Necula, M., and J. Kuret, 2004, Pseudophosphorylation and glycation of tau protein enhance but do not trigger fibrillization in vitro: J Biol Chem, v. 279, p. 49694-703.
Neve, R. L., P. Harris, K. S. Kosik, D. M. Kurnit, and T. A. Donlon, 1986, Identification of cDNA clones for the human microtubule-associated protein tau and chromosomal localization of the genes for tau and microtubule-associated protein 2: Brain Res, v. 387, p. 271-80.
Nezis, I. P., A. Simonsen, A. P. Sagona, K. Finley, S. Gaumer, D. Contamine, T. E. Rusten, H. Stenmark, and A. Brech, 2008, Ref(2)P, the Drosophila

melanogaster homologue of mammalian p62, is required for the formation of protein aggregates in adult brain: J Cell Biol, v. 180, p. 1065-71.
Nishimura, I., Y. Yang, and B. Lu, 2004, PAR-1 kinase plays an initiator role in a temporally ordered phosphorylation process that confers tau toxicity in Drosophila: Cell, v. 116, p. 671-82.
Noh, M. Y., K. Chun, B. Y. Kang, H. Kim, J. S. Park, H. C. Lee, Y. H. Kim, S. Ku, and S. H. Kim, 2013, Newly developed glycogen synthase kinase-3 (GSK-3) inhibitors protect neuronal cells death in amyloid-beta induced cell model and in a transgenic mouse model of Alzheimer's disease: Biochem Biophys Res Commun, v. 435, p. 274-81.
Nussbaum, J. M., S. Schilling, H. Cynis, A. Silva, E. Swanson, T. Wangsanut, K. Tayler, B. Wiltgen, A. Hatami, R. Ronicke, K. Reymann, B. Hutter-Paier, A. Alexandru, W. Jagla, S. Graubner, C. G. Glabe, H. U. Demuth, and G. S. Bloom, 2012, Prion-like behaviour and tau-dependent cytotoxicity of pyroglutamylated amyloid-beta: Nature, v. 485, p. 651-5.
O'Brien, R. J., and P. C. Wong, 2011, Amyloid precursor protein processing and Alzheimer's disease: Annu Rev Neurosci, v. 34, p. 185-204.
Ollmann, M., L. M. Young, C. J. Di Como, F. Karim, M. Belvin, S. Robertson, K. Whittaker, M. Demsky, W. W. Fisher, A. Buchman, G. Duyk, L. Friedman, C. Prives, and C. Kopczynski, 2000, Drosophila p53 is a structural and functional homolog of the tumor suppressor p53: Cell, v. 101, p. 91-101.
Omalu, B. I., J. Bailes, J. L. Hammers, and R. P. Fitzsimmons, 2010, Chronic traumatic encephalopathy, suicides and parasuicides in professional American athletes: the role of the forensic pathologist: Am J Forensic Med Pathol, v. 31, p. 130-2.
Ong, S. E., B. Blagoev, I. Kratchmarova, D. B. Kristensen, H. Steen, A. Pandey, and M. Mann, 2002, Stable isotope labeling by amino acids in cell culture, SILAC, as a simple and accurate approach to expression proteomics: Mol Cell Proteomics, v. 1, p. 376-86.
Osterwalder, T., K. S. Yoon, B. H. White, and H. Keshishian, 2001, A conditional tissue-specific transgene expression system using inducible GAL4: Proceedings of the National Academy of Sciences, v. 98, p. 12596-12601.
Otvos, L., L. Feiner, E. Lang, G. I. Szendrei, M. Goedert, and V. M. Lee, 1994, Monoclonal antibody PHF-1 recognizes tau protein phosphorylated at serine residues 396 and 404: J Neurosci Res, v. 39, p. 669-73.
Overbye, A., M. Fengsrud, and P. O. Seglen, 2007, Proteomic analysis of membrane-associated proteins from rat liver autophagosomes: Autophagy, v. 3, p. 300-22.
Paganini-Hill, A., and V. W. Henderson, 1994, Estrogen Deficiency and Risk of Alzheimer's Disease in Women: American Journal of Epidemiology, v. 140, p. 256-261.
Pankiv, S., T. H. Clausen, T. Lamark, A. Brech, J. A. Bruun, H. Outzen, A. Overvatn, G. Bjorkoy, and T. Johansen, 2007, p62/SQSTM1 binds directly to Atg8/LC3 to facilitate degradation of ubiquitinated protein aggregates by autophagy: J Biol Chem, v. 282, p. 24131-45.
Pantaloni, D., and M. F. Carlier, 1993, How profilin promotes actin filament assembly in the presence of thymosin beta 4: Cell, v. 75, p. 1007-14.
Papanikolopoulou, K., and E. C. Skoulakis, 2011, The Power and Richness of Modelling Tauopathies in Drosophila: Molecular Neurobiology, v. 44, p. 122-133.

Park, H., M. Kim, and D. K. Fygenson, 2008, Tau-isoform dependent enhancement of taxol mobility through microtubules: Arch Biochem Biophys, v. 478, p. 119-26.
Park, J. H., and J. C. Hall, 1998, Isolation and Chronobiological Analysis of a Neuropeptide Pigment-Dispersing Factor Gene in Drosophila melanogaster: Journal of Biological Rhythms, v. 13, p. 219-228.
Park, J. H., C. Helfrich-Forster, G. Lee, L. Liu, M. Rosbash, and J. C. Hall, 2000, Differential regulation of circadian pacemaker output by separate clock genes in Drosophila: Proc Natl Acad Sci U S A, v. 97, p. 3608-13.
Patton, R. L., W. M. Kalback, C. L. Esh, T. A. Kokjohn, G. D. Van Vickle, D. C. Luehrs, Y. M. Kuo, J. Lopez, D. Brune, I. Ferrer, E. Masliah, A. J. Newel, T. G. Beach, E. M. Castano, and A. E. Roher, 2006, Amyloid-beta peptide remnants in AN-1792-immunized Alzheimer's disease patients: a biochemical analysis: Am J Pathol, v. 169, p. 1048-63.
Pei, J. J., E. Braak, H. Braak, I. Grundke-Iqbal, K. Iqbal, B. Winblad, and R. F. Cowburn, 1999, Distribution of active glycogen synthase kinase 3beta (GSK-3beta) in brains staged for Alzheimer disease neurofibrillary changes: J Neuropathol Exp Neurol, v. 58, p. 1010-9.
Peng, Y., D. Stoleru, J. D. Levine, J. C. Hall, and M. Rosbash, 2003, Drosophila free-running rhythms require intercellular communication: PLoS Biol, v. 1, p. E13.
Petersen, R. C., J. E. Parisi, D. W. Dickson, K. A. Johnson, D. S. Knopman, B. F. Boeve, G. A. Jicha, R. J. Ivnik, G. E. Smith, E. G. Tangalos, H. Braak, and E. Kokmen, 2006, Neuropathologic features of amnestic mild cognitive impairment: Arch Neurol, v. 63, p. 665-72.
Pittman, A. M., H.-C. Fung, and R. de Silva, 2006, Untangling the tau gene association with neurodegenerative disorders: Human Molecular Genetics, v. 15, p. R188-R195.
Plautz, J. D., M. Straume, R. Stanewsky, C. F. Jamison, C. Brandes, H. B. Dowse, J. C. Hall, and S. A. Kay, 1997, Quantitative analysis of Drosophila period gene transcription in living animals: J Biol Rhythms, v. 12, p. 204-17.
Pope, S. K., V. M. Shue, and C. Beck, 2003, Will a healthy lifestyle help prevent Alzheimer's disease?: Annu Rev Public Health, v. 24, p. 111-32.
Quirion, R., J. C. Martel, Y. Robitaille, P. Etienne, P. Wood, N. P. Nair, and S. Gauthier, 1986, Neurotransmitter and receptor deficits in senile dementia of the Alzheimer type: Can J Neurol Sci, v. 13, p. 503-10.
Quraishe, S., C. M. Cowan, and A. Mudher, 2013, NAP (davunetide) rescues neuronal dysfunction in a Drosophila model of tauopathy: Mol Psychiatry, v. 18, p. 834-42.
Ramain, P., K. Khechumian, L. Seugnet, N. Arbogast, C. Ackermann, and P. Heitzler, 2001, Novel Notch alleles reveal a Deltex-dependent pathway repressing neural fate: Curr Biol, v. 11, p. 1729-38.
Ramsden, M., L. Kotilinek, C. Forster, J. Paulson, E. McGowan, K. SantaCruz, A. Guimaraes, M. Yue, J. Lewis, G. Carlson, M. Hutton, and K. H. Ashe, 2005, Age-dependent neurofibrillary tangle formation, neuron loss, and memory impairment in a mouse model of human tauopathy (P301L): J Neurosci, v. 25, p. 10637-47.
Reed, L. A., Z. K. Wszolek, and M. Hutton, 2001, Phenotypic correlations in FTDP-17: Neurobiol Aging, v. 22, p. 89-107.

Refinetti, R., G. C. Lissen, and F. Halberg, 2007, Procedures for numerical analysis of circadian rhythms: Biol Rhythm Res, v. 38, p. 275-325.

Reichstein, E., and E. D. Korn, 1979, Acanthamoeba profilin. A protein of low molecular weight from Acanpthamoeba castellanii that inhibits actin nucleation: Journal of Biological Chemistry, v. 254, p. 6174-6179.

Ribé, E. M., M. Pérez, B. Puig, I. Gich, F. Lim, M. Cuadrado, T. Sesma, S. Catena, B. Sánchez, M. Nieto, P. Gómez-Ramos, M. A. Morán, F. Cabodevilla, L. Samaranch, L. Ortiz, A. Pérez, I. Ferrer, J. Avila, and T. Gómez-Isla, 2005, Accelerated amyloid deposition, neurofibrillary degeneration and neuronal loss in double mutant APP/tau transgenic mice: Neurobiol Dis, v. 20, p. 814-22.

Rodriguez-Martin, T., K. Anthony, M. A. Garcia-Blanco, S. G. Mansfield, B. H. Anderton, and J.-M. Gallo, 2009, Correction of tau mis-splicing caused by FTDP-17 MAPT mutations by spliceosome-mediated RNA trans-splicing: Human Molecular Genetics, v. 18, p. 3266-3273.

Rodriguez-Rocha, H., A. Garcia-Garcia, M. I. Panayiotidis, and R. Franco, 2011, DNA damage and autophagy: Mutation Research/Fundamental and Molecular Mechanisms of Mutagenesis, v. 711, p. 158-166.

Rodríguez-Asiain, A., G. Ruiz-Babot, W. Romero, R. Cubí, T. Erazo, R. M. Biondi, J. R. Bayascas, J. Aguilera, N. Gómez, C. Gil, E. Claro, and J. M. Lizcano, 2011, Brain Specific Kinase-1 BRSK1/SAD-B associates with lipid rafts: modulation of kinase activity by lipid environment: Biochimica et Biophysica Acta (BBA) - Molecular and Cell Biology of Lipids, v. 1811, p. 1124-1135.

Rong, Y., C. K. McPhee, C. McPhee, S. Deng, L. Huang, L. Chen, M. Liu, K. Tracy, E. H. Baehrecke, E. H. Baehreck, L. Yu, and M. J. Lenardo, 2011, Spinster is required for autophagic lysosome reformation and mTOR reactivation following starvation: Proc Natl Acad Sci U S A, v. 108, p. 7826-31.

Roote, J., and S. Russell, 2012, Toward a complete Drosophila deficiency kit: Genome Biol, v. 13, p. 149.

Rosenmann, H., N. Grigoriadis, D. Karussis, M. Boimel, O. Touloumi, H. Ovadia, and O. Abramsky, 2006, Tauopathy-like abnormalities and neurologic deficits in mice immunized with neuronal tau protein: Arch Neurol, v. 63, p. 1459-67.

Samura, E., M. Shoji, T. Kawarabayashi, A. Sasaki, E. Matsubara, T. Murakami, X. Wuhua, S. Tamura, M. Ikeda, K. Ishiguro, T. C. Saido, D. Westaway, P. St George Hyslop, Y. Harigaya, and K. Abe, 2006, Enhanced accumulation of tau in doubly transgenic mice expressing mutant betaAPP and presenilin-1: Brain Res, v. 1094, p. 192-9.

Santa-Maria, I., A. Haggiagi, X. Liu, J. Wasserscheid, P. T. Nelson, K. Dewar, L. N. Clark, and J. F. Crary, 2012, The MAPT H1 haplotype is associated with tangle-predominant dementia: Acta Neuropathol, v. 124, p. 693-704.

Santa-Maria, I., F. Hernández, J. Del Rio, F. J. Moreno, and J. Avila, 2007, Tramiprosate, a drug of potential interest for the treatment of Alzheimer's disease, promotes an abnormal aggregation of tau: Mol Neurodegener, v. 2, p. 17.

Santacruz, K., J. Lewis, T. Spires, J. Paulson, L. Kotilinek, M. Ingelsson, A. Guimaraes, M. DeTure, M. Ramsden, E. McGowan, C. Forster, M. Yue, J. Orne, C. Janus, A. Mariash, M. Kuskowski, B. Hyman, M. Hutton, and K. H.

Ashe, 2005, Tau suppression in a neurodegenerative mouse model improves memory function: Science, v. 309, p. 476-81.
Sawyer, L. A., J. M. Hennessy, A. A. Peixoto, E. Rosato, H. Parkinson, R. Costa, and C. P. Kyriacou, 1997, Natural Variation in a Drosophila Clock Gene and Temperature Compensation: Science, v. 278, p. 2117-2120.
Schaeffer, S. W., A. Bhutkar, B. F. McAllister, M. Matsuda, L. M. Matzkin, P. M. O'Grady, C. Rohde, V. L. Valente, M. Aguade, W. W. Anderson, K. Edwards, A. C. Garcia, J. Goodman, J. Hartigan, E. Kataoka, R. T. Lapoint, E. R. Lozovsky, C. A. Machado, M. A. Noor, M. Papaceit, L. K. Reed, S. Richards, T. T. Rieger, S. M. Russo, H. Sato, C. Segarra, D. R. Smith, T. F. Smith, V. Strelets, Y. N. Tobari, Y. Tomimura, M. Wasserman, T. Watts, R. Wilson, K. Yoshida, T. A. Markow, W. M. Gelbart, and T. C. Kaufman, 2008, Polytene chromosomal maps of 11 Drosophila species: the order of genomic scaffolds inferred from genetic and physical maps: Genetics, v. 179, p. 1601-55.
Schaeffer, V., I. Lavenir, S. Ozcelik, M. Tolnay, D. T. Winkler, and M. Goedert, 2012, Stimulation of autophagy reduces neurodegeneration in a mouse model of human tauopathy: Brain, v. 135, p. 2169-2177.
Schenck, A., B. Bardoni, C. Langmann, N. Harden, J.-L. Mandel, and A. Giangrande, 2003, CYFIP/Sra-1 Controls Neuronal Connectivity in Drosophila and Links the Rac1 GTPase Pathway to the Fragile X Protein: Neuron, v. 38, p. 887-898.
Schenk, D., R. Barbour, W. Dunn, G. Gordon, H. Grajeda, T. Guido, K. Hu, J. Huang, K. Johnson-Wood, K. Khan, D. Kholodenko, M. Lee, Z. Liao, I. Lieberburg, R. Motter, L. Mutter, F. Soriano, G. Shopp, N. Vasquez, C. Vandevert, S. Walker, M. Wogulis, T. Yednock, D. Games, and P. Seubert, 1999, Immunization with amyloid-beta attenuates Alzheimer-disease-like pathology in the PDAPP mouse: Nature, v. 400, p. 173-7.
Schneider, A., J. Biernat, M. von Bergen, E. Mandelkow, and E. M. Mandelkow, 1999, Phosphorylation that detaches tau protein from microtubules (Ser262, Ser214) also protects it against aggregation into Alzheimer paired helical filaments: Biochemistry, v. 38, p. 3549-58.
Schneider, J. A., Z. Arvanitakis, W. Bang, and D. A. Bennett, 2007, Mixed brain pathologies account for most dementia cases in community-dwelling older persons: Neurology, v. 69, p. 2197-204.
Scott, R. C., O. Schuldiner, and T. P. Neufeld, 2004, Role and Regulation of Starvation-Induced Autophagy in the Drosophila Fat Body: Developmental Cell, v. 7, p. 167-178.
Serenó, L., M. Coma, M. Rodríguez, P. Sánchez-Ferrer, M. B. Sánchez, I. Gich, J. M. Agulló, M. Pérez, J. Avila, C. Guardia-Laguarta, J. Clarimón, A. Lleó, and T. Gómez-Isla, 2009, A novel GSK-3β inhibitor reduces Alzheimer's pathology and rescues neuronal loss in vivo: Neurobiology of Disease, v. 35, p. 359-367.
Seward, M. E., E. Swanson, A. Norambuena, A. Reimann, J. N. Cochran, R. Li, E. D. Roberson, and G. S. Bloom, 2013, Amyloid-beta signals through tau to drive ectopic neuronal cell cycle re-entry in Alzheimer's disease: J Cell Sci, v. 126, p. 1278-86.
Shang, Y., L. C. Griffith, and M. Rosbash, 2008, Light-arousal and circadian photoreception circuits intersect at the large PDF cells of the Drosophila brain: Proc Natl Acad Sci U S A, v. 105, p. 19587-94.

Shin, R. W., T. Kitamoto, and J. Tateishi, 1991, Modified tau is present in younger nondemented persons: a study of subcortical nuclei in Alzheimer's disease and progressive supranuclear palsy: Acta Neuropathol, v. 81, p. 517-23.
Shipton, O. A., J. R. Leitz, J. Dworzak, C. E. Acton, E. M. Tunbridge, F. Denk, H. N. Dawson, M. P. Vitek, R. Wade-Martins, O. Paulsen, and M. Vargas-Caballero, 2011, Tau protein is required for amyloid {beta}-induced impairment of hippocampal long-term potentiation: J Neurosci, v. 31, p. 1688-92.
Shiryaev, N., Y. Jouroukhin, E. Giladi, E. Polyzoidou, N. C. Grigoriadis, H. Rosenmann, and I. Gozes, 2009, NAP protects memory, increases soluble tau and reduces tau hyperphosphorylation in a tauopathy model: Neurobiol Dis, v. 34, p. 381-8.
Shulman, J. M., and M. B. Feany, 2003, Genetic modifiers of tauopathy in Drosophila: Genetics, v. 165, p. 1233-42.
Skipper, L., K. Wilkes, M. Toft, M. Baker, S. Lincoln, M. Hulihan, O. A. Ross, M. Hutton, J. Aasly, and M. Farrer, 2004, Linkage disequilibrium and association of MAPT H1 in Parkinson disease: Am J Hum Genet, v. 75, p. 669-77.
Sokolove, P. G., and W. N. Bushell, 1978, The chi square periodogram: its utility for analysis of circadian rhythms: J Theor Biol, v. 72, p. 131-60.
Soutar, M. P. M., W.-Y. Kim, R. Williamson, M. Peggie, C. J. Hastie, H. McLauchlan, W. D. Snider, P. R. Gordon-Weeks, and C. Sutherland, 2010, Evidence that glycogen synthase kinase-3 isoforms have distinct substrate preference in the brain: Journal of Neurochemistry, v. 115, p. 974-983.
Spires-Jones, T. L., K. J. Kopeikina, R. M. Koffie, A. de Calignon, and B. T. Hyman, 2011, Are tangles as toxic as they look?: J Mol Neurosci, v. 45, p. 438-44.
Stambolic, V., L. Ruel, and J. R. Woodgett, 1996, Lithium inhibits glycogen synthase kinase-3 activity and mimics wingless signalling in intact cells: Curr Biol, v. 6, p. 1664-8.
Steinhilb, M. L., D. Dias-Santagata, E. E. Mulkearns, J. M. Shulman, J. Biernat, E. M. Mandelkow, and M. B. Feany, 2007, S/P and T/P phosphorylation is critical for tau neurotoxicity in Drosophila: J Neurosci Res, v. 85, p. 1271-8.
Sydow, A., A. Van der Jeugd, F. Zheng, T. Ahmed, D. Balschun, O. Petrova, D. Drexler, L. Zhou, G. Rune, E. Mandelkow, R. D'Hooge, C. Alzheimer, and E. M. Mandelkow, 2011, Tau-induced defects in synaptic plasticity, learning, and memory are reversible in transgenic mice after switching off the toxic Tau mutant: J Neurosci, v. 31, p. 2511-25.
Takashima, A., K. Noguchi, G. Michel, M. Mercken, M. Hoshi, K. Ishiguro, and K. Imahori, 1996, Exposure of rat hippocampal neurons to amyloid β peptide (25–35) induces the inactivation of phosphatidyl inositol-3 kinase and the activation of tau protein kinase I/glycogen synthase kinase-3β: Neuroscience Letters, v. 203, p. 33-36.
Tarhan, M. C., Y. Orazov, R. Yokokawa, S. L. Karsten, and H. Fujita, 2013, Biosensing MAPs as "roadblocks": kinesin-based functional analysis of tau protein isoforms and mutants using suspended microtubules (sMT): Lab on a Chip.
Terry, R. D., L. A. Hansen, R. DeTeresa, P. Davies, H. Tobias, and R. Katzman, 1987, Senile dementia of the Alzheimer type without neocortical neurofibrillary tangles: J Neuropathol Exp Neurol, v. 46, p. 262-8.

Tharp, W. G., and I. N. Sarkar, 2013, Origins of amyloid-beta: BMC Genomics, v. 14, p. 290.
Theriot, J. A., and T. J. Mitchison, 1993, The three faces of profilin: Cell, v. 75, p. 835-8.
Thies, W., and L. Bleiler, 2011, 2011 Alzheimer's disease facts and figures: Alzheimers Dement, v. 7, p. 208-44.
Thornton, C., N. J. Bright, M. Sastre, P. J. Muckett, and D. Carling, 2011, AMP-activated protein kinase (AMPK) is a tau kinase, activated in response to amyloid beta-peptide exposure: Biochem J, v. 434, p. 503-12.
Tomioka, K., M. Sakamoto, Y. Harui, N. Matsumoto, and A. Matsumoto, 1998, Light and temperature cooperate to regulate the circadian locomotor rhythm of wild type and period mutants of Drosophila melanogaster: Journal of Insect Physiology, v. 44, p. 587-596.
Tomlinson, A., D. D. L. Bowtell, E. Hafen, and G. M. Rubin, 1987, Localization of the sevenless protein, a putative receptor for positional information, in the eye imaginal disc of Drosophila: Cell, v. 51, p. 143-150.
Tseng, B. P., K. N. Green, J. L. Chan, M. Blurton-Jones, and F. M. LaFerla, 2008, Aβ inhibits the proteasome and enhances amyloid and tau accumulation: Neurobiology of Aging, v. 29, p. 1607-1618.
Van Dongen, H. P., E. Olofsen, J. H. VanHartevelt, and E. W. Kruyt, 1999, A procedure of multiple period searching in unequally spaced time-series with the Lomb-Scargle method: Biol Rhythm Res, v. 30, p. 149-77.
Verheyen, E. M., and L. Cooley, 1994, Profilin mutations disrupt multiple actin-dependent processes during Drosophila development: Development, v. 120, p. 717-28.
Voss, K., B. Combs, K. R. Patterson, L. I. Binder, and T. C. Gamblin, 2012, Hsp70 alters tau function and aggregation in an isoform specific manner: Biochemistry, v. 51, p. 888-98.
Wainwright, M., and L. Amaral, 2005, The phenothiazinium chromophore and the evolution of antimalarial drugs: Trop Med Int Health, v. 10, p. 501-11.
Wang, J. W., Y. Imai, and B. Lu, 2007, Activation of PAR-1 kinase and stimulation of tau phosphorylation by diverse signals require the tumor suppressor protein LKB1: J Neurosci, v. 27, p. 574-81.
Wassarman, D. A., M. Therrien, and G. M. Rubin, 1995, The Ras signaling pathway in Drosophila: Current Opinion in Genetics & Development, v. 5, p. 44-50.
Weber, U., W. J. Gault, P. Olguin, E. Serysheva, and M. Mlodzik, 2012, Novel regulators of planar cell polarity: a genetic analysis in Drosophila: Genetics, v. 191, p. 145-62.
Wegmann, S., I. D. Medalsy, E. Mandelkow, and D. J. Muller, 2013, The fuzzy coat of pathological human Tau fibrils is a two-layered polyelectrolyte brush: Proc Natl Acad Sci U S A, v. 110, p. E313-21.
Weingarten, M. D., A. H. Lockwood, S. Y. Hwo, and M. W. Kirschner, 1975, A protein factor essential for microtubule assembly: Proc Natl Acad Sci U S A, v. 72, p. 1858-62.
Weisenberg, R. C., G. G. Borisy, and E. W. Taylor, 1968, The colchicine-binding protein of mammalian brain and its relation to microtubules: Biochemistry, v. 7, p. 4466-79.
Whitehouse, P. J., A. M. Martino, P. G. Antuono, P. R. Lowenstein, J. T. Coyle, D. L. Price, and K. J. Kellar, 1986, Nicotinic acetylcholine binding sites in Alzheimer's disease: Brain Res, v. 371, p. 146-51.

Wischik, C. M., P. C. Edwards, R. Y. Lai, M. Roth, and C. R. Harrington, 1996, Selective inhibition of Alzheimer disease-like tau aggregation by phenothiazines: Proc Natl Acad Sci U S A, v. 93, p. 11213-8.
Wischik, C. M., M. Novak, P. C. Edwards, A. Klug, W. Tichelaar, and R. A. Crowther, 1988a, Structural characterization of the core of the paired helical filament of Alzheimer disease: Proc Natl Acad Sci U S A, v. 85, p. 4884-8.
Wischik, C. M., M. Novak, H. C. Thøgersen, P. C. Edwards, M. J. Runswick, R. Jakes, J. E. Walker, C. Milstein, M. Roth, and A. Klug, 1988b, Isolation of a fragment of tau derived from the core of the paired helical filament of Alzheimer disease: Proc Natl Acad Sci U S A, v. 85, p. 4506-10.
Wittmann, C. W., M. F. Wszolek, J. M. Shulman, P. M. Salvaterra, J. Lewis, M. Hutton, and M. B. Feany, 2001, Tauopathy in Drosophila: neurodegeneration without neurofibrillary tangles: Science, v. 293, p. 711-4.
Wolozin, B., and P. Davies, 1987, Alzheimer-related neuronal protein A68: specificity and distribution: Ann Neurol, v. 22, p. 521-6.
Wolozin, B. L., A. Pruchnicki, D. W. Dickson, and P. Davies, 1986, A neuronal antigen in the brains of Alzheimer patients: Science, v. 232, p. 648-50.
Woodgett, J. R., 1990, Molecular cloning and expression of glycogen synthase kinase-3/factor A: EMBO J, v. 9, p. 2431-8.
Woods, D. F., C. Hough, D. Peel, G. Callaini, and P. J. Bryant, 1996, Dlg protein is required for junction structure, cell polarity, and proliferation control in Drosophila epithelia: J Cell Biol, v. 134, p. 1469-82.
Wortmann, M., 2012, Dementia: a global health priority - highlights from an ADI and World Health Organization report: Alzheimers Res Ther, v. 4, p. 40.
Wszolek, Z. K., Y. Tsuboi, B. Ghetti, S. Pickering-Brown, Y. Baba, and W. P. Cheshire, 2006a, Frontotemporal dementia and parkinsonism linked to chromosome 17 (FTDP-17): Orphanet J Rare Dis, v. 1, p. 30.
Wszolek, Z. K., Y. Tsuboi, B. Ghetti, S. Pickering-Brown, Y. Baba, and W. P. Cheshire, 2006b, Frontotemporal dementia and parkinsonism linked to chromosome 17 (FTDP-17): Orphanet J Rare Dis, v. 1.
Wszołek, Z. K., J. Słowiński, M. Golan, and D. W. Dickson, 2005, Frontotemporal dementia and parkinsonism linked to chromosome 17: Folia Neuropathol, v. 43, p. 258-70.
Wu, C. H., C. Fallini, N. Ticozzi, P. J. Keagle, P. C. Sapp, K. Piotrowska, P. Lowe, M. Koppers, D. McKenna-Yasek, D. M. Baron, J. E. Kost, P. Gonzalez-Perez, A. D. Fox, J. Adams, F. Taroni, C. Tiloca, A. L. Leclerc, S. C. Chafe, D. Mangroo, M. J. Moore, J. A. Zitzewitz, Z. S. Xu, L. H. van den Berg, J. D. Glass, G. Siciliano, E. T. Cirulli, D. B. Goldstein, F. Salachas, V. Meininger, W. Rossoll, A. Ratti, C. Gellera, D. A. Bosco, G. J. Bassell, V. Silani, V. E. Drory, R. H. Brown, Jr., and J. E. Landers, 2012, Mutations in the profilin 1 gene cause familial amyotrophic lateral sclerosis: Nature, v. 488, p. 499-503.
Wu, J. W., M. Herman, L. Liu, S. Simoes, C. M. Acker, H. Figueroa, J. I. Steinberg, M. Margittai, R. Kayed, C. Zurzolo, G. Di Paolo, and K. E. Duff, 2013a, Small Misfolded Tau Species Are Internalized via Bulk Endocytosis and Anterogradely and Retrogradely Transported in Neurons: Journal of Biological Chemistry, v. 288, p. 1856-1870.
Wu, T. H., Y. N. Lu, C. L. Chuang, C. L. Wu, A. S. Chiang, D. E. Krantz, and H. Y. Chang, 2013b, Loss of vesicular dopamine release precedes tauopathy in degenerative dopaminergic neurons in a Drosophila model expressing human tau: Acta Neuropathol, v. 125, p. 711-25.

Xu, P., S. Y. Vernooy, M. Guo, and B. A. Hay, 2003, The Drosophila MicroRNA Mir-14 Suppresses Cell Death and Is Required for Normal Fat Metabolism: Current biology : CB, v. 13, p. 790-795.

Xu, T., and S. Artavanis-Tsakonas, 1990, deltex, a locus interacting with the neurogenic genes, Notch, Delta and mastermind in Drosophila melanogaster: Genetics, v. 126, p. 665-77.

Yamada, M., 2003, Senile dementia of the neurofibrillary tangle type (tangle-only dementia): neuropathological criteria and clinical guidelines for diagnosis: Neuropathology, v. 23, p. 311-7.

Yanamandra, K., N. Kfoury, H. Jiang, Thomas E. Mahan, S. Ma, Susan E. Maloney, David F. Wozniak, Marc I. Diamond, and David M. Holtzman, 2013, Anti-Tau Antibodies that Block Tau Aggregate Seeding In Vitro Markedly Decrease Pathology and Improve Cognition In Vivo: Neuron, v. 80, p. 402-414.

Yoshida, H., and M. Goedert, 2011, Phosphorylation of Microtubule-Associated Protein Tau by Ampk-Related Kinases: J Neurochem.

Yoshiyama, Y., V. M. Lee, and J. Q. Trojanowski, 2013, Therapeutic strategies for tau mediated neurodegeneration: J Neurol Neurosurg Psychiatry, v. 84, p. 784-95.

Yu, Y., X. Run, Z. Liang, Y. Li, F. Liu, Y. Liu, K. Iqbal, I. Grundke-Iqbal, and C. X. Gong, 2009, Developmental regulation of tau phosphorylation, tau kinases, and tau phosphatases: J Neurochem, v. 108, p. 1480-94.

Zempel, H., E. Thies, E. Mandelkow, and E. M. Mandelkow, 2010, Abeta oligomers cause localized Ca(2+) elevation, missorting of endogenous Tau into dendrites, Tau phosphorylation, and destruction of microtubules and spines: J Neurosci, v. 30, p. 11938-50.

Zhang, B., J. Carroll, J. Q. Trojanowski, Y. Yao, M. Iba, J. S. Potuzak, A. M. Hogan, S. X. Xie, C. Ballatore, A. B. Smith, 3rd, V. M. Lee, and K. R. Brunden, 2012, The microtubule-stabilizing agent, epothilone D, reduces axonal dysfunction, neurotoxicity, cognitive deficits, and Alzheimer-like pathology in an interventional study with aged tau transgenic mice: J Neurosci, v. 32, p. 3601-11.

Zhou, G., R. Myers, Y. Li, Y. Chen, X. Shen, J. Fenyk-Melody, M. Wu, J. Ventre, T. Doebber, N. Fujii, N. Musi, M. F. Hirshman, L. J. Goodyear, and D. E. Moller, 2001, Role of AMP-activated protein kinase in mechanism of metformin action: J Clin Invest, v. 108, p. 1167-74.

Zhou, J., B. Wan, R. Li, X. Gu, Z. Zhong, Y. Wang, and L. Yu, 2012, Jab1 interacts with brain-specific kinase 2 (BRSK2) and promotes its degradation in the ubiquitin–proteasome pathway: Biochemical and Biophysical Research Communications, v. 422, p. 647-652.

Zilka, N., Z. Kazmerova, S. Jadhav, P. Neradil, A. Madari, D. Obetkova, O. Bugos, and M. Novak, 2012, Who fans the flames of Alzheimer's disease brains? Misfolded tau on the crossroad of neurodegenerative and inflammatory pathways: J Neuroinflammation, v. 9, p. 47.

9| Appendix 1 – *Drosophila* strains used in this work

Table 9.1 Full genotypes of stocks described in this work

Label	Description	Full Genotype	Source
GMR	Driver of GAL4 in eye photoreceptors	$w^{[1118]}$; P{w[$^{+}$mc], UAS-GMR::GAL4}/CyO ; MKRS/TM6B	Lab stock
ELAV	Temperature sensitive driver of GAL4 throughout the nervous system	$w^{[1118]}$; P{w[$^{+}$mc], UAS-ELAV::GAL4},P{w[$^{+}$mc], UAS-ELAV::GAL4}/CyO ; MKRS/TM6B	Kind gift of Kyung-An Han
PDF	Driver of GAL4 in lateral ventral neurons	$yw^{[1118]}$; P{w[$^{+}$mc], UAS-PDF::GAL4}/ P{w[$^{+}$mc], UAS-PDF::GAL4} ; +/+	Lab stock
0N4R	WT human 0N4R tau	$w^{[1118]}$; + ; P{w[$^{+}$mc], UAS-4Rtau}/TM6B	Lab stock
B2WT5	WT human BRSK2	$w^{[1118]}$; + ; P{w[$^{+}$mc], UAS-B2WT5}/TM3	Lab stock
0N4R/B2WT5	Recombinant WT human 0N4R tau and WT human BRSK2	$w^{[1118]}$; CyO/If ; P{w[$^{+}$mc], UAS-B2WT5},P{w[+mc], UAS-4Rtau} /TM6B	Lab stock
2N4R tau T212A	2N4R human tau with T212A mutation	$w^{[1118]}$; CyO/If ; P{w[$^{+}$mc], UAS-2N4Rtau T212A}/MKRS	A kind gift of Guy Tear and Giulia Povellato
2N4R tau T231A	2N4R human tau with T231A mutation and FLAG tag	$w^{[1118]}$; CyO/If ; P{w[$^{+}$mc], UAS-2N4Rtau T231A}/MKRS	Generated by Alessia Galasso
2N4R tau S262A	2N4R human tau with S262A mutation and FLAG tag	$w^{[1118]}$; CyO/If ; P{w[$^{+}$mc], UAS-2N4Rtau S262A}/MKRS	Generated by Alessia Galasso
2N4R tau T212D	2N4R human tau with T212D mutation and FLAG tag	$w^{[1118]}$; CyO/If ; P{w[$^{+}$mc], UAS-2N4Rtau T212D}/MKRS	This work
2N4R tau T231D	2N4R human tau with T231D mutation and FLAG tag	$w^{[1118]}$; CyO/If ; P{w[$^{+}$mc], UAS-2N4Rtau T231D}/MKRS	This work
2N4R tau S262D	2N4R human tau with S262D mutation and FLAG tag	$w^{[1118]}$; CyO/If ; P{w[$^{+}$mc], UAS-2N4Rtau S262D}/MKRS	This work
2N4R tau T212D S262D	2N4R human tau with T212D and S262D mutations, and FLAG tag	$w^{[1118]}$; CyO/If ; P{w[$^{+}$mc], UAS-2N4Rtau T212D S262D}/MKRS	This work
Chic 4891	Mutated gene *chickadee*, amorphic allele	$w^{[1118]}$; P{PZ}chic01320 cn1/CyO ; ry506	BDSC
Chic 4892	Disruption of gene *chickadee* by transposable element insertion	$w^{[1118]}$; chic221 cn1/CyO; ry506	BDSC

Table 9.2 Details of additional chromosome 2 deficiencies acquired from Bloomington

Stock	Insertion	Full Genotype	Donor
7648	87F2;87F10, 3R:9369363;9509679	w[1118]; Df(3R)Exel6169, P{w[+mC]=XP-U}Exel6169/TM6B, Tb[1]	Exelixis, Inc.
7804	27F2;28A3, 2L:7364976;7495492	w[1118]; Df(2L)Exel7031/CyO	Exelixis, Inc.
7859	44A4;44B3, 2R:3948670;4019248	w[1118]; Df(2R)Exel7094/CyO	Exelixis, Inc.
7885	52E11;52F1, 2R:12030362--12030372;12046356	w[1118]; Df(2R)Exel9060, PBac{w[+mC]=RB5.WH5}Exel9060	Exelixis, Inc.
7886	53B1;53C4, 2R:12176759;12312794	w[1118]; Df(2R)Exel7142/CyO	Exelixis, Inc.
8876	43A3;43F6	Df(2R)CA58/CyO	Michael Ashburner
9275	43F8;44D4, 2R:3849654;4487956	w[1118]; Df(2R)ED1735, P{w[+mW.Scer\FRT.hs3]=3'.RS5+3.3'}ED1735/SM6a	DrosDel Project
9413	55B8;55E3, 2R:14028250;14526773	w[1118]; Df(2R)ED3636, P{w[+mW.Scer\FRT.hs3]=3'.RS5+3.3'}ED3636/SM6a	DrosDel Project
23664	45A9;45E3, 2R:5009694;5403346	w[1118]; Df(2R)BSC279/CyO	Kevin Cook
23665	45C4;45F4, 2R:5180164;5466121	w[1118]; Df(2R)BSC280/CyO	Kevin Cook
23692	52F11;53B1, 2R:12117729--12117731;12176803	w[1118]; Df(2R)BSC309/CyO	Kevin Cook
24128	27F7;28C4, 2L:7423926;7800182	w[1118]; Df(2L)ED501, P{w[+mW.Scer\FRT.hs3]=3'.RS5+3.3'}ED501/SM6a	DeosDel Project
24339	42A8;42B2, 2R:1911160;2536218	w[1118]; Df(2R)BSC313/CyO	Kevin Cook
24351	42A14;42C7, 2R:2123567;2633535	w[1118]; Df(2R)BSC326/CyO	Kevin Cook
24362	54F1;55B1, 2R:13742225--13742255;13928168	w[1118]; Df(2R)BSC338/CyO	Kevin Cook
24912	45D4;45F4, 2R:5296452;5466121	w[1118]; Df(2R)BSC408/CyO	Kevin Cook
24987	55A1;55B7, 2R:13778659;14015980	w[1118]; Df(2R)BSC483/CyO	Kevin Cook
25442	52F6;53A5, 2R:12075259;12169783	w[1118]; Df(2R)BSC609/CyO	Kevin Cook
7493	22D1;22E1, 2L:2175607;2362917	w[1118]; Df(2L)Exel6007, P{w[+mC]=XP-U}Exel6007/CyO	Exelixis, Inc.

Stock	Insertion	Full Genotype	Donor
7528	38C2;38C7, 2L:20205107;20449190—20458307	w[1118]; Df(2L)Exel6046, P{w[+mC]=XP-U}Exel6046/CyO	Exelixis, Inc.
7779	22B2;22B8, 2L:1737960;2010136	w[1118]; Df(2L)Exel8005/CyO	Exelixis, Inc.
7780	22B8;22D1, 2L:1989057--1989058;2152458	w[1118]; Df(2L)Exel7008/CyO	Exelixis, Inc.
7813	30B1;30B4, 2L:9388129;9448660—9448833	w[1118]; Df(2L)Exel8022/CyO	Exelixis, Inc.
7814	30B2;30B3, 2L:9415663;9431473	w[1118]; Df(2L)Exel9064, PBac{w[+mC]=RBr}Exel9064/CyO	Exelixis, Inc.
7851	38C7;38D5, 2L:20449190--20458307;20680624	w[1118]; Df(2L)Exel7078/CyO	Exelixis, Inc.
7852	38E9;38F3, 2L:20770538;20874804	w[1118]; Df(2L)Exel7079/CyO	Exelixis, Inc.
8000	22B5;22D1, 2L:1911627;2175599	w[1118]; Df(2L)Exel6006, P{w[+mC]=XP-U}Exel6006/CyO	Exelixis, Inc.
9175	38D1;38F5, 2L:20638580;20917519	w[1118]; Df(2L)ED1317, P{w[+mW.Scer\FRT.hs3]=3'.RS5+3.3'}ED1317/SM6a	DrosDel Project
9222	38B4;38C6, 2L:20085397;20382385	w[1118]; Df(2L)ED1305, P{w[+mW.Scer\FRT.hs3]=3'.RS5+3.3'}ED1305/SM6a	DrosDel Project
9704	28E8;29B1, 2L:8155863;8346414	w[1118]; Df(2L)BSC227/CyO	Kevin Cook
26500	44A2;44D1, 2R:3885081;4350143	w[1118]; Df(2R)BSC266/CyO	Kevin Cook
9705	28E5;28F4, 2L:8092128--8092225;8221250	w[1118]; Df(2L)BSC228/CyO	Kevin Cook
24357	38F1;39A6, 2L:20831386;21155355	w[1118]; Df(2L)BSC333/CyO	Kevin Cook

Table 9.3 Details of RNAi stocks from VDRC examined in this work

Gene	Transformant ID	Construct ID	Library
CG4238	41982	11260	GD
Su(dx)	103814	102798	KK
DPR3	106517	111766	KK
GlyP	109596	100434	KK
CG7261	105428	101739	KK
AIF	109615	101231	KK
Spire	107335	109380	KK
Arpc2	104396	108258	KK
Debcl	106669	100738	KK
CG8726	109451	108815	KK
CG14763	104043	112546	KK
CSN4	103803	100065	KK
Hey	103570	101381	KK
Sut3	4009	1865	GD
Sut2	102028	110424	KK
Sut1	104983	112749	KK
Nup50	100564	108150	KK
Pnut	11791	1512	GD

10| Appendix 2 – primers used in this work

Tau mutagenic primers:

T212D sense: 5’ CAGCCGCTCCCGCGACCCGTCCCTTCCA 3’

T212D antisense: 5’ TGGAAGGGACGGGTCGCGGGAGCGGCTG 3’

T231D sense: 5’ AGAAGGTGGCAGTGGTCCGTGATCCACCCAAGTC 3’

T231D antisense: 5’ GACTTGGGTGGATCACGGACCACTGCCACCTTCT 3’

S262D sense: 5’ GTCAAGTCCAAGATCGGCGACACTGAGAACCTGAAGCA 3’

S262D antisense:
5’ TGCTTCAGGTTCTCAGTGTCGCCGATCTTGGACTTGAC 3’

Tau sequencing primers:

Tau sense 24: 5’ CGA AGTGATGGA AGATCACG 3’

Tau sense 508: 5’ AGGATTCCAGCA AAA ACCCC 3’

Tau sense 550: 5’ AGCTCTGGTGAACCTCCAAAAT 3’

Tau sense 1074: 5’ CAATATCACCCACGTCCCTG 3’

Tau sense 1199: 5’ CTGGGGACACGTCTCCACG 3’

Tau amtisense 123: 5’ AATGCCTGCTTCTTCAGCTG 3’

Subcloning primers for pUAST attP2:

pUASTattP2 sense: 5’ TGCAACTACTGAAATCTGCC 3’

pUASTattP2 antisense: 5’ ACACCACAGAAGTAAGGTTCC 3’